PSEUDOTUMOURS FOLLOWING

METAL-ON-METAL HIP RESURFACING ARTHROPLASTY

A DISSERTATION SUBMITTED TO THE
UNIVERSITY OF OXFORD



IN PARTIAL FULFILMENT OF THE REQUIREMENTS
FOR THE DEGREE OF
DOCTOR OF PHILOSOPHY

BY
YOUNG-MIN KWON
FRCS(Orth) FRACS(Orth)

WADHAM COLLEGE
OXFORD
AND
NUFFIELD DEPARTMENT OF ORTHOPAEDICS, RHEUMATOLOGY
AND MUSCULOSKELETAL SCIENCES
UNIVERSITY OF OXFORD

TRINITY TERM 2009

I dedicate this thesis to my parents, my wife, and my son.
For all they have given me.

Acknowledgements

First of all, I would like to express my sincere gratitude to my distinguished supervisors: Professor David W. Murray, Dr. Harinderjit S. Gill, and Dr. David J. Beard. They have provided me with invaluable guidance, support and most importantly academic freedom to pursue throughout this journey. I thank Mr. Peter McLardy-Smith for warmly welcoming me to Oxford and to his College. I am eternally indebted to Mrs. Barbara Marks who has, from the very beginning, always been a source of wisdom and who has graciously provided advice throughout this research endeavour. I am to grateful Ms. Jo Copp for her kind administrative support. During this cross-disciplinary project, it has been a privilege to work with and learn from my highly respected colleagues at the Nuffield Department of Orthopaedics, Rheumatology and Musculoskeletal Sciences, University of Oxford. In particular, I would like to acknowledge Dr. Simon Ostlere, Professor Nick Athanasou, Dr. Afsie Sabokbar, Dr. Guillaume Mabilleau, Dr. Zhidao Xia, and Dr. Stephen Mellon. Lastly, I thank all the patients who have generously given up time during their busy lives to participate in the research studies, without whom this thesis would not have been made possible.

Abstract

Pseudotumours Following Metal-on-Metal Hip Resurfacing Arthroplasty

Young-Min Kwon — Doctor of Philosophy
Wadham College — Trinity Term 2009

Metal-on-metal hip resurfacing arthroplasty (MoMHRA) has undergone a recent resurgence as an alternative treatment option for young and active patients with significant hip osteoarthritis. Despite the satisfactory short-term implant survivorship, abnormal periprosthetic soft-tissue masses relating to the hip joint (pseudotumours) are being increasingly reported. These were found to be locally destructive, requiring revision surgery in a high proportion (75%) of patients, the outcome of which is poor. However, there is currently no definitive evidence of potential mechanisms involved in the occurrence of such destructive soft tissue masses. The broad aims of this thesis were: 1) to determine the extent of this emerging clinical complication (pseudotumour) with a high revision burden; and 2) to determine whether pseudotumour results from a local biological reaction to an increased wear debris burden generated by excessive MoMHRA implant wear.

A clinical study investigated the prevalence of, and association between, pseudotumours and serum metal ion levels in 158 MoMHRA patients (201 hips). The overall prevalence of pseudotumour was found to be 4%, considerably higher than previously reported. The study also established that pseudotumour only occurred with elevated metal ion levels, suggesting the underlying cause is increased wear.

It was postulated that pseudotumours are likely to be a biological reaction to the large amount of metal debris generated *in vivo* due to excessive wear. Two potential biological reactions mediating the occurrence of pseudotumours were then investigated. An *in vitro* clinical study demonstrated that systemic hypersensitivity type IV reaction, mediated by lymphocyte reactivity to these metals, is not the dominant biological response involved in pseudotumours. A further *in vitro* experiment demonstrated that metal particle-induced cytotoxicity is likely to be an important factor leading to pseudotumours.

Subsequent research focused, firstly, on assessing the magnitude of bearing surface wear that occurs in pseudotumour patients, and secondly on elucidating the potential wear mechanism responsible for the increased implant wear in these patients. A retrieval study demonstrated that MoMHRA implants revised due to pseudotumour were associated with significantly greater linear wear rates. This combined with the metal ion data confirmed that pseudotumour is associated with increased wear at the MoM articulation. An edge-loading wear pattern was always found in the pseudotumour group. An *in vivo* study was then developed to investigate whether the edge-loading occurs during functional activities. Edge-loading in the pseudotumour group was found to occur with up to 4-fold increase in duration and up to 7-fold increase in force. This *in vivo* finding supported the *in vitro* retrieval study finding of an edge-loading wear pattern in the pseudotumour group, suggesting that edge-loading during functional activities is an important *in vivo* mechanism responsible for localised high wear and subsequent elevation of metal ion levels in MoMHRA patients with pseudotumours.

It is concluded that pseudotumour is likely to result from a local biological reaction to increased metal debris load, generated by excessive MoMHRA implant wear due to edge-loading. In susceptible patients, the dose-dependent cytotoxicity of wear debris leads to subsequent necrosis of periprosthetic soft tissues. Clinicians need to be aware of pseudotumours and surgeons should undertake MoMHRA with great care in the knowledge that even with satisfactory component positioning, the problem can occur. In evaluating MoMHRA patients with unexplained symptoms with normal plain radiographs, further investigation with soft-tissue imaging modalities such as ultrasound or MRI is recommended.

Table of Content

CHAPTER 1 INTRODUCTION 1

1.1 OVERVIEW 1
1.2 OVERALL SCOPE OF THE PROPOSED THESIS 5
1.3 SPECIFIC OBJECTIVES 5
1.4 STRUCTURE OF THE THESIS 6

CHAPTER 2 LITERATURE REVIEW 8

2.1 METAL-ON-METAL HIP RESURFACING 8
2.1.1 Evolution of Hip Resurfacing Implant Design 8
2.1.2 Contemporary Design 9
2.1.3 Implant Survivorship 11
2.2 METAL WEAR PARTICLES & IONS 13
2.2.1 Metal-on-Metal Articulation Wear 14
2.2.2 Metal Wear Particles 15
2.2.3 Metal Ions 16
2.2.4 Metal Excretion 18
2.2.5 Metal Ion Levels *In Vivo* 19
2.2.5.1 Measurement Methods 19
2.2.5.2 Metal Ion Levels in General Population 20
2.2.5.3 Metal Ion Levels Following MoM Hip Arthroplasty 21
2.2.5.4 Serum Metal Ion Level as a Marker for Wear 24
2.3 SYSTEMIC ADVERSE CONSEQUENCES OF SERUM METAL IONS 25
2.3.1 Chromosomal Abnormality 25
2.3.2 Carcinogenesis 26
2.3.3 Teratogenicity 27
2.3.4 Metal Hypersensitivity 27
2.4 LOCAL ADVERSE PERIPROSTHETIC SOFT TISSUE MASSES 30
2.5 SUMMARY 35

CHAPTER 3 PREVALENCE AND METAL ION STUDY 37

3.1 INTRODUCTION 37
3.2 STUDY DESIGN 38
3.3 MATERIALS AND METHODS 39
3.3.1 MoMHRA Patient Recruitment 39
3.3.2 Imaging 40
3.3.3 Histology & SEM/EDX Examinations 43
3.3.4 Metal Ion Level Measurements 44
3.3.5 Functional Outcome Measurement 46
3.3.6 Statistics 46
3.4 CONTROL MEASUREMENTS 47
3.4.1 Venous Sampling 47
3.4.2 Hip Aspiration 48
3.5 RESULTS 49
3.5.1 Prevalence 49
3.5.2 Metal Ion Levels 54
3.6 DISCUSSION 58
3.7 SUMMARY 64

CHAPTER 4 *IN VITRO* ASSESSMENT OF METAL HYPERSENSITIVITY 65

4.1 INTRODUCTION 65
4.2 THE NULL HYPOTHESIS 66
4.3 STUDY DESIGN 66

4.4 MATERIALS AND METHODS 66
4.4.1 Patients 66
4.4.2 Implant-Related Hypersensitivity Tests 68
4.4.3 Lymphocyte Transformation Test 69
4.4.4 Serum Metal Ion Analysis 71
4.4.5 Statistics 72
4.5 RESULTS 72
4.5.1 Incidence of Enhanced Metal-Induced Lymphocyte Reactivity 72
4.5.2 Level of Metal-Induced Lymphocyte Reactivity 74
4.5.3 Serum Metal Ion Levels vs. Lymphocyte Reactivity 75
4.6 DISCUSSION 78
4.7 SUMMARY 82

CHAPTER 5 *IN VITRO* METAL CYTOTOXICITY 83

5.1 INTRODUCTION 83
5.2 THE NULL HYPOTHESES 84
5.3 MATERIALS AND METHODS 84
5.3.1 *In Vitro* Experimental Considerations 84
5.3.2 Cell Cultures with Metal Nanoparticles and Ions 87
5.3.3 Cytotoxicity Assays 88
5.3.4 Metal Ion Release into Culture Medium by Co and Cr Nanoparticles 91
5.3.5 Statistics 92
5.4 CONTROL EXPERIMENTS 92
5.4.1 Alamar Blue Assay 92
5.4.2 Live/Dead Assay 95
5.4.3 Repeatability of Live/Dead Assay 96
5.4.4 Verification of Nanoparticle Size 98
5.5 RESULTS 101
5.5.1 Effects of Nanoparticles on the Viability of Macrophages 101
5.5.2 Effects of Metal Ions on the Viability of Macrophages 104
5.5.3 Metal Ion Release into the Culture Medium 106
5.6 DISCUSSION 107
5.7 SUMMARY 113

CHAPTER 6 *IN VITRO* MEASUREMENT OF MOMHRA WEAR 114

6.1 INTRODUCTION 114
6.2 THE NULL HYPOTHESES 115
6.3 MATERIALS AND METHODS 115
6.3.1 Ethics Approval 115
6.3.2 Selection of Retrieved Implants 116
6.3.3 Collection of Retrieval Implants 118
6.3.4 Study Power Estimation 119
6.3.5 MoMHRA Implant Wear Measurement 120
6.3.6 Linear Wear Assessment Using a Roundness Machine 122
6.3.7 Statistics 126
6.4 CONTROL MEASUREMENTS 126
6.5 RESULTS 127
6.5.1 Qualitative Assessment 127
6.5.2 Linear Wear Rate 128
6.5.3 Edge-Loading 130
6.6 DISCUSSION 131
6.7 SUMMARY 137

CHAPTER 7 *IN VIVO* ASSESSMENT OF EDGE-LOADING 138

7.1 INTRODUCTION 138
7.1.1 *In Vivo* Hip Joint Force 139
7.1.2 Acetabular Component Orientation 142
7.1.3 Study Aim 143
7.2 THE NULL HYPOTHESIS 143
7.3 MATERIALS AND METHODS 144
7.3.1 MoMHRA Patient Recruitment 144
7.3.2 Three-Dimensional Lower Limb Motion Analysis 146
7.3.3 Justification of Motion Analysis Protocol 150
7.3.4 Computed Tomography (CT) Scans 152
7.3.5 Data Presentation 157
7.3.6 Definition of Edge-Loading 159
7.3.7 Statistics 160
7.4 ERROR ASSESSMENTS 161
7.4.1 Motion Analysis System 161
7.4.2 Inter-Trial Variability 163
7.4.3 CT Measurement Error Assessments 165
7.4.4 Hip Joint Centre Determination 167
7.4.5 Validity of CT Cup Orientation Measurements 171
7.5 RESULTS 173
7.5.1 Edge-Loading 173
7.5.2 Zone Duration of Force Paths 174
7.5.3 Force Impulse Distribution of Force Paths 177
7.5.4 Acetabular Cup Orientation 179
7.5.5 Serum Metal Ion Levels 180
7.6 DISCUSSION 182
7.7 SUMMARY 193

CHAPTER 8 CONCLUSIONS, CLINICAL RELEVANCE AND FUTURE WORK 194

8.1 REVIEW OF RESEARCH OBJECTIVES 194
8.2 CONCLUSIONS 195
8.3 CLINICAL RELEVANCE 199
8.4 RECOMMENDATIONS FOR FUTURE STUDIES 202

APPENDIX 1: OXFORD HIP SCORE I

APPENDIX 2: *IN VITRO* CYTOTOXICITY EXPERIMENTAL PROTOCOL III

APPENDIX 3: MOTION ANALYSIS PROTOCOL XI

APPENDIX 4: LOW DOSE HIP CT SCANNING PROTOCOL XV

APPENDIX 5: RISK ASSESSEMENT FOR IONISING RADIATION XVI

APPENDIX 6: CT VS. EBRA ACETABULAR CUP ANGLES XVII

APPENDIX 7: PUBLICATIONS AND CONFERENCE PROCEEDINGS XVIII

REFERENCES XXII

List of Figures

Figure 2-1: The Birmingham Hip Resurfacing (BHR) system. 10

Figure 3-1: (a) Extended field of view of sagittal ultrasound image of a mass (arrows) arising from the anterior aspect of the hip joint in Case 2; (b) Coronal STIR MRI image of a predominantly solid low signal intensity mass (arrows) seen in Figure 3-1(a). 51

Figure 3-2: Peri-implant soft tissue showing coagulative necrosis with granulomas containing macrophages (arrows) (hematoxylin and eosin stain, magnification 100×). 53

Figure 3-3: Pseudomembrane showing numerous perivascular lymphoid aggregates (arrows) and a diffuse lymphocyte infiltrate (hematoxylin and eosin stain, 100×)..... 53

Figure 3-4: EDX spectrum obtained from metal particulate analysis, confirming the presence of cobalt (Co) and chromium (Cr)..... 54

Figure 3-5: Boxplots showing differences in serum cobalt (a) and serum chromium (b) level measurements between the three patient groups. The number of patient per group is denoted by *n*. 55

Figure 3-6: Boxplots showing differences in cobalt (a) and chromium (b) levels in hip aspirates between the two MoMHRA patient groups. The number of patient per group is denoted by *n*. 56

Figure 3-7: Serum cobalt and chromium concentrations correlated with hip aspirate cobalt and chromium concentrations. 57

Figure 4-1: Mean lymphocyte reactivity (stimulation index) measured (at 10^{-4}M) in the three patient groups for cobalt, chromium and nickel. Asterisk (*) indicates $p<0.05$ versus the control group with no metal implants (medium only). 75

Figure 4-2: Serum cobalt and chromium ion levels from all patients in the three groups are plotted against cobalt and chromium challenged lymphocyte reactivity. 77

Figure 4-3: Serum cobalt and chromium ion levels from patients in the pseudotumour group are correlated with cobalt and chromium challenged lymphocyte reactivity. 77

Figure 5-1: The cell numbers plotted against the relative fluorescent unit (RFU). 93

Figure 5-2: Micrographs of scanning electron microscopy (SEM) showing control RAW 264.7 cells and RAW 264.7 cells cultured with Cr nanoparticles *in vitro* for four days. No particles were observed in control cells at either low (a, b) or high magnification (c). Aggregation of nanoparticles could form large clumps (up to 30 μm in diameter) (d) or small particles (1-3 μm in diameter) (e). However, the majority of particles sizes

were found to be 30-60 nm in diameter, which were attached to the surface of RAW 264.7 cells (f). 100
Figure 5-3: The effect of metal nanoparticles on RAW263.7 macrophage cell numbers at day 1 and day 4. Asterisk (*) indicates $p<0.05$ against the control cells (no particles added, concentration 0 particles/ml)..... 102
Figure 5-4: Confocal microscopic micrographs of Live/Dead staining at Day 1, with metal nanoparticle concentrations at 1×10^{12} particles/ml and metal ion concentrations at 1000 μM: (a) control (medium only); (b) Co nanoparticles; (c) Cr nanoparticles; (d) Ti nanoparticles; (e) Co ions; and (f) Cr ions. Live cells are stained green and dead cells are stained red (original magnification 200×). 103
Figure 5-5: The effect of metal nanoparticles (1×10^{12} particles/ml) and ions (1000μM) on RAW263.7 macrophage viability at day 1 and day 4. Asterisk (*) indicates $p<0.05$ against the control cells (no particles added, concentration 0 particles/ml)..... 104
Figure 5-6: The effect of Co and Cr ions on RAW263.7 macrophage cell numbers at day 1 and day 4. Asterisk (*) indicates $p<0.05$ against the control cells (no metal ions added, concentration 0 μM)..... 105
Figure 5-7: A linear correlation between the level of Co ions released from the particulate form of Co nanoparticles (corrosion) and the level of Co ions measured in the culture medium from cobalt (II) sulphate heptahyrate solution following 24 hours of incubation in the culture medium. 107
Figure 6-1: Photographs of the roundness machine set-up used to measure linear wear of the retrieved femoral head (a) and acetabular cup (b) components. 123
Figure 6-2: Roundness profiles of a) edge-loaded and b) non-edge loaded acetabular cup components. The maximum wear area (shaded in yellow) is located at the edge of the cup for the edge-loaded (a), while the maximum wear area occurs well within the cup in the non-edge loaded cups (b). 125
Figure 6-3: Boxplots showing differences in the linear wear rates of the a) femoral head and b) acetabular cup components between the two implant groups. 129
Figure 6-4: Linear wear rates of all retrieved implants are plotted against time *in vivo*. 130
Figure 7-1: A reconstructed motion analysis image of a patient with labelled retro-reflective markers placed at anatomical landmarks (Appendix 3) during a level-ground walking. A vertical red arrow represents the ground reaction force measured by the force platform of the right lower limb during a stance phase. 148

Figure 7-2: Edge of the acetabular cup coordinates was selected (red dots) on the on three non-consecutive slices using medical imaging software SliceOmatic. 155
Figure 7-3: Force paths projected on the acetabular cup viewed in the direction that is through the centre of the cup. In patient A (shown in blue), the force path does not enter the outer most radial zone (zone 1), thus no edge-loading is observed. In patient B (shown in red), the force path enters the outer most radial zone (zone 1), indicating edge-loading. The black circles (●) indicate force path at heelstrike and the black triangles (▲) indicate force path locus at toe-off. 160
Figure 7-4: Intra- and inter-observer mean differences (mm) in x- and y- coordinates is presented for pelvic markers (PM), bony landmarks (anterior superior iliac spines), and acetabular and femoral components. The error bars indicate limits of agreement (95% confidence intervals with two standard deviation of the mean difference). Abbreviations: medio-lateral (ML), antero-posterior (AP), right ASIS pelvic marker (PM1), left ASIS pelvic marker (PM2), sacrum pelvic marker (PM3), right ASIS (ASIS1), left ASIS (ASIS2), acetabular component (AC), femoral component (FC). ... 166
Figure 7-5: A schematic diagram illustrating the parameters used to calculate hip joint centre. 170
Figure 7-6: EBRA digital measurement system with the reference lines drawn in red..... 172
Figure 7-7: Distribution of zone duration during functional activities: walking (a), stair climbing (b), and rising from a chair (c). Zone 1 is defined as the edge-loading zone. The error bars represent standard errors of mean. Asterisk (*) indicates significant difference between the two MoMHRA patient groups. 176
Figure 7-8: Distribution of normalised hip joint force impulse (calculated from the area under force vs. time curve) in each zone during functional activities: walking (a), stair climbing (b), and rising from a chair (c). Zone 1 is defined as the edge-loading zone. The error bars represent standard errors of mean. Asterisk (*) indicates significant difference between the two MoMHRA patient groups. 178
Figure 7-9: Values for the acetabular cup inclination and anteversion of the hips with pseudotumours (n = 9) and the hips without pseudotumours (n = 21). The safe zone, as defined by Lewinnek *et al* [202], is outlined by the dotted rectangle. 180
Figure 7-10: Boxplots showing differences in median serum cobalt (a) and serum chromium (b) level measurements between the patient groups. The number of patient per group is denoted by *n*. 181

List of Tables

Table 2-1: Currently available hip resurfacing systems. 10
Table 2-2: Survivorship for the currently used hip resurfacing systems. 13
Table 2-3: A list of cobalt and chromium ion level studies. 22
Table 2-4: Published reports of periprosthetic soft-tissue mass in hip MoM bearings. 31
Table 3-1: Serum Co and Cr levels in healthy volunteers. 47
Table 3-2: Control tests for hip aspiration using metal needles. 48
Table 3-3: Summary of pseudotumour prevalence. 49
Table 3-4: Summary of imaging findings. 50
Table 4-1: Summary of patient group demographics. 67
Table 4-2: Incidence of positive metal reactivity (SI≥2.0) within each patient group (at 10^{-4}M). 74
Table 5-1: The relative fluorescent units (RFU) in Alamar Blue Assay. 94
Table 5-2: Live/Dead cell counts in wells 1 to 4. 95
Table 5-3: Intra-observer and inter-observer repeatability for Live/Dead cell counts. 97
Table 5-4: Summary of repeatability errors. 98
Table 6-1: Summary of retrieved implants. 119
Table 7-1: A summary of study patient groups. 146
Table 7-2: Inter-trial repeatability of the components of the peak ground reaction force, in five patients during three walking trials. 164

List of Abbreviations

MoMHRA	Metal-on-metal hip resurfacing arthroplasty
MoM	Metal-on-metal
Co	Cobalt
Cr	Chromium
CoCr	Cobalt-chromium alloy
MRI	Magnetic resonance imaging
RFU	Relative fluorescent unit
SEM	Scanning electron microscopy
PM	Pelvic markers
ML	Medio-lateral
AP	Anteroposterior
ASIS	Anterior superior iliac spine
AC	Acetabular component
FC	Femoral component
CT	Computed tomography
THA	Total hip arthroplasty
FDA	Food and Drug Administration
MoP	Metal-on-polyethylene
BHR	Birmingham Hip Resurfacing
CoC	Ceramic-on-ceramic
GF-AAS	Graphite furnace atomic absorption spectrophotometry
ICP-MS	Inductively-coupled plasma mass spectroscopy
BEI	Biological exposure indicies
DNA	Deoxyribose nucleic acid
ALVAL	Aseptic lymphocytic-dominated vascular associated lesion
LTT	Lymphocyte transformation testing
IL-1	Interleukin-1
TNF-α	Tumour necrosis factor-α
ESR	Erythrocyte sedimentation rate
CRP	C reactive protein
EDX	Energy-dispersed analysis of X-rays
FSE	Fast spin echo

STIR	Short-tau inversion recovery
SEM/EDX	Scanning electron microscopy with energy-dispersed analysis of X-rays
OHS	Oxford Hip Score
PBMC	Peripheral blood mononuclear cells
ANOVA	One-way analysis of variance
Ni	Nickel
SI	Stimulation index
αMEM	Alpha modified Eagle minimum essential medium
FBS	Foetal bovine serum
AB	Alamar Blue assay
LD	Live/Dead assay
PBS	Phosphate-buffered solution
Ethd-1	Ethidium homodimer-1
Ti	Titanium
RASIS	Right anterior superior iliac spine
LASIS	Left anterior superior iliac spine
SACR	Sacrum
HJC	Hip joint centre
PCS	Pelvis-embedded coordinate system
ICC	Intra-class correlation coefficient
EBRA	Ein Bild Roentgen Analyse digital measurement system
FE	Finite element
MW	Molecular weight

CHAPTER 1 INTRODUCTION

1.1 Overview

Metal-on-metal hip resurfacing arthroplasty (MoMHRA) has undergone a recent resurgence as an alternative treatment option for young and active patients with significant hip osteoarthritis. This is due to the proposed advantages of MoMHRA over conventional total hip arthroplasty (THA) such as bone conservation, greater implant stability, and assumed easier revision surgery [1]. According to the 2008 National Joint Registry England and Wales Annual Report [2], the total number of hip resurfacing procedures accounted for 46% (1585 of 3471) of all primary hip arthroplasty procedures performed in the patient group younger than 55 years of age**.** In Australia, hip resurfacing procedures accounted for 29% of the overall number of primary total hip arthroplasties for patients in the same age group [3]. Furthermore, the annual increase in hip resurfacing procedures in the United States has been projected to be around 100% following the recent approval by the Food and Drug Administration (FDA) of these devices in 2006 [4].

The results of published short-term survivorship studies of the current generation of metal-on-metal (MoM) hip resurfacing prostheses, with improved implant materials, design and manufacturing processes, vary between 93% and 100% at a mean of five years [5-10]. This represents a significant improvement from the previous generation of hip resurfacing prostheses [11-13]. However, the National Joint Registry data also recorded the cause of failure of MoMHRA as unexplained in 21% of revision cases [2], suggesting that the modes of failures for MoMHRA is not yet fully understood. A possible cause of

unexplained failures in the MoMHRA is an adverse biological reaction to metal wear debris.

There is a concern that metal-on-metal resurfacing implants generate up to 500 times the number of *nanometer*-sized metal particles than the number of *micrometer*-sized particles generated by metal-on-polyethylene bearings [14]. Metal nanoparticles corrode to produce either a protective passive layer on the surface or dissolve into charged free metal ions in solution [15]. Both cobalt (Co) and chromium (Cr) ions have been detected in solution during corrosion of the metal alloys used for resurfacing implants [16]. Furthermore, the published reports on patients with modern MoM bearings have uniformly shown higher levels of blood cobalt and chromium (the principal elements in the CoCr alloy used in metal-on-metal hip resurfacing implants), when compared to pre-operative values, and in comparison to the levels in patients with conventional metal-on-polyethylene (MoP) bearings [17-21].

The long-term biological consequences of exposure to these metal particles and ions remain largely unknown. As metal-on-metal hip resurfacing procedures are increasingly being used in younger active patients, with a life expectancy significantly longer than the traditional elderly THA patients, there are now heightened concerns over the unknown risks of long-term exposure to metal debris. Adverse biological responses to metal particles and ions can be local or systemic. Potential systemic adverse biological effects, such as risk of cancer and hypersensitivity reactions, are being studied and debated [22-25]. There is also concern about chromosomal aberrations and trans-placental passage of

elevated metal ions to the next generation [26-28]. Although the available data on risk of cancer associated with total joint arthroplasty does not support a causal link, there are limitations of drawing such conclusions based on these studies containing a small number of patients and a relatively short follow up period [29, 30].

One of the local adverse biological responses is the occurrence of periprosthetic soft-tissue masses, with anecdotal evidence of association with either metallosis or elevated levels of blood metal, in patients with MoMHRA. Soft-tissue masses, with or without cystic elements, following MoM hip implants are increasingly being reported in the literature [31-38]. In addition, the reports of these soft-tissue masses are emerging from a number of orthopaedic centres across the United Kingdom [39-41]. Therefore, this is a growing concern for orthopaedic surgeons performing MoMHRA. As it was often difficult to distinguish morphologically from a necrotic tumour, the term 'pseudotumour' has been used to describe these periprosthetic soft–tissue masses around MoMHRA [42]. The term is controversial and the soft-tissue masses have also been described by other names such as bursae [32], cysts [34], or inflammatory masses [31]. These pseudotumours were found to be locally destructive, requiring revision surgery in a high proportion (75%) of patients. The massive local soft tissue destruction by the pseudotumour mass often requires plastic surgical reconstruction and can also cause neurovascular compromise such as femoral nerve palsy and femoral artery stenosis/fibrosis. Moreover, the outcome of revision surgery for pseudotumour is inferior to the outcome of other MoMHRA revisions as well as to the outcome of matched primary THA [43]. Histologically, pseudotumour was characterized by the presence of T-

lymphocytes and macrophages where extensive necrosis was noted. Metallic wear particles in the soft tissue specimens were identified in most cases. The anecdotal evidence of elevated serum cobalt and chromium ion level measurements and joint fluid aspirates have been reported [37].

Despite increasing cases of pseudotumours being reported by multiple centres across the United Kingdom, definitive evidence of mechanisms involved in the occurrence of pseudotumours is lacking. This is because the currently available published information is limited to a small number of descriptive studies. There have been no published studies specifically designed to explore and delineate the potential biological reactions involved in the pathogenesis of soft tissue masses, or their potential association with the level of metal ions in patients with MoMHRA. Furthermore, additional studies are also necessary firstly to establish whether the excessive bearing surface wear occurs in MoMHRA patients with pseudotumours, and secondly to elucidate the potential wear mechanism responsible for the increased implant wear in these patients. Evidence that supports a relationship between the increased metal wear particle generation and the occurrence of an adverse local biological reaction with a high revision burden, such as pseudotumour, would highlight wear as an important factor in the potential failure of MoMHRA. Such evidence-based knowledge would be pivotal for patient selection, surgical technique and design of future hip resurfacing implants in order to ensure long-term prosthesis survivorship.

1.2 Overall Scope of the Proposed Thesis

The scope of this thesis was to determine whether an emerging clinical complication, pseudotumour, with a high revision burden results from a local biological reaction to increased wear product burden, generated by excessive MoMHRA implant wear. Thus, the broad aims of the thesis were to investigate: (1) the potential biological reactions involved in the occurrence of pseudotumours, and their potential association with the elevated levels of metal ions; and (2) the potential mechanism that leads to elevated production of metal wear debris burden in patients with MoMHRA.

1.3 Specific Objectives

The specific objectives were:

1. To establish the extent of this clinical complication (pseudotumour) by investigating its prevalence in patients with MoMHRA.
2. To explore the relationship between metal ion levels and presence of pseudotumours in patients with MoMHRA.
3. To investigate the role of systemic metal-induced hypersensitivity as a potential biological reaction mediating the occurrence of pseudotumours in patients with MoMHRA.
4. To investigate whether adverse biological reactions to large amounts of metal nanoparticles and metal ions are mediated by the local cytotoxic effects.
5. To establish whether increased MoMHRA implant bearing surface wear occurs in patients with pseudotumours.

6. To investigate edge-loading as a potential wear mechanism that leads to elevated production of metal particles and metal ion levels in MoMHRA patients with pseudotumours.

1.4 Structure of the Thesis

The thesis is presented in the following structure:

Chapter 2 presents a literature review of the current opinions and research into metal wear particles and ions as well as the available evidence of periprosthetic soft tissue pseudotumours in patients with the metal on metal hip resurfacing arthroplasty.

Chapter 3 reports a clinical study undertaken in MoMHRA patients in order to establish the prevalence of pseudotumour and explore any association between metal ion levels and pseudotumours.

Chapter 4 describes an *in vitro* clinical study of MoMHRA patients to assess systemic metal hypersensitivity in patients with pseudotumours.

Chapter 5 reports an *in vitro* experiment conducted to investigate the possible role of local metal particle-induced cytotoxicity as a potential biological reaction involved in mediating the occurrence of pseudotumours.

Chapter 6 reports an *in vitro* retrieval study conducted to measure wear of MoMHRA implants revised due to pseudotumours.

Chapter 7 describes an *in vivo* motion analysis study developed to investigate *in vivo* edge-loading as a mechanism that can lead to the increased wear in MoMHRA patients with pseudotumours.

The final chapter (Chapter 8) summarises the important results and conclusions of the studies outlined in the thesis, discusses the clinical relevance of the work presented, and finally provides recommendations for future work.

CHAPTER 2 LITERATURE REVIEW

2.1 Metal-on-Metal Hip Resurfacing

2.1.1 Evolution of Hip Resurfacing Implant Design

The original femoral hemi-resurfacing, termed mold arthroplasty, pre-dated the use of stemmed femoral components when it was introduced by Smith-Petersen in 1948 [44]. In the early 1950's, Charnley developed the first total resurfacing arthroplasty using a Teflon-on-Teflon bearing, which failed early due to the poor wear characteristics of Teflon.

The first-generation of total metal-on-polyethylene hip resurfacing, in which the large diameter femoral component articulated with thin polyethylene cups or liners, resulted in accelerated wear and production of large volumes of particulate debris [11, 13, 45]. This led to extensive osteolysis and implant loosening. Hip resurfacing was largely abandoned by the mid-1980's due to the failures of procedures performed during 1970's and early 1980's. As the mechanism for particle-induced osteolysis was yet to be elucidated at the time, the failure was attributed to avascular necrosis of the femoral head and acetabular component loosening due to high frictional torque.

The second-generation of total hip resurfacing was introduced in early 1990s after the renaissance of metal-on-metal articulation for THA with the development of the Metasul (Sulzer Inc. Winterthur, Switzerland) bearing. Metasul was a high-carbon (>0.2%)

containing, wrought cobalt-chromium (CoCr) alloy with excellent wear characteristics [46]. The Wagner system, implanted in a small number of patients, was cementless, with both components consisting of a titanium alloy and a Metasul articulation [45]. McMinn's initial hip resurfacing system was based on a cast high carbon CoCr alloy. The cementless system resulted in early failure of the initial implants due to aseptic loosening of both components. A cemented version with the smooth finish of the backside had early acetabular loosening due to cement-cup debonding.

2.1.2 Contemporary Design

Based on the lessons learned from the history of resurfacing and metal-on-metal bearing, the contemporary third-generation hip resurfacing systems are characterised by the use of CoCr alloy with high carbon content (> 0.2%) for the bearing couple, with cementless fixation for the acetabular component, and cemented fixation for the femoral component. In 1997, McMinn introduced the Birmingham Hip Resurfacing (Midland Medical Technologies, Birmingham, UK) which was machined from 'as cast' CoCr alloy in accordance with British Standard 7252 part 4, with 5% carbide content (Figure 2-1). In the same year in the US, Amstutz introduced the Conserve Plus (Wright Medical Technology, Arlington, Tennessee). All components were made of cast cobalt-chromium alloy that were heat treated and solution annealed. The acetabular component had sintered beads ranging from 50 to 150 μm in diameter for cementless press-fit fixation. The contemporary MoMHRA systems currently available are summarized in Table 2-1.



Figure 2-1: The Birmingham Hip Resurfacing (BHR) system.

Table 2-1: Currently available hip resurfacing systems.

System	Introduced	Process	Heat Treatment	Acetabular Shape	Acetabular Surface	Acetabular Thickness (mm)	Cement Mantle (mm)	Femoral Stem
Conserve Plus	1996	Cast	HIP, SHT	Truncated hemisphere	Sintered CoCr beads ± HA	3.5 or 5	1	± Load bearing
Birmingham	1996	Cast	None	Hemisphere	CoCr bead cast-in + HA	3 (rim)	0	Not defined
Cormet	1997	Cast	HIP, SHT	Equatorial expansion	Ti-VPS + HA	6 (dome)	0	Not defined
Durom	2001	Wrought	NA	Truncated hemisphere	Ti-VPS	3 and 4 (2 cups per head)	1	Non-load bearing
ASR	2003	Cast	HIP	Truncated hemisphere	Sintered CoCo beads + HA	4	0.5	Non-load bearing
ReCap	2004	Cast	None	Hemisphere	Ti-VPS ± HA	5 - 6	0.5	Not defined
Icon	2004	Cast	None	Hemisphere	CoCr cast in + HA	Not defined	0	Not defined

HIP: Hot Isostatically Pressed
SHT: Solution Heat Treated
Ti-VPS: Titanium Vacuum Plasma Sprayed
NA: Non-Applicable
HA: Hydroxyapatite

2.1.3 Implant Survivorship

In the orthopaedic literature, implant survival analysis is used to report the long term results of a series of joint prostheses such as MoMHRA and to compare the results of different prostheses. Survival analysis is a statistical technique that is used to determine the survival rate or failure rate [47], but often does not provide information about outcome or quality. For the analysis, it is assumed that all patients received their operation at the same time. The chance of the implant surviving for a particular length of time is then calculated [48]. Any definition of failure can be used, although revision is usually considered to be the end point. Defining revision surgery as a failure can often overestimate the success of an implant because it does not assess pain or function unless they are included in the definition of failure. However, revision due to any cause is still regarded as a valid final end-point in joint replacement analysis and remains the most commonly used end point in reporting MoMHRA. The methods of survival analysis used to report MoMHRA survivorship include the product limit method described by Kaplan and Meier and life-time table [48]. The life-time table provides more detailed information such as the number of joints followed, the number of failures and the number lost to follow-up.

The results of published short-term survivorship studies of the current generation of MoM hip resurfacing prostheses, with improved implant materials, design and manufacturing process, vary between 93% to 100% (Table 2-2). This represents a significant improvement from the earlier generation of hip resurfacing prostheses. Treacy *et al* [9] reported a 98% survivorship of Birmingham Hip Resurfacing (BHR) at five

years. A recent independent study by Steffen *et al* [8] reported a survival analysis of 610 BHRs implanted with a minimum follow-up of 2 years and a review of patients five years post-operatively. The survivorship was 95% at 5 years. Another independent prospective review of 230 BHRs by Hing *et al* [6] reported a 98% survivorship at a mean of 5 years. Amstutz *et al* compared the outcome of Conserve Plus implants in patients younger than 50 years of age to those patients 50 years and older [5]. The study found no differences in survivorship and post-operative clinical scores between the two groups. Despite the satisfactory short-term implant survivorship, however, the National Joint Registry data also recorded the cause of failure of MoMHRA as "unexplained" in 21% of failed cases, more than treble that found in traditional total hip arthroplasty (THA) [2]. This suggests that the mechanism of MoMHRA failures is not yet fully understood. This may be related to the long-term biological consequences of exposure to metal particles and ions generated by MoMHRA.

Table 2-2: Survivorship for the currently used hip resurfacing systems.

Study	*Prosthesis*	*Age at surgery (years, range)*	*Number of Hips*	*Follow-up (years, range)*	*Survivorship for revision*
Steffen 2008 [8]	BHR	51 (16-81)	610	4.2 (2-7.6)	95%
Hing 2007 [6]	BHR	52 (18-82)	230	5 (4-6)	98%
Amstutz 2007 [5]	Conserve Plus	41 (14-49) 57 (50-78)	350 337	5.5 (2-9)	94%
Nishii 2007 [7]	BHR	51 (19-73)	50	5.6 (5-7)	96%
Revell 2006 [49]	Corin (18) BHR (55)	43 (16-69)	73	6.1 (2-12)	93%
Mont 2006 [50]	Conserve Plus	40 44	42 42	3.4 (2-5)	94%
Shimmin 2005 [51]	BHR	Not Reported	3429	Not Reported	97%
Lilikakis 2005 [52]	Cormet 2000	51 (23-72)	70	2.3 (2- 3)	97%
Treacy 2005 [9]	BHR	52 (17-76)	144	5	98%
Grigoris 2005 [44]	Durom	48 (22-72)	200	2.2 (1-3)	100%
De Smet 2005 [53]	BHR	49 (16-75)	252	2.8 (2-5)	98%
Mont 2005 [54]	Conserve Plus	49	50	1.5 (1-2)	100%
Beaulé 2004 [55]	Conserve Plus	34 (15-40)	94	3.0 (2-5.6)	97%
Beaulé 2004 [56]	Conserve Plus	39 (16-56)	56	4.9	95%
Daniel 2004 [10]	BHR (403) McMinn (43)	48 (26-55)	446	3.3 (1-8)	99%

2.2 Metal Wear Particles & Ions

There are heightened concerns over the unknown risks of long-term exposure to metal debris generated from metal-on-metal resurfacing implants, especially as MoMHRA procedures are increasingly being performed in younger active patients. Therefore, it was important to understand the wear that occurs in MoM bearing surfaces, the characteristics of the metal wear debris particles and their metal ions generated, as well as the factors

that influence blood metal ion levels in patients following MoMHRA. These will be outlined in the following sub-sections.

2.2.1 Metal-on-Metal Articulation Wear

Wear of bearings is a progressive loss of bearing substance from the implant material. Wear is measured either as the mass of material removed from interacting surfaces per unit of time, or as the volume lost [57]. Unlike the traditional metal-on-polyethylene bearing system, which has a linear wear rate, metal-on-metal prostheses have an early high wear rate or run-in phase, followed by a low wear rate, or steady-state phase [58]. The run-in wear is thought to result from the removal of surface asperities of either the passive oxide surface layer or the substrate by abrasive (removal of softer material by harder material) and adhesive (removal of asperities by cold welding and breakage of asperities) mechanisms, or it may result from the forced conformity of the components during loading until the correction of any asphericity between head and cup [59]. The wear rates are sensitive to material parameters (carbon content, alloy processing and heat treatment), design parameters (radial clearance), and manufacturing parameters (surface roughness and sphericity) [60]. As there are significant differences in designs, materials, tolerances, and manufacturing between various metal-on-metal hip resurfacing implants available (Table 2-1), conclusions regarding wear of one implant cannot necessarily be applied to other implants.

The renewed interest in hip resurfacing follows the introduction of the MoM articulation. This was, in part, based on the observation that some of the early MoM prostheses have

survived for over 20 years, with low wear and no incidence of osteolysis [61, 62]. The reported volumetric wear from metal-on-metal bearings is significantly lower than those for metal-on-polyethylene (MoP). Based on measurements of 118 retrieved specimens of Metasul metal-on-metal bearing THA, an average annual linear wear rate of 25 μm for the whole articulation per year has been calculated for the first year [14]. The low wear measurements of retrieved components verified the findings of hip simulator studies. The wear rate decreases to 5 μm per year after the third year. This represents at least 20 times less wear than that of a standard MoP bearing. The volumetric wear was estimated to be 0.3 mm^3/year, 60-fold less than that of metal-on-polyethylene bearings measured to be 18 mm^3/year [63].

2.2.2 Metal Wear Particles

Cobalt and chromium, the principal elements in the CoCr alloy used in metal-on-metal implants, are naturally occurring essential trace metals [64], the depletion of which in the body results in physiological deficiencies syndromes. Cobalt is a cofactor in vitamin B12 and chromium is an essential cofactor in the interaction between insulin and its receptor.

Particles generated from the articular surfaces of MoM prostheses have a size range in the nanometer scale. Doorn *et al* [65] used transmission electron microscopy to visualize the wear particles generated *in vivo* following enzymatic digestion of periprosthetic tissues from around 13 revised MoM prostheses. The study has reported that the majority of the particles were round in shape, although a small proportion were needle-like in morphology. Most of the CoCr wear particles were smaller than 50 nm.

Although the wear rates in MoM bearing surfaces are lower than conventional MoP, the number of *nanometre*-sized metal particles generated is much greater than the number of *micrometer*-sized particles from MoP bearings [14]. From the volumetric wear and the average volume of a single particle, the numbers of particles produced by MoM bearing surfaces was calculated. On average, 6.7×10^{12} to 2.5×10^{14} particles are estimated to be produced per year. This is up to 500 times the number of particles produced by a metal-on-polyethylene bearing estimated to be about 5×10^{11} particles per year [65]. Thus, metal-on-metal bearings generate greater numbers of smaller diameter particles than metal-on-polyethylene implants.

2.2.3 Metal Ions

The precise details of metal ion production, transport and excretion processes, which determine the *in vivo* levels of cobalt and chromium, remain unknown. An increase in levels *in vivo* may result from an increased metal ion production either from bearing and/or modular interfaces, or impaired renal excretion.

In contrast to particulate wear debris generated in MoP and ceramic-on-ceramic (CoC) bearings, metal particles corrode to either produce a protective passive layer or dissolve into charged free metal ions in solution. As body fluid is comprised of electrolytes, metals undergo corrosion and release metal ions into its surroundings [66]. The released metal ions from the metal particles are thought to be more important than the metal particles themselves in terms of immuno-suppressive effects, as the soluble form of a

metal can circulate freely in the body [67]. The metal ions may stay bound to local tissues or may form complexes with proteins (organometallic complexes) or anions (inorganic metal oxides or salts) [68]. Cobalt II (Co^{2+}) and chromium III (Cr^{3+}) have been detected in solution during corrosion of metal alloys [23].

In a well fixed, clinically well-functioning metal-on-metal bearing couple system, metal ions may derive from a number of potential sources [15]. The majority of the metal ions are generated from the bearing surface. Thus, metal ions are released directly from the bearing surfaces as they wear by corrosion, as well as by degradation of the nanometer sized metal wear particles [69]. There are additional contributions from corrosion and fretting from modular connections in total hip arthroplasty, porous coatings of resurfacing implants, component impingement and other orthopaedic implants *in situ*. It is not possible, however, to isolate the amount of metal ions generated from the bearing surface versus the amount generated from other sources.

The rate of corrosion is not known, but will depend on the local tissue environment [69]. Germain *et al* [14], while investigating the effect of the metal particulate on cell cultures, observed *in vitro* that metal ion levels in solution increased rapidly in the first 24 hours. It has been suggested that the majority of metal particles generated corrode rapidly and thus the circulating metal ion levels reflect the rate of metal wear particle debris.

2.2.4 Metal Excretion

Unlike the majority of organic chemicals, metals cannot be eliminated from tissues by metabolic degradation. Thus, the metals can only be eliminated from tissues by renal or gastrointestinal excretion [69]. As these metals are essential trace elements in the body, there are effective renal clearance mechanisms. Cobalt and chromium are excreted by the kidneys, with negligible amounts lost through sweat and stools. The loss of renal function leads to an increase in serum metal ion levels [70].

Potential adverse effects on kidney function due to Co and Cr wear in MoM bearings have been reported. Daniel *et al* investigated whether the renal excretion threshold is exceeded at higher metal levels in an animal model [71]. There was no evidence of a cumulative build-up even at high levels of metal generation. Marker *et al* [72] investigated serum metal ion levels and creatinine clearance at the 10-year follow-up in 75 patients with MoM THA. The serum creatinine clearance was in the normal range for all patients. The study cohort included 7 patients with bilateral THA, whose creatinine clearance did not differ from the values of patients with unilateral THA. A similar result was reported by Daniel *et al* [73] who found there was no evidence of elevation of the early markers of nephrotoxicity in patients with BHR after 10 years [74].

2.2.5 Metal Ion Levels *In Vivo*

2.2.5.1 Measurement Methods

In measuring trace metals with concentrations in the part-per-billion range, the risk of contamination is a major technical challenge. Adherence to stringent protocols is required from specimen collection to sample introduction into the furnace or plasma [75]. The venepuncture needs to be performed with needles, syringes, and tubes that have been verified to be free of trace metal contamination at the part per billion level. A plastic needle instead of a metal needle is preferred for venepuncture. Contamination with a metal needle should be minimised by flushing the collection system with the initial 5 millilitres (ml) of blood. Specimens need to be stored and processed in plastic vessels verified to be contamination-free by appropriate testing.

The matrices that can be analysed include whole blood, serum, erythrocytes, urine and solid tissues. Spot urine samples tend to yield variable metal concentrations due to variations in hydration that occur throughout the day. Although there is a good correlation between blood and a 24-hour urine sample, the latter is more difficult to obtain, with a higher likelihood of contamination by the patient. Thus, blood sample analysis is usually reported in the literature.

In blood, metal ions are transported both in the plasma and within the blood cells. Some metals, particularly chromium which tends to concentrate within erythrocytes, may not be in dynamic equilibrium with extracellular chromium [76]. For this reason, serum analysis

may underestimate the metal levels. However, blood analysis that includes cells (whole blood or erythrocytes) requires a matrix digestion protocol to improve the recovery of the metal. This may predispose to introduction of contaminants and interference from the large iron storage within the erythrocytes. In a consensus statement on metal ions in metal-on-metal hip arthroplasties, MacDonald *et al* [75] recommended, due to the relative ease of analysis, that all futures studies report on the metals in serum for comparison purposes.

The use of inductively coupled-plasma mass spectroscopy (ICP-MS) improves the detection limits compared to graphite furnace atomic absorption spectrophotometry (GF-AAS) [75]. This is important because cobalt and chromium are normally present in body fluids and tissues in trace amounts that may be at below or slightly higher than the detection limits. The high temperature of an inductively coupled argon plasma ion source, in the range of 7,000 K to 10,000 K, breaks the sample components into primarily charged atomic ions that are detected by the mass spectrometer. The ICP-MS technique allows multi-element determinations, which improves throughput and reduces the amount of sample required. High-resolution ICP-MS overcomes the interference caused by the complex matrix in whole blood [77].

2.2.5.2 Metal Ion Levels in General Population

The reference values for normal control subjects, based on analysis methods using ICP-MS in 59 normal control subjects, have been established [78]; these were serum cobalt levels <0.15 μg/l with a limit of detection of 0.02 μg/l and serum chromium levels <0.26

μg/L with the detection limit of 0.01 μg/l. The biological exposure indices (BEI), published by the American Conference of Government Industrial Hygienists, generally indicate a metal ion concentration below which nearly all workers should not experience adverse health effects [75]. The indices are guidelines that are used by industry for workers in trades such as stainless steel welding operations. They correspond to the uptake levels expected in workers exposed to cobalt and chromium in the workplace, most commonly through air-borne exposure. However, they do not necessarily correlate to an increased risk of adverse outcomes. The recommended maximum BEI for cobalt in blood, at the end of the work week, is 1 μg/l.

2.2.5.3 Metal Ion Levels Following MoM Hip Arthroplasty

The published reports on the modern MoM bearings have uniformly shown higher serum Co and Cr levels when compared to pre-operative values, and in comparison to the levels in patients with conventional MoP [16-20]. The serum Co and Cr levels have been prospectively monitored following implantation of BHR prostheses [17, 79]. The peak serum levels of Co (2.4 μg/l; 10-fold increase) and Cr (4.0 μg/l; 16-fold increase) occurred at 6 and 9 months respectively, compared to the pre-operative levels. These peaks were followed by a gradual decline during the next 15 months. A list of the literature review of the cobalt and chromium ion levels studies is presented in Table 2-3.

Table 2-3: A list of cobalt and chromium ion level studies.

Study	***Samples***	***Implant***	***Number of cases***	***Analysis***	***Follow-up (years)***
Marker 2007 [72]	Serum	MoM THA[1]	75	GF-AAS[2]	10
Vendittoli 2007 [80]	Whole blood, Serum, Erythrocyte	Durom HRA[3]	45	ICP-MS[4]	2
Rasquinha 2006 [81]	Serum	MoM THA	10	GF-AAS	5
Hart 2006 [82]	Whole blood	BHR[5] Durom HRA	32 2	ICP-MS	2
Back 2005 [83]	Serum	BHR	16	ICP-MS (Co), GF-AAS (Cr)	2
Heisel 2005 [84]	Serum Urine (Cr)	MoM THA Conserve Plus	4 4	GF-AAS	1
Brodner 2004 [85]	Serum	MoM THA	60	GF-AAS	3 - 5
Brodner 2004 [86]	Serum & umbilical cord serum	MoM THA	3	GF-AAS	2 - 5
Ladon 2004 [27]	Whole blood	MoM THA	95	ICP-MS	2
Clarke 2003 [19]	Serum	MoM THA BHR Conserve Plus	22 16 6	ICP-MS	1
MacDonald 2003 [20]	Erythrocytes	MoM THA MoP[6] THA	22 18	ICP-MS	2
Brodner 2003 [18]	Serum	MoM THA CoP[7] THA	36 37	GF-AAS	5
Lhotka 2003 [87]	Whole blood	MoM THA	259	GF-AAS	4
Savarino 2002 [21]	Serum	MoM THA MoP	26 15	GF-AAS	3
Jacobs 1998 [64]	Serum, Urine (Cr)	MoP THA	25	GF-AAS	3
Jacobs 1996 [88]	Serum, Urine	MoM THA McMinn HRA	8	GF-AAS	25
Coleman 1973 [89]	Whole Blood	Cast alloy THA	16	Neutron activation	1

[1] Total Hip Arthroplasty (THA)
[2] Atomic-absorption spectrophotometry (AAS)
[3] Hip resurfacing arthroplasty (HRA)
[4] Inductively coupled plasma mass spectrometry (ICP-MS)
[5] Brimingham hip resurfacing (BHR)
[6] Metal-on-Polyethylene (MoP)
[7] Ceramic-on-Polyethylene (CoP)

There is recent evidence to suggest that Co and Cr levels are influenced by factors such as the type of MoM implant, implant design, and positioning of the implant. However, it is often difficult to compare these studies due to variations in the study design, the sources of the samples (serum, whole blood, erythrocyte and urine), the methods of laboratory analysis techniques used, and the various types of combination of implants [90].

The effect of the diameter of MoM bearings on metal levels remains controversial. For instance, a significantly greater increase in Co and Cr levels in patients with MoM hip resurfacing (mean diameter 48 mm, range 38-54 mm) in comparison to the patients with 28 mm MoM THA has been demonstrated [19]. On the contrary, a more recent study found no significant difference in Co and Cr levels between the resurfacing group (50 mm or 54 mm diameter) and 28 mm diameter MoM THA group [91]. A comparison of these study results is limited due to the different sources of samples that have been used to measure Co and Cr levels. Serum analysis was used in one study while the whole blood levels were measured in the other study. Furthermore, implant design variables between the different types of MoM hip resurfacing arthroplasties and MoM THA investigated in each study may have influenced the Co and Cr levels.

Metal ion levels have been demonstrated to be influenced by specific MoM resurfacing implant design systems. Vendittoli *et al* [80] measured the whole blood Co and Cr ion concentrations in patients with Durom hip resurfacing system (Zimmer, Winterthur, Switzerland), which has a high carbon-content, wrought MoM resurfacing hip

arthroplasty design. The authors reported lower mean serum Co and Cr levels in patients with this implant in comparison with other hip resurfacing arthroplasty prostheses.

In addition to the design and the diameter of the MoM bearings, the implant position, which is significantly influenced by the technical skill of the surgeon implanting the prosthesis, may also play a role in the extent of metal ion release. The effect of the acetabular component abduction angle on the serum metal levels has been investigated. Elevated serum and joint fluid levels of chromium and cobalt ions have been measured with steep acetabular component positioning in MoMHRA patients [85, 92, 93].

2.2.5.4 Serum Metal Ion Level as a Marker for Wear

Metal concentration analysis is a powerful research tool in the evaluation of MoM hip arthroplasty systems [94]. As it is not possible to measure wear of bearing couples radiographically in metal-on-metal hip systems, blood concentrations of metal ions have been considered as potential surrogate markers of bearing surface wear. This assumption is supported by wear measurements of retrieved components [14] and rapid corrosion of metal particles *in vitro* [16].

More recently, the wear measurements of retrieved femoral components were correlated with serum metal ion measurements. The serum metal ion concentrations were significantly correlated with the measured femoral component linear wear (measurement of the maximum depth of the wear scar) in 26 patients undergoing revision surgery [95].

Patients with metallosis had significantly higher metal ion concentrations and significantly greater amounts of femoral component wear. It has been suggested that serum metal levels can be used to both estimate wear and as a diagnostic tool. The authors reported that serum levels greater than 17 μg/l for chromium and 19 μg/l for cobalt were more likely to be associated with metallosis and recommended consideration for early revision surgery.

2.3 Systemic Adverse Consequences of Serum Metal Ions

Adverse biological responses to metal particles and ions can be local or systemic. Systemic adverse biological effects of elevated metal particles and ion levels are poorly defined. However, they have been associated with chromosomal aberrations, risk of carcinogenesis [22, 23, 27, 30], and hypersensitivity reactions [25] in patients. There is also concern about passing chromosomal problems to the next generation [26, 28].

2.3.1 Chromosomal Abnormality

There is an increasing body of evidence to suggest that metal ions can lead to the generation of free radicals: reactive oxygen species and reactive nitrogen species, which can, in turn, cause cellular dysfunction. Free radicals can react with DNA (nuclear and mitochondrial), and induce damage to purine and pyrimidine bases as well as to the deoxyribose backbone [96]. They can also induce DNA cross-links [97, 98]. Ladon *et al* investigated changes in metal ion levels and chromosome aberrations in patients within two years of receiving MoM hip arthroplasties [27]. The authors noted a statistically significant increase in both chromosome translocations and aneuploidy in peripheral

blood lymphocytes at 6, 12 and 24 months post surgery. The authors also noted that these changes were progressive with time. The change in aneuploidy was greater than chromosomal translocations. However, the authors did not find any statistically significant correlations between chromosomal translocation indices and Co or Cr concentrations in whole blood. Permanent modification of genetic material may represent the first step involved in carcinogenesis.

2.3.2 Carcinogenesis

There is an on-going concern that MoM total hip arthroplasty may be associated with an increased cancer risk due to an increased exposure to metal particles or ions. The carcinogenic potential of cobalt and chromium wear particles have been demonstrated in animal models [99]. However, the results from an epidemiological study assessing the relative risk of cancer following MoM THA demonstrated that there is no apparent increased risk [100]. Although the available data on the cancer risk associated with total joint arthroplasty does not support a causal link, there are limitations of drawing such a conclusion based on these studies with a small number of patients and short follow up period [29, 30]. The long-term follow-up is important because the latency of known carcinogens, such as tobacco, asbestos, and ionizing radiation, is several decades. Therefore, future studies of large patient populations adjusted for comorbidities, with focus on patients who had surgeries more than ten years ago, are required in order to define the relationship between MoM joint arthroplasty and cancer.

2.3.3 Teratogenicity

As MoMHRA procedures are being increasingly performed in young patients, including females of child bearing age, there is a concern that mutagenic or teratogenic effects could manifest in children conceived. Brodner *et al* [26] analysed umbilical cord serum and corresponding maternal serum of three women with metal-on-metal total hip arthroplasty. The cobalt and chromium levels in the cord serum were below the detection limit of the graphite furnace atomic absorption spectrometry. The authors reported that there was no evidence of a passage of metal ions across the placenta at the time of surgery. This finding was recently contradicted by Ziaee *et al* [28], who measured maternal and cord blood using the high-resolution ICP-MS. This study found that the cord blood levels of cobalt and chromium were 60% and 29% respectively of the mean maternal blood levels in patients with hip resurfacing. There was also a free-passage of metal ions across the placenta in the control group (mothers without metal devices). This was thought to suggest that these essential trace elements are needed by the developing foetus. Although it is possible that the placenta exerts a modulatory effect on the rate of metal transfer to provide a constant level to the foetus, there is currently no consensus on this issue.

2.3.4 Metal Hypersensitivity

The prevalence of metal sensitivity among patients with a well-functioning implant is approximately 25%, twice that of the general population [101]. Nickel is the most common metal sensitiser in humans followed by cobalt and chromium, and cross reactivity between nickel and cobalt is common. The average prevalence of metal

sensitivity among patients with a failed or poorly functioning implant is 60% [101]. However, this association does not prove a causal relationship. It is not known whether these patients are sensitive because the implants have failed or whether the implants failed because the patient had a pre-existing metal sensitivity.

Adverse metal sensitivity reactions in patients with MoM THA have been reported since its introduction in 1970's [102, 103]. There is recent evidence from retrieval studies that metal particles induce an acquired or antigen-specific immune response, type IV delayed hypersensitivity reaction driven by T-lymphocytes. This type of hypersensitivity reaction is generally associated with responses to intracellular pathogens and autoimmune diseases [25, 104]. In this type of hypersensitivity reaction, T-lymphocytes are responsible for sustaining the chronic inflammatory response, and for providing a mechanism for memory of the specific antigen [101]. This involves a specific antigen, co-stimulatory molecules, an antigen presenting cell and T-lymphocytes. Activated T-lymphocytes slow their rate of migration, begin to proliferate, and release various cytokines, which result in accumulation and activation of macrophages [105]. Macrophages can act as antigen presenting cells. The periprosthetic tissue analysis has shown that metal particles are contained within macrophages [104, 106, 107].

The histological examination of periprosthetic tissues, from failed MoM THA implants due to pain, revealed chronic inflammatory cells located perivascularly or as lymphocyte follicles, often with extensive necrosis, suggestive of cell-mediated delayed type hypersensitivity reaction. This has been described as aseptic lymphocytic-dominated

vascular associated lesion (ALVAL) [25]. The metal-protein complexes are considered to be candidate antigens for eliciting hypersensitivity responses. The metal-protein complexes produced from degradation of metal alloys have been shown to be immunologically active *in vitro* [101].

The role of metal-induced delayed hypersensitivity reaction in pathogenesis of poor implant performance such as aseptic osteolysis has been investigated by Hallab *et al* [108]. These authors measured the lymphocyte responses to implant metals. Lymphocyte proliferation, measured using lymphocyte transformation testing (LTT), and cytokine release were used as quantitative reactivity measurements. THA subjects were greater than three-fold more reactive to Cr than were controls or osteoarthritis subjects. THA subjects with osteolysis were more reactive to Co (43% vs. 0% incidence). This is consistent with the clinical reports of metal sensitivity related failures of modern MoM THA, including cases associated with osteolysis. Periprosthetic osteolysis was observed in 7 out of 19 metal-on-metal hip implants revised for pain and swelling [25]. Park *et al* [109] reported 6% (10/169) incidence of periprosthetic osteolysis at 27 months following second generation MoM THA. The osteolysis was confined to the greater trochanter. A significantly higher rate of hypersensitivity reactions to cobalt chloride skin testing was observed in patients with osteolysis compared to controls without osteolysis, implicating a delayed type hypersensitivity reaction. The histological examination showed a perivascular accumulation of T-lymphocytes. The immunohistochemical analysis demonstrated elevated levels of bone-resorbing cytokines such as IL-1 and TNF-α produced by infiltrating lymphocytes and activated macrophages. Although a causal

relationship could not be established from the study, the findings suggested that early osteolysis is associated with abnormalities consistent with delayed-type hypersensitivity to metal.

However, the relationship between these metal sensitivity histological features and MoM implant failure has not been fully established. This is due to the fact that ALVAL-like features have been observed in patients with no clinical symptoms of metal allergy and in retrieval studies of failure from mechanical causes [110, 111] and from pain for other reasons [112].

2.4 Local Adverse Periprosthetic Soft Tissue Masses

One of the local adverse biological responses is the occurrence of periprosthetic soft-tissue masses, with anecdotal evidence of association with either metallosis or elevated levels of blood metal, in patients with MoMHRA. These represent a class of complication that has recently been causing a growing concern for orthopaedic surgeons. Periprosthetic soft-tissue masses are being increasingly reported in the literature [31-38]. A review of the published cases in the literature is presented in Table 2-4. Furthermore, the reports of these soft-tissue masses are emerging from a number of orthopaedic centres across the United Kingdom [39-41]. Clinically, patients often presented with a mass that resembled a neoplasm and caused a diagnostic challenge. In addition, the initial biopsy of these cases was difficult to distinguish morphologically from a necrotic tumour. Based on these observations, these soft–tissue masses were termed ‘pseudotumours’ [42]. However, the use of the term is controversial and these soft-tissue masses have also been described by

other names such as bursae [32], cysts [34], or inflammatory mass [31]. Pseudotumours were found to be locally destructive, requiring revision surgery in a high proportion (75%) of patients. Moreover, the outcome of revision surgery for pseudotumour is inferior to the outcome of other MoMHRA revisions as well as the outcome of primary THA in matched cases [43]. During revision surgery, additional plastic surgery reconstruction is often required to address the massive local soft tissue destruction by pseudotumour mass. In some cases, femoral nerve palsy and femoral artery stenosis/fibrosis requires vascular surgery to address these neurovascular compromises. Histologically, pseudotumour was characterized by the presence of T-lymphocytes and macrophages where extensive necrosis was noted. Metallic wear particles in the soft tissue specimens were identified in most cases. The serum cobalt and chromium ion level measurements (measured in six patients) and joint fluid aspirate (measured in one patient) in one study were elevated [37].

Table 2-4: Published reports of periprosthetic soft-tissue mass in hip MoM bearings.

Study	*Cases*	*Gender*	*Implant Type*	*Symptoms*	*Mass*
Hart 2009 [35]	16	Females (8) Male (7)	BHR	Pain	Cystic (lateral or posterior), Solid (iliopsoas)
Pandit 2008 [37]	20	Female	BHR (14) Conserve Plus (4) Cormet (2)	Pain, dislocation, rash, nerve palsy	Cystic (lateral or posterior), Solid (anterior around psoas)
Toms 2008 [38]	20	Females (11) Males (8)	MoM THA	Pain	Cystic (gluteal compartment)
Gruber 2007 [34]	2	Female	MoM THA (1 bilateral)	Pain, swelling	Cystic (anterior to femoral head)
Boardman 2006 [31]	1	Female	BHR	Pain, swelling	Solid (psoas tendon)

A recent study reported the presence of soft-tissue periprosthetic hip lesions in 15 (8 females and 7 males) out of 26 patients with unexplained pain following MoMHRA [35]. In another study, symptomatic soft-tissue masses were found in a series of 20 MoM resurfaced hips in 17 female patients [37]. The mass was locally highly destructive and produced various presenting symptoms including pain, rash, dislocation, femoral nerve palsy and the presence of a lump. In all cases, the white cell count was normal. The inflammatory markers ESR (Erythrocyte Sedimentation Rate) and CRP (C reactive protein) were within normal limits in the majority of cases (17/20).

Radiological imaging characteristics of pseudotumours have recently been described [33]. The study presented the magnetic resonance imaging (MRI), computed tomography (CT) and ultrasound findings from a series of pseudotumour cases. Although the soft tissue masses could be detected on ultrasound, CT or MRI, the authors recommended ultrasound as the preferred initial imaging modality as CT scans and MRI images may be degraded by metal artefact. MRI was used to assess the extent of the masses. The two main imaging abnormalities included either a cystic mass located lateral or posterior to the joint, or a predominantly solid mass located anteriorly involving the psoas bursa and muscle.

In the case-series report, fifteen patients (75%) with pseudotumours required revision surgery to a conventional hip replacement with metal-on-polyethylene, ceramic-on-polyethylene or ceramic-on-ceramic bearing couples and this led to the resolution of symptoms in most patients [37]. The precise incidence is unknown, however, the authors

estimated an incidence of 1% in the first five years post-operatively. Histologically, the pseudotumour was characterized by the presence of T-lymphocytes and granulomas containing macrophages where extensive necrosis was noted. Metallic wear particles were identified in most cases. The serum metal ion measurements, reported in the study for less than a third of the patient cohort were elevated. The authors reasonably suggested that the soft tissue mass represented either an allergic response to a normal level of metal wear particles, or a toxic effect of a very high level of particles.

The presence of similar cystic soft tissue reactions have been reported in a review of MRI findings in 19 patients (11 females and 8 males) with early post-operative pain following MoM THA prostheses (De Puy International Ltd., Leeds UK) [38]. The median postoperative time to MRI was 35 months (range 11-63 months). The soft-tissue abnormalities were of intermediate T1-weighted signal (19/20) and a high T2-weighted signal (18/20), which were consistent with fluid collection. These collections, surrounded by irregular walls, always maintained contact with the neck of the prosthesis, and extended into the gluteal compartment in 18 cases. The MRI appearances could also be consistent with periprosthetic abscess, but inflammatory markers and microscopy were normal in all cases. At the time of revision surgery, discrete peri-prosthetic soft tissue thickening, a fluid filled cavity, or a combination of these findings was present in all 15 revised hips. Corrosion and severe pitting of the femoral components was demonstrated in 8 hips. Histological examination showed necrosis in 12 cases and perivascular lymphocytic infiltration in 5 cases. The authors suggested that early post-operative pain (less than 3 years) following MoM THA may be due to an abnormal soft tissue reaction.

Isolated case reports of periprosthetic soft-tissue masses in patients with MoM hip resurfacing or MoM THA have been also reported in the literature [31, 34, 36]. A solid psoas mass containing a high concentration of metal particles following a successful BHR (Smith & Nephew, Birmingham, UK) has been described [31]. In another report, a recurrent intra-pelvic cyst caused a vascular compromise in a male patient, which occurred 14 years after McKee-Farrar total hip arthroplasty [36]. Campbell *et al* [113] reported 4 cases (3 female, 1 male) out of a 1,500 patient pool presenting with early groin pain within 3-12 months following BHR. The periprosthetic tissues revealed extensive lymphocytic infiltrates suggestive of immunological reaction. There was complete resolution of symptoms following revision surgery. In one patient with bilateral BHR implants, one side had osteolysis and the other side had an effusion.

In conclusion, pseudotumours represent an emerging complication that occurs in MoMHRA patients, recently causing a growing concern for the orthopaedic community. Pseudotumours are locally destructive, requiring revision surgery in a high proportion of cases, who also have poor outcome following revision surgery. A review of the literature demonstrated that despite increasing cases of pseudotumours being reported, the published information currently available is limited to a small number of descriptive studies with anecdotal association of elevated metal ion levels in patients with pseudotumour. There have been no published studies specifically designed to explore the potential biological reactions involved in the occurrence of soft tissue masses, or their potential association with the elevated level of metal ions in patients with MoMHRA.

Furthermore, additional studies are also necessary to establish whether the excessive bearing surface wear occurs in MoMHRA patients with pseudotumours, as well as to elucidate the potential wear mechanism responsible for implant wear in these patients. It was, therefore, justified to investigate this clinically important complication with studies designed to explore potential mechanisms involved in the occurrence of pseudotumours in order to provide evidence-based recommendations to minimise such an adverse clinical outcome in the future.

2.5 Summary

- MoMHRA is increasingly being used in young and active patients with hip osteoarthritis. Despite the satisfactory short-term implant survivorship, there are heightened concerns over the unknown risks of long-term exposure to metal wear debris particles and their metal ions.
- Adverse biological responses to the metal particles and ions can be local or systemic. The potential systemic adverse biological effects such as risk of cancer, carcinogenesis, genotoxicity, teratogenicity and hypersensitivity reactions are being studied and debated.
- Destructive local periprosthetic soft tissue masses (pseudotumours) are increasingly being reported in MoMHRA patients. These represent a class of complication that has recently been causing a growing concern for orthopaedic surgeons and patients.

- Pseudotumours are locally destructive, requiring revision surgery in a high proportion (75%) of patients. The outcome of revision surgery for pseudotumour is also inferior to the outcome of other MoMHRA revisions.
- Despite anecdotal reports of elevated metal ion levels associated with pseudotumours, there is currently no definitive evidence of potential mechanisms involved in the occurrence of such destructive soft tissue masses.
- Therefore, further studies designed to explore potential mechanisms involved in occurrence of soft tissue pseudotumours are warranted in order to provide evidence-based recommendations to minimise such an adverse clinical outcome in the future.

CHAPTER 3 PREVALENCE AND METAL ION STUDY

3.1 Introduction

Pseudotumour is an emerging complication of MoMHRA that has recently been causing a growing concern for the orthopaedic surgeons and their patients alike. A review of the literature in the previous chapter (Chapter 2) demonstrated that these pseudotumours are locally destructive, requiring revision surgery in a high proportion (75%) of patients [37]. Moreover, the outcome of revision surgery for pseudotumour is inferior to the outcome of other MoMHRA revisions as well as the outcome of primary THA in matched cases [43]. The prevalence has been estimated to be 1% [37] in a case-series study, based on the number of identified cases during the first five post-operative years. This estimation is limited by its study design and its inherent assumption that only those patients who have presented with significant or severe symptoms have pseudotumours. Furthermore, the current evidence for the elevated cobalt and chromium levels in patients with pseudotumour is limited to serum metal ion measurements in less than a third of the patient cohort reported in the same study. Thus, a clinical study designed to establish the prevalence of, and the relationship between, metal ion levels and presence of pseudotumours in patients with MoMHRA was necessary in order to assess the extent of this emerging complication and also to establish a framework for this thesis. The aims of this study were therefore firstly to accurately determine the prevalence of pseudotumours in MoMHRA patients and secondly, to measure serum metal ion levels in MoMHRA patients with and without pseudotumours.

3.2 Study Design

A cross-sectional study measures the prevalence of health outcomes in a population at a single point in time. As cross-sectional studies cannot distinguish between newly occurring and long-established conditions, they provide information about the prevalence of health-related states and conditions, rather than incidence. These studies demonstrate associations, and such information can be used to explore aetiology. Therefore, in this local Research Ethics Committee approved study (Oxford Research Ethics Committee B: 07/H0605/151), a cross-sectional study design was used to measure the prevalence of pseudotumour in patients with MoMHRA and to investigate its possible association with serum metal levels.

A bias is a systemic error that causes tendency towards erroneous results [114]. Selection bias is the preferential inclusion of subjects with certain treatment outcomes. A cross-sectional study must include representative samples of the population for valid generalisation of the findings. In order to minimize patient selection bias in this study, the patients were recruited using the following criteria:

1. Inclusion criteria: Patients who were identified from the hospital database as having had MoMHRA performed at least three years previously (1999-2004) at the Nuffield Orthopaedic Centre, Oxford were invited on an all-comer basis to participate in this study. The minimum three-year post-operative period was selected to minimise the confounding factors of higher levels of wear during the run-in period [115] and the potential effects of the soft tissue healing process following surgery.

2. Exclusion criteria: In accordance with recommendations from the Ethics Committee, patients who were identified on the database as either having previously participated or were currently participating in any other MoMHRA clinical studies were excluded from the study. No other exclusion criteria were applied.

3.3 Materials and Methods

3.3.1 MoMHRA Patient Recruitment

A total of 228 consecutive patients identified on the database met the selection criteria. Those patients were sent an invitation letter together with a patient information sheet to participate in the study. The patients had two weeks to consider their decision, during which time they could discuss any queries or concerns with the investigator. There were 170 patients who confirmed their willingness to participate by returning the signed research participant response form. Of 170 patients, 12 patients either cancelled or failed to attend the scheduled clinic appointments.

The total study group evaluated consisted of 201 MoMHRA implanted hips in 158 patients (97 male, 61 female) with a mean age of 56 years (range 33-73 years). The two main underlying diagnoses were osteoarthritis (89%), and dysplasia (7%), with the remaining 4% being avascular necrosis, slipped upper femoral epiphysis or trauma. The mean follow-up was 61 months (range 36-88 months). All surgeries were performed using the posterior approach to the hip. Resurfacing devices implanted included 128 Birmingham Hip Resurfacing (BHR), 66 Conserve Plus (Wright Medical Technology,

Memphis, USA) and 7 ReCap (Biomet, Bridgend, South Wales, UK). The component size of all resurfaced hips was recorded. A control group for the serum metal levels consisted of 20 patients (10 male, 10 female), with a mean age 68 years (range 57-80 years) who had received a hybrid metal-on-polyethylene (MoP) total hip arthroplasty using the Trilogy acetabular component (Zimmer, Warsaw, IN, USA) and Exeter femoral stem (Stryker Howmedica Osteonics, Newbury, UK) at least three years previously at the Nuffield Orthopaedic Centre, Oxford.

All patients in the study group underwent imaging studies (ultrasound, with or without magnetic resonance imaging, and plain radiographs) in order to detect the presence of pseudotumours, as well as serum metal ion measurements. In addition, the tissue specimens of pseudotumours obtained from percutaneous biopsy, when available, were examined histologically and using scanning electron microscopy with energy-dispersed analysis of X-rays (EDX) in order to determine the size and composition of metal particle aggregates seen during histological examination. The Oxford Hip Score (OHS) [116] was also used to measure the functional outcomes in these patients.

3.3.2 Imaging

Ultrasound:

The use of ultrasound scanning in the evaluation of the hip joint and its surrounding tissues as a first-line investigation tool in a wide range of musculoskeletal conditions is well established and described in the radiology literature [117-120]. Ultrasound examination, often coupled with ultrasound-guided aspiration, frequently provides

sufficient information to enable a firm diagnosis. In accordance with the recommendation from a previous radiological study (a study which characterised the imaging features of pseudotumours), ultrasound was used as the initial imaging modality in the current study [33]. Ultrasound can differentiate solid lesions from cystic lesions, and can also be used to guide biopsy and aspirations. In addition, ultrasound is not affected by metal artefacts from the MoMHRA implants.

Ultrasound images (Sonoline Antares, Siemens AG, NY, USA) were obtained with a high linear array transducer (4-12 MHz) with the assistance of an experienced musculoskeletal radiologist. The patients were positioned supine and in lateral decubitus. Standard sagittal oblique images were obtained by placing the probe parallel to the long axis of the femoral neck. The probe was placed anteriorly, posteriorly and directly lateral to the femoral neck to obtain dynamic views of these areas. The standard images stored were sagittal views along the axis of femoral neck (anteriorly and posteriorly) and coronally over the greater trochanter. Any abnormality was examined in multiple planes. The examination included the inspection of the psoas muscle. Probes of varying frequency were used depending on the size of the patient.

The ultrasound findings were documented on a proforma. In order to consistently record the ultrasound findings, the following categorical classification was devised to include the ultrasound appearance of two common hip pathological conditions (trochanteric bursa thickening and joint effusion), whose appearances are distinct from that of pseudotumours:

I: Normal appearance

II: Trochanteric bursa thickening

III: Hypoechoic abnormality conforming to the anatomy of the joint, representing either joint effusion or capsular thickening.

IV: Cystic or solid mass arising from the joint extending beyond the confines of the anatomical joint.

In accordance with the published radiological study, the type IV appearance was considered to represent abnormal periprosthetic soft tissue mass (pseudotumour) [33].

Percutaneous hip joint aspiration and/or biopsy were performed in the study patients. This invasive investigation was considered necessary in order to obtain tissue specimens for the histological analysis and to measure metal ion levels in hip aspirates. This was performed in patients with a soft-tissue mass as well as in those patients without a soft tissue mass who agreed to partake in the procedure (n=13). The hip aspiration was performed under ultrasound guidance. The core biopsy was similarly taken in cases of solid mass using a biopsy trocar.

Magnetic Resonance Imaging:

Although MRI is more accurate for detecting soft-tissue masses than ultrasound, it was not a practical method of screening a large number of patients. Therefore, in the current study, MRI was used to assess the anatomical extent of any cystic or solid masses detected on the screening ultrasound (US) scan. MRI was performed using a Siemens 1.5 Tesla system (Siemens AG, NY, USA). A standard MRI protocol, consisting of axial T1-

weighted and T2-weighted fast spin echo (FSE) and coronal T1-weighted sequences and short-tau inversion recovery (STIR) sequences, was used.

Plain Radiograph:

Standard supine anteroposterior pelvis and shoot-through lateral radiographs of the operated hips were taken to measure the acetabular cup component inclination. This was of interest in the current study as elevated serum and joint fluid levels of chromium and cobalt ions have been measured with steep acetabular component positioning in MoMHRA patients [85, 92, 93]. Therefore, the acetabular component abduction angle relative to the pelvic horizontal was measured (Picture Archiving and Communication Systems, PACS) on the anteroposterior view in all MoMHRA study patients.

3.3.3 Histology & SEM/EDX Examinations

Histological examination of soft tissue is an important component of pseudotumour analysis [37, 42]. The core needle biopsy samples were fixed in formalin and processed in a routine manner. The samples were stained with haematoxylin and eosin and other standard stains (Ziehl-Neelsen, PAS, Grocott or Giemsa staining) for histological examination. In addition, scanning electron microscopy (JSM-840F, JEOL Ltd, Tokyo, Japan) with energy-dispersed analysis of X-rays (SEM/EDX) was used to analyse the tissue specimens. The SEM/EDX is an electron probe microanalysis method that has been used extensively to characterize the size, morphology and elemental composition of submicron-sized particles [121]. The SEM/EDX was necessary in this study in order to determine the size and composition of metal particle aggregates seen during histological

examination. This involved sectioning the core biopsy specimens, which were then deparaffinised and carbon coated for 8 seconds in preparation for electron image using EDX. The operating conditions of the scanning electronic microscope were set at 15 mm working distance, 15 kV accelerating voltage. Digital secondary electron image images were taken at 200 or 2000 magnification and captured. Each tissue specimen was scanned for the presence of metal particulates.

3.3.4 Metal Ion Level Measurements

Metal ion level measurements were measured from patients' serum. In addition, percutaneous hip joint aspiration performed in a limited number of patients allowed determination of metal ion concentration localised within the pseudotumour mass or hip joint. The venous blood samples were collected in the current study in accordance with the consensus protocol described by MacDonald *et al* [75]. Venepuncture was performed using disposable Venosafe (Terumo Europe NV, Leuven, Belgium) 21-gauge stainless-steel needles. The first 5 ml of withdrawn blood was discarded to minimise contamination with a metal needle by flushing the collection system with the initial 5 ml of blood. All collected samples were placed into 6 ml vacuum tubes (Venosafe VF-106SAHL, Terumo Europe NV, Leuven, Belgium), kept at room temperature, and transported overnight. These tubes had been verified to be free of trace metal contamination at the part per billion level.

As previously outlined in Chapter 2, the matrices that can be analysed include whole blood, serum, erythrocytes, urine and solid tissues. However, blood analysis that includes

cells (whole blood or erythrocytes) requires a matrix digestion protocol to improve the recovery of the metal, during which the digestion process presents a potential source of contamination. Thus, the serum analysis for comparison purposes has been recommended [75]. As the focus of this study was to compare the metal ion levels between patient groups, the serum analysis was selected for the current study. The use of inductively-coupled plasma mass spectroscopy (ICP-MS) for serum analysis was based on the fact that it allows multi-element determinations, which reduced the amount of sample material required [75]. This was an important consideration in the current study, as there was limited volume of hip aspirate available on each patient for microbiological tests as well as metal ion level measurements.

The analysis was performed at the Laboratory of Clinical Biology, Department of Toxicology, University Hospital, Ghent, Belgium. This laboratory has a well established collaboration with the Nuffield Department of Orthopaedics, Rheumatology and Musculoskeletal Sciences in providing metal ion levels for a number of clinical studies. The laboratory has demonstrated its capacity to accurately perform multiple specimen analysis in a relatively short period of time. This was an important consideration in the current study as there were a large number of participating patients. Therefore, serum cobalt and chromium levels were analysed in a blinded fashion using ICP-MS (ELAN DRC II, PerkinElmer Life and Analytical Sciences, Shelton, CT, USA). The laboratory's quoted detection limit of cobalt and chromium in serum was 0.25 μg/l.

3.3.5 Functional Outcome Measurement

The Oxford Hip Score (OHS) was used to measure the functional outcomes of patients in this study (Appendix 1), as it is a valid and practical means of monitoring outcomes of hip replacement surgery [122]. The Oxford Hip Score is a disease specific patient self-assessed score with 12 items [123]. This was used with a 0 to 48 scale, with 48 being the best score [116].

3.3.6 Statistics

The data set was assessed for normality using the Shapiro-Wilks test. The prevalence of pseudotumours in each gender was compared using the chi-squared statistic. Inter-group comparisons of non-normally distributed serum levels of Co and Cr between the patient group with MoP THA (control group), the MoMHRA patient group without pseudotumour (non-pseudotumour group), and the MoMHRA patient group with pseudotumour (pseudotumour group) were performed using the Kruskal-Wallis non-parametric analysis of variance. Mann-Whitney tests were used to compare serum and hip aspirate metal levels, OHS values, acetabular cup inclination angle, femoral component size, and implant type between the pseudotumour and non-pseudotumour groups. Differences at $p < 0.05$ were considered to be significant. SPSS® statistical software release 13.0 (SPSS Inc. Chicago, IL, USA), was used for performing the statistical analysis.

3.4 Control Measurements

Control measurements were performed in order to verify that the sample collection techniques used in this study did not introduce metal contamination during both venous sampling and hip aspiration procedures.

3.4.1 Venous Sampling

Venous blood samples were collected using the recommended technique in five healthy volunteers (5 males, age range 25-35 years). All collected samples were placed into the Terumo Venosafe VF-106SAHL 6 ml tubes (lot 0604027), kept at room temperature, transported overnight and analysed in a blinded fashion at the laboratory. The results of the Co and Cr ion level measurements were all below the detection limits of the ICP-MS (0.25 μg/L). This is summarised in Table 3-1.

Table 3-1: Serum Co and Cr levels in healthy volunteers.

Healthy Volunteer	Co level (μg/l)	Cr level (μg/l)
1	< 0.25	< 0.25
2	< 0.25	< 0.25
3	< 0.25	< 0.25
4	< 0.25	< 0.25
5	< 0.25	< 0.25

The results were consistent with the reference values for normal control subjects: serum cobalt levels <0.15 μg/L and serum chromium levels <0.26 μg/L [78]. It was concluded that the current sample collection technique, transport and analysis methods can reliably be used to measure the serum cobalt and chromium levels in this study.

3.4.2 Hip Aspiration

The recommended non-metallic needle was not practical for hip aspiration. It was difficult to manoeuvre the plastic needle while performing hip aspiration due to its pliable nature. Therefore, metal spinal needles were tested for potential metal contaminations in a control experiment. The metal spinal needles were used to aspirate 2 ml of sterile normal saline solution. In order to simulate hip aspiration in patients, where sampling may require repeated attempts, aspiration of 2 ml of normal saline was performed up to three 'passes' through the needle before being placed into the sterile plastic collection tube. The results are summarised in Table 3-2.

Table 3-2: Control tests for hip aspiration using metal needles.

Normal Saline Aspirate	Co level (μg/l)	Cr level (μg/l)
1 Aspiration (2 ml)	< 0.25	< 0.25
2 Aspiration (4 ml)	< 0.25	< 0.25
3 Aspiration (6 ml)	< 0.25	< 0.25

All samples recorded below the detection levels for Co and Cr. Therefore, it was concluded that hip aspirations can be performed using metal spinal needles in this study without introducing significant metal contamination.

3.5 Results

3.5.1 Prevalence

Pseudotumours were found in seven patients (6 female, 1 male) from the 158 patients (97 male, 61 female) with MoMHRA. The overall prevalence of pseudotumours estimated per patient and per resurfaced hip was 4.4% (95% confidence interval (CI) 2.5% - 8.0%), and 6.5% (95% CI 3.6% - 9.8%), respectively (Table 3-3). For female patients, the overall pseudotumour prevalence was up to 10-fold higher than for male patients (9.8% vs. 1.0%) (chi-square test, p=0.04). Pseudotumours were approximately 14-fold more prevalent in the patients with bilateral MoMHRA implants (13.9%) compared to the patients with unilateral MoMHRA implants (0.9%). Pseudotumours were detected in approximately one third of female patients (30%) with bilateral resurfacing implants, far exceeding the prevalence in male bilateral patients (3.8%). This is in contrast to the prevalence in patients with unilateral MoMHRA implants, in whom the prevalence was low for both genders (0% vs. 1.5%). In four out of six bilateral MoMHRA patients (3 females, 1 male), pseudotumours were found in both hips.

Table 3-3: Summary of pseudotumour prevalence.

	All Patients			*Unilateral Arthroplasty*			*Bilateral Arthroplasty*		
	Total	Male	Female	Total	Male	Female	Total	Male	Female
Pseudotumour	7	1	6	1	0	1	6	1	5
Non-pseudotumour	151	96	55	114	71	67	37	25	12
Total Number	158	97	61	115	71	68	43	26	17
Pseudotumour Prevalence	4.4%	1.0%	9.8%	0.9%	0%	1.5%	13.9%	3.8%	29.4%

The ultrasound and MRI appearances of all masses, summarised in Table 3-4, were consistent with the characteristic imaging features previously described for pseudotumours [33]. On MRI images, the cyst walls and solid masses showed low signal intensity on T2-weighted images and STIR images, either similar to or lower than the signal of muscles. The fluid component had a high signal on T2 and low signal on T1. Solid masses in 5 hips were located at the anterior aspect of the joint in the region of the psoas bursa (Figures 3-1a & 3-1b), whereas cystic fluid collections found in 6 hips were located at the lateral or posterior aspect of the joint.

Table 3-4: Summary of imaging findings.

Patient	Gender	Hip	Diagnosis	Implant	FC Size (mm)	Location	Appearance	Dimensions* (cm)
1	Female	R	OA	BHR	46	Posterior/lateral	Cystic	2.1×1.5×2.2
		L	OA	BHR	46	Anterior	Solid	3.1×2.5×3.0
2	Female	L	OA	BHR	46	Anterior	Solid	5.6×3.3×3.2
3	Female	R	DDH	BHR	42	Anterior	Solid	3.2×2.5×1.5
		L	DDH	BHR	46	Anterior	Solid	5.1×4.5×2.5
4	Female	R	OA	BHR	46	Posterior/lateral	Solid	4.3×3.1×3.4
		L	OA	BHR	46	Anterior	Cystic	8.0×7.1×6.5
5	Female	R	OA	BHR	50	Posterior/lateral	Cystic	6.2×4.5×2.1
		L	OA	BHR	50	No Pseudotumour Detected		
6	Male	R	OA	BHR	54	Posterior/lateral	Cystic	5.5×5.3×1.8
		L	OA	BHR	50	Posterior/lateral	Cystic	3.1×3.5×1.0
7	Female	R	OA	C+	48	No Pseudotumour Detected		
		L	OA	C+	50	Posterior/lateral	Cystic	4.0×3.0×2.0

* Dimensions refer to the maximum width, height, and depth as measured on MRI.

Abbreviations: Right (R), left (L), osteoarthritis (OA), developmental dysplasia of hip (DDH), Birmingham Hip Resurfacing (BHR), Conserve Plus hip resurfacing (C+), femoral component (FC).

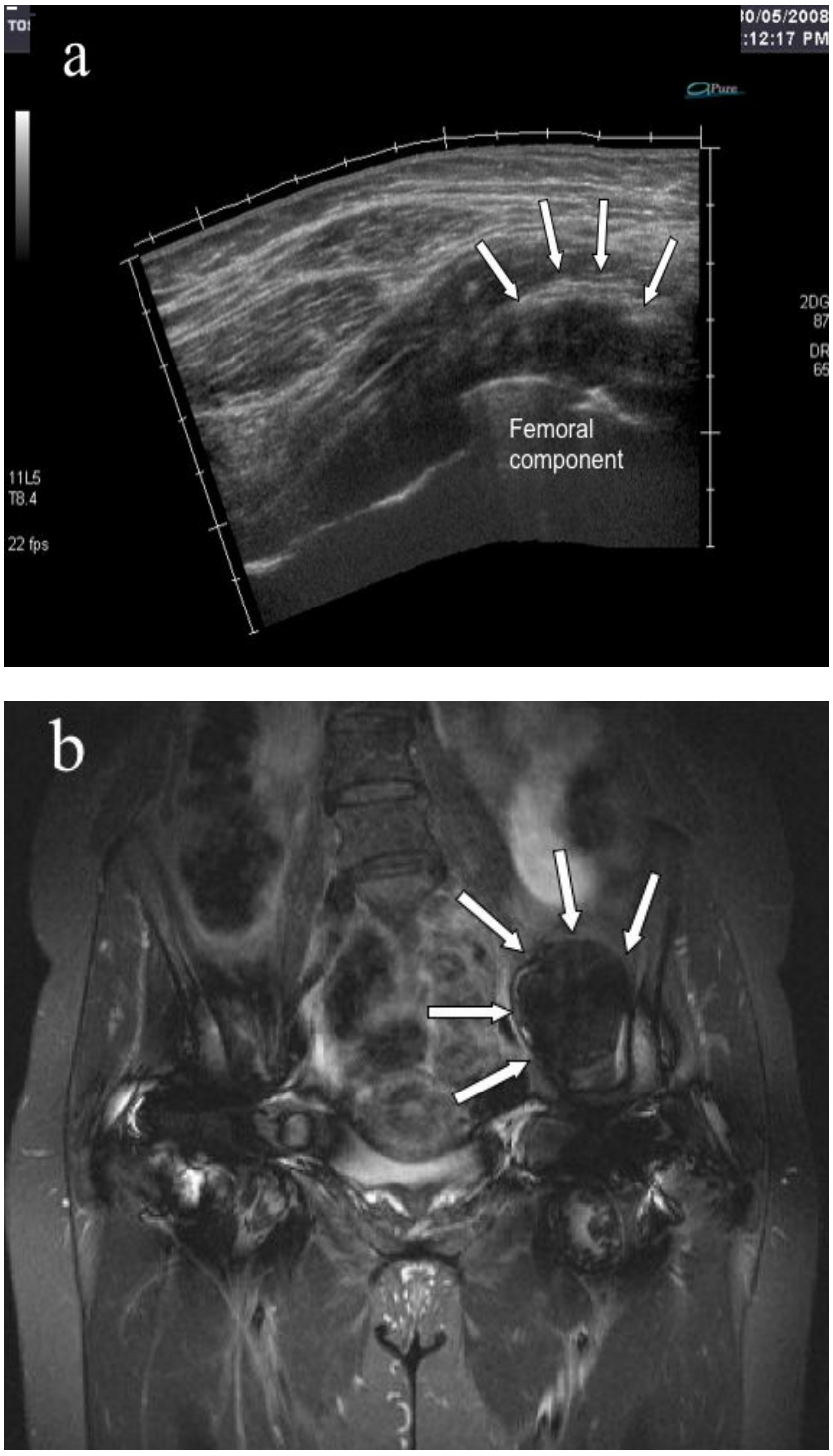


Figure 3-1: (a) Extended field of view of sagittal ultrasound image of a mass (arrows) arising from the anterior aspect of the hip joint in Case 2; (b) Coronal STIR MRI image of a predominantly solid low signal intensity mass (arrows) seen in Figure 3-1(a).

Ultrasound-guided aspiration and/or core biopsy was obtained from five out of seven patients with a soft-tissue mass. The two remaining patients declined to partake in the procedure. Hip joint aspiration was also performed in 13 MoMHRA patients without a soft tissue mass. No organisms were isolated on microbiological culture of hip aspirates and periprosthetic tissues. Histological examinations of biopsy specimens of the pseudotumour tissue showed extensive necrosis of connective tissue, in which there were scattered aggregates of metal particles within necrotic macrophages in extracellular tissue (Figure 3-2). Discrete granuloma-like collections of viable macrophages and giant cells were seen around the areas of necrosis. There was a variable diffuse lymphocytic infiltrate in the superficial and deep fibrous tissues and scattered perivascular lymphoid aggregates (Figure 3-3).

The scanning electron microscopy examination of the pseudotumour tissues identified: (1) aggregates of metal particles up to 10 μm in diameter; and (2) metal particles sized 30-60 nm in diameter, located in the extracellular tissue. Elemental analysis using scanning electron microscopy with energy-dispersed analysis of X-rays (SEM/EDX) conducted on the individual particles identified on specimen tissues confirmed the presence of both Co and Cr (Figure 3-4).

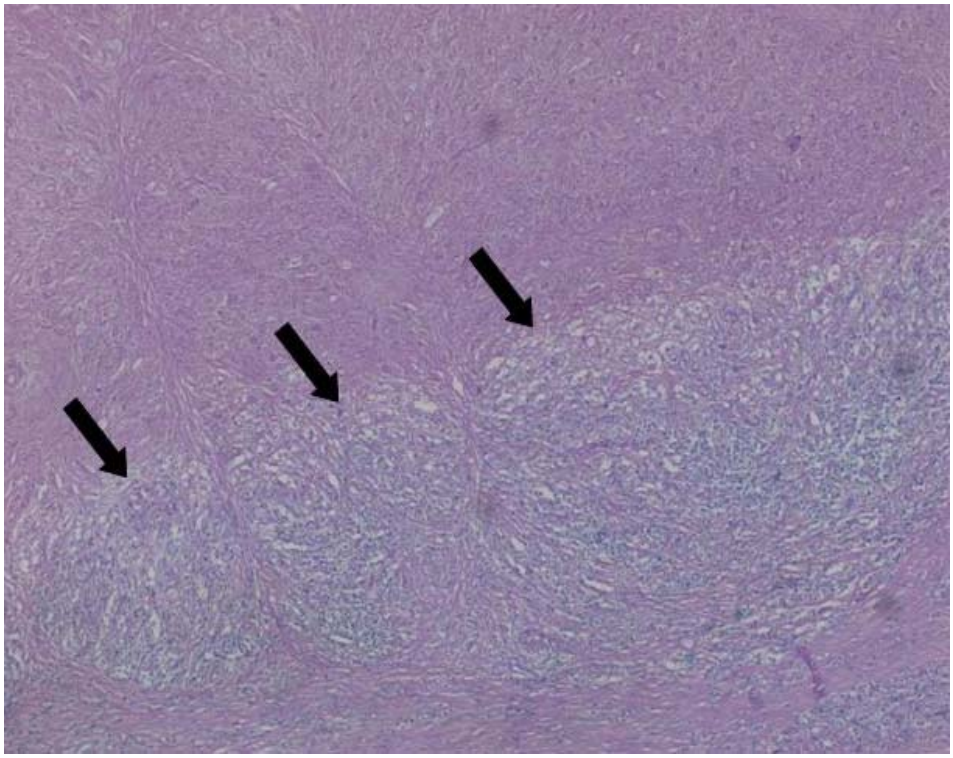


Figure 3-2: Peri-implant soft tissue showing coagulative necrosis with granulomas containing macrophages (arrows) (hematoxylin and eosin stain, magnification 100×).

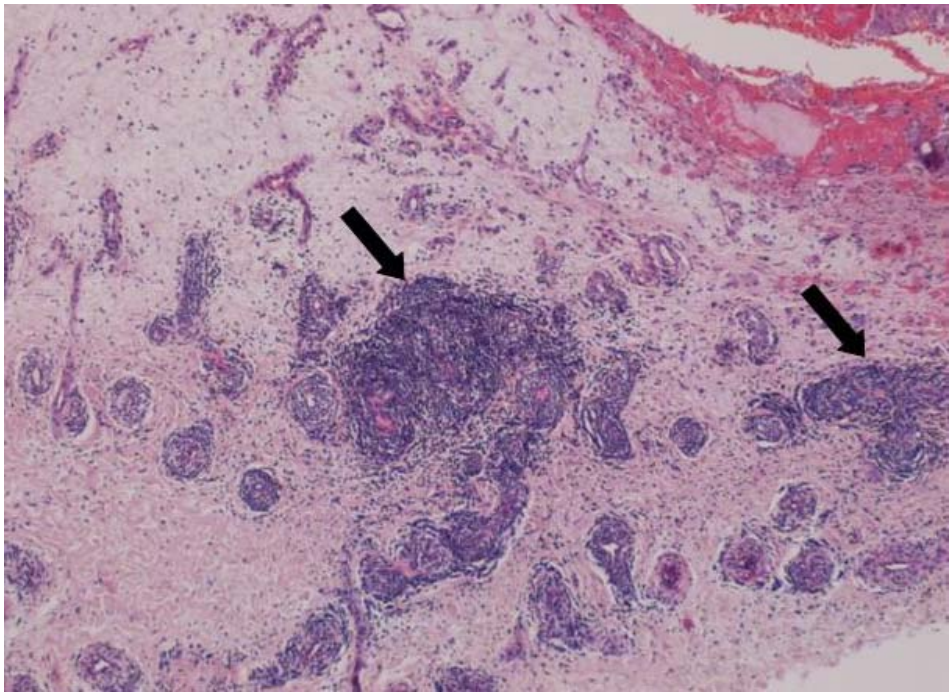


Figure 3-3: Pseudomembrane showing numerous perivascular lymphoid aggregates (arrows) and a diffuse lymphocyte infiltrate (hematoxylin and eosin stain, 100×).

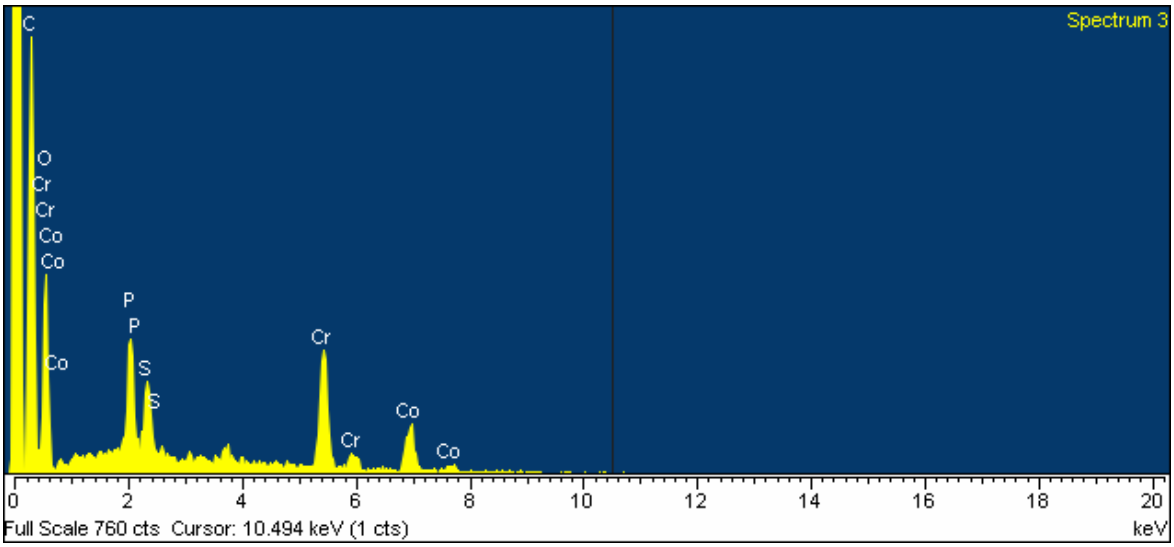


Figure 3-4: EDX spectrum obtained from metal particulate analysis, confirming the presence of cobalt (Co) and chromium (Cr).

3.5.2 Metal Ion Levels

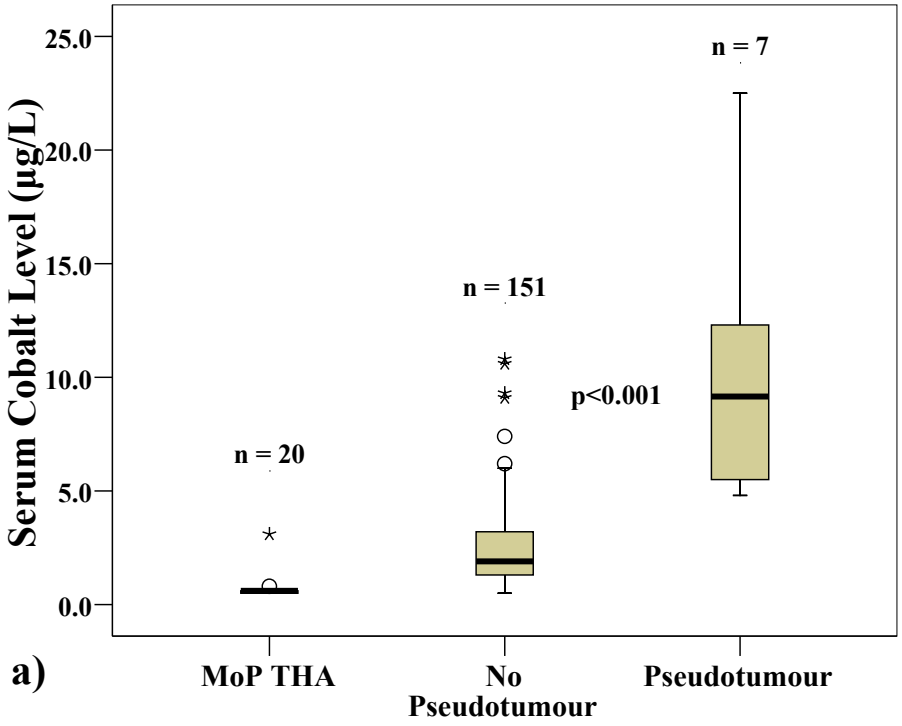
In comparison with the non-pseudotumour group and the control group with MoP THA, the pseudotumour group was associated with:

(1) significantly higher median serum cobalt levels: 9.2 µg/l (range 4.8-22.5 µg/l) vs. 1.9 µg/l (range 0.5-10.8 µg/l) vs. control group 0.6 µg/l (range 0.5-3.1 µg/l), $p<0.001$, (Figure 3-5);

(2) significantly higher median serum chromium levels: 12.0 µg/l (range 3.8-22.8 µg/l) vs. 2.1 µg/l (range 0.5-14.3 µg/l) vs. control group 0.5 µg/l (range 0.5-1.1 µg/l), $p<0.001$;

(3) significantly higher median hip aspirate cobalt levels: 1182 µg/l (range 206-1802 µg/l) vs. 86.2 µg/l (range 1.0-158 µg/l), $p=0.003$ (Figure 3-6); and

(4) significantly higher median aspirate chromium levels: 883.0 µg/l (range 221-1322 µg/l) vs. 114.8 µg/l (range 3-230 µg/l), $p=0.001$.



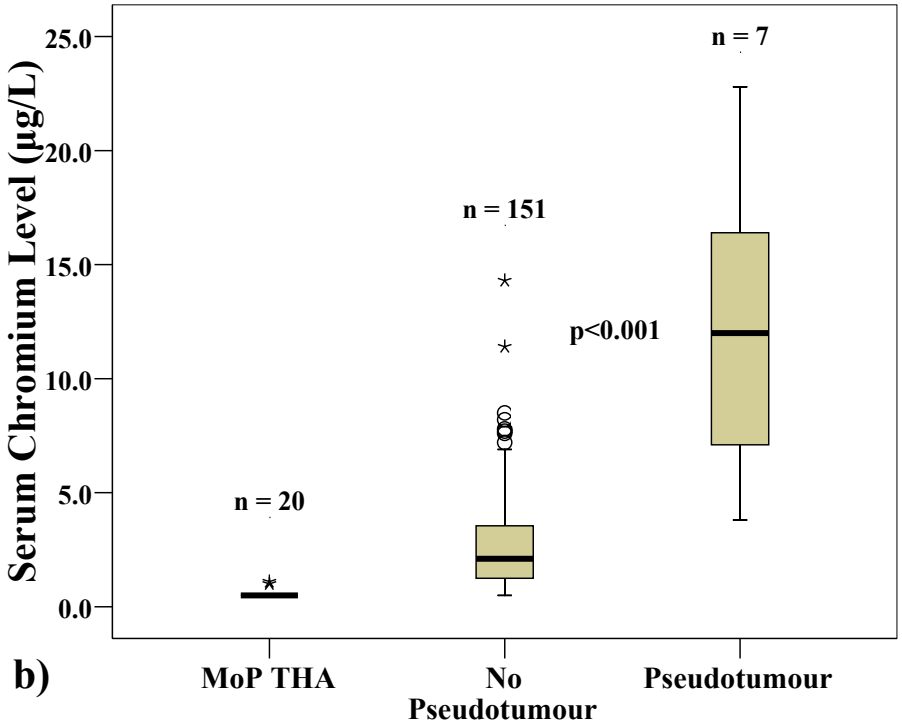


Figure 3-5: Boxplots showing differences in serum cobalt (a) and serum chromium (b) level measurements between the three patient groups. The number of patient per group is denoted by *n*.

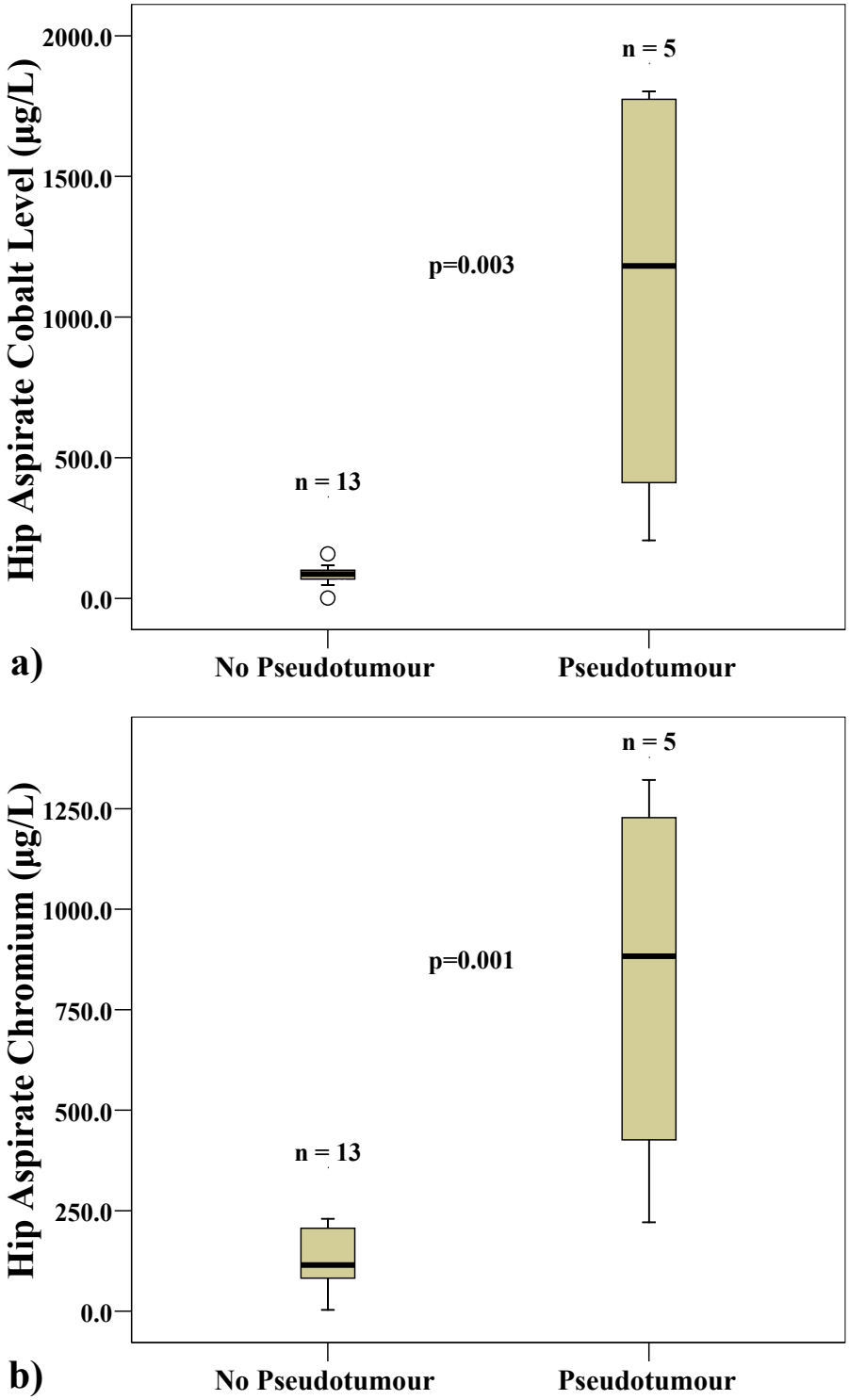


Figure 3-6: Boxplots showing differences in cobalt (a) and chromium (b) levels in hip aspirates between the two MoMHRA patient groups. The number of patient per group is denoted by *n*.

In addition, there was a high degree of linear correlation between serum and hip aspirate metal levels: Pearson's correlation coefficient (r): r = 0.841 for Co, $p < 0.001$ and r = 0.847 for Cr, $p < 0.001$ (Figure 3-7). Three out of five patients in the non-pseudotumour group with either extreme or outlier median serum Co and Cr values reported the presence of other orthopaedic metal implants *in situ* (e.g. spinal fusion and metal implants for fractures).

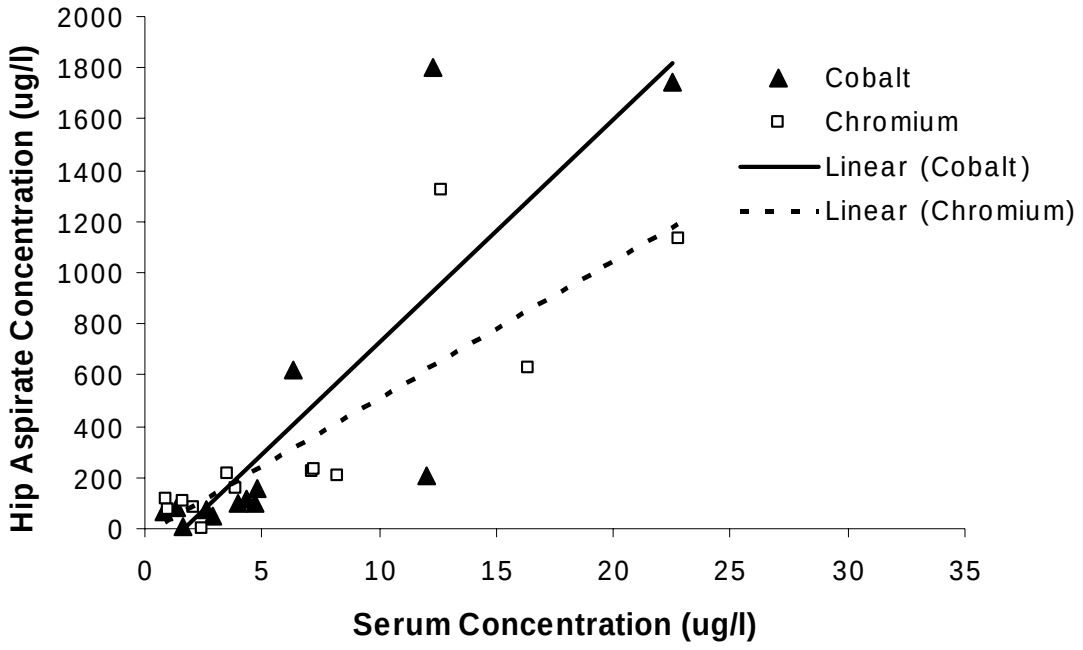


Figure 3-7: Serum cobalt and chromium concentrations correlated with hip aspirate cobalt and chromium concentrations.

The pseudotumour group reported significantly inferior OHS: 41 (range 48-32) vs. 47 (range 52-35) $p<0.001$. Although the femoral component size in the majority of hips in the pseudotumour group (7 out of 13 hips) was equal to or less than 46 mm, this was not

statistically different to the non-pseudotumour group (47 mm, 95% confidence interval 44 – 50 mm vs. 49 mm, 95% confidence interval 48 – 49 mm, p=0.11). There was no significant difference between pseudotumour and non-pseudotumour groups in terms of acetabular cup inclination angle (48.2°, 95% confidence interval 42.2°- 54.2° vs. 46.9°, 95% confidence interval 45.5°- 48.1°, p=0.51), or implant type (p=0.2). There was no radiographic evidence of component loosening or osteolysis in either group.

3.6 Discussion

The prevalence of pseudotumours has recently been estimated to be 1% [37] in a case-series study, based on number of identified cases during the first five post-operative years. This estimation is, however, limited by its study design and its inherent assumption that only those patients who have presented with significant or severe symptoms have pseudotumours. The results of the current cross-sectional study estimated that the overall prevalence of soft tissue mass in MoMHRA patients was considerably higher (4%) than the previously reported prevalence.

The current study also shows a very high (30%) prevalence of pseudotumours in females with bilateral MoMHRA implants, in whom pseudotumours were detected in both hips in two thirds of cases. A high female prevalence and the bilateral nature of the pathology, in part, would be consistent with a theory that a systemic metal-induced hypersensitivity is a dominant biological reaction involved in pseudotumours. A high incidence of exposure to jewellery in females may lead to sensitisation to metals in these patients, thereby

increasing the likelihood of eliciting delayed-type hypersensitivity reaction to metals upon the implantation of MoMHRA. The systemic nature of a hypersensitivity reaction would account for the bilateral nature of the pathology. Furthermore, a diffuse lymphocyte infiltration pattern seen on histological examinations in the current study has also been observed in the first and second generation MoM THA [25, 104, 106] as well as following MoM hip resurfacing arthroplasty [37, 38, 42]. This has been described as aseptic lymphocyte-dominated vasculitis associated lesion (ALVAL). This histological feature is thought to be a characteristic histological pattern of tissue reactions to MoM bearings and to represent a metal-induced T-lymphocyte-mediated hypersensitivity reaction of type IV (delayed-type hypersensitivity). The metal particle clusters seen on histology in the current study were confirmed to be Co and Cr particles from the SEM/EDX elemental analysis.

However, an ALVAL response was not seen histologically in all pseudotumours, whereas necrosis and a macrophage infiltrate were consistently seen. Furthermore, the prevalence of pseudotumour exceeds the prevalence of metal hypersensitivity reactions leading to an adverse clinical outcome, which are currently estimated to affect less than 1% of the patients with implants [101]. These factors suggest that another mechanism is likely to be involved. The presence of extensive necrosis and heavy macrophage infiltrate would be in keeping with a local metal-induced cytotoxic effect. Cytotoxicity may lead to a vicious cycle in which metal wear particle generation leads to macrophage recruitment, particle phagocytosis, cell death, with resultant metal particle release, leading to further macrophage recruitment, and repetition of this process.

The results of this study demonstrated that a soft tissue pseudotumour in patients with MoMHRA is associated with elevated serum and hip aspirate cobalt and chromium ion levels. Patients with a pseudotumour had up to a six-fold elevation of median serum levels and up to a twelve-fold elevation of median hip aspirate levels of Co and Cr ions in comparison to patients without pseudotumours. The median serum ion levels measured in the pseudotumour patients were up to four times higher than the peak post-operative levels reported in patients with well functioning MoMHRA [17, 79]. Potential confounding factors that may lead to elevated serum metal levels include renal impairment and Cr and Co from other sources. None of the patients in the study had renal impairment. Patients in the pseudotumour group did not report occupational exposure to metals or ingestion of health supplements containing Co and Cr. The median serum cobalt and chromium levels in female patients with bilateral arthroplasty in the pseudotumour group were 9.0 μg/l (range 4.8-22.5 μg/l) and 12.0 μg/l (range 3.8-22.8 μg/l), respectively. These metal ion levels were significantly greater than the median serum cobalt and chromium levels in female patients with bilateral arthroplasty without pseudotumour, which were 2.9 μg/l (range 0.9-6.0 μg/l, $p< 0.001$) and 3.2 μg/l (range 1.2-8.1 μg/l, $p< 0.001$), respectively. The presence of other orthopaedic metal implants *in situ* such as metal implants for fracture fixation, which may have contributed to the serum metal ion level, were present in three out of five patients in the non-pseudotumour group with either extreme or outlier median serum Co and Cr values, however, none were present in the pseudotumour group.

Recently, serum levels have been used to estimate the MoM wear, based on the positive correlation that exists between the wear measurements and the serum metal ion measurements [124]. Patients with metallosis had significantly higher metal ion concentrations and significantly greater amounts of femoral component wear. In the current study, pseudotumours were not detected in those patients who had 'normal' median serum and aspirate levels of cobalt and chromium ions as reported for well functioning MoMHRA [17, 79, 82, 125]. This suggests that pseudotumours do not occur if MoM articulations are functioning well. Therefore, it is hypothesised that pseudotumours occur in patients with contemporary MoMHRA implants when there is increased wear at the MoM articulation, as wear is positively correlated with the elevation of metal ion concentrations *in vivo*. Interestingly, the elevated Co and Cr levels in the pseudotumour group could not be attributed to the factors that have been reported to influence the serum metal ions levels such as type of implant [80], femoral component size [19, 91] or acetabular component inclination angle [85, 92, 93]. This may be due to relatively small number of pseudotumours detected in the study. This may, in part, also reflect the fact that localised high amounts of wear may occur, even in well-fixed implants without obvious radiographic evidence of malalignment, because of implant impingement. Impingement is a dynamic phenomenon which is determined by the orientation of the implant components combined with the movement patterns of the patient.

There are several limitations to this prevalence study. In order to reduce selection bias, patients were recruited on all-comer basis. However, the study group may not have been

a representative sample because patients with concerns may have preferentially agreed to participate, thereby over-estimating the prevalence. In addition, a relatively small number of pseudotumour cases have been identified. Thus, interpretation of any trend present within this patient group should be done so with caution. This was a cross sectional study, thus it cannot be used to establish a cause and effect relationship for the associations identified. Ultrasound was used as the initial imaging modality [33]. Ultrasound may have under-reported smaller soft-tissue masses. However, ultrasound was used in preference to MRI, as it was a more practical method of screening a large number of patients. Moreover, ultrasound is a well established method for detecting soft tissue masses and is not affected by artefacts from the prosthesis. MRI is arguably more sensitive for small deep lesions, but the anatomy immediately adjacent to the prosthesis is obscured by metal artefact. Thus, ultrasound scans were performed with the assistance of an experienced musculoskeletal radiologist. Serum metal ion analysis was used in this study. As some metals, particularly chromium, tend to concentrate within erythrocytes [76], serum analysis may have underestimated the metal levels. However, this study focused on the relative values between different groups rather than absolute values. Furthermore, the most appropriate blood fraction for the measurement of metal ions in patients with metal-on-metal implants remains controversial [90, 126].

In conclusion, the current study estimated the prevalence of pseudotumour to be considerably higher than previously reported, thereby justifying the case for further studies designed to explore potential mechanisms involved in the occurrence of this clinically important complication. The study also established an association between the

elevated serum and hip aspirate metal ion levels and the occurrence of an adverse local biological reaction (pseudotumour) with a high revision burden. This suggests that pseudotumour may be a biological reaction to the large amount of metal wear products generated from excessive wear *in vivo*.

The pertinent findings from the current clinical study also provide a framework for the remainder of the thesis. Further studies are therefore required to investigate potential biological reactions involved in mediating the occurrence of pseudotumours, such as systemic hypersensitivity reaction and local metal particle-induced cytotoxicity. Furthermore, a study focused on assessing the magnitude of bearing surface wear that occurs in pseudotumour patients would be required to confirm the *in vivo* findings of elevated metal ion concentrations in serum and hip aspirates in patients with pseudotumours. Lastly, it is important to investigate any potential wear mechanism responsible for the increased implant wear in these patients.

3.7 Summary

- There was 4% overall prevalence of an abnormal soft tissue mass, 'pseudotumour', in patients with MoMHRA, considerably higher than previously reported. The prevalence of pseudotumours in females was particularly high, especially in females with bilateral MoMHRA implants (30%).
- Pseudotumours were associated with elevated serum and hip aspirate levels of Co and Cr ions, the principal elements in the CoCr alloy used in MoMHRA implants.
- Pseudotumours were not detected in those patients who had 'normal' median serum and aspirate levels of cobalt and chromium ions reported in well functioning MoMHRA. This suggested that pseudotumours do not occur if MoM articulations are well functioning. Therefore, it was postulated that pseudotumours are likely to be a biological reaction to the large amount of metal debris generated *in vivo* due to excessive wear.
- Studies were required to investigate the potential biological reactions mediating the occurrence of pseudotumours: a systemic metal hypersensitivity reaction and a local metal-induced cytotoxicity. These are reported in the next two chapters.

CHAPTER 4 *IN VITRO* ASSESSMENT OF METAL HYPERSENSITIVITY

4.1 Introduction

Results of the clinical study in the previous chapter (Chapter 3) estimated a high (30%) prevalence of pseudotumours in females with bilateral MoMHRA implants, in whom pseudotumours were detected in both hips in two thirds of cases. This suggested that a systemic metal-induced hypersensitivity may be an important biological mechanism involved in pseudotumours. A high incidence of exposure to jewellery in females may lead to sensitisation to metals in these patients, thereby increasing the likelihood of eliciting delayed-type hypersensitivity reaction to metals upon the implantation of MoMHRA. The systemic nature of the hypersensitivity reaction would also account for the bilateral nature of the pathology. Furthermore, lymphocyte infiltrations seen in histological examinations were similar to the observations reported in aseptic lymphocyte vasculitis associated lesion (ALVAL) cases, which is thought to represent a systemic metal-induced T-lymphocyte-mediated hypersensitivity reaction of type IV (delayed type hypersensitivity). Hence, these findings indicated that a systemic delayed hypersensitivity reaction to nickel (Ni), a common metal sensitiser present in jewellery, and chromium or cobalt, the principal elements in the CoCr alloy used in MoMHRA implants, may play a role in the biological reactions of pseudotumours. The aim of the next study was therefore to investigate the incidence and level of systemic metal-induced hypersensitivity in MoMHRA patients with and without pseudotumours by measuring lymphocyte proliferation responses to these metals.

4.2 The Null Hypothesis

H_0: There is no difference in the lymphocyte proliferative responses, as measured by the lymphocyte transformation tests, between MoMHRA patients with pseudotumours and MoMHRA patients without pseudotumours.

4.3 Study Design

A case-control study compares subjects with a specified outcome (the cases) with subjects who do not have this outcome (the controls) with respect to risk factors of interest [114]. Case-control studies are an efficient method to evaluate risk factors that lead to adverse outcomes that occur infrequently. Therefore, in this local Research Ethics Committee approved study (Oxford Research Ethics Committee B: 07/H0605/151, Amendment 1), lymphocyte transformation tests (LTT) were performed to compare metal sensitivity in MoMHRA patients with pseudotumour (Group 1) with two control groups: MoMHRA patients without pseudotumour (Group 2) and patients without any MoMHRA (Group 3).

4.4 Materials and Methods

4.4.1 Patients

A total of 92 patients were investigated. There were 3 patient groups: (1) Group 1 – MoMHRA patients with pseudotumours (n=10), a cystic or solid mass relating to the resurfaced hip, detected using ultrasound and confirmed with MRI. This cohort consisted

of seven patients from the prevalence study (Chapter 3) and three additional patients who have been diagnosed with pseudotumours since the prevalence study has been completed; (2) Group 2 – patients with well functioning MoMHRA without pseudotumours detected on ultrasound (n=60); and (3) Group 3 – age-matched control patients without metal implants and no clinical history of metal allergy (n=22) (Table 4-1). The patients in the first two groups (Groups 1 and 2) were recruited using the selection criteria identical to those previously outlined in Chapter 3. Resurfacing devices implanted included 75 Birmingham Hip Resurfacing (BHR), 19 Conserve Plus and 2 ReCap. The subjects without any MoMHRA (Group 3) consisted of pre-operative patients scheduled for hip resurfacing arthroplasty. A clinical history of metal allergy manifested as a dermal reaction to metal jewellery was obtained. In addition, venous blood samples were collected in all patients for lymphocyte transformation tests, and serum Co and Cr ion level analysis.

Table 4-1: Summary of patient group demographics.

Patient Group	Total Patient Number	Bilateral Arthroplasty	Mean Age (range, years)	Mean Follow-up (range, months)
Pseudotumour	10 (1M, 9F)	8 (1M, 7F)	56 (45-62)	65 (36-79)
Non-pseudotumour	60 (30M, 30F)	18 (10M, 8F)	55 (40-69)	61 (36-88)
Control	22 (13M, 9F)	None	55 (50-58)	Pre-operative

Abbreviations: Male (M), Female (F).

4.4.2 Implant-Related Hypersensitivity Tests

Testing for delayed type IV hypersensitivity has been historically conducted *in vivo* using skin patch testing [105]. Skin patch testing involves incorporating an antigen in a carrier, and exposing this to dermal tissue by means of an affixed bandage. After exposure of approximately 48-96 hours (the maximal time for a type IV response), reactions are graded on a scale of 1 (mild or absent response) to 4 (severe red rash with blisters). The concerns about the applicability of skin patch testing to assess *in vivo* immune responses to metal implants include: (1) no consensus regarding the suitable standardised testing battery of relevant orthopaedic metals; (2) unknown antigen presenting potential of metals in the peri-prosthetic environment, which is likely to be different from the dermis where Langerhan cells are the primary antigen presenting cells; (3) development of immunological tolerance, whereby a loss of pre-operative positive cutaneous metal sensitivity may occur [127]; (4) presence of an impaired host immune response; (5) the possibility of inducing metal hypersensitivity in a previously insensitive patient; and (6) the duration of exposure is different from the actual peri-prosthetic environment.

Due to the limitations of skin patch testing, the use of the lymphocyte transformation test (LTT) to investigate metal sensitivity related implant failure has been described in the literature [108, 128]. Metal particles induce an acquired or antigen-specific immune response, type IV delayed hypersensitivity reaction driven by T-lymphocytes. The LTT measures the proliferative response of lymphocytes following activation [129]. Therefore, *in vitro* lymphocytic proliferation testing (LTT) is considered to represent a more

clinically appropriate method of assessing lymphocyte reactivity to metals [108]. Thus, the lymphocyte transformation tests were used to measure metal sensitivity in this study.

4.4.3 Lymphocyte Transformation Test

The LTT is a labour-intensive process requiring specialised equipment and expertise, and thus is performed by a limited number of specialised laboratories. There was no local laboratory which routinely performed the tests. For this reason, a collaboration was sought and established with a specialist allergy laboratory in Munich, Germany. The LTT methodology utilised by the laboratory in assessing implant-induced hypersensitivity is well documented in the literature [130, 131]. Thus, all LTT analyses were performed in a blinded fashion at the Ludwig-Maximilians-University, Munich, Germany.

In the current study, three metals were selected as challenging agents for lymphocyte reactivity: cobalt, chromium and nickel. Cobalt and chromium are the principal elements in the CoCr alloy used in MoMHRA implants, accounting for greater than 90% of the alloy [44]. Moreover, in the prevalence study (Chapter 3), these metal levels were found to be elevated in pseudotumour patients. In addition, the metal aggregates seen in histology of pseudotumour were also confirmed to contain these metals (Chapter 3). Although nickel constitutes approximately 1% of MoMHRA CoCr alloy [44], it was selected as it is the commonest metal sensitiser in humans [132] and it is frequently present in jewellery; Thus, lymphocyte reactivity of these metals were compared to a negative control (medium only without a challenging agent) and a positive control (phytohaemagglutinin, which activates lymphocytes) [130].

The testing protocol involved isolation of peripheral blood mononuclear cells (PBMC) from heparinized blood samples using standard Ficoll–Hypaque® (Pharmacia, Uppsala, Sweden) density gradient centrifugation. The PBMC's were cultured in tubes at a cell density of 10^6 cells/ml in an enriched RPMI1640 culture medium (Sigma, Deisenhofen, Germany). Proliferation assays were performed in triplicate, in 96-well microtiter plates (Greiner, Frickenhausen, Germany; 2×10^5 cells/well). The cultures were set up in the presence of either: (1) medium alone as a negative control; (2) phytohaemagglutinin (PHA) (Biochrom, Berlin, Germany; 2 μg/ml), which activates lymphocytes as a positive control; (3) three concentrations of nickel sulfate ($NiSO_4$) (Sigma N-4882, Germany; 10^{-4}M, 10^{-5}M, and 10^{-6}M); (4) three concentrations of cobalt chloride ($CoCl_3$) (10^{-4}M, 10^{-5}M, and 10^{-6}M); or (5) three concentrations of chromium chloride ($CrCl_3$) (10^{-4}M, 10^{-5}M, and 10^{-6}M). After 5 days in culture, the cells were pulsed overnight with [^{3}H]-thymidine, which is incorporated into the cellular DNA. Lymphocyte proliferation was assessed by scintillation counting of incorporated radioactivity and expressed as stimulation index.

Stimulation Index

The stimulation index (SI) was calculated as the ratio of mean counts per minute (cpm) of stimulated to the control (culture medium only) cultures. The stimulation index was used to compare the lymphocyte proliferative (or reactivity) response. In order to determine the incidence of metal reactivity, a positive result was defined when there was a greater than 2-fold lymphocyte proliferative response compared to the negative control cultures containing medium only (SI≥2.0). This is an arbitrary definition which is the most

commonly used in the literature [133]. A positive response is interpreted as a sign of lymphocyte sensitisation (metal-sensitivity) specific to the challenging metal. In addition to measuring the incidence of positive LTT results in the groups based on a threshold of SI value greater than 2.0, the level of the lymphocyte proliferation response to metals in each patient group was also assessed. This was thought to be necessary as the threshold for a positive test is arbitrary, thus the absolute SI values were also of interest. The highest SI values for each patient, generally observed with the highest concentrations of metal ions (10^{-4}M), were used for analysis.

4.4.4 Serum Metal Ion Analysis

A potential correlation between serum Co and Cr ion levels and lymphocyte reactivity to Co and Cr was of interest in the current study, as a positive linear correlation would support metal-induced systemic hypersensitivity in MoMHRA patients with pseudotumour. Therefore, the venous blood samples were collected in accordance with the consensus protocol previously described in Chapter 3 [75]. Venepuncture was performed using disposable Venosafe (Terumo Europe NV, Leuven, Belgium) 21-gauge stainless-steel needles. The first 5 ml of withdrawn blood was discarded to avoid metal contamination from the needle. All collected samples were placed into 6 ml vacuum tubes (Venosafe VF-106SAHL, Terumo Europe NV, Leuven, Belgium), kept at room temperature, and transported overnight. Serum cobalt and chromium levels were analysed in a blinded fashion using ICP-MS. The analysis was performed at the Laboratory of Clinical Biology, Department of Toxicology, University Hospital, Ghent, Belgium. The detection limit of cobalt and chromium in serum was 0.25 μg/l.

4.4.5 Statistics

The data set was assessed for normality and presented as mean ± standard error. The incidence of positive LTT results in each group was compared using the Pearson chi-square statistic. Inter-group comparisons of the normally distributed mean SI values for Ni, Co and Cr were calculated using one-way ANOVA analysis of variance with post-hoc Tukey test. Inter-group comparisons of the non-normally distributed serum levels of Co and Cr were performed using Kruskal-Wallis non-parametric analysis of variance. Correlation between the mean SI values and serum metal levels was calculated using non-parametric Spearman rank correlation analysis, expressed as Spearman's correlation rho. Differences at $p < 0.05$ were considered to be significant. SPSS® statistical software release 13.0 (SPSS Inc. Chicago, IL, USA) was used to perform the statistical analyses.

4.5 Results

4.5.1 Incidence of Enhanced Metal-Induced Lymphocyte Reactivity

For Co and Cr, none of the patients in the pseudotumour and control groups had positive metal-reactivity to these metals (Table 4-2). In the non-pseudotumour group, the incidence of metal-sensitivity to these metals was also very low (<5%). The highest incidence of metal sensitivity to Ni was seen in the pseudotumour group (80%). This represented a significant elevation: 6-fold increase compared to the control group (13%) and a 1.8-fold increase compared to the non-pseudotumour group (45%) (χ^2=10.6; $p<0.01$). As the pseudotumour group consisted predominantly of female patients with

bilateral MoMHRA (7 out of 10), the incidence of positive metal-reactivity to Ni in this sub-group was measured. Interestingly, for female patients with bilateral MoMHRA, the incidence of positive LTT reactivity to Ni was similar in the non-pseudotumour group (75%) and in the pseudotumour group (71%) (χ^2=0.1; p=0.71). The incidence of positive LTT reactivity in the total female patient sub-groups was higher in the pseudotumour group (78%) than the non-pseudotumour group (50%), although the difference was not statistically significant (χ^2=5.62; p=0.08). Comparison of the incidence of positive LTT between the male patients with bilateral MoMHRA implants was limited as the only male patient in the pseudotumour group had bilateral implants and tested positive for lymphocyte reactivity to nickel. The incidence of patient-reported clinical history of metal allergy manifested as a dermal reaction to metal jewellery was limited to two female patients with bilateral MoMHRA in the pseudotumour group (20%), three females (2 with bilateral MoMHRA) in the non-pseudotumour group (5%), and none in the control group. All of these patients had positive lymphocyte proliferation to Ni, as measured by LTT.

Table 4-2: Incidence of positive metal reactivity (SI≥2.0) within each patient group (at 10^{-4}M).

Patient Groups	Sub-Groups	Nickel	Cobalt	Chromium
Pseudotumour	Overall	8/10 (80%)	0%	0%
	Male	1/1 (100%)	0%	0%
	Female	7/9 (78%)	0%	0%
	Male Bilateral	1/1 (100%)	0%	0%
	Female Bilateral	5/7 (71%)	0%	0%
Non-Pseudotumour	Overall	29/60 (45%)	1/60 (2%)	3/60 (5%)
	Male	12/30 (40%)	1/30 (3%)	2/30 (7%)
	Female	15/30 (50%)	0/30 (0%)	1/30 (3%)
	Male Bilateral	3/10 (30%)	0/10 (0%)	1/10 (10%)
	Female Bilateral	6/8 (75%)	0/8 (0%)	0/8 (0%)
Control	Overall	3/22 (13%)	0%	0%
	Male	2/13 (15%)	0%	0%
	Female	1/9 (11%)	0%	0%

4.5.2 Level of Metal-Induced Lymphocyte Reactivity

Inter-group comparisons of the mean SI values for phytohaemagglutinin (positive control) showed no significant differences (p=0.80). Similarly, there was no significant difference in the mean SI values for Co (p=0.81) and Cr (p=0.87) among the three groups (Figure 4-1). However, for nickel, a significant difference in the inter-group mean SI values existed (p=0.02). The lymphocyte proliferation response to Ni was significantly greater in the patient groups with MoMHRA (groups 1 and 2), with a greater than 2-fold increase in the mean SI values, in comparison with the control subjects without MoMHRA (group 3) (p=0.04). However, there was no significant difference

demonstrated in the lymphocyte proliferation response to Ni between the pseudotumour group and the non-pseudotumour group (p=0.65).

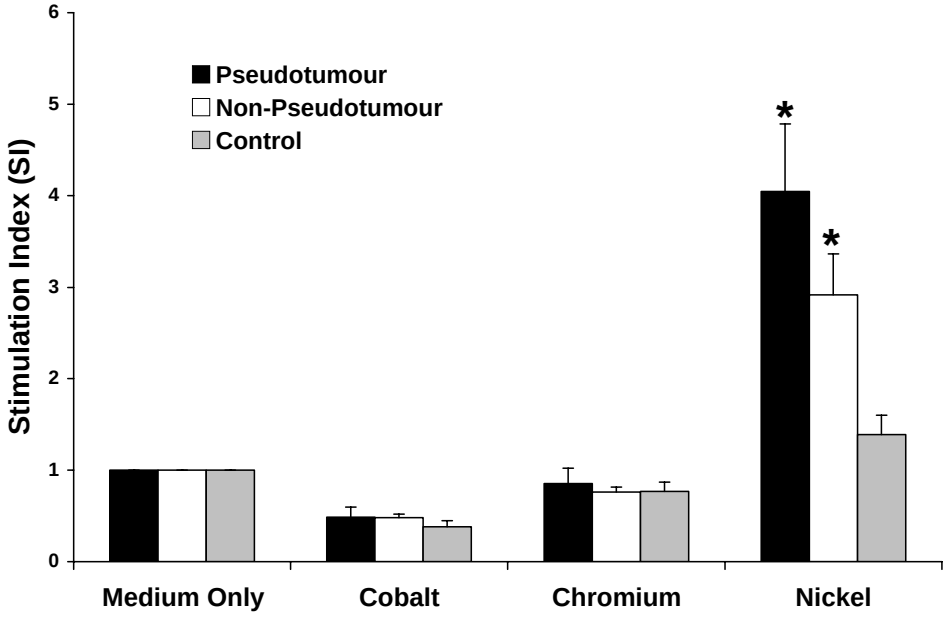


Figure 4-1: Mean lymphocyte reactivity (stimulation index) measured (at 10^{-4}M) in the three patient groups for cobalt, chromium and nickel. Asterisk (*) indicates $p<0.05$ versus the control group with no metal implants (medium only).

4.5.3 Serum Metal Ion Levels vs. Lymphocyte Reactivity

Venous blood samples collected from all patients were analysed for serum concentrations of Co and Cr. The patient groups with MoMHRA (Groups 1 and 2) demonstrated significant elevation of both serum Co and Cr compared to the control group ($p<0.001$). In comparison with the non-pseudotumour and control groups, the pseudotumour group was associated with:

(1) significantly higher median serum cobalt levels: 13.3 μg/l (range 4.8-34.1 μg/l) vs. 2.4 μg/l (range 0.5-9.3 μg/l) vs. control group 0.5 μg/l (range 0.5-0.8 μg/l), $p<0.001$; and (2) significantly higher median serum chromium levels: 15.1 μg/l (range 3.8-35.2 μg/l) vs. 2.1 μg/l (range 0.5-8.3 μg/l) vs. control group 0.5 μg/l (range 0.5-0.7 μg/l), $p< 0.001$.

When all patients in the three groups were considered together, correlation analysis between serum metal ion levels and lymphocyte reactivity to Co and Cr demonstrated no significant correlations: the Spearman's correlation coefficients for Co and Cr were 0.02 ($p=0.67$) and 0.02 ($p=0.52$), respectively (Figure 4-2). However, in the pseudotumour group, the median serum Cr level demonstrated a significant negative correlation with the mean lymphocyte proliferation reactivity (the mean SI values obtained after challenging with Cr at 10^{-4}M) within the observed SI range: the Spearman's correlation coefficient was –0.68 ($p=0.04$) (Figure 4-3). This indicated an inverse relationship between serum Cr levels and lymphocyte reactivity to Cr. In contrast, no significant correlation was found between the SI values and median serum Co levels: correlation coefficient was 0.01 ($p=0.99$).

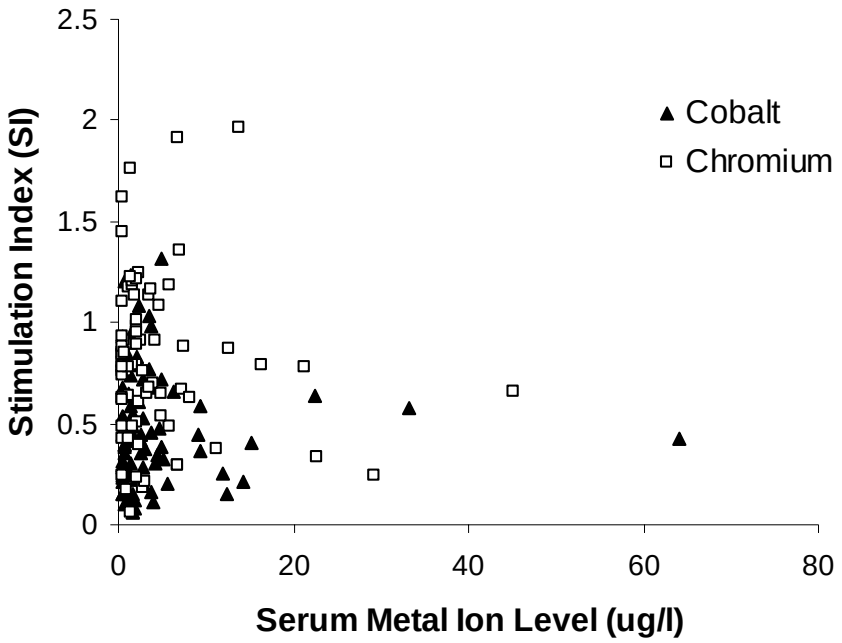


Figure 4-2: Serum cobalt and chromium ion levels from all patients in the three groups are plotted against cobalt and chromium challenged lymphocyte reactivity.

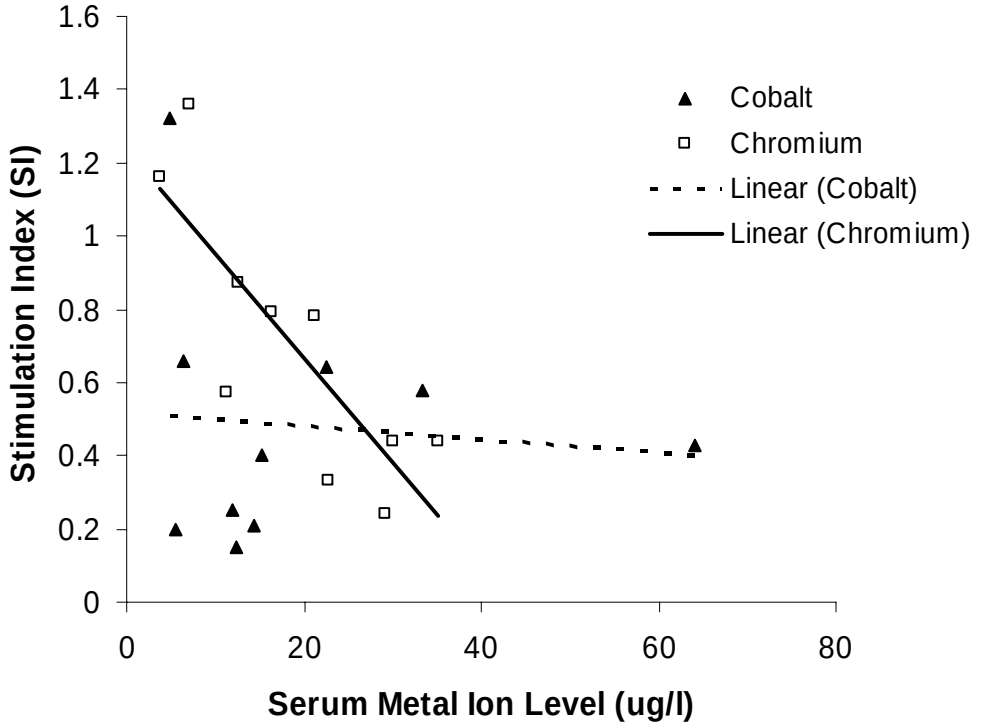


Figure 4-3: Serum cobalt and chromium ion levels from patients in the pseudotumour group are correlated with cobalt and chromium challenged lymphocyte reactivity.

4.6 Discussion

The true incidence of clinically important metal hypersensitivity reactions in patients with MoM bearings remains unknown [134]. Historically, skin patch testing has been used to determine metal sensitivity in patients with MoM implants, with the reported incidence varying between 10% to 74% [102, 103]. A high (30%) prevalence of pseudotumours was found in females with bilateral MoMHRA implants (Chapter 3), who displayed the histological feature of lymphocyte infiltrations. The histological appearance was similar to the aseptic lymphocyte vasculitis associated lesion (ALVAL), indicating that a systemic delayed hypersensitivity reaction to metals may be an important biological mechanism of pseudotumours. The metals investigated in this study included nickel (Ni), a common metal sensitiser present in jewellery, and chromium (Cr) or cobalt (Co), the principal elements in the CoCr alloy used in MoMHRA implants.

In the current study, both the incidence (45% to 80%) and the magnitude of enhanced lymphocyte response to metals in patients with MoMHRA (groups 1 and 2) was significantly higher than the control group without metal implants (13% incidence), supporting a link between metal exposure and metal sensitivity. However, the significant increase in lymphocyte reactivity was only demonstrated with Ni, which is the commonest metal sensitiser in humans [132], despite nickel constituting only 1% of MoMHRA CoCr alloy [44]. There was no significant increase with Co and Cr, the principal elements of metal alloy used for MoMHRA implants. This finding is in contrast with the previous studies of MoM THA implants [108, 135, 136], which have reported predominant reactivity to these metals. Thus, metal sensitivity in patients with MoMHRA

appears to be mediated by lymphocyte reactivity to Ni, rather than Co and Cr. This suggests that metal debris released from MoMHRA, which has a larger bearing diameter compared to small head diameter MoM THA, may lead to differential *in vivo* effects on lymphocytes.

The histological features of pseudotumours, characterised by the presence of lymphocyte infiltrates, lymphoid aggregates, as well as marked necrosis with macrophages, were similar to those of ALVAL. A high incidence of exposure to jewellery in females would lead to sensitisation to metals in these patients, thereby increasing the likelihood of eliciting delayed-type hypersensitivity reaction to metals upon the implantation of MoMHRA. Continuous release of metal ions from the metal-on-metal articulation would facilitate sensitisation and consequent cell-mediated immunological response, in which proliferation of sensitised T-lymphocytes could be induced following a second contact with the antigen [25]. These factors suggested that pseudotumours may represent a delayed hypersensitivity reaction to nickel, chromium or cobalt.

However, in comparison with non-pseudotumour MoMHRA patients, there was no significant difference in the incidence or level of lymphocyte reactivity to metal, as measured by LTT, in patients with pseudotumour. The majority of the pseudotumour group consisted of female patients with bilateral hip resurfacings (7 out of 10). Thus, a 2-fold increase in the overall incidence of positive lymphocyte proliferation to Ni in the pseudotumour group (80%) compared with the non-pseudotumour group (38%) did not reflect a comparable subset of patients. When the sub-groups consisting of female

patients with bilateral implants were compared, the incidence of enhanced lymphocyte proliferation to Ni was similar between the pseudotumour group (71%) and the non-pseudotumour group (75%).

The apparent lack of differences in lymphocyte reactivity between the pseudotumour and non-pseudotumour groups demonstrated in the current study may be explained by several observations. Firstly, the relationship between these metal sensitivity histological features and MoM implant failure has not been fully established. This is due to the fact that the ALVAL-like features have been observed in patients with no clinical symptoms of metal allergy, as well as in retrieval studies of failed implants from mechanical causes [110, 111] and pain for other reasons [112]. Thus, ALVAL is not pathognomonic for implant failure due to metal hypersensitivity. Secondly, the current study finding is consistent with the clinical study finding (Chapter 3) that an ALVAL response was not seen histologically in all pseudotumours, whereas necrosis and a macrophage infiltrate were always observed. Lastly, the prevalence of pseudotumour, estimated to be 4% in the clinical study (Chapter 3) exceeds the prevalence of metal hypersensitivity reactions leading to an adverse clinical outcome, which are currently estimated to affect < 1% of patients [101]. These observations, combined with the current study findings suggest that another mechanism, such as a local metal-induced cytotoxic effect, is likely to be involved.

Within the highly elevated serum Cr level range (5 μg/l to 35 μg/l) found only in the pseudotumour group, the lymphocyte reactivity to Cr was negatively correlated to serum

Cr levels. The inverse relationship is contradictory to the proportional relationship reported between lymphocyte reactivity and serum Co and Cr levels at a lower concentration range (0.5 μg/l to 3.5 μg/l) [133]. This suggests that there may be dose-dependent *in vivo* modulation of lymphocyte reactivity to metals: Cr has proliferative effects on lymphocytes at lower concentrations, but it has inhibitory effects at high concentration ranges. A similar dose-dependent relationship on the number of lymphocytes has been reported in the literature: a threshold whole blood level of combined Co and Cr greater than 5 μg/l was found to be associated with a significant reduction in the circulating levels of T cytotoxic (CD8+) subsets in patients with MoMHRA implants [82]. In the current study, a significant correlation did not exist between lymphocyte activity and serum Co ion levels in the pseudotumour group, suggesting that Co and Cr may differ in dose and exposure time required to induce lymphocyte reactivity.

In conclusion, patients with MoMHRA have a higher incidence and level of enhanced lymphocyte response only to Ni ions compared to the control patients without MoMHRA, reflecting exposure and immune reactivity to Ni. However, Co and Cr, the principal elements in the CoCr alloy used in metal-on-metal hip resurfacing implants, did not induce enhanced lymphocyte reactivity in patients with MoMHRA. In the current study, local periprosthetic hypersensitivity cannot be excluded due to the inherent limitations of the test used. Furthermore, the individual biologic response to the presence of wear debris may vary, reflecting a different toxic-effect threshold or immunological intolerance. However, the current study results also demonstrated that systemic exposure and immune

reactivity to Co, Cr and Ni did not differ in MoMHRA patients with pseudotumour compared to those MoMHRA patients without pseudotumours. This suggests that systemic hypersensitivity type IV reactions, mediated by lymphocyte reactivity to these metals, is not the dominant biological reaction involved in the occurrence of soft tissue pseudotumours.

4.7 Summary

- The current study results demonstrated that systemic exposure and immune reactivity to Co, Cr (the principal elements in the CoCr alloy used in MoMHRA implants) and Ni (common metal sensitiser present in jewellery) did not differ in MoMHRA patients with pseudotumour compared to those MoMHRA patients without pseudotumours. Therefore, the null hypothesis, which stated that there is no difference in lymphocyte proliferative responses between MoMHRA patients with pseudotumour and patients without pseudotumours, could not be rejected.
- This finding suggests that a systemic hypersensitivity response to Co, Cr and Ni is not a dominant biological reaction involved in the occurrence of pseudotumour.
- Therefore, the hypothesis that a local cytotoxic effect of large amounts of metal wear debris is implicated as the potential biological reaction involved in mediating the occurrence of pseudotumours was warranted and tested in the next chapter.

CHAPTER 5 *IN VITRO* METAL CYTOTOXICITY

5.1 Introduction

Histological examinations of soft tissue pseudotumour were characterised by extensive necrosis of connective tissue, in which there were scattered aggregates of metal particles within necrotic macrophages in the extracellular tissue (Chapter 3). Elemental analysis, using scanning electron microscopy with energy-dispersed analysis of X-rays (SEM/EDX) conducted on the individual particles identified on specimen tissues confirmed these metal aggregates contained both Co and Cr. Moreover, patients with pseudotumours had up to a twelve-fold elevation of median hip aspirate levels of Co and Cr ions in comparison to patients without pseudotumours (Chapter 3). Hence, the presence of extensive necrosis and granuloma-like collections of macrophages would be in keeping with a local metal-induced cytotoxic effect. Cytotoxicity is postulated to lead to a vicious cycle in which metal wear particle generation leads to macrophage recruitment, particle phagocytosis and cell death, with resultant metal particle release. This would, in turn, lead to further macrophage recruitment, and repetition of this process. However, the effect of phagocytosis of clinically relevant metal nanoparticles on macrophages has not been elucidated. Thus, it was hypothesised that a local cytotoxic effect of chromium or cobalt may play a role in the biological reactions involved in pseudotumours. The aim of this study was therefore to investigate the local cytotoxicity to ions and particles of cobalt and chromium on macrophage viability *in vitro*.

5.2 The Null Hypotheses

H_0: There is no difference in the viability of macrophages *in vitro* in the presence of cobalt nanoparticles and ions, when compared to a control environment not containing metal particles and ions.

H_0: There is no difference in the viability of macrophages *in vitro* in the presence of chromium nanoparticles and ions, when compared to a control environment not containing metal particles and ions.

5.3 Materials and Methods

5.3.1 *In Vitro* Experimental Considerations

It is important to provide justification for a number of critical *in vitro* experimental parameters utilised in the current study to investigate the local cytotoxicity of metal ions and particles. Important parameters that needed to be considered during *in vitro* experiments included: the selection of cell type and source; selection of metal particles/ions and their source; and the concentration range of metal particles/ions to be tested.

The macrophage is the major differentiated cell of the mononuclear phagocyte system, which responds rapidly to biomaterial implantation in soft and hard tissue [137]. Necrotic macrophages in extracellular tissue containing metal aggregates were the dominant cell type observed in the clinical study of patients with pseudotumour (Chapter 3), which is

also consistent with the published report [42]. In addition, macrophages also act as antigen presenting cells in type IV delayed hypersensitivity reactions driven by T-lymphocytes [105], indicating that activation of lymphocytes during the hypersensitivity reaction depends on viable macrophages. Initially, the use of primary human cells obtained from patients with MoMHRA was considered, as this would have been most relevant to the clinical situations. However, obtaining a further volume of venous blood from the pseudotumour patients during the clinical studies (Chapters 3 and 4) was not feasible because this would have required a substantial increase in the total volume of blood sample of 50 ml above the already required for the metal ion level analysis and subsequent lymphocyte tests. In addition, a variable degree of heterogenicity in macrophage responses to wear debris materials between individuals has been reported [138-140]. Thus, a source of cells with minimal variability was required in order to obtain reproducible and consistent results between experiments. The RAW 264.7 murine macrophage cell line has been well characterised and is widely used to assess the cytotoxicity of various types of wear particles in the literature [141, 142]. It is also readily available. For these reasons, murine macrophages were selected to assess the biological effects of metal nanoparticles and ions in this study.

In the current study, three metals and two metal ions were investigated with respect to their *in vitro* cytotoxicity on murine macrophages: cobalt nanoparticles and ions, chromium nanoparticles and ions, and titanium nanoparticles. Cobalt and chromium nanoparticles and ions were chosen for the following reasons: (1) they are the principal elements in the CoCr alloy used in MoMHRA implants [44]; (2) these metal ion levels

were found to be elevated in pseudotumour patients; and (3) the metal aggregates seen in histology of pseudotumour contained Co and Cr metals (Chapter 3). Titanium has outstanding biocompatibility, with its corrosion resistance exceeding that of CoCr alloys [143]. In fact, commercially-pure titanium is the material of choice for the porous layer in the cementless THA. The titanium particles used in this study were of the same nanometer-size as the cobalt and chromium nanoparticles. This was necessary in order to investigate whether the process of nanoparticle phagocytosis by macrophages, by its self, affected cell viability.

It was important to use the metal nanoparticles that are representative of the particles generated *in vivo*. Particles generated from the articular surfaces of MoM prostheses have a size range in the nanometer scale [65]. Although aggregates of metal particles were observed, the majority of metal particles identified by the scanning electron microscopy examination of pseudotumour tissues were 30-60 nm in diameter (Chapter 3). Thus, the particle size in a similar nanometer range was necessary in the current study. The use of CoCr alloy particles generated from a pin-on-plate tribometer or hip simulator was considered. However, the various digestion methods used in the isolation of these particles from simulator lubricants have been found to adversely affect particle size, shape and composition [144]. Therefore, commercially-manufactured Co and Cr nanoparticles were used in the current study. This ensured the uniformity of size (range 30-50 nm) and composition as well as availability of sufficient quantity. Furthermore, the use of commercially-manufactured Co and Cr nanoparticles allowed assessment of the relative cytotoxicity of Co compared to Cr, which was one of the study aims.

It was also important to test *in vitro* cytotoxicity using clinically relevant doses of metal nanoparticles and ions. For metal ions, the *in vitro* metal concentration range was based on *in vivo* hip aspirate metal ion levels (instead of serum levels) found in patients with pseudotumours (Chapter 3) in order to assess the effect of local periprosthetic concentrations. An upper limit of the concentration range was set at two orders of magnitude increase from the hip aspirate level to account for a short *in vitro* incubation period. For metal nanoparticles, the concentration range was based on that reported by a study on cytotoxicity of metal nanoparticles on histiocytes [16].

5.3.2 Cell Cultures with Metal Nanoparticles and Ions

A RAW 264.7 murine macrophage cell line (supplied by the Botnar Research Centre, University of Oxford, Oxford, UK) was recovered from stock in liquid nitrogen, and cultured in alpha modified Eagle minimum essential medium (αMEM) (Gibco BRL, Invitrogen Ltd., Paisley, UK) supplement with 10% foetal bovine serum (FBS) (M.B. Meldrum Ltd., UK) and penicillin/streptomycin (Gibco BRL, Invitrogen Ltd., Paisley, UK) at a seeding density of 1×10^5 cells/cm^2 in 10 cm diameter tissue culture dishes and 96 well tissue culture plates. For cell viability assays, a culture was set up in the presence of either:

(1) a negative control: cells were cultured in medium alone;

(2) metal nanoparticles: cobalt nanoparticles (purity 99.8%, a mean size of 30 nm, American Elements, Merelex Corp. Los Angeles, USA), chromium nanoparticles (purity 99%, a mean size of 30 nm, American Elements, Merelex Corp. Los Angeles, USA) and

titanium (Ti) nanoparticles (purity 99.8%, a mean size of 35 nm, American Elements, Merelex Corp. Los Angeles, USA) which were all individually suspended in culture medium at concentrations of 10^7,10^8,10^9,10^{10}, 10^{11}, 10^{12},10^{13} particles/ml); or

(3) Co and Cr ions: cobalt (II) sulphate heptahydrate (Sigma-Aldrich Company Ltd. Dorset, UK) and chromium (III) chloride hexahydrate (Sigma-Aldrich Company Ltd. Dorset, UK) solutions were prepared at concentrations of 1μM, 10μM, 100μM, 1000μM in culture medium.

The cells were examined under a light microscope at magnifications of 200× and 400× prior to the cell viability assays. All experiments were repeated three times. A more detailed *in vitro* cell culture protocol utilised in the current study is provided in Appendix 2.

5.3.3 Cytotoxicity Assays

Numerous biological assays are aimed towards the measurement of survival and proliferation of mammalian cells [145]. Alamar Blue (AB) is a sensitive non-radioactive homogeneous assay for the measurement of cell viability. The assay involves the addition of a fluorogenic redox indicator to growing cells in culture. The oxidized form of Alamar Blue is a dark blue colour and has little intrinsic fluorescence. When taken into cells, the dye becomes reduced and turns red. This reduced form of Alamar Blue is highly fluorescent. The extent of this conversion, which is an indication of cell viability, can be quantified by its optical density of fluorescence for greater sensitivity. This is measured as the relative fluorescent unit (RFU). Alamar Blue assay was selected to be used in the

current study for several reasons. First, it is simple to use. The indicator is added directly to cells in culture towards the end of the incubation period. Second, Alamar Blue is non-toxic to the cells and user. Third, it is sensitive, detecting as few as 10 living cells [146].

The use of overall number of viable cells alone to measure cell viability can be misleading. This is because the overall cell number is influenced by both cell proliferation rate as well as cell death rate. Thus, the cell number reflects the balance between cell proliferation and death. In order to more accurately measure cell death, or cytotoxicity caused by challenging metal particles/ions, a second assay was necessary to quantify the numbers of both viable (live) and non-viable (dead) cells. Live/Dead (LD) Assay is one such assay. It is a simple and safe cytotoxicity assay that contains two fluorescent dyes: calcein to stain living cells green and ethidium homodimer-1 (Ethd-1) to stain damaged or dead cells red. The cells are subsequently counted and quantified using fluorescence microscopy [147]. The use of Live/Dead in the study allowed calculation of cell viability as:

Cell Viability (%) = [live cells / total cell numbers (live + dead)] × 100. (Equation 5-1)

Therefore, the Alamar Blue assay and the Live/Dead assay were used in this study to measure proliferative and cytotoxic responses, respectively.

Alamar Blue Assay

At the end of day 1 and day 4, cells were harvested for Alamar Blue proliferation assay to measure the overall number of viable cells. After removal of the culture medium, cells were incubated in fresh serum-free αMEM containing 5% Alamar Blue (BioSource

Europe, Invitrogen, UK) at 37°C for 2 hours for the cell proliferation assay. As stated previously, the Alamar Blue assay incorporates a fluorimetric redox indicator, and the fluorescence signal correlates with metabolic activity and viability of the cells. The system incorporates an oxidation-reduction indicator, which is detected using a SpectraMAX GeminiXS microplate fluorometer at an excitation wavelength of 530 nm and an emission wavelength of 590 nm, with a cut-off at 570 nm and was analysed using its associated software SoftMAX®PRO (Molecular Devices, Sunnyvale, CA) and reported as relative fluorescent units (RFU). RFU values were converted to the total viable cell number by plotting the RFU against standard curves that were produced by sequential dilution of the same cells. This method was repeated for each microplate used in the experiment in order to calculate the overall viable cell number from the measured RFU values. A more detailed description of Alamar Blue assay protocol is provided in Appendix 2.

Live/Dead Assay

At the end of day 1 and day 4, cells were also harvested for Live/Dead assay to measure the proportion of viable cells relative to the total number of cells (cell viability). Cells were washed twice in phosphate-buffered solution (PBS) (Cambrex Bio Science Workingham, Berkshire, UK) to remove any serum derived from the cell culture medium. Samples were stained using a Live/Dead stain kit (Molecular Probes, Invitrogen, Carlsbad, California, USA). As stated previously, the kit contains two fluorescent dyes: calcein to stain living cells green and ethidium homodimer-1 (Ethd-1) to stain damaged or dead cells red. Samples were stained using 4 μM calcein and 2 μM Ethid-1 (final

concentration) in PBS for 30 minutes at (37 ± 1) °C. Samples were rinsed twice using PBS to remove any dye, mounted in PBS and observed by using fluorescence microscopy. A more detailed description of Live/Dead assay protocol is provided in Appendix 2.

Images were captured using a Radiance 2000 Laser Confocal scanning microscope (Bio-Rad Microscience Ltd. Herts, UK) at 200× magnification using the associated LaserSharp 2000 software. For each sample, three representative images were captured. Images were analysed with Cell Imaging software for Life Science Microscopy, version 1.20 (Soft Imaging System GmbH, Munster, Germany). Living and dead cells were counted to estimate the cell numbers in an image. Cell viability was calculated using Equation 5-1.

5.3.4 Metal Ion Release into Culture Medium by Co and Cr Nanoparticles

Metal particles corrode to either produce a protective passive layer or dissolve into charged free metal ions in solution. Thus, the biological effect of the nanoparticles on the macrophages may be due to the particulate form of nanoparticles themselves or mediated by their ions in solution. In order to quantify the degree of corrosion of metal nanoparticles in the culture medium, Co and Cr nanoparticles were incubated in culture medium at 10^{10}, 10^{11}, 10^{12},10^{13} particles/ml for one day. The particles were then centrifuged (2100*g*) to obtain the particles-free supernatants, which were analysed for Co and Cr ion levels using ICP-MS (ELAN DRC II, PerkinElmer Life and Analytical Sciences, Shelton, CT, USA). In addition, the centrifuged cobalt (II) sulphate heptahydrate and chromium (III) chloride hexahydrate at concentrations of 1μM, 10μM,

100μM, 1000 μM were also analysed for ion levels following incubation in culture medium for one day. The analysis was performed at the Laboratory of Clinical Biology, Department of Toxicology, University Hospital, Ghent, Belgium. The detection limit of cobalt and chromium was 0.25 μg/l.

5.3.5 Statistics

SPSS® statistical software release 13.0 (SPSS Inc. Chicago, IL, USA) was used to perform the statistical analyses. The data set was assessed for normality and presented as mean ± standard error. Inter-group comparisons of the normally distributed data were performed using one-way ANOVA with Tukey post-hoc test. Differences at $p < 0.05$ were considered to be significant.

5.4 Control Experiments

Validity and repeatability control experiments were required to demonstrate utility of the investigative procedures. Control experiments were therefore performed to: (1) demonstrate the utility of cytotoxic assays (Alamar Blue and Live/Dead assays); and (2) verify the size of commercially-manufactured Co and Cr nanoparticles used in the current study.

5.4.1 Alamar Blue Assay

Validity refers to the system's ability to measure what it was designed to measure. Firstly, as the reduction of Alamar Blue is enzymatic in nature, it was critical to study the reaction conditions in order to obtain valid results. Each cell line has unique metabolic

properties and must be individually characterised to determine the experimental parameters. For this reason, a control experiment was performed to explore a correlation between the cell numbers of the RAW 264.7 murine macrophage cells and the measured relative fluorescent unit (RFU). RAW 264.7 murine macrophages cultured in alpha modified Eagle minimum essential medium were added to the microplate in sequential dilutions of 1:2 and the relative fluorescent units were measured.

The cell number was plotted against the relative fluorescent unit (RFU). This is shown in Figure 5-1. The linear regression analysis showed there was a very high degree of correlation: the Pearson's correlation coefficient was 0.98 ($p < 0.05$). The process of plotting cell numbers against the measured relative fluorescent unit (RFU) was repeated for each microplate in order to calculate the cell numbers.

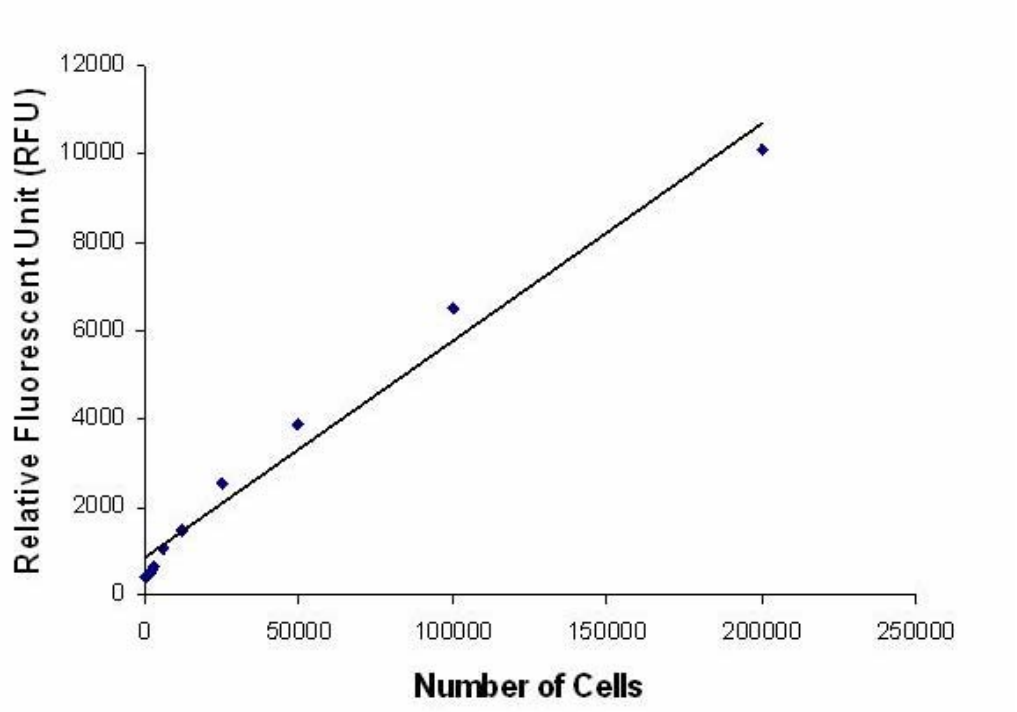


Figure 5-1: The cell numbers plotted against the relative fluorescent unit (RFU).

A second control experiment was performed to verify that the RFU measures the metabolic activity of live RAW 264.7 murine macrophage cells. The relative fluorescent units were measured in three groups: (1) the control 'live' cell group; RAW 264.7 murine macrophage cells cultured in αMEM; (2) the 'dead cell' group; the control cells were treated with acetone/methanol (50%), a known cytotoxic agent; and (3) the 'no cell' group; 5% Alamar Blue alone (without cells). The RFU values for the three groups are listed in the Table 5-1.

Table 5-1: The relative fluorescent units (RFU) in Alamar Blue Assay.

Sample	Control Live Cell Group	Dead Cell Group	Background No Cell Group
1	19899.7	999.2	1040.2
2	20592.5	1029.4	1066.7
3	23036.1	1039.3	1041.8
4	21703.5	1034.5	1074.1
5	19075.5	1021.4	1079.8

The data was assessed for normality. One-way ANOVA with post-hoc Tukey tests showed that there was no difference in RFU values between the dead cells group and the background (Alamar Blue solution only) group ($p = 0.998$); whereas there was a statistically significant difference between the control group and the no cell group as well as versus the dead cell group ($p < 0.001$). Therefore, the results of the control experiments demonstrated that any RFU value above the background RFU value reflected metabolic activity of viable RAW 264.7 murine macrophage cells.

5.4.2 Live/Dead Assay

For Live/Dead assay, a control experiment was performed to ensure that the assay could reliably be used to calculate the viability of the the RAW 264.7 murine macrophage cells in this study. There were two cell groups: (1) the 'live' cell group; the RAW 264.7 murine macrophage cells cultured in αMEM; and (2) the 'dead' cell group; control cells treated with acetone/methanol (50%), a known cytotoxic agent. The live cell group was placed into wells numbered 1 and 2; while the dead cells were placed into the wells numbered 3 and 4. All wells contained coverslips. The two cell groups were stained using the Live/Dead assay containing: (1) 4 μM calcein (stains living cells green); and (2) 2 μM Ethid-1 (stains dead cells red) in PBS for 30 minutes at (37 ± 1) °C. Three images were captured in each well. Live cells (green) and dead cells (red) were counted to estimate the cell numbers per image. The results are presented in Table 5-2.

Table 5-2: Live/Dead cell counts in wells 1 to 4.

	Wells Containing Live Cells		Wells Containing Dead Cells	
	Well 1	Well 2	Well 3	Well 4
Live Cell (Green) Count	89	95	0	0
	105	97	0	0
	99	100	1	0
Dead Cell (Red) Count	1	0	95	100
	0	0	98	104
	0	0	108	97

The results demonstrated that the alive (viable) and dead (non-viable) RAW 264.7 murine macrophage cells were stained green and red, respectively. Therefore, it was concluded that the two fluorescent dyes in the Live/Dead assay (calcein to stain living cells green and ethidium to stain damaged or dead cells red) could reliably be used to calculate the viability of the the RAW 264.7 murine macrophage cells in this study.

5.4.3 Repeatability of Live/Dead Assay

Repeatability refers to a system's ability to reproduce the same results in repeated trials with no change in experimental conditions. A visual counting process is required in calculating the viability using the Live/Dead assay. The repeatability of this quantitative assessment was assessed by calculating the intra-observer and inter-observer error in counting the number of green and red stained cells per image. Ten images obtained during the control experiment were counted by the investigator and a second observer. One of the investigators repeated the count the following day. The results are listed in Table 5-3.

Table 5-3: Intra-observer and inter-observer repeatability for Live/Dead cell counts.

	Investigator 1 Day 1		Investigator 1 Day 2	
Sample	Live Green	Dead Red	Live Green	Dead Red
1	89	95	90	93
2	87	78	85	80
3	97	88	95	86
4	89	78	90	80
5	79	75	81	73
6	90	84	89	85
7	85	88	85	90
8	98	84	99	86
9	78	95	77	95
10	88	99	90	97

	Investigator 1 Day 1		Observer Day 1	
Sample	Live Green	Dead Red	Live Green	Dead Red
1	89	95	87	92
2	87	78	85	75
3	97	88	91	84
4	89	78	85	75
5	79	75	80	70
6	90	84	87	85
7	85	88	83	85
8	98	84	95	80
9	78	95	75	93
10	88	99	84	97

There are a number of methods that can be used to assess repeatability. The repeatability coefficient and the limits of agreement for the measurements were calculated according to the method described by Bland and Altman [148]:

The repeatability coefficient = 2 × standard deviations

The limits of agreement (95% confidence interval) = the mean differences ± 2 × standard deviations.

A summary of repeatability errors is presented in the Table 5-4.

Table 5-4: Summary of repeatability errors.

	Intra-observer Error		Inter-observer Error	
	Green	Red	Green	Red
Mean Difference	-0.1	-0.1	2.8	2.7
Standard Deviation	1.5	1.9	1.8	1.6
Repeatability Coefficient	3.0	3.8	3.6	3.2
95% Confidence Interval	-3.1–2.9	-2.9–2.7	-0.8-6.4	-0.5–5.9

The counts indicated that for a new image, one can expect the two observers to differ by a maximum of 6.4 for green cells and 5.9 red cells, whereas the repeated counting by the same observer may differ by a maximum of 3.1 green cells and 2.9 red cells. One observer (the investigator) was responsible for all subsequent Live/Dead cell counting in order to minimise repeatability error.

5.4.4 Verification of Nanoparticle Size

As stated previously, it was important to use the metal nanoparticles that are representative of the particles generated *in vivo* in the current *in vitro* study. The size of metal particles identified in pseudotumour tissues was found to be 30-60 nm in diameter in the clinical study (Chapter 3). The size of wear particles has been reported to be an important factor that influences *in vitro* cytotoxic effects [149]. The manufacturer's stated average production nanoparticle size was 35 nm (range 30-50 nm). However, this value

may not reflect the true variation in particle size. Therefore, this represented a potential error which needed to be verified.

A control experiment was designed and performed. Various chemical solutions, such as those used in the isolation of nanoparticles from simulator lubricants, have been shown to adversely affect nanoparticle size [144]. Therefore, it was considered important to verify the commercially-manufactured nanoparticle size under the same *in vitro* culture conditions as those utilised in the current study. Thus, the nanoparticle size was determined after it had been co-cultured with the macrophages. The RAW264.7 cells were seeded on 5 mm diameter glass coverslips for 2 hours before 1×10^{13} nanoparticles/ml were added to the culture medium. After 4 days in the culture, the cell–biomaterial constructs were fixed in 4% glutaraldehyde for 48 hours. They were then serially dehydrated in 40, 70, 80, 90, 95, and 100% ethanol each for 15 minutes, and subsequently infiltrated in 50% hexamethyldisilazane in absolute ethanol and 100% hexamethyldisilazane for 20 minutes. These were replaced with fresh 100% hexamethyldisilazane before leaving the samples in a fume cabinet overnight to dry. The dried samples were carbon coated for examination with scanning electron microscopy (JEOL (UK) Ltd, Herts, UK).

Scanning electron microscopy (SEM) examinations demonstrated that the majority of metal particle sizes were 30-60 nm in diameter, which often formed large aggregates (up to 30 μm in diameter) (Figure 5-2). Thus, the variation in particle size was similar to the stated size range. Therefore, it was concluded that the size of commercially-manufactured

Co, Cr and Ti nanoparticles were representative of the particle size generated *in vivo* (Chapter 3) and subsequently could reliably be used to assess *in vitro* cytotoxicity in the current study.

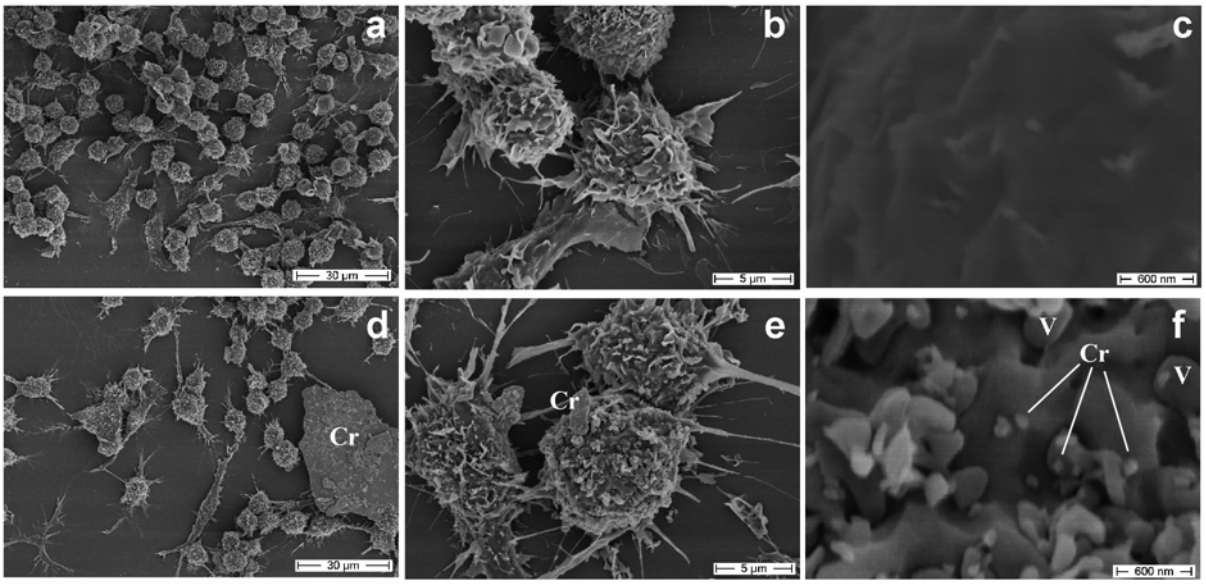
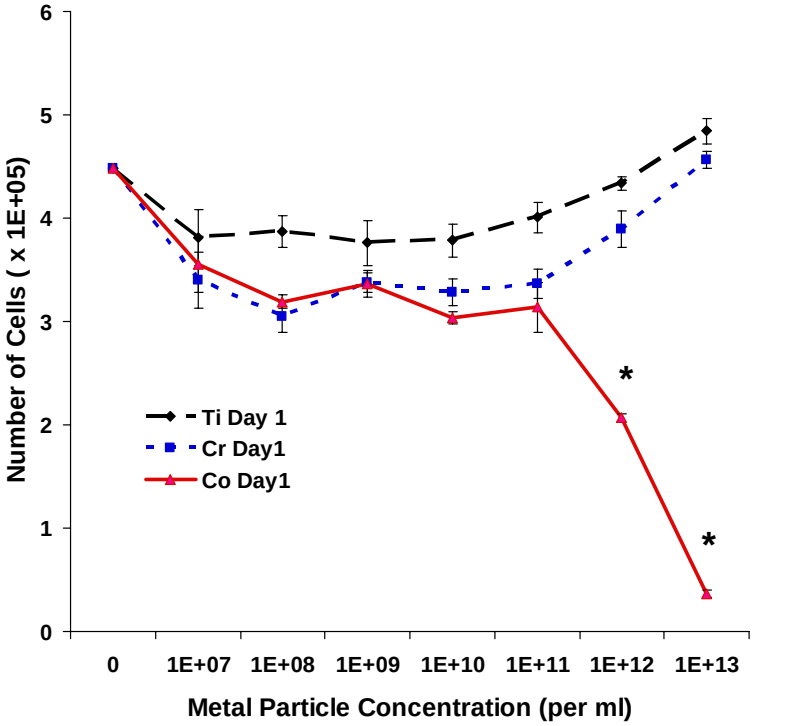


Figure 5-2: Micrographs of scanning electron microscopy (SEM) showing control RAW 264.7 cells and RAW 264.7 cells cultured with Cr nanoparticles *in vitro* for four days. No particles were observed in control cells at either low (a, b) or high magnification (c). Aggregation of nanoparticles could form large clumps (up to 30 µm in diameter) (d) or small particles (1-3 µm in diameter) (e). However, the majority of particles sizes were found to be 30-60 nm in diameter, which were attached to the surface of RAW 264.7 cells (f).

5.5 Results

5.5.1 Effects of Nanoparticles on the Viability of Macrophages

Light microscopic examinations suggested that the cytoplasm of the RAW 264.7 macrophages contained aggregates of Co, Cr and Ti particles at all concentration ranges (10^8 - 10^{13} particles/ml), except at 10^7 particles/ml. The overall number of viable cells, as measured with the Alamar Blue assay at day 1 and day 4 for metal nanoparticle groups, is shown in Figure 5-3. Compared to the control cells (no particles added, concentration 0 particles/ml), the Alamar Blue assay showed non-significant reductions in the total number of viable cells in all three metal nanoparticle groups for 1×10^7 to 1×10^{11} particles/ml concentrations ($p=0.11$). Both day 1 and day 4 showed the same trend. Interestingly, when particle concentrations were 1×10^{12} particles/ml, there was a striking difference between Co, Cr and Ti. In the Co group, the total number of viable cells sharply declined at concentrations between 1×10^{12} and 1×10^{13} particles/ml at both day 1 and day 4 ($p<0.05$). In the Cr and Ti group, there was no significant difference in the total viable number of cells compared to the control group at day 1 and 4 ($p=0.45$).



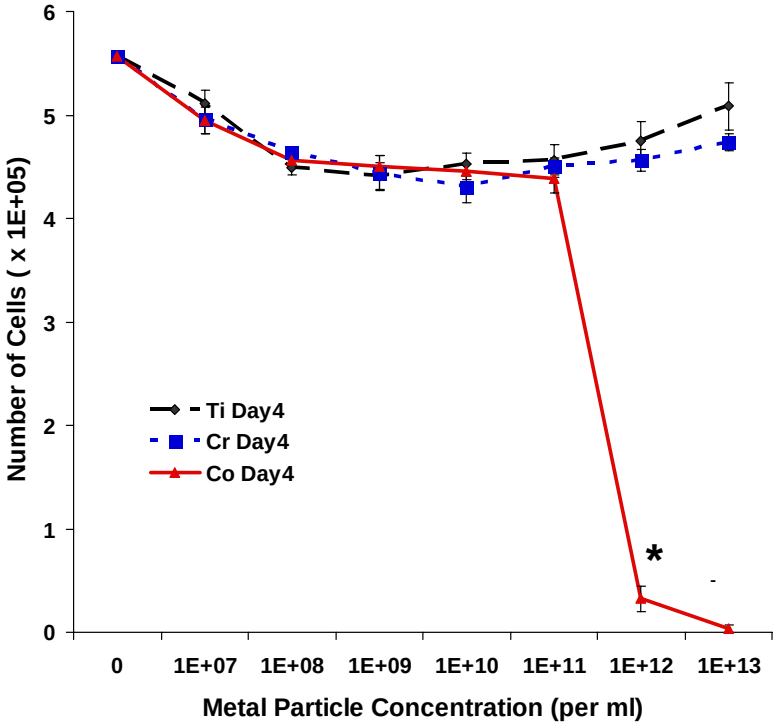


Figure 5-3: The effect of metal nanoparticles on RAW263.7 macrophage cell numbers at day 1 and day 4. Asterisk (*) indicates $p<0.05$ against the control cells (no particles added, concentration 0 particles/ml).

The Live/Dead staining showed that at high concentrations of nanoparticles (greater than 10^{12} particles/ml), Co nanoparticles were cytotoxic to the majority of cells (Figure 5-4). At 10^{12} particles/ml, Co significantly reduced the viability of the macrophages to 25% and 3% of the control group at day 1 and day 4, respectively. Thus, Co nanoparticles were cytotoxic to 75% and 97% of the overall number of macrophages at day 1 and day 4 ($p<0.001$) (Figure 5-5) respectively. In contrast, Cr and Ti nanoparticles demonstrated no significant reduction in cell viability at both day 1 and day 4 in comparison with the control group ($p=0.53$). Live/Dead assays performed at the concentrations less than 10^{12} particles/ml demonstrated no significant effect on the cell viability for all three metals.

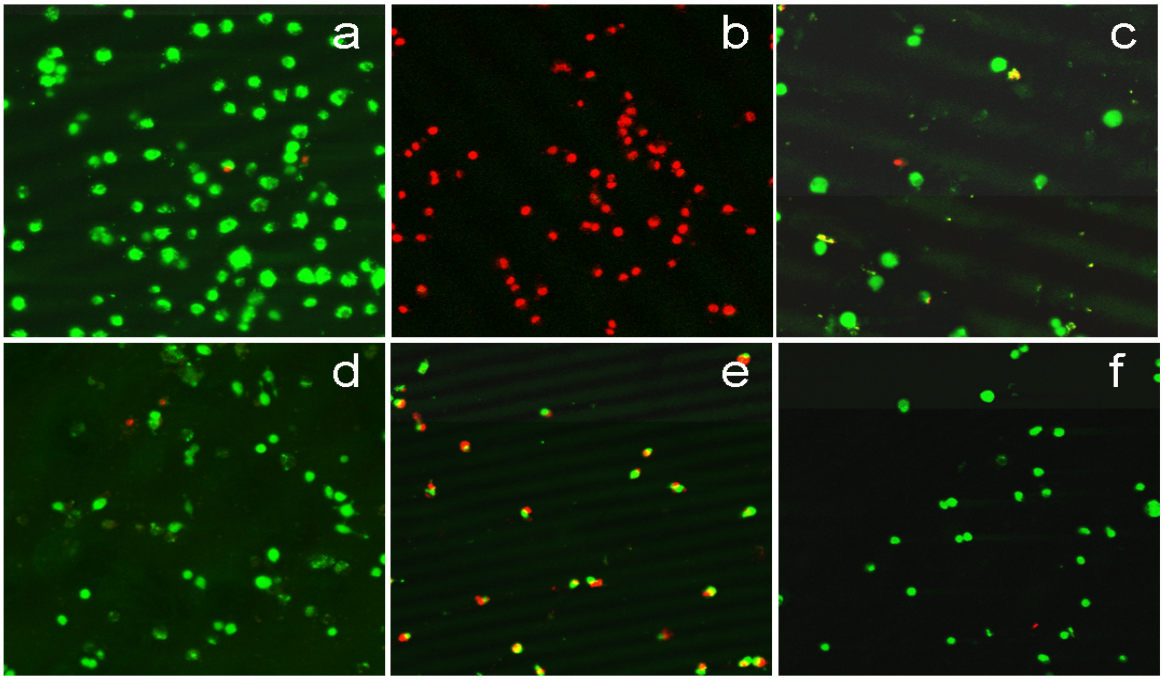


Figure 5-4: Confocal microscopic micrographs of Live/Dead staining at Day 1, with metal nanoparticle concentrations at 1×10^{12} particles/ml and metal ion concentrations at 1000 μM: (a) control (medium only); (b) Co nanoparticles; (c) Cr nanoparticles; (d) Ti nanoparticles; (e) Co ions; and (f) Cr ions. Live cells are stained green and dead cells are stained red (original magnification 200×).

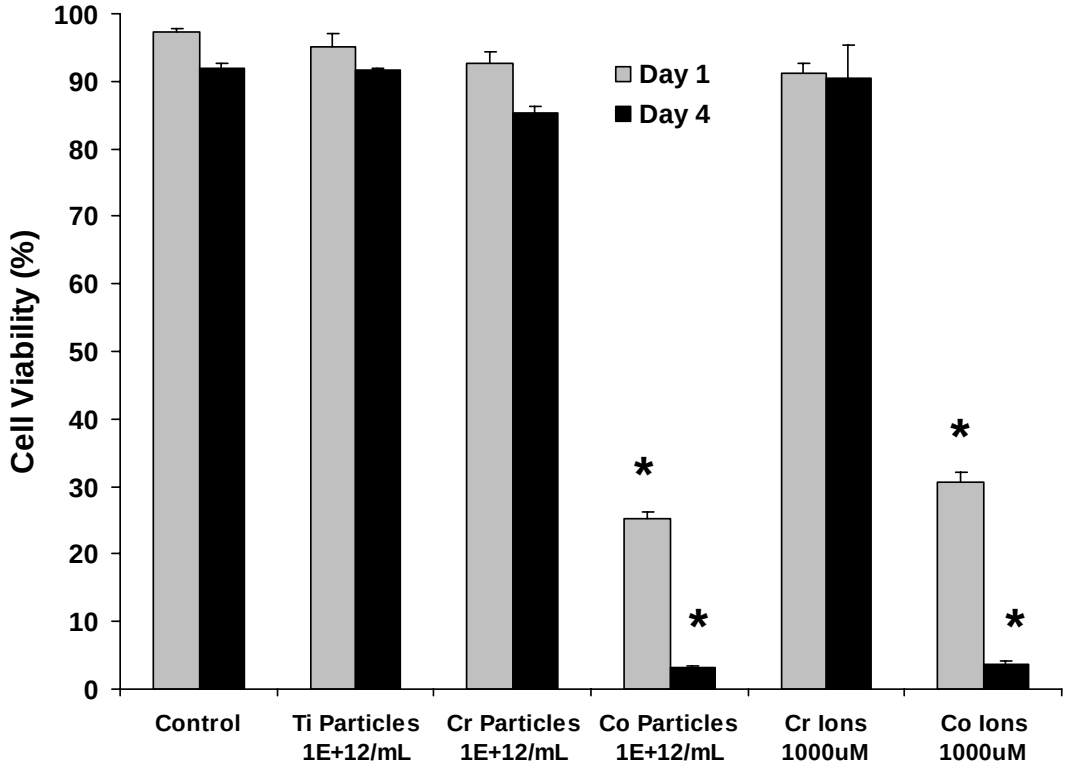
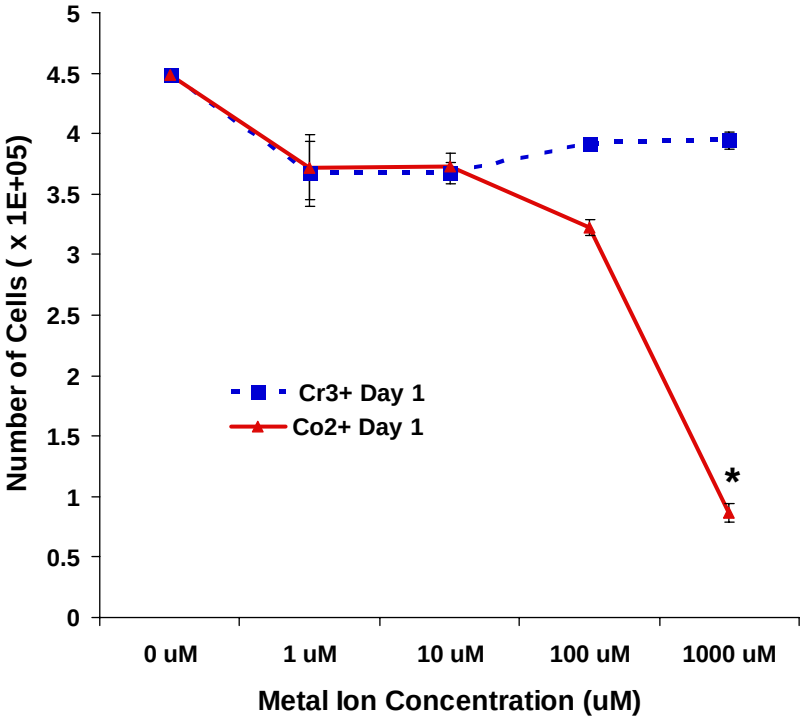


Figure 5-5: The effect of metal nanoparticles (1×10^{12} particles/ml) and ions (1000μM) on RAW263.7 macrophage viability at day 1 and day 4. Asterisk (*) indicates $p<0.05$ against the control cells (no particles added, concentration 0 particles/ml).

5.5.2 Effects of Metal Ions on the Viability of Macrophages

The overall number of viable cells, as measured with the Alamar Blue assay at day 1 and day 4 for metal ion groups, is shown in Figure 5-6. At concentrations between 1 μM to 100 μM, exposure to both metal ions led to a non-significant reduction in the overall viable cell numbers compared with control cells (no particles added, concentration 0 particles/ml) ($p=0.15$). Both day 1 and day 4 showed the same trend. At 1000 μM, Co^{2+} caused a dramatic decrease in total number of viable cells ($p<0.001$).



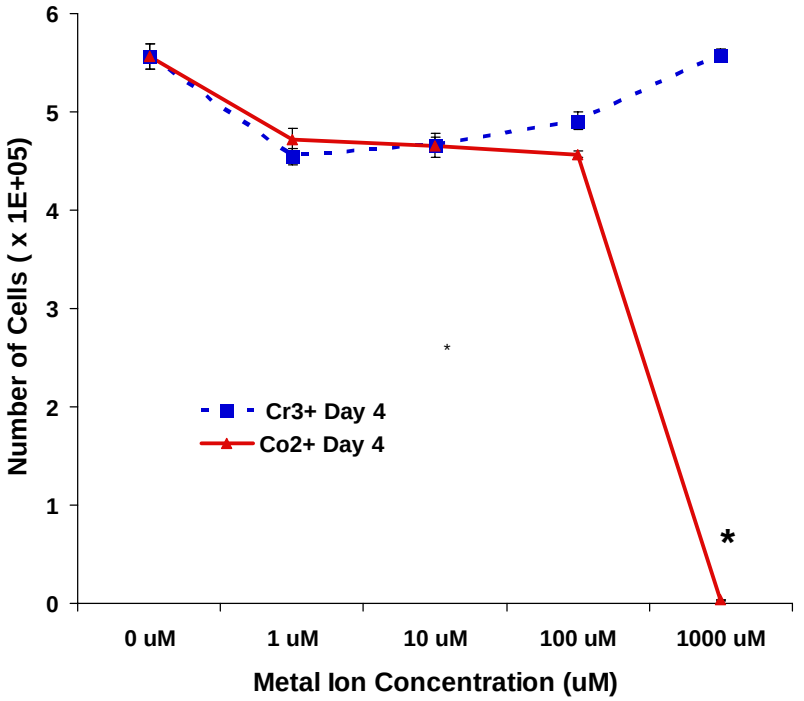


Figure 5-6: The effect of Co and Cr ions on RAW263.7 macrophage cell numbers at day 1 and day 4. Asterisk (*) indicates $p<0.05$ against the control cells (no metal ions added, concentration 0 μM).

At concentrations lower than 1000 μM, the Live/Dead staining showed that Co^{2+} and Cr^{3+} ions had no significant effects on the cell viability. However, at 1000 μM, Co^{2+} ions were cytotoxic to the macrophages: Co^{2+} ions significantly reduced the viability of the macrophages to 30% and 3% of the control group at day 1 and day 4, respectively. This indicates that Co^{2+} ions were cytotoxic to 70% and 97% of the overall number of macrophages ($p<0.001$) (Figure 5-5). Cell viability in the Cr^{3+} ion groups showed no significant reduction at day 1 and day 4 ($p=0.89$).

5.5.3 Metal Ion Release into the Culture Medium

Cobalt nanoparticles at concentrations of 10^{10}, 10^{11}, 10^{12},10^{13} particles/ml released 66 μg/l, 630 μg/l, 4777 μg/l, 14019 μg/l of Co ions into the culture medium, respectively. Cobalt ion levels measured in the culture medium with cobalt (II) sulphate heptahydrate at concentrations 1 μM, 10 μM, 100 μM, 1000 μM were 35 μg/l, 412 μg/, 4307 μg/l, 12958 μg/l, respectively. Thus, there was a high degree of linear correlation between Co ions released from Co nanoparticles and Co ion levels measured in the culture medium with cobalt (II) sulphate heptahydrate: Pearson's correlation coefficient (r): $r = 0.99$, $p < 0.001$ (Figure 5-7). Therefore, the particulate form of Co nanaparticles at concentrations of 10^{10}, 10^{11}, 10^{12}, 10^{13} particles/ml released equivalent concentrations of Co ion into the culture medium as corresponding 1 μM, 10 μM, 100 μM, 1000μM of cobalt (II) sulphate heptahydrate solutions. The linear correlation was not observed with Cr nanoparticles as they did not appear to corrode in the culture medium within 24 hours: Cr nanoparticles at concentrations 10^{10}, 10^{11}, 10^{12},10^{13} particles/ml released 1.0μg/l, 1.1 μg/l, 1.4 μg/l, 7.3 μg/l of Cr ions into the culture medium, respectively.

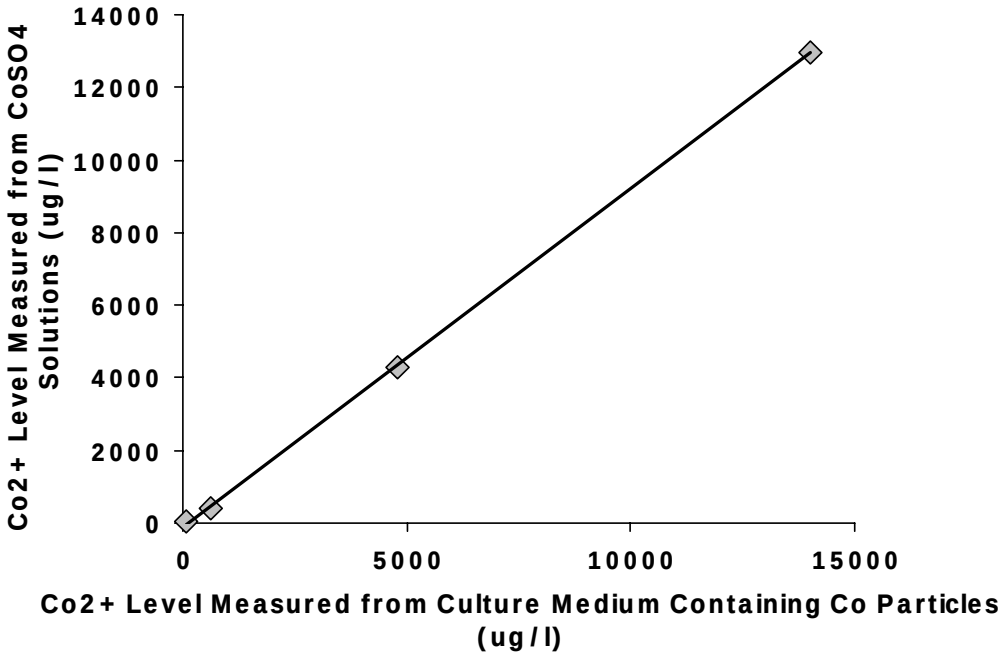


Figure 5-7: A linear correlation between the level of Co ions released from the particulate form of Co nanoparticles (corrosion) and the level of Co ions measured in the culture medium from cobalt (II) sulphate heptahyrate solution following 24 hours of incubation in the culture medium.

5.6 Discussion

The presence of extensive necrosis and heavy macrophage infiltrate were key histological features of pseudotumours (Chapter 3). Aggregates of metal particles within necrotic macrophages in extracellular tissue were found to contain both Co and Cr. Moreover, patients with pseudotumours had up to a twelve-fold elevation of median hip aspirate levels of Co and Cr ions in comparison to patients without pseudotumours (Chapter 3). These findings suggested that a local cytotoxic effect of chromium or cobalt on

macrophages may play a role in biological reactions involved in pseudotumours. However, potential cytotoxic effects of the phagocytosis of clinically relevant Co and Cr nanoparticles by macrophages *in vitro* have not been previously investigated.

Recently, the biological effects of nanometer-sized CoCr alloy particles on fibroblasts have been published [16, 149]. These studies have found that metal nanoparticles, in comparison with metal microparticles and ceramic particles, led to increased amounts of cellular damage, suggesting that there may be fundamentally different biological responses of human cells to metal wear particles *in vitro* which depend on the particle size. In the current study, potential cytotoxic effects were investigated on a different cell type, macrophages, using Co and Cr particles that were representative of the nanometer-sized metal wear particles generated from articular surfaces of MoM prostheses *in vivo* (Chapter 3). However, biological effects differed between the similarly-sized Co, Cr and Ti nanoparticles. Although both Co and Cr are the principal elements in the CoCr alloy used in metal-on-metal hip resurfacing implants, the dose-dependent cytotoxicity was observed only with Co nanoparticles. The *in vitro* cytotoxicity of Co nanoparticles and ions are consistent with previous reported studies on the toxicity of micrometer-sized Co particles and their ions on macrophages and osteoblasts [150, 151]. The release of soluble ions from the surface of the particles is influenced not only by particle size, but also depends on shape and chemical composition. Thus, a greater release of metal ions in solution from Co nanoparticles in comparison to Cr nanoparticles may, in part, explain why Co is more cytotoxic.

Cytotoxicity of the Co nanoparticles on the macrophages may be due to the nanoparticles themselves or mediated by Co ions in solution. The correlation of Co ion concentrations in the culture medium following corrosion of Co nanoparticles indicates that 1×10^{12} particles/ml of Co nanoparticles (the cytotoxic concentration) released equivalent concentrations of Co ions into the culture medium as 100 μM of cobalt (II) sulphate heptahydrate, which is one order of magnitude less than the cytotoxic Co ion concentration (1000 μM). Although synergistic effects of nanoparticles together with ions cannot be excluded, the results suggest that cytotoxicity of Co nanoparticles *in vitro* is likely to be a result of nanoparticles (once they are phagocytosed into cells in their particulate form), rather than diffusion of metal ions, produced from corrosion of nanoparticles extracellularly in the culture medium. Furthermore, the critical cytotoxic Co ion concentration of 1000 μM found *in vitro* is two orders of magnitude higher than the concentration range than that found in hip aspirate (20μM, Chapter 3), and five orders of magnitude higher than the concentration range found in serum (0.1μM, Chapter 3) *in vivo* in MoMHRA patients with pseudotumours. Although it is possible that prolonged duration of continuous exposure at lower concentrations *in vivo* may lead to cytotoxicity, Co ion concentrations present in serum and hip aspirates may not be sufficient to cause cytotoxicity.

Inside the cells, Co ions have been shown to participate in Fenton-like reactions with hydrogen peroxide, leading to the generation of free radicals which result in cellular damage [96]. Thus, corrosion of phagocytosed nanoparticles may lead to toxic levels of

intra-cellular ion concentration. Therefore, cytotoxic processes occurring in macrophages *in vivo* is also likely to be mediated predominantly by Co nanoparticles, in which phagocytosed nanoparticles lead to a direct effect on cells via intra-cellular corrosion.

Phagocytosis of nanoparticle aggregates by RAW 264.7 macrophages were suggested by microscopical observations. The metal nanoparticle concentrations present in the periprosthetic tissues of patients with pseudotumour have not been established. However, the high concentrations of metal nanoparticles required for cytotoxic effects *in vitro* (greater than 10^{12} particles/ml) are unlikely to be achieved in the periprosthetic environment *in vivo* under normal kinematic conditions with well functioning contemporary MoM bearing implants, which have been estimated to generate a total number of metal particles around 6.7 x 10^{12} per year [65]. Therefore, the high cytotoxic concentrations are likely to result *in vivo* only when there is increased production of Co nanoparticles due to excessive implant wear [124].

The presence of metal particles contained within macrophages, juxtaposed with extensive necrosis of connective tissue, has been observed in the periprosthetic tissues from failed MoM bearing implants including those with pseudotumours [37, 42, 104, 106, 107]. The *in vitro* cytotoxicity of metal nanoparticles would be consistent with the observed areas of necrosis surrounded by macrophages in pseudotumours *in vivo*, where there is likely to be a long exposure time and a high level of metal wear debris. It is postulated that phagocytosis of Co nanoparticles by macrophages leads to cytotoxicity due to Co ions released during intra-cellular corrosion. This would lead to a vicious cycle of necrosis,

recruitment of macrophages to areas of clustered dead macrophages and re-phagocytosis leading to an expanding necrotic zone. The necrosis may be caused in a dose-dependent manner, where the saturation threshold is dependent on the duration of exposure and magnitude of metal debris. Pseudotumour-like histological appearance of an extensive area of tissue necrosis separated from viable tissue by macrophages containing large numbers of intracellular metal particles has been observed in a post-mortem study in subjects with cobalt-chrome prostheses [152]. Necrosis was observed only in organs with high metal concentrations whereas it was not observed in the liver and the kidney, which had lower concentrations of metal debris.

There are several study limitations. Although the combined effects of cobalt and chromium nanoparticles were not investigated in the current study, the use of commercially-manufactured Co and Cr nanoparticles allowed assessment of the relative cytotoxicity of Co compared to Cr, which has not been investigated previously. Chromium exists in the body in two valencies: trivalent (Cr^{3+}) and hexavalent (Cr^{6+}) [64, 153]. Hexavalent chromium was not investigated in this study. However, hexavalent chromium has been shown to be much more unstable in solution, as it undergoes rapid reduction to the less biologically active trivalent Cr. In addition, the predominant valency that exists *in vivo* remains controversial [126]. Measurements of various cytokines would have provided additional information regarding the inhibition or activation of macrophages. However, the current study focused on the cytotoxic effect upon macrophages rather than cellular activation. In order to more accurately measure cell death, or cytotoxicity in the current study, a second assay, the Live/Dead assay, was used

to quantify the numbers of both viable (live) and non-viable (dead) cells. Cell viability was then calculated relative to the total numbers of macrophages.

In conclusion, cobalt nanoparticles and ions have dose-dependent cytotoxic effects on macrophages *in vitro*, which is likely to be mediated by the particulate form of nanoparticles themselves rather than by their corrosion into ions in the culture medium. The high concentration of cobalt nanoparticles required for cytotoxicity of macrophages *in vitro* suggests that increased production of cobalt nanoparticles *in vivo*, due to excessive MoM implant wear, may lead to local adverse biological effects. However, the individual biologic response to the presence of wear debris may vary, resulting in a different toxic-effect threshold or immunological intolerance. Therefore, in susceptible patients, cytotoxicity of high concentrations of Co nanoparticles phagocytosed by macrophages located in the periprosthetic tissues, leading to necrosis, may be an important factor in the occurrence of pseudotumours.

5.7 Summary

- The results of this study demonstrated that cobalt nanoparticles and ions have dose-dependent effects on the viability of macrophages *in vitro*. Therefore, the first null hypothesis, which stated that there is no difference in the viability of macrophages *in vitro* in the presence of cobalt nanoparticles and ions, when compared to a control, could be rejected. The second null hypothesis, which stated that there is no such difference for chromium nanoparticles and ions, could not be rejected.
- This *in vitro* finding suggests that the local cytotoxicity of high concentrations of cobalt nanoparticles phagocytosed by macrophages located in the periprosthetic tissues, with subsequent tissue necrosis, may be an important biological reaction involved in mediating the occurrence of pseudotumours in patients with MoMHRA.
- Therefore, it is concluded that further studies focused firstly on assessing the magnitude of bearing surface wear that occurs in pseudotumour patients, and secondly on elucidating potential mechanisms responsible for the increased implant wear in these patients are warranted.

CHAPTER 6 *IN VITRO* MEASUREMENT OF MOMHRA WEAR

6.1 Introduction

Blood concentrations of metal ions have been considered as potential surrogate markers of MoM bearing surface wear, as it is not possible to measure wear of bearing couples radiographically in metal-on-metal hip systems. This assumption is supported by recent wear measurements of retrieved femoral components [124]. Elevated serum metal ion concentrations were significantly correlated with greater amounts of femoral component linear wear. Thus, it has been suggested that serum metal levels can be used to estimate wear.

The results of the prevalence study (described in Chapter 3) demonstrated that a soft tissue pseudotumour in patients with MoMHRA was associated with elevated serum and hip aspirate cobalt and chromium ion levels. Patients with a pseudotumour had up to a six-fold elevation of median serum levels and up to a twelve-fold elevation of median hip aspirate levels of Co and Cr ions in comparison to patients without pseudotumours. As wear is positively correlated with the elevation of metal ion concentrations *in vivo*, this suggests that pseudotumours occur in patients with contemporary MoMHRA implants when there is increased wear at the MoM articulation. Furthermore, edge-loading, a phenomenon whereby the femoral component comes into contact with the edge of the acetabular component, has been suggested as a possible mechanism that leads to increased wear in MoMHRA implants [95, 124, 154, 155]. However, direct assessment of

wear and occurrence of edge-loading in MoMHRA implants has not been previously investigated in patients with pseudotumours.

The importance of retrieved implant analysis in understanding the pattern and the magnitude of MoM implant wear is well established in the literature [61, 154]. The aims of this study were therefore firstly to quantify the wear of MoMHRA implants revised for pseudotumours using direct measurement (i.e. not by metal ion assessment) and compare this measurement to that for a control group of MoMHRA implants revised for other reasons of failure, and secondly, to establish whether the edge-loading phenomenon occurs in implants revised for pseudotumours.

6.2 The Null Hypotheses

H_0: There is no difference in the linear wear rates between MoMHRA implants revised due to pseudotumours and a control group of MoMHRA implants revised due to other reasons of failure.

H_0: There is no difference in the incidence of edge-loading between MoMHRA implants revised due to pseudotumours and a control group of MoMHRA implants revised due to other modes of failure.

6.3 Materials and Methods

6.3.1 Ethics Approval

MoMHRA implants retrieved at the time of revision surgery usually contain small amounts of residual bone adherent to the implant. The study objective was to analyse the

surfaces of the implant for evidence of wear rather than the adherent bone, which had already been routinely examined for diagnostic information. However, as the adherent bone can be difficult to remove from the implants, it was considered that the retrieved implant-bone units constituted human tissue. According to the Human Tissue Act 2004, there are no statutory requirements to the need for consent to the storage or use of tissue from existing holdings for research. However, this study adhered to the Human Tissue Authority's (Department of Health, United Kingdom) recommended code of practice by formally seeking and subsequently obtaining approval from the local Research Ethics Committee (Oxford Research Ethics Committee B: 07/H0605/151, Amendment 2) prior to accessing implants from the existing holdings.

6.3.2 Selection of Retrieved Implants

The current study aimed to investigate two groups of retrieved implants: (1) Group 1 – MoMHRA implants retrieved from patients who underwent revision surgery due to the presence of pseudotumour; and (2) Group 2 (control) – MoMHRA implants retrieved from patients who underwent revision surgery due to other causes of failure. The study needed to be performed on representative samples in each implant group to ensure a valid generalisation of the findings. This was of particular concern in selecting implants for the pseudotumour group, because the presence of pseudotumour is not a well-established revision indication. In order to minimise selection bias, the retrieved implants were selected using the following selection criteria:

1. Inclusion criteria:

(a) MoMHRA implants of a contemporary design that are currently in use. This was imposed to reflect the design of MoMHRA implants in the prevalence study (Chapter 3) in whom the elevated metal ion concentrations were found.

(b) MoMHRA revision surgery diagnosis of pseudotumour was confirmed by medical records, operative notes as well as the final histopathology reports. Specifically, the following requirements were set: (i) the presence of soft tissue pseudotumour mass was documented in the revised resurfaced hip pre-operatively; (ii) the stated indication for revision surgery was solely due to the presence of pseudotumour; and (iii) the final diagnosis of the histopathology report of the tissue specimen by the musculoskeletal pathologist was pseudotumour, in accordance with the published histological features of pseudotumour [37, 42].

(c) MoMHRA revision surgery diagnosis in the non-pseudotumour group was limited to femoral neck fracture and infection. Femoral neck fractures and infection represented two MoMHRA failures that could be reliably established from the operative notes and/or histopathology reports. Other reasons for failure such as component loosening can have multiple underlying causes and thus, the diagnosis is often difficult to establish. Therefore, the revision indications of femoral neck fractures and infection were chosen for the non-pseudotumour group.

2. Exclusion criteria:

(a) MoMHRA implants that had been severely damaged at removal were excluded, as these would have led to unreliable roundness measurement and hence wear estimation.

(b) MoMHRA implants in the pseudotumour group which showed discrepancy between the operative indication and the histopathology report were excluded. This exclusion ensured that diagnosis of pseudotumour was confirmed by medical records, operative notes as well as the final histopathology report in all MoMHRA implants in the pseudotumour group.

6.3.3 Collection of Retrieval Implants

Archived holdings at the Histopathology Department, Nuffield Department of Orthopaedic Surgery contained retrieved MoMHRA implants obtained from revision surgeries performed at the Nuffield Orthopaedic Centre. In order to maximise the number of specimens in the study, implants were also collected from an additional centre. This was necessary largely due to the stringent selection criteria for implants. A collaboration was established with the researchers at the Implant Development Centre (IDC), Leamington Spa, UK, which holds a collection of retrieved BHR implants. A limited number of MoMHRA implants held by the IDC met the selection criteria and these were included in the study. A total of 16 implants were collected from the archived holdings at the Histopathology Department, Nuffield Department of Orthopaedic Surgery. This cohort included all MoMHRA implants in the pseudotumour group. A further 14 implants were available from the IDC.

In total, 30 MoMHRA implants were investigated. There were 8 MoMHRA implants retrieved from the patients who underwent revision surgery due to the presence of pseudotumour (Group 1) and 22 MoMHRA implants retrieved from the patients who

underwent revision surgery due to femoral neck fractures or infection (Group 2). A summary of the implants in each group is provided in Table 6-1. Although seven out of eight implants in the pseudotumour group contained both the acetabular and the femoral components, the acetabular components were not available for analysis in four femoral neck fracture cases as they were not always replaced when the femoral component was revised.

Table 6-1: Summary of retrieved implants.

	Pseudotumour Group	Non-Pseudotumour Group
Number of implants	8	22
Gender (female: male)	8: 0	13: 9
Age (years)	52 (range 39 - 65)	54 (range 45 - 70)
Time *in vivo* (years)	3.6 (SD ± 2.3)	2.3 (SD ± 1.2)
Implant Type	BHR (5) Conserve Plus (2) Cormet (1)	BHR (18) Conserve Plus (4)
Femoral component size (mm) (± Standard deviation, SD)	47 (± SD 4)	48 (± SD 5)

6.3.4 Study Power Estimation

Due to a limited number of available retrieved implants that met the selection criteria, it was important to estimate the power of the study. Power of a test is the probability of correctly concluding that a treatment difference of a specified size exists. There are various methods that can be used to determine the power of a study for a specified sample size. Specific formulae can be used to test different hypotheses, however, these formulae are complex and their use time-consuming. An alternative and simple approach is to use the nomogram described by Altman [156]. It incorporates a number of relevant factors

into the calculations: the study sample size, the significance level, and the standardised difference defined as a ratio of the difference of interests to the standard deviation of the observations.

For linear wear rate of MoMHRA, a significant difference of interest was 10 μm, which represented a 2-fold increase from the reported steady-state wear rate of 5 μm for MoM bearings [14]. Based on repeated measures taken during a pilot study on five implants, the expected measurement standard deviation was estimated to be 8 μm. Thus, a standardised difference of 1.25 was calculated. The statistical significance level was set at 0.05. Using Altman's nomogram, the current study sample size of 30 estimated the power at 0.90. This implied that the study had 90% probability of correctly concluding that a difference of 10 μm exists. However, study power estimation is not a precise process because the parameters used for calculations are imprecisely estimated. In addition, the nomogram is used under the assumption that equal sized samples are required, thus the unequal sized samples in this study would have further reduced the power. Despite these limitations, it was concluded that the current study had sufficient power to detect wear rate differences between the two implant groups.

6.3.5 MoMHRA Implant Wear Measurement

Wear of bearings is a progressive loss of bearing substance from the implant bearing surfaces [143]. There are two methods that are commonly used to measure bearing surface wear. The wear can be quantified gravimetrically by sequential measurements of any weight loss of a material. Wear is then presented as weight loss, which is converted

to volumetric wear. Alternatively, linear wear can be quantified as the maximum deviation from ideal sphericity. This method calculates the highest local wear for a component, allowing determination of both the magnitude as well as location of wear. These two parameters were of interests in this study. Linear wear, in turn, can be measured using either a coordinate measurement machine or roundness machine.

The established method using a coordinate measuring machine involves digitisation of the coordinates of approximately 300 to 400 points along equally spaced traces radiating from the centre of implant bearing surfaces [62]. Computer software is then used to fit a perfect sphere. The radial distance of the data points from the surface of this sphere indicates the local depth of wear. However, the wear data on the acetabular cup has been reported to be unreliable in cases where there is insufficient non-worn surface for accurate fitting of the nominal sphere [62]. Alternatively, roundness machine measurement is another well established technique that has been used to measure wear in ceramic-on-ceramic bearings [157, 158] and more recently in MoMHRA [155]. A roundness machine has a higher accuracy compared to a coordinate measurement machine (0.02 μm vs. 1 μm) [158]. Moreover, these devices have been used to demonstrate a morphological pattern of wear occurring at the edge of the MoMHRA acetabular cup (edge-loading). Therefore, a roundness machine was considered best suited to the aim of this work and was selected to measure linear wear in this study.

6.3.6 Linear Wear Assessment Using a Roundness Machine

All implants were catalogued with an identification number to ensure patient anonymity. The components were not autoclaved between removal and examination. The bearing surfaces of the retrieved components were first inspected with the naked eye under bright lighting. The linear wear of retrieved MoMHRA femoral and acetabular bearing surfaces was assessed using a Taylor-Hobson Talyrond 290 Roundness machine (Taylor Hobson Ltd., Leicester, United Kingdom). The roundness testing machine measures both partial and full circles. The machine was used to measure the radial sphericity of the femoral and acetabular components in several planes. The maximum linear wear, recorded in micrometers (μm), was measured by subtracting the wear profile from an ideal circle.

Firstly, the component was centred in the roundness machine measurement plate until the measuring gauge was in contact with the bearing surface. Multiple equatorial roundness profiles were then taken from the skirt of the femoral component and the edge of the acetabular component toward their polar regions to locate the maximum wear on each component (Figure 6-1). This was done in a sequential manner in 5 μm increments. The wear area was defined as deviation from an ideal sphericity greater than 2 μm, as this value corresponded with the reported manufacturing tolerances. Thus, a deviation above this value was likely to be due to wear. Once the wear area was located, further equatorial roundness profiles were taken in 1 μm increments away from the area in order to identify the maximum wear area. Polar measurements perpendicular to the equatorial axis were also taken at the maximum wear area. The location of the wear scar (maximum depth of wear) was recorded in degrees from the centre of polar region on the prosthesis.

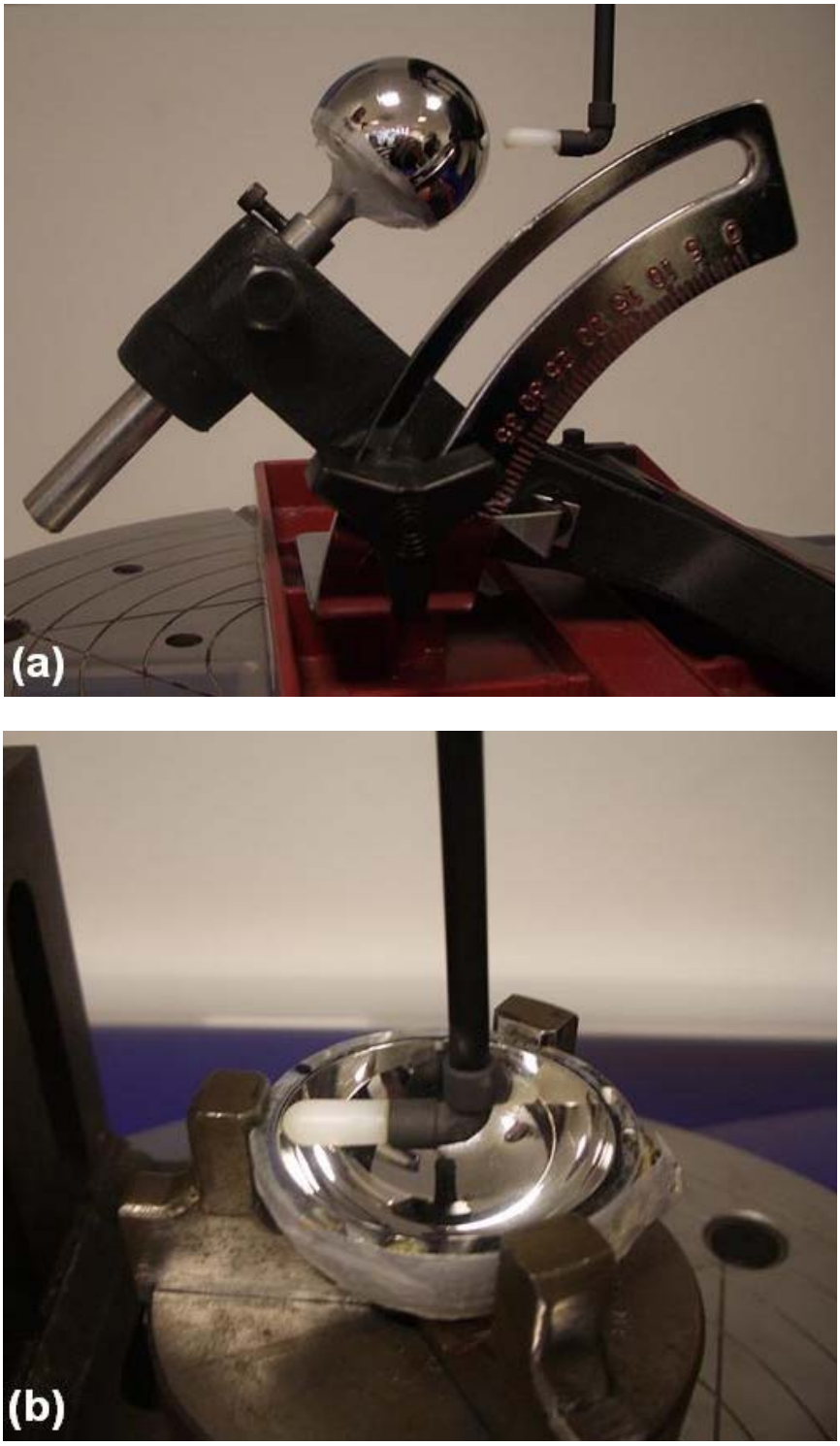


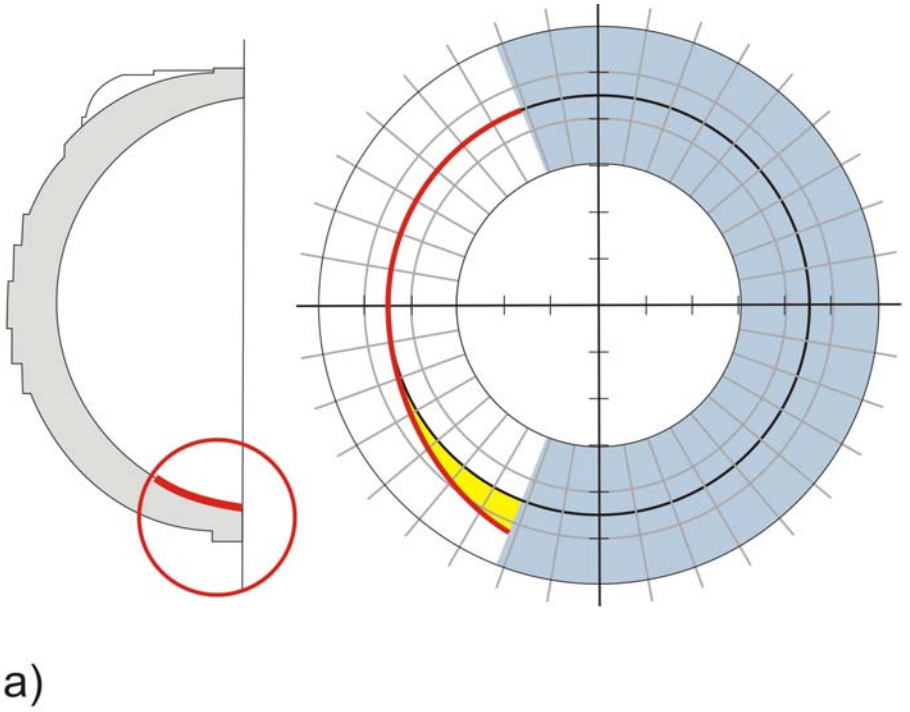
Figure 6-1: Photographs of the roundness machine set-up used to measure linear wear of the retrieved femoral head (a) and acetabular cup (b) components.

Estimation of Linear Wear Rate

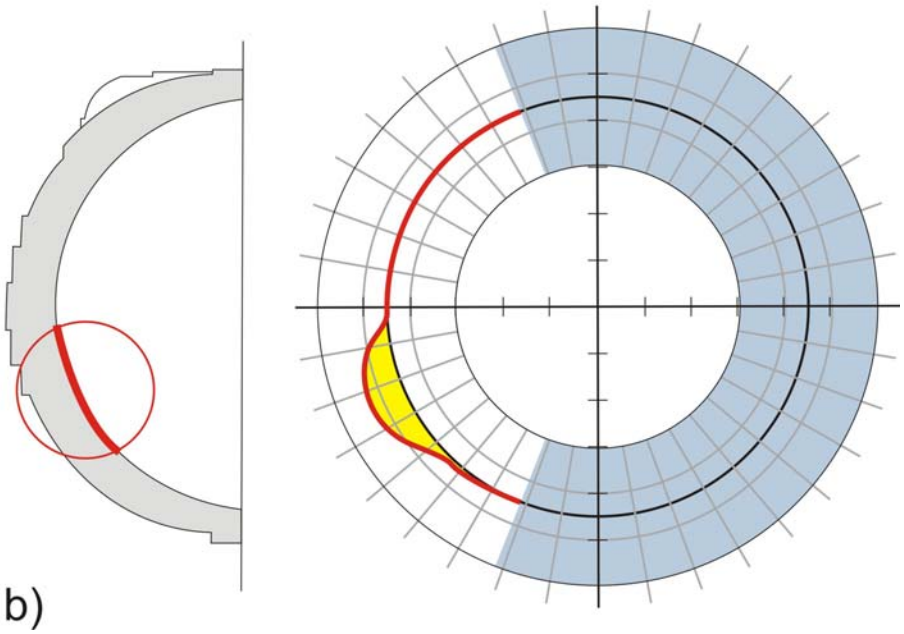
The linear wear depth was defined as the maximum value of the distance between the wear profile from an ideal circle recorded in micrometer (μm). For each MoMHRA femoral and acetabular component, the average linear wear rate was defined as the maximum linear wear scar depth divided by the duration of the implant *in vivo* (years).

Edge-Loading Definition

Edge-loaded components were defined as acetabular cups which showed the maximum area of wear crossing over the edge of the cup (Figure 6-2). Non-edge-loaded components were defined as acetabular cups which showed the maximum wear area on the cup occurring within the hemispheric bearing surface of the cup.



a)



b)

Figure 6-2: Roundness profiles of a) edge-loaded and b) non-edge loaded acetabular cup components. The maximum wear area (shaded in yellow) is located at the edge of the cup for the edge-loaded (a), while the maximum wear area occurs well within the cup in the non-edge loaded cups (b).

6.3.7 Statistics

The data set was assessed for normality. Mann-Whitney non-parametric tests were used to calculate the level of statistical significance for the differences in the non-normally distributed linear wear rate between the pseudotumour and non-pseudotumour implant groups. Pearson's correlation analyses, expressed as Pearson's correlation coefficient, were calculated to assess the strength of correlation between the linear wear rate and time to revision. The incidence of edge-loading in each group was compared using the Fisher's exact test. Differences at $p < 0.05$ were considered to be significant. SPSS® statistical software release 13.0 (SPSS Inc. Chicago, IL, USA) was used to perform the statistical analyses.

6.4 Control Measurements

In this study, linear wear rate, a calculation based on the dimensions of the retrieved components, was used as an objective measure of wear. This method requires an assumption of the initial sphericity of each component in order to determine wear as a deviation from perfect roundness. Thus, measuring linear wear was dependent on an accurate knowledge of the sphericity of the MoMHRA implants at insertion. The manufacturers' stated production tolerance for implant sphericity is ± 2 μm. However, this value may not reflect the true variation in implant roundness. This represented a potential error which needed to be quantified.

A control experiment was designed and performed. Ten unused MoMHRA implant pairs were measured using an identical method used in measuring the retrieved implants. The implants were BHR's, which was the most common implant type measured in the current study. The sizes of the BHR pairs tested were: 42 – 54 mm for the femoral components; and 48 – 60 mm for the corresponding acetabular components. The results of the control experiment demonstrated that the true variation in implant sphericity was 0.74 μm (standard deviation ± 0.3 μm) and 1.0 μm (standard deviation ± 0.4 μm) for the femoral and acetabular component, respectively. Thus, the uncertainty in the sphericity of each MoMHRA implant was within 1.0 μm, indicating that the variation remained well within the stated tolerance. The control experiment has also indicated that the roundness machine could reliably be used to measure sphericity of MoMHRA implants. Therefore, this measurement method was subsequently used to calculate linear wear (deviation from an ideal sphericity) of the retrieved implants.

6.5 Results

6.5.1 Qualitative Assessment

Qualitative assessment of wear of MoMHRA implants was performed by inspecting the bearing surfaces of implants under bright lighting. Post-retrieval damage artefacts were evident in a number of implants as isolated scratches or dents. In all cases, fine scratches were observed on the polar regions of bearing surfaces of the femoral head and the acetabular cup. There was no evidence of delamination or pitting appearances reported in MoP bearings [159], or stripe wear reported in ceramic-on-ceramic bearing couples [160]. This may be explained by the ability of MoM bearings to self-polish by wearing

down the surface surrounding a scratch, which may hide any distinctive visible stripe on the head. Thus, there was minimal wear damage visible to the naked eye in all implants.

6.5.2 Linear Wear Rate

In comparison with the non-pseudotumour implant group, the pseudotumour implant group was associated with (Figure 6-3):

(1) significantly higher median linear wear rate of the femoral component: 8.1 μm/year (range 2.75 - 25.4 μm/year) vs. 1.97 μm/year (range 0.82 - 13.00 μm/year), p=0.002; and

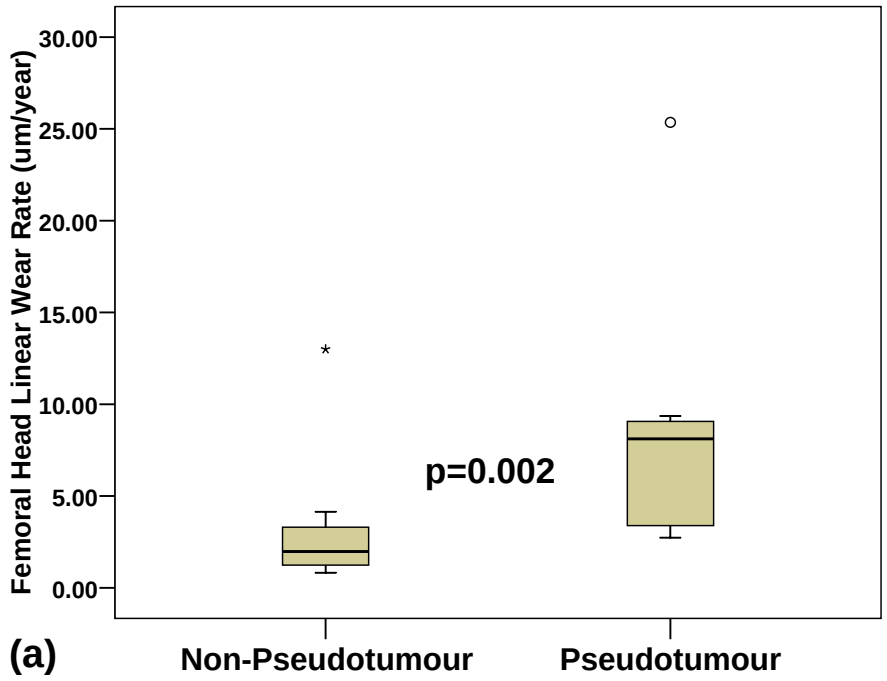
(2) significantly higher median linear wear rate of the acetabular component: 7.36 μm/year (range 1.61 - 24.9 μm/year) vs. 1.28 μm/year (range 0.18 - 3.33 μm/year), p=0.001.

Similarly, differences were also measured in absolute wear values. The median absolute linear wear was significantly higher in the pseudotumour implant group:

(1) 21.05 μm (range 2.74 - 164.80 μm) vs. 4.25 μm (range 1.30 - 8.80 μm) for the femoral component, p=0.005; and

(2) 14.87 μm (range 1.93 - 161.68 μm) vs. 2.51 μm (range 0.23 - 6.04 μm) for the acetabular component, p=0.008.

In all cases, the maximum wear occurred in localised zones.



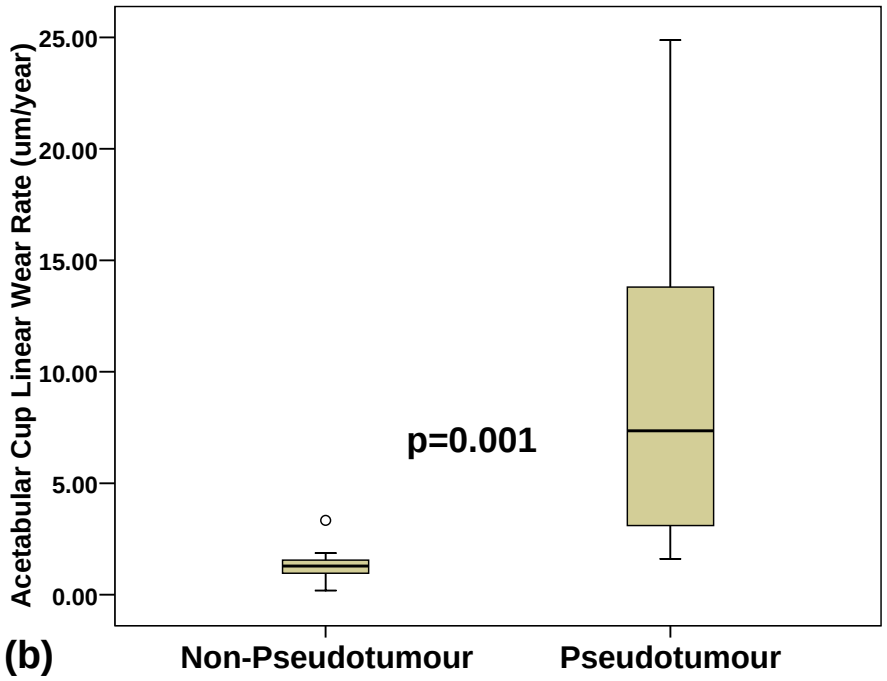


Figure 6-3: Boxplots showing differences in the linear wear rates of the a) femoral head and b) acetabular cup components between the two implant groups.

There was a poor linear correlation between the linear wear rate and the time *in vivo*: Pearson's correlation coefficient (r): r = 0.33 for femoral component, and r = 0.32 for acetabular component (Figure 6-4). In addition, there was no significant difference in linear wear rate between the fracture and infection sub-groups within the non-pseudotumour group (p=0.41).

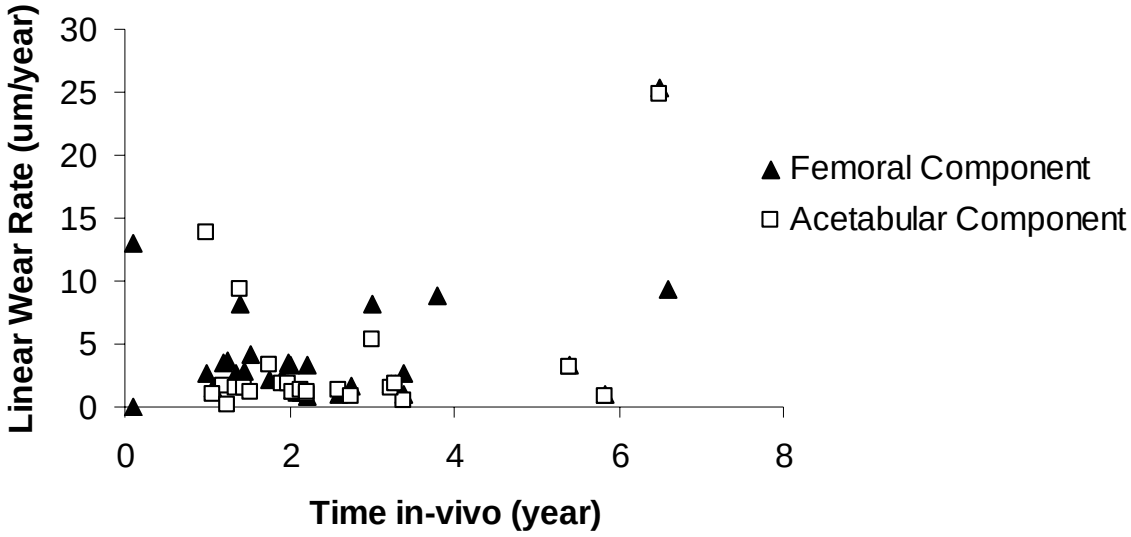


Figure 6-4: Linear wear rates of all retrieved implants are plotted against time *in vivo*.

6.5.3 Edge-Loading

Using the definition of edge-loading previously described (Figure 6-2), edge-loading was observed in all acetabular components (100%) in the pseudotumour group. In contrast, edge-loading was observed in only one acetabular component (6%) in the non-pseudotumour group of implants. The deepest wear was observed well within the bearing surface in the rest of this group. The difference in the incidence of edge-loading between the two groups was statistically significant (Fisher's exact test, p=0.03).

6.6 Discussion

Wear debris from MoM bearing surfaces is generated by mechanical wear, surface corrosion or a combination of both. It consists of both insoluble particles and soluble metal ions, the latter disseminating into the systemic circulation [15]. MoMHRA patients with pseudotumours were found to have up to a six-fold elevation of median serum levels and up to a twelve-fold elevation of median hip aspirate levels of cobalt and chromium ion levels in comparison to patients without pseudotumours (Chapter 3). In fact, pseudotumours were not detected in those patients who had normal cobalt and chromium levels. In light of the recently reported positive correlation between the elevated serum metal ion concentrations and the greater amounts of MoMHRA implant wear [124], these study results suggested that pseudotumours occur when there is increased wear at the MoM articulation. However, direct wear measurement of MoMHRA implants has not been previously investigated in patients with pseudotumours.

The results of the current retrieval study demonstrated that MoMHRA implants revised due to pseudotumour were associated with significantly greater linear wear of both femoral head and acetabular cup components. Implants in the pseudotumour group had up to a four-fold increase of median linear wear rate of the femoral component and greater than a five-fold increase of median linear rate of the acetabular component, in comparison with implants in the non-pseudotumour group. Interestingly, the median linear wear rates of the femoral components measured in the pseudotumour group in this study were, however, similar to the wear rates recently reported in 8 BHR femoral

components revised for non-pseudotumour-related failures [161]. Seven out of eight implants in the report were revised within 15 months of surgery. It is difficult to compare these values as the values determined from short-term retrievals during the run-in phase are higher than the steady state values. In fact, a five-fold reduction in annual wear rate from the first year run-in phase to the third year steady-state has been measured in MoM bearings [14]. The mean time *in vivo* for both implant groups in the current study was during or beyond the third year of implantation (3.6 years for the pseudotumour group and 2.3 years for the non-pseudotumour group). Furthermore, a variation in the methods of measurement used between the current study (roundness machine) and the short term published report (coordinate measurement machine) may have also contributed to differing estimations of the absolute linear wear rates. However, these factors do not diminish the differences found in relative values between the two implant groups in this study.

Potential confounding factors that may have led to increased wear rates in the pseudotumour implant group include relative differences in time from implantation to retrieval, femoral component size and heterogenicity of subgroups in the non-pseudotumour group. However, there was a poor correlation between the linear wear rate and the time *in vivo* for implants in both groups. Furthermore, there was no significant differences in femoral component sizes between the pseudotumour and non-pseudotumour groups (47 mm vs. 49 mm, $p=0.75$). Lastly, the linear wear rates between the two sub-groups (femoral neck fracture and infection) in the non-pseudotumour implants did not differ significantly ($p=0.41$). Therefore, significantly greater linear wear

rates measured *in vitro* from the retrieved MoMHRA implants revised due to pseudotumour support the *in vivo* study findings of elevated metal ion concentrations in serum and hip aspirates in patients with pseudotumours (Chapter 3), thereby confirming that pseudotumour in contemporary MoMHRA implants is associated with increased wear at the MoM articulation.

Wear on the acetabular cup components in the pseudotumour group always involved the edge, indicating edge-loading of the bearing. Edge-loading is a phenomenon whereby the femoral component comes into contact with the edge of the acetabular component. It has been recently suggested as a possible mechanism that leads to increased wear in MoMHRA implants [92, 124, 154, 155]. Edge-loading has the potential to disrupt the favourable fluid film lubrication that occurs in MoMHRA bearing surfaces [162, 163]. Metal-on-metal bearing surfaces which do not function under conditions of full fluid-film lubrication may be prone to more frequent surface-to-surface contact. Furthermore, when contact occurs, stresses may be transmitted over a smaller surface area. Computational wear modelling of MoMHRA has demonstrated that a significant wear area leads to re-distribution of contact stress along the boundary of the worn zone [164]. This may lead to a self-perpetuating cycle that results in so-called runaway wear: edge-loading would lead to loss of favourable fluid film lubrication and production of metallic wear debris leading to a third body abrasive wear with subsequent increased production of metal wear debris. As edge-loading and the thickness of the lubricating fluid-film influence the extent of metal ion generation [154], these conditions would lead to increased metal ion levels in hip joint aspirate and serum, such as those measured in patients with pseudotumours.

Therefore, edge-loading with an associated loss of fluid film lubrication may be the dominant wear generation mechanism in MoMHRA patients with pseudotumour.

There are several limitations to the study. Linear wear measurement method is limited to estimating the local deepest wear (worst case) and not the mean wear of the component. However, wear was found to be highly localised in the MoMHRA implant couples. The topographical surface shape of the wear scar was not mapped. It would have been informative to fully characterise the corresponding wear scars located on the femoral components. Anatomical orientation of the implants is difficult without landmarks provided at the time of revision surgery as MoMHRA implants, unlike stemmed THA, are symmetrical in appearance without distinctive geometrical markers that can be used for orientation. As the retrieved implants were not marked with *in vivo* orientation at the time of retrieval, information regarding the specific anatomical orientation of the wear scar could not be assessed. Despite these limitations, the pattern of edge-loading was clearly demonstrated on the acetabular components. Complete good-quality plain radiographs were only available in fewer than half of the selected retrieved implants. Therefore, radiographic acetabular component inclination, which has been reported to influence MoM bearing wear [92, 93], could not reliably be assessed.

It was assumed in the current study that the rate of wear is linear with time. Data from hip simulator studies and clinical metal ion level measurement suggest a biphasic rate of wear with an initial high run-in wear followed by a lower steady state wear [17, 60]. Although the vast majority of implants in both groups were from or beyond the third year of

implantation, several implants in the non-pseudotumour group had failed earlier within the higher wearing run-in period. This may have led to under-estimation of the wear difference between the implant groups. Furthermore, the effects of manufacturing tolerance error of MoM bearing sphericity would have a proportionally greater impact on estimated linear wear rate in implants that have been revised at an early stage. However, the effect of this on the wear rates would have been minimal as manufacturing tolerance was estimated from the control measurements to be less than 1μm.

The wear rates are sensitive to material parameters (carbon content, alloy processing and heat treatment), design parameters (radial clearance), and manufacturing parameters (surface roughness and sphericity) [60, 115]. There are differences in designs, materials, and manufacturing processes between three types of metal-on-metal hip resurfacing implants measured in the current study. This confounding factor could be controlled if only one type of implant from a single manufacturer was measured. However, this would have further reduced the available number of retrieved implants, thereby reducing the power of study. Moreover, a proportionally similar number of implant types were studied in each group, and thus minimising this confounding effect on comparative values.

In conclusion, significantly higher linear wear rates were measured in the retrieved femoral head and acetabular cup components revised due to pseudotumour than those revised for other reasons in the current *in vitro* retrieval study; this supports the *in vivo* study findings of elevated metal ion concentrations in patients with pseudotumours (Chapter 3). The results of this study, therefore, confirm that pseudotumour in

contemporary MoMHRA implants is associated with increased wear at the MoM articulation. Furthermore, wear on the acetabular cup components in the pseudotumour group indicated edge-loading of the bearing. This suggests that highly localised wear occurring due to edge-loading with an associated loss of fluid film lubrication may be the dominant wear mechanism in MoMHRA patients with pseudotumours. Further *in vivo* investigation into the importance of edge-loading as a mechanism responsible for increased wear is required.

6.7 Summary

- The results of the current retrieval study demonstrated that MoMHRA implants revised due to pseudotumour were associated with significantly greater linear wear rates of both femoral head and acetabular cup components. Therefore, the first null hypothesis, which stated that there is no difference in the linear wear rates between the two groups, was rejected.
- This *in vitro* finding supports the *in vivo* findings of elevated metal ion concentrations in serum and hip aspirates in patients with pseudotumours (Chapter 3), thereby confirming that pseudotumour in contemporary MoMHRA implants is associated with increased wear at the MoM articulation.
- Wear on the acetabular cup components in the pseudotumour group always involved the edge, indicating edge-loading of the bearing. Therefore, the second null hypothesis, which stated that there is no difference in the incidence of edge-loading between the two groups, was also rejected.
- This suggests that edge-loading with the loss of fluid film lubrication may be the dominant wear generation mechanism in MoMHRA patients with pseudotumour.
- Therefore, *in vivo* investigation of edge-loading as a mechanism that can lead to the increased wear in patients with pseudotumours is discussed in the next chapter.

CHAPTER 7 *IN VIVO* ASSESSMENT OF EDGE-LOADING

7.1 Introduction

The results of the previous chapter (Chapter 6) have indicated that edge-loading occurred in implants retrieved from failed MoMHRA due to pseudotumours, thereby suggesting that edge-loading is a wear mechanism that leads to increased wear in MoMHRA implants. Although *in vitro* assessment of retrieved implants provides valuable information, it has limitations. Retrieval studies of total joint components are limited by the fact that the implants were retrieved because of failure, resulting in selection bias. This selection bias excludes examination of implants from well functioning hip joints. Thus, extrapolation of *in vitro* retrieval study results to *in vivo* conclusions is not always appropriate. Therefore, an *in vivo* study is required to investigate edge-loading in MoMHRA patients with pseudotumours as well as in patients with well functioning MoMHRA without pseudotumours in order to make a valid conclusion.

Edge-loading *in vivo* has not been previously investigated in MoMHRA patients. The current chapter focuses on determining whether edge-loading occurs in patients with pseudotumours *in vivo* during functional activities. Edge-loading *in vivo* may be represented by projecting the resultant segment reaction force vector at the hip joint onto the inner surface of acetabular cup component. In the case of edge-loading, the resultant hip joint force would be directed towards the edge of the acetabular cup component, consistent with the localised wear morphology observed in the retrieval study. This representation requires accurate measurement of both the *in vivo* hip joint force and the

acetabular component orientation in patients with MoMHRA. Measuring *in vivo* hip joint forces in patients with implants *in situ* during functional activities presents numerous difficulties. Furthermore, there is considerable variability in the post-operative position of the acetabular components following hip resurfacing. In order to accurately measure *in vivo* resultant segment reaction force at the hip and acetabular component orientation, it was important to consider a number of different methods. A brief background of various available methods that were considered and justification for those methods that were selected for this study are discussed in the following sub-sections.

7.1.1 *In Vivo* Hip Joint Force

In vivo hip joint forces measurement in patients with implants *in situ* presents numerous challenges. Consequently, only a limited number of such studies have been conducted on small cohorts of subjects. Researchers have utilised both telemetry [165-168] and mathematical modelling [164, 169-171] to measure or predict *in vivo* forces across the hip joint. Resultant hip joint moments and contact forces have been investigated using instrumented total hip prostheses with in-built force transducers [167, 172]. Force data from these instrumented prosthesis is relayed to a computer via telemetry. This method can only be applied prospectively prior to index surgery in a limited number of patients. Thus, this method was not appropriate to be used in this study. However, the results of instrumented prostheses studies have been useful in providing experimental validation of mathematical lower limb models, such as those utilised in this study [173].

More recently, video fluoroscopy has been used to determine the *in vivo* kinematics of the hip joint [174, 175]. This method involves determining *in vivo* motion patterns of the hip joint in three-dimensions (3D) using video fluoroscopy and model-fitting techniques, during which 3D models of the acetabular and femoral head component are projected into the two-dimensional fluoroscopic images. Computer aided design (CAD) models of the prosthesis are then used to reconstruct 3D position and orientation in space. Although this method can provide important information regarding component motion, it does not provide any information regarding the direction or magnitude of resultant hip joint force. Furthermore, the total radiation exposure for the participating patients would be greater with fluoroscopy-based activity measurement than with radiographs or single session of computed tomography (CT). In order to comply with the local Research Ethics Committee guidelines, which recommend limiting all non-clinical (research) radiation exposure to a minimum, an alternate method was considered.

Although there are important measurement limitations [176, 177], three-dimensional motion measurement in the context of clinical and biomechanical analyses of joint replacement is becoming a key instrument for investigating the joint dynamic behaviour. This has led to development of modern motion analysis systems with efficient and reliable measurement techniques and representation tools [178]. In fact, modern quantitative motion analysis is increasingly being utilised in clinical and biomechanical research in patients with MoMHRA [179, 180].

Modern motion analysis measures human movement, and then uses models to estimate the forces and moments transmitted across the joints. The two important components of motion analysis are kinematics and kinetics. Kinematics is the study of motion, in isolation from the forces that generate the motion. Kinetics, in the context of mechanics, is the study of forces giving rise to motion. The motion analysis system consists of an optometric tracking system and force platforms. Specialised cameras are used in conjunction with motion analysis software to provide a frame-by-frame representation of the subject's limbs, based on the location of spherical markers attached to the subject's skin, in a three-dimensional coordinate system. The markers are aligned with bone landmarks to define body segments and are tracked throughout the movement by the optometric system. The motion analysis system relates the kinematic variables to the kinetic variables by determining the position in space of the limb segment relative to the position and direction of the ground reaction force measured using force platforms. Mathematical models are used to calculate the total resultant force and moment acting at each joint segment.

Recently, three-dimensional lower limb motion analysis has been used to model the *in vivo* loci of movement on the inner surface of the acetabular component over which the femoral component moves (wear paths) in relatively large cohorts of THA patients [181-183]. These studies have demonstrated that motion analysis can reliably be used to quantify the *in vivo* wear path with respect to the acetabular component. Modern motion analysis can also be used to calculate the resultant joint force acting at each joint of any given segment. Therefore, motion analysis was chosen in the current study to quantify the

in vivo loci of the projection of the resultant segment reaction force vectors at the hip joint onto the acetabular component inner bearing surface (force path), in order to investigate *in vivo* edge-loading. One important limitation of the method described by Bennett *et al* [181-183] was the determination of acetabular component orientation only in the coronal plane using plain radiographs. The location of the projected force path relies on accurate representation of acetabular cup orientation for each resurfaced hip. Therefore, the current study sought to overcome this limitation by using an alternate method to accurately determine acetabular component orientation in three dimensions.

7.1.2 Acetabular Component Orientation

A common limitation to radiographic methods for determining the position of the components [184, 185] is that they are dependent on the patient's positioning during examination. This arises because the radiographic calculations involve the projection of a three-dimensional pelvis on to a two-dimensional plane. Thus, measurements of precise orientation cannot be reliably measured. For this reason, computed tomography (CT) scanning has been used to measure anatomical implant angles of the acetabular component in relation to pelvis [186, 187]. Anatomical anteversion and inclination are referred to as the true or three-dimensional anteversion and inclination [188]. Anatomical inclination is the angle between the acetabular axis and the longitudinal axis, and anatomical anteversion is the angle between the transverse axis and the acetabular axis [187]. The acetabular axis passes through the centre of the socket and is perpendicular to the plane of the socket face. Anatomical anteversion is best determined from CT images, since it is measured in the transverse plane. In order to accurately determine the

anatomical acetabular component orientation, three-dimensional CT-based orientation of the acetabular component was measured in this study. This method involved measuring three-dimensional coordinates of both the acetabular cup and anatomical pelvic landmarks (anterior superior iliac spines and pubic tubercle) within the CT coordinate system. This ensured that the measured position of cup relative to pelvis was independent of the patient positioning.

7.1.3 Study Aim

The aim of this *in vivo* study was to investigate whether edge-loading occurs in MoMHRA patients with and without pseudotumours by quantifying the dynamic loci of resultant hip joint segment force relative to the acetabular component (force path) during functional activities, using integrated data from three-dimensional motion analysis and CT information.

.

7.2 The Null Hypothesis

H_0: There is no difference in the *in vivo* edge-loading, as measured by locus of the hip joint segment force vector intersection with the acetabular cup during functional activities of daily living, between MoMHRA patients with pseudotumours and MoMHRA patients without pseudotumours.

7.3 Materials and Methods

All patients in the current study underwent three-dimensional lower limb motion analysis in order to estimate the hip joint segment force during functional activities. In addition, computed tomography scans were utilised to determine each patient's specific acetabular component orientation and hip joint centre. The details of the patient selection, the motion analysis, computed tomography scanning, as well as data presentation including the definition of edge-loading are discussed in the following sub-sections.

7.3.1 MoMHRA Patient Recruitment

Patients with confirmed diagnosis of pseudotumour and patients without pseudotumour from the earlier MoMHRA prevalence study (Chapter 3) were invited to participate in the current study. An additional approval from the local Research Ethics Committee (Oxford Research Ethics Committee B: 07/H0605/151, Amendment 3) was obtained and all patients gave informed written consent. Patients were recruited from the previous study cohort in order to avoid the need to expose additional patients to the identical clinical, laboratory and radiological investigations necessary to detect pseudotumours. This may have introduced a potential selection bias, as the patients with pseudotumour in the current study were 'mildly' symptomatic. However, pseudotumour patients with significant or severe symptoms would have had difficulty in performing the required functional activities during motion analysis and their results would have been confounded by pain. In order to minimize patient selection bias in this study, the patients were recruited using the following selection criteria:

1. Inclusion criteria: All patients with and without abnormal soft tissue reactions, as confirmed by ultrasound and MRI in the MoMHRA prevalence study (Chapter 3), were invited to participate in the current study.

2. Exclusion criteria: Exclusion criteria were the presence of pain or impairment which would restrict walking, stair climbing, or sitting onto or rising from a chair. This was to ensure patients were able to comfortably perform these functional activities for the motion analysis study.

Patients

A total of 21 patients were investigated. There were 2 patient groups: (1) Group 1 – MoMHRA patients with pseudotumours, a cystic or solid mass relating to the resurfaced hip, detected using ultrasound and confirmed with MRI (n = 6); and (2) Group 2 (control) – patients with well functioning MoMHRA implants without pseudotumours detected on ultrasound (n = 15). The patients in both groups had previously participated in the earlier MoMHRA pseudotumour prevalence study (Chapter 3). A summary of patients' details is provided in Table 7-1. Approximately two individuals from the control arm (Group 2) were matched for gender, age, femoral component size, and time since surgery to one individual from the pseudotumour arm (Group 1) of the study. All patients in the study underwent both lower limb motion analysis and hip CT scanning. In addition, the serum concentrations of cobalt and chromium had been measured in all patients.

Table 7-1: A summary of study patient groups.

	Pseudotumour Patient Group	Non-Pseudotumour Patient Group
Total Patient Number	6	15
Male	1 (1B)	3 (3B)
Female	5 (2B)	12 (6B)
Mean Age (years)	55 (range 44-58)	56 (range 46-60)
Implant Type	BHR (8) Conserve Plus (2)	BHR (18) Conserve Plus (6)
Femoral Component Size (mm)	45 (range 44-50)	46 (range 46-50)
Mean Time Since Surgery (months)	60 (range 36-79)	64 (range 36-88)

Abbreviations: Bilateral implants (B).

7.3.2 Three-Dimensional Lower Limb Motion Analysis

Motion Analysis System

Data collection for the three-dimensional lower limb motion analysis was conducted at the Oxford Gait Laboratory (Nuffield Orthopaedic Centre, Oxford, UK). The laboratory comprises a twelve-metre long walkway incorporating two force platforms at the centre of the capture volume surrounded by the infra-red measurement cameras. The laboratory is equipped with a 12 camera Vicon Nexus Motion Analysis System (Oxford Metrics Ltd., Oxford, UK) and two OR6 AMTI R6-6-1000 force platforms (Advanced Medical Technology Inc., MA, USA).

Full three-dimensional lower limb motion analysis was performed on all patients in the study. Twenty-three spherical retro-reflective markers (14 mm diameter) were attached on specific anatomical landmarks (Figure 7-1) in accordance with the Plug-In-Gait lower body marker set [189] (Appendix 3). These comprised the anterior superior iliac spines,

the mid-point of posterior superior iliac spines, thigh, knee markers at the femoral epicondyles, tibial markers, ankle markers at the malleoli and foot markers at the heel and the metatarsal heads. Data was captured with a video capture rate of 100 Hz and an analogue data capture rate of 1000 Hz, while patients performed functional activities including level walking, rising from and sitting down onto a chair, and stair climbing. All patients were able to complete these activities easily and without pain. Three trials of each activity were captured for each patient. The average testing time for each patient was approximately three hours. For each functional activity, ground reaction force data obtained from the force platforms were used to define heel contact and toe-off events in the motion analysis. A detailed experimental protocol for the motion analysis trials is provided in the Appendix 3.

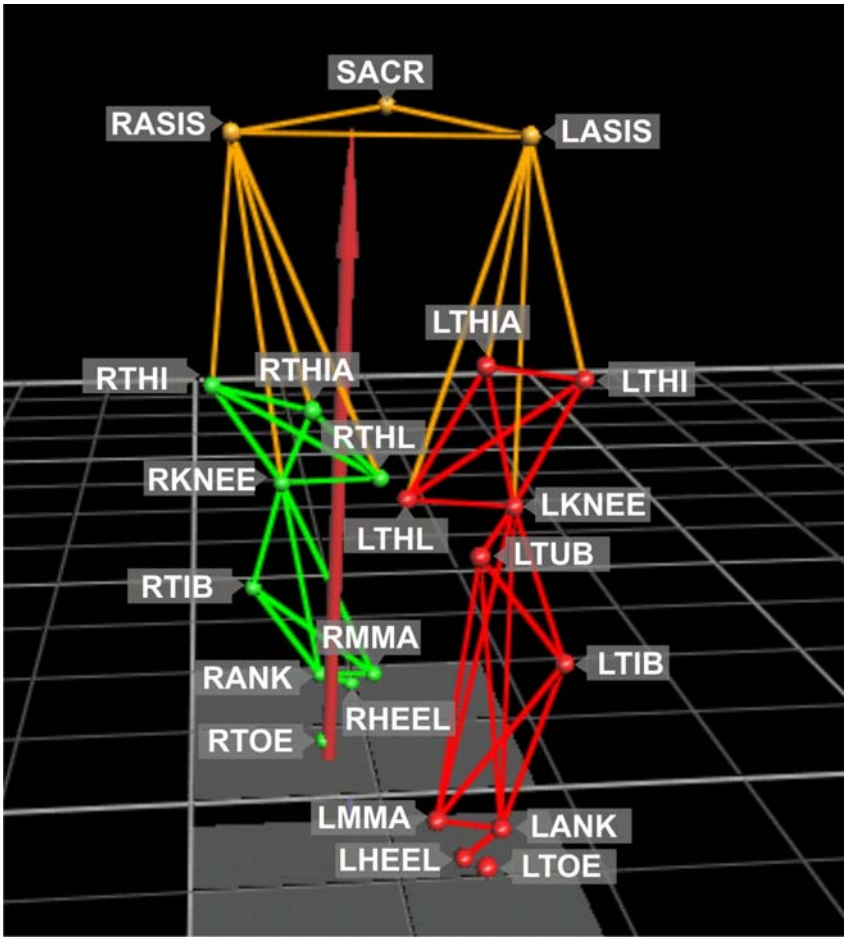


Figure 7-1: A reconstructed motion analysis image of a patient with labelled retro-reflective markers placed at anatomical landmarks (Appendix 3) during a level-ground walking. A vertical red arrow represents the ground reaction force measured by the force platform of the right lower limb during a stance phase.

Motion Analysis Data Processing

Kinematic and kinetic data processing in this study was performed with commercially available software (BodyBuilder, Vicon Motion Systems) using the Plug-In-Gait model implemented in the BodyBuilder language, with customisation of the model on subject specific basis to account for individual hip joint centre location. Plug-In-Gait (Version 1.9) is a validated mathematical lower body model [190]. BodyBuilder is a

biomechanical modelling application designed to automate three-dimensional vector algebra calculations. The software calculates the values of quantities which cannot be measured directly, such as resultant hip joint segment force, based on ground reaction force (measured directly from the force platforms) using a mathematical model. Plug-In-Gait modelling is based on kinematic and kinetic data reduction protocols described in the literature [191-194].

The calculated kinematic and kinetic variables are obtained by processing the recorded trajectories of the motion analysis markers in combination with the data from the force platforms. In brief, this processing relies upon the use of kinematic and kinetic models to construct a system of embedded coordinates from the marker sets throughout functional activity. The kinematic model assumes that the individual segments comprising the lower limb behave as rigid bodies. The model allows the orientation and location of each limb segment to be determined. Inter-segmental hip joint force and moments are calculated in a sequential process using inverse dynamics technique, in which the joint reactions at the hip are determined using more distal segment joint reaction results. Thus, the joint reaction force calculation is first performed for the foot segment. The distal forces and moments acting upon this segment and the point at which they are acting are known from the force platform measurements. Since the motion of the segment is known, the proximal resultant forces and moments acting at and about the ankle joint, can be determined. Next the analysis is performed for the shank segment; the distal forces and moments for this segment are equal in magnitude and directed opposite to the

foot segment's proximal forces and moments. The process is then repeated for the thigh segment.

The kinematic variables such as temporal-spatial parameters (including step length, cadence, velocity), and joint angles in patients with MoMHRA have been recently reported in the literature [179, 180]. Although these temporal-spatial parameters may be useful in assessing quantitative functional gait recovery following surgery, the clinical implications and significance of these variables calculated using modern analysis techniques remain unknown. Furthermore, the range of hip motion during functional activities such as stair climbing and rising from a chair is greatly influenced by the height of the chair and inclination of staircase used, thus it can not be reliably used to characterise differences between patient groups [195]. Therefore, it would be difficult to establish any clinically significant difference between groups based on these kinematic variables. The objective of the motion analysis used in the current study was to estimate the dynamic hip joint segment force during functional activities, and thus, the intention was not to document the gait characteristics of patients with MoMHRA. In order to achieve the study aim, the processing of motion analysis parameter in the current study was therefore focused on, and limited to, the resultant hip joint segment force estimation.

7.3.3 Justification of Motion Analysis Protocol

There is no standardised protocol for lower limb motion analysis of MoMHRA patients. Therefore, it is important to provide justification for a number of important experimental parameters utilised in the motion analysis protocol used in this study.

Selection of Functional Activities:

Experimental activities that were relevant in terms of activities of daily living were selected to collect data on patients with MoMHRA. The experimental protocol consisted of a set of three groups of activities: walking, stair ascent and stair descent, rising from and sitting onto a chair. Walking was included as it is a fundamental activity of daily living. Analysis of more strenuous activities of daily living was thought to be required to identify differences between the two patient groups, as challenging physical tasks have higher sensitivity as a tool [180]. Rising from a chair and stair climbing are two activities that result in high joint loads. During rising from a chair, the peak hip joint reaction force has been calculated to be twice body weight [195]. Forces as high as 5.5 times body weight are transferred from the femur to the acetabulum during stair climbing [167].

Motion Trials:

Important parameters that needed to be considered during motion trials included speed, footwear, and number of trials. All activities were performed at the patient's self-selected speed in this study. This was because individual subject's natural speed has been reported to be constant throughout activities such as walking and stair climbing [196]. Thus, self-selection of speed by each patient ensured that patients retained their natural gait characteristics. Patients were required to perform all activities barefoot in order to avoid the varying influence of different footwear on motion patterns during functional activities [167]. Patient fatigue before the completion of activities and data collection would result in unrepresentative data. Although none of the functional activities were extremely

strenuous in nature, the maximum number of repeated trials per functional activity was limited to three.

Equipment:

A commercially available chair and staircase were used in this study. An adjustable-height chair (specifications: seat 381 mm^2, height 457-610 mm, maximum permissible weight 114 kg) was used. The chair was armless and back-less. This design was selected as it has been shown to generate greater joint moments while minimising patient errors due to inadvertent use of upper limbs to rise from a chair [195]. A commercially available non-instrumented two-step staircase was used in this study. It had a rise of 180 mm and a staircase slope of 33°. These dimensions comply with the UK private and public building regulations [197]. The second step was also a platform, where the patient could safely turn around and commence stair descent. A simplified two-stair step was selected as it has been shown to have similar kinematic and kinematic results in comparison to staircases with three or more steps [198].

7.3.4 Computed Tomography (CT) Scans

CT Scanning Protocol

Computed tomography (CT) scans of the patients' pelvis and lower limbs were obtained in the transverse plane using a high-resolution 64-slice CT scanner (Siemens Somatom, Siemens Medical Solutions USA, Inc., NY, USA) using a metal artefact reduction sequence. CT scanning protocol was performed in accordance with 'low dose CT scan protocol' as recommended by Hart *et al* (Appendix 4) [199]. The protocol lowers the

effective radiation dose by reducing the volume of the patient imaged. Instead of continuous scanning from pelvis to lower limbs, the protocol recommends scanning a set of sequential regional areas: anterior superior iliac supine bi-laterally, the hip region (extending from above the acetabulum down to the lesser trochanter), and at the knee. The reduction in radiation dose was an important consideration as CT scans represented additional radiation exposure to the current study patients, who had already undergone plain radiographs during their participation in the previous research study (Chapter 3). For this reason, a risk assessment was sought and obtained from clinical radiation experts (Appendix 5). Thus, the low-dose protocol was used to minimise radiation exposure without compromising image quality. The protocol also utilises an extended scale for the minimisation of metal artefacts. The CT scanner parameters were 100 kV and an x-ray tube current of 60 – 100 mA.

Integration of the three-dimensional anatomical reconstruction of acetabular component orientation based on the CT scan with the hip joint segment force calculated from the three-dimensional motion analysis system was required to accurately relate output from one system relative to another. This integration would be possible if both systems shared a common reference coordinate system. In the motion analysis model, a pelvic coordinate system was defined by three pelvic markers placed on the anterior superior iliac spines (ASIS) and mid-point between posterior superior iliac spines. In order to ensure that the same pelvic coordinate system could also be defined within CT data, the pelvic motion analysis markers were replaced with radio-opaque markers at the end of the motion analysis, prior to CT scanning.

Pre-requisite requirements for CT markers were as follows: (1) markers were easily identifiable (no metal artefacts or scatter) on CT scan images; (2) markers were comfortable for patients; and (3) markers remained *in situ* (i.e. no fall-out) while patients transferred from the motion analysis laboratory to the CT scanner. A number of different markers were trialled. Multi-Modality MM3002 markers (Intermark Medical, Innovations Ltd. in Bromley Kent, UK) were selected for this study. These are made of a hydrogel component with a medical grade adhesive. The Multi-Modality Markers provided a clear and accurate reference point on CT scan. They were easy to securely attach and remove from the patient.

Measurements in CT Coordinate System

A medical imaging software package, SliceOmatic (Version 4.2 Rev-9b, TomoVision, Virtual Magic Inc., Montreal, Canada), was used to locate the coordinates of multi-modality markers, anatomical pelvic landmarks and MoMHRA prostheses within the CT DICOM (Digital Images and Communications in Medicine) images. Four points for each of multi-modality markers placed on the right and left anterior superior iliac spine (RASIS, LASIS) and the sacrum (SACR) were recorded. The first point was in the middle of the marker close to the skin surface where the marker first appeared in the CT slices. The second and third points were on the outside of the marker by the skin surface on different slices. The fourth point was in the middle of the marker by the skin surface in the final slice before the marker disappeared from view. For acetabular components, the points most easily defined for the cup were the edges where the line of the edge of the

cup was visible (Figure 7-2). Two points at the edges of the cup were selected for three slices. These slices were selected such that they were separated as much as possible. A minimum of 30 points was chosen on the edge of the head with maximum of 5 points per slice.

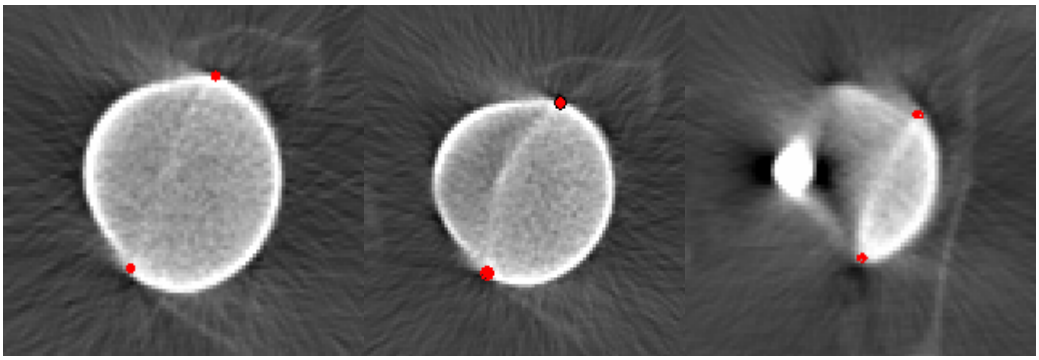


Figure 7-2: Edge of the acetabular cup coordinates was selected (red dots) on the on three non-consecutive slices using medical imaging software SliceOmatic.

Acetabular Component Orientation Measurement

The origin of the acetabular coordinate system was defined at the hip joint centre (HJC). A general plane can be expressed in vector form by any vector point on the plane and any given vector direction in the plane. In the case of the acetabular coordinate system, the plane to be calculated was the plane through the cup opening (cup face plane) defined by the CT coordinates on the rim of the acetabular component. The normal axis to this plane, passing through the cup centre, was referred to as the acetabular axis. Acetabular cup inclination and anteversion were described by the angles this made, in the coronal and sagittal planes, relative to the anterior pelvic plane in the bone coordinate system. The anterior pelvic plane was defined by the most anterior prominences of the anterior

superior iliac spines and pubic tubercle identified on CT images. In addition, a combined angle was also calculated, which was defined as the sum of inclination and anteversion angles. The combined angle was of interest in the study, in light of the recent report of increased anteversion combined with increased inclination being associated with elevated concentration of whole blood metal ions [93]. Therefore, three different angles of the acetabular cup component orientation were measured in the current study: (1) inclination angle; (2) anteversion angle; and (3) combined angle (inclination + anteversion) representing the aggregate orientation in the coronal and sagittal plane.

Furthermore, it was considered important to assess the acetabular inclination and anteversion angles measured in each patient group relative to the published recommendations for the acetabular cup orientation. There are a number of recommendations for an 'optimal' position of the acetabular component [92, 200, 201]. However, these recommended positions all fall within a 'safe zone' for the cup orientation with inclination of 40 ± 10° and anteversion of 15 ± 10°, as described by Lewinneck *et al* [202]. Therefore, the safe zone of Lewinnek was used in the study.

As the measured points were in the coordinate system of the CT scanner, the coordinates of three CT multi-modality pelvic markers (right and left ASIS, SACR) were used to define the same pelvis-embedded coordinate system (PCS) as that defined by the motion analysis kinematic model. The axis system directions were in accordance with International Society of Biomechanics standards [203], whereby the coordinate system origin is located halfway between the two ASIS markers. All points in one arbitrary local

coordinate system can be 'transformed' into another arbitrary coordinate system. The spatial transformation is a mathematical process which involves translation of the origin and rotations of axes of one coordinate system relative to another. All transformation calculations were done by mathematical routines in Matlab (Matlab Version 7.8.0.347 (R2009a); The MathsWorks, Natick, MA, USA), which were written with the assistance of an engineer. The Matlab routines transformed three-dimensional point locations between coordinate systems and incorporated an algorithm that computed the best-fit plane from a set of points.

7.3.5 Data Presentation

Three-dimensional projection of the hip joint segment force loci onto the inner surface of the acetabular component was generated in order to quantify the location, time duration and magnitude of hip joint segment force. The numerical processes integrating the data generated from motion analysis and CT scanning were implemented in a custom routine written in Matlab (Version 7.8.0.347 (R2009a), The MathsWorks, Natick, MA, USA) with the assistance of an engineer. The steps used were as follows:

(1). From the CT data, the orientation of the acetabular cup was determined (SliceOmatic medical imaging software package, Version 4.2 Rev-9b, TomoVision, Virtual Magic Inc., Montreal, Canada), allowing the transform from the pelvic coordinate system to an acetabular cup embedded coordinate system to be calculated.

(2). The segment reaction force at the hip joint centre was calculated in the pelvic coordinate system and then transformed into the acetabular cup coordinate system. This allowed the loci of the intersection of force vector with the inner bearing surface of the

cup to be calculated throughout the load bearing phase of all measured activities. The locus of the force vector intersection with the cup throughout the load bearing was termed the "force path".

(3). The distance from the intersection point of the force vector and the cup inner surface to the centre of the cup was normalised by the radius of the cup face. The inner bearing surface of the cup was thus divided into concentric zones defined in 10% increments of the cup face radius, with the zone furthest from the centre of the cup designated as zone 1. Thus, an intersection occurring at the cup edge corresponded to the ratio value equal to 1.0. The zones were defined using the ratio as follows (Figure 7-3):

Zone 1: Ratio 1.0 – 0.9

Zone 2: Ratio 0.9 – 0.8

Zone 3: Ratio 0.8 – 0.7

Zone 4: Ratio 0.7 – 0.6

Zone 5: Ratio 0.6 – 0.5

Zone 6: Ratio less than 0.5

(4). Calculations were performed to determine the total time duration for the weight bearing phase for any given activity (each frame represented 1/100th of a second, as cameras operated at 100 Hz). The percentage of total stance time spent by the force path in each zone was then calculated. This was called the "zone duration", with duration for a particular zone termed zone *n* duration, where *n* was the number of the zone in question.

(5). In addition, it was considered important to quantify the variation in the magnitude of the segment force throughout activity, in particular to obtain a way to compare how segment force magnitude varied between the zones defined above. Taking a peak or

average value would not have been representative as the magnitude of the segment force varied with time. It was therefore necessary to estimate the cumulative effect over time by calculating the area under the force/time curve for each zone [204]. This was termed the "force impulse".

Normalisation of Parameters

In order to allow inter-patient comparison, calculated variables were normalised. The duration of loci of hip joint force vector in each zone was normalised as a percentage of the total duration of the weight bearing phase. Hip joint segment force impulse was normalised to patient body weight (mass multiplied by the acceleration due to gravity).

7.3.6 Definition of Edge-Loading

Edge-loading was defined to occur when the force path was within a distance equal to or less than 10% of the cup radius from the edge of the acetabular cup (i.e. the ratio 1.0-0.9 in zone 1) (Figure 7-3). The figure of 10% was based on observations from the retrieval study (Chapter 6) that the maximum area of wear in the non-edge-loaded acetabular cups occurred around the polar region that was well within the sphere of the cup. Representative force path plots for non-edge-loading and edge-loading patients are shown in Figure 7-3.

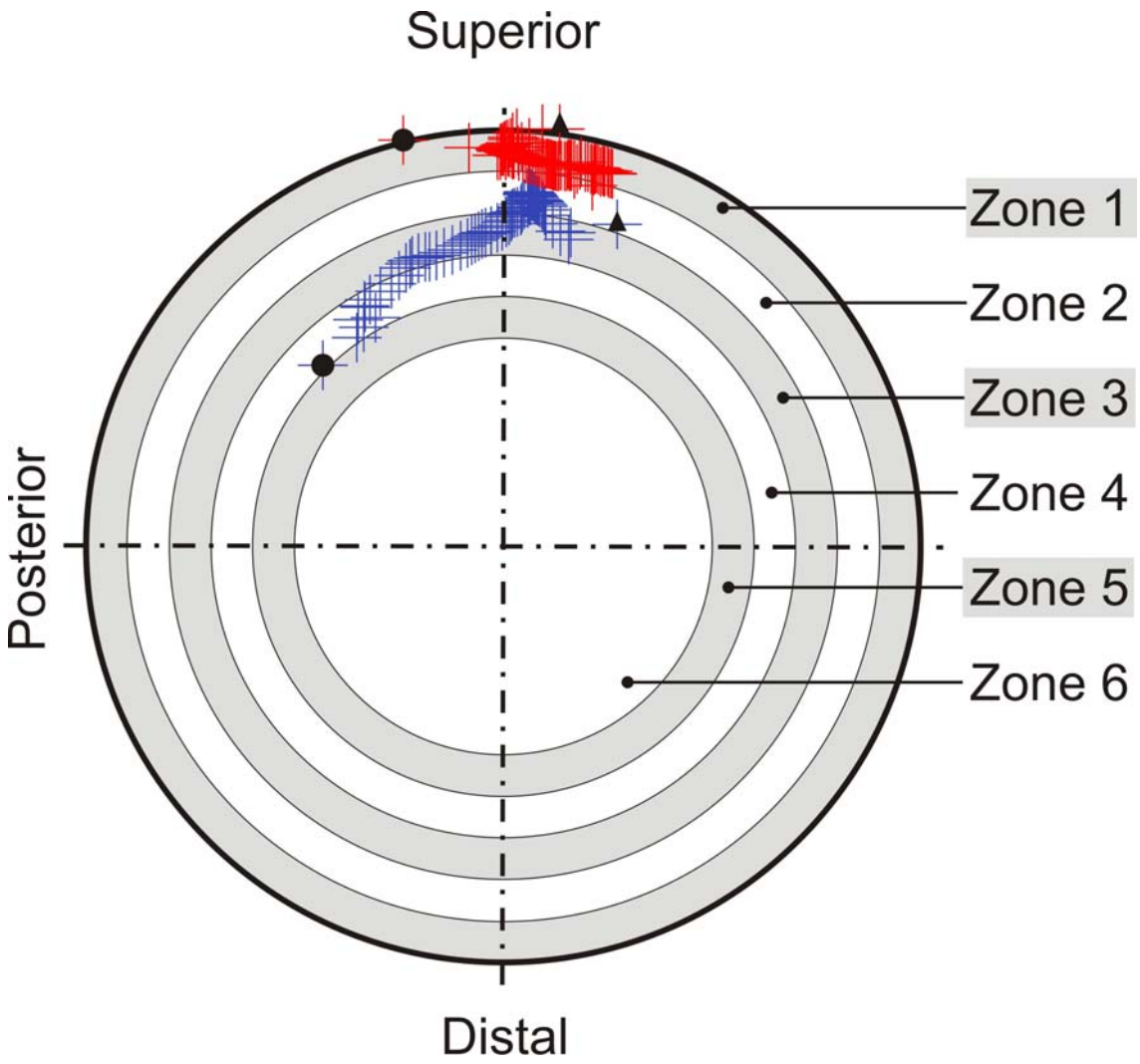


Figure 7-3: Force paths projected on the acetabular cup viewed in the direction that is through the centre of the cup. In patient A (shown in blue), the force path does not enter the outer most radial zone (zone 1), thus no edge-loading is observed. In patient B (shown in red), the force path enters the outer most radial zone (zone 1), indicating edge-loading. The black circles (●) indicate force path at heelstrike and the black triangles (▲) indicate force path locus at toe-off.

7.3.7 Statistics

The data set was assessed for normality. Correlation of acetabular angles measured using CT scans and plain radiographs were calculated using Pearson's correlation analyses, expressed as Pearson's correlation coefficient. Inter-group comparisons of the zone

duration and the force impulse variables between the patient group without pseudotumour (non-pseudotumour group) and the patient group with pseudotumour (pseudotumour group) were performed using the Student's t-test. In order to determine significant variations in acetabular cup orientation between the right and the left resurfaced hips in all patients with bilateral MoMHRA in the study, the paired t-test was utilised. Inter-group comparisons of the non-normally distributed acetabular cup angles were performed using the Mann-Whitney non-parametric tests. Differences at $p < 0.05$ were considered to be significant. SPSS® statistical software release 13.0 (SPSS Inc. Chicago, IL, USA) was used to perform the statistical analyses.

7.4 Error Assessments

Methodologies utilised in this study are subject to measurement inaccuracies and model assumptions. Therefore, it was important to identify the potential sources of errors, quantify errors to assess whether they were acceptable and, where possible, institute measures to minimise errors.

7.4.1 Motion Analysis System

The systematic error of the motion analysis system refers to the calibration error of cameras and force platforms.

Camera Calibration:

A calibration residual is the average error between the constructed and actual marker position for all the markers on the calibration reference object. The residuals therefore reflect the accuracy of system. Static calibration calculates the origin of the capture volume and determines the orientation of the global coordinate system. An L-shaped rigid bar, with four 14 mm marker balls (three co-linear) 100 mm apart, was used to collect data for the static calibration. Dynamic calibration allows optimisation of the calibration throughout the capture volume. This was conducted using a Vicon wand, which is a rigid bar with two 14 mm marker balls 100 mm apart. The wand was moved through the reconstructed volume and dynamic data was captured. Static and dynamic trials were performed prior to each of the motion analysis experiment to determine the residual error of the system. The mean camera calibration residual for all seven testing session days was 0.66 ± 0.12 mm (95% CI) with a standard deviation of 0.6 mm. The residual error was within the two millimetres deemed acceptable by the system manufacturer.

Force Platform Calibration:

Prior to each experimental session, the force platforms were zeroed. Calibration of force platforms was assessed by placing a 10 kg weight and recording the readings from each force platform. Both force platforms were measured to be accurate within ± 0.5% for all sessions. This was considered to be acceptable for the current study. In addition, a more rigorous quantitative assessment of the accuracy of force platforms with custom-built calibration jig has been previously well established [205, 206]. This was of critical importance in the current study as the ground reaction force measured by the force

platforms was a primary direct kinetic variable used to calculate the hip joint segment force. In fact, a study by Gill *et al* has demonstrated that the mean error of force platforms in determining the centre of pressure and hence the direction and magnitude of the joint segment force was less than 1.6 mm [207].

7.4.2 Inter-Trial Variability

Repeatability refers to a system's ability to reproduce the same results in repeated trials with no change in experimental conditions. Thus, a system that has poor repeatability is unreliable. Inter-trial repeatability was assessed in the first five patients by selecting three walking trials in which clean heel-strike and toe-off events were recorded. As the ground reaction force was an important direct kinetic measurement of interest in this study, the repeatability of the three-components of the peak ground reaction force measured by the force platforms at heel-strike among three walking trials was assessed using the intra-class correlation coefficient (ICC). Intra-class correlation coefficient is a statistical method which quantifies repeatability relative to the normal variation between trials. This differs from the limits of agreement and coefficient of repeatability as described by Bland and Altman [148]. These values, which are in the same units as the variables, are less meaningful in cases where the numeric values that would represent clinical importance are not known. In assessing inter-trial repeatability of force platform vectors (measured in newtons), the numeric values of clinical significance were not known. Therefore, the ICC was calculated by taking the ratio of the estimated subject variance component to the sum of all estimated variance component: ICC value of 1 represents a perfect agreement between trials. Reliable measurements are those for which the subject variance

component is dominant over the other variance component (i.e. ICC greater than 0.5) [208].

A high degree of agreement was measured between trials in the data from both force platforms in all three force components (Table 7-2). The ICC values between 0.80 and 0.85 implied that 80% to 85% of the total variance in ground reaction force measured during three trials could be explained by the variability between different patients. This indicated that potential sources of error such as variation in walking cadence and velocity in each patient were repeatable and systematic. Therefore, it was concluded that ground reaction force vectors measured using the motion analysis system could reliably be used to compare patients in the study. In addition, it was concluded that a single representative trial could be used for subsequent analysis.

Table 7-2: Inter-trial repeatability of the components of the peak ground reaction force, in five patients during three walking trials.

	Inter-trial ICC
Force Platform A	
x component	0.83
y component	0.80
z component	0.81
Force Platform B	
x component	0.85
y component	0.81
z component	0.80

7.4.3 CT Measurement Error Assessments

Accurate three-dimensional coordinate measurement of the locations of the multi-modality markers and MoMHRA implant was essential. It influenced the orientation of the pelvic coordinate system, the resulting implant orientation and the final location of the hip joint centre (HJC). This process needed to be carried out with as much repeatability as possible to ensure accuracy of the results.

In order to assess the repeatability of this method, 30 CT scan slices of the first two patients were used to quantify the intra- and inter-observer error in identifying the coordinates of the markers and MoMHRA implants. The CT images were assessed in the medical imaging software package SliceOmatic (Version 4.2 Rev-9b, TomoVision, Virtual Magic Inc., Montreal, Canada). The x- and y-coordinates of the anatomic landmark markers (z- coordinate, representing longitudinal axis, is constant for each CT image slice) and the edges of the implants within the CT images were measured by the investigator and a second observer. The CT coordinate system was calibrated such that the numerical values of CT coordinates corresponded to length in millimetres. The investigator repeated the measurement the next day. A summary of repeatability errors, calculated using the Bland & Altman method as described in Chapter 5, is presented in Figure 7-4.

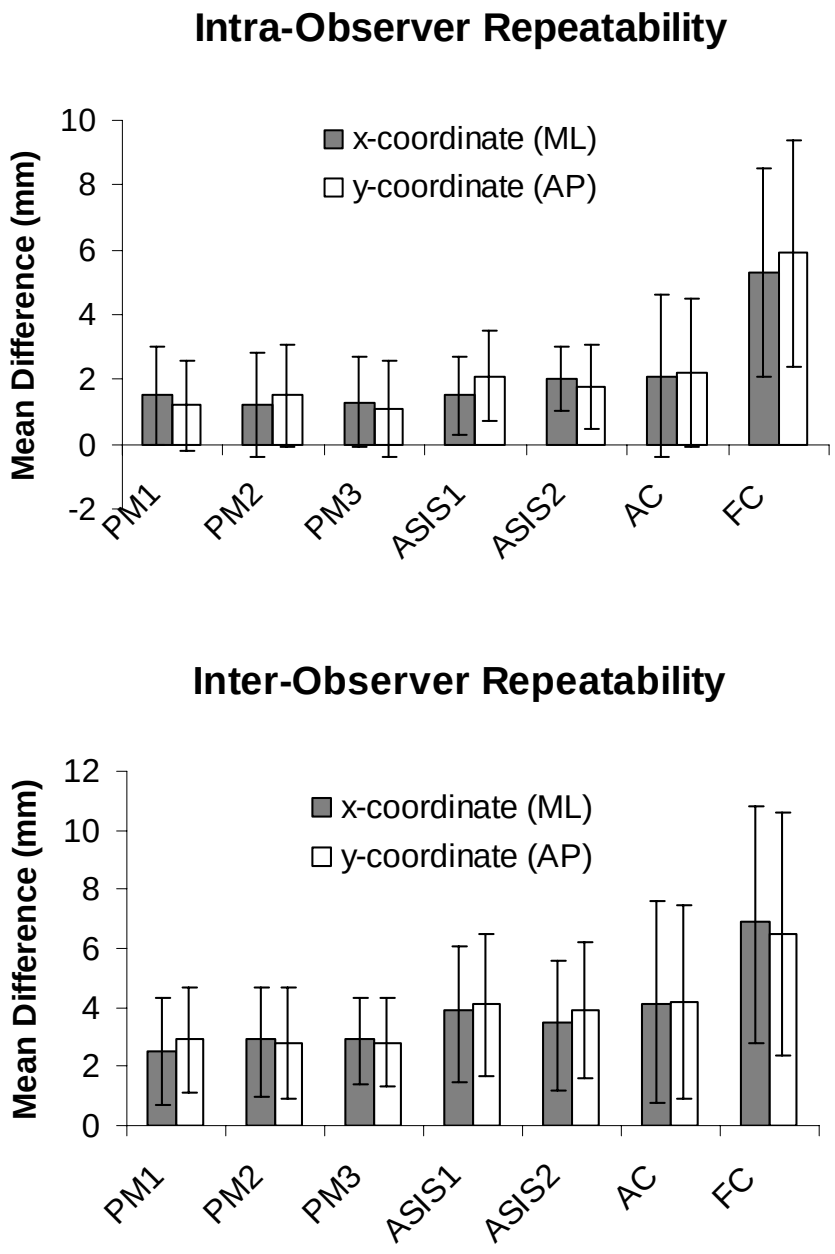


Figure 7-4: Intra- and inter-observer mean differences (mm) in x- and y- coordinates is presented for pelvic markers (PM), bony landmarks (anterior superior iliac spines), and acetabular and femoral components. The error bars indicate limits of agreement (95% confidence intervals with two standard deviation of the mean difference). Abbreviations: medio-lateral (ML), antero-posterior (AP), right ASIS pelvic marker (PM1), left ASIS pelvic marker (PM2), sacrum pelvic marker (PM3), right ASIS (ASIS1), left ASIS (ASIS2), acetabular component (AC), femoral component (FC).

For intra-observer measurements, the mean difference in locating x and y coordinates was less than 1.8 mm for pelvic markers and bony landmarks. The mean difference for locating the edges of the femoral component, however, was 6.0 mm, compared to 2.2 mm for locating the edges of the acetabular components. The maximum absolute difference for the same assessor was up to 9.5 mm for locating the edges of the femoral components. For inter-observer measurements, the mean difference was higher for all markers than the intra-observer measurements. Therefore, one observer (the investigator) was responsible for all subsequent measurement of CT coordinates in order to minimise repeatability error. The relatively high variability of locating the edge of the femoral component was of concern. The edge of the head of the femoral component, unlike the edges of the acetabular component, was not easily discernable on the CT images. This was because the head of the femoral component was largely obscured by the acetabular component in most CT images. For this reason, the hip centre calculation was estimated based on the points on the acetabular component rather than points on the femoral component in order to minimise error. This is discussed in the following sub-section.

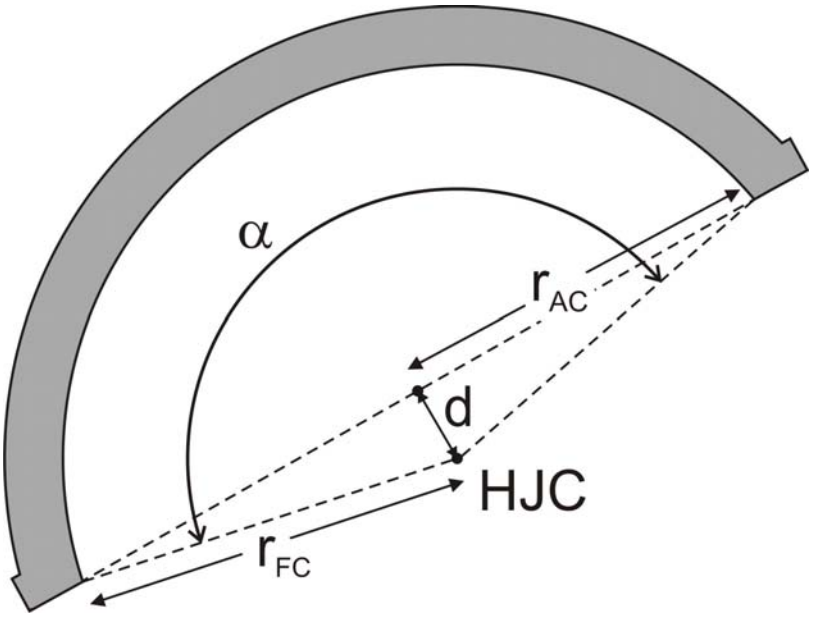
7.4.4 Hip Joint Centre Determination

Hip joint centre (HJC) is the point about which hip moments and forces are calculated. As it is not a bony landmark that can be palpated, its location must be calculated. The Plug-In-Gait model in the BodyBuilder software uses an algorithm to calculate the hip joint centre, which has been devised based on radiographic examination of 25 non-operated hips [189]. Thus, this represents a potential source of error, especially in

MoMHRA patients in whom the degree of anatomical restoration of resurfaced hip offset and height is variable, and influenced by implant insertion techniques [154, 209]. In fact, in comparison to methods based on radiological images, the inaccuracy of the regression equation method used in the Plug-In-Gait model has been reported to have a mean error of 29 mm [210-212]. Asymmetry in HJC location, which can be up to 26 mm [212], is also not accounted for by the predictive equations, which assume symmetry. This level of inaccuracy can lead to unacceptable errors because calculated output variables such as segment hip joint force are extremely sensitive to the assumptions made about the location of the centre of the joints. Errors in the range of 30 mm in HJC in the anterior-posterior direction have been reported to cause errors of 22% in the magnitude of hip flexion/extension moments [213].

In order to improve the accuracy of HJC determination in this study, the location of HJC in resurfaced hips was determined using the CT images and an optimisation procedure. It was assumed that the HJC was located at the centre of the femoral component, which could be represented by a sphere. A sphere was fitted by minimising the sum of squares of the distances from each data point relative to the surface of the sphere (Matlab Version 7.8.0.347 (R2009a); The MathsWorks, Natick, MA, USA). This calculation was initially performed by extracting the three-dimensional coordinates of a minimum of 30 points distributed over the head of the femoral component using the medical imaging software SliceOmatic (Version 4.2 Rev-9b, TomoVision, Virtual Magic Inc., Montreal, Canada).

However, the edge of the head of the femoral component was not easily discernable on the CT images. This was reflected in relatively high intra- and inter-observor errors in identifying the coordinates of the femoral component; difference for the same assessor was up to 9.5 mm. Thus, determining the HJC locations using sphere-fitting of points on the femoral component would have led to unacceptable error. Therefore, an alternative method (illustrated in Figure 7-5) using coordinates of the acetabular component was utilised to calculate the centre of the femoral component. This method involved calculating the offset (*d* in Figure 7-5) from the face of the acetabular component (determined from CT data) which is equal to the position of the origin of a sphere that corresponds to the centre of the femoral component (*HJC* in Figure 7-5). Although the angle subtended by the acetabular component (included angle α in Figure 7-5) of Conserve Plus implants was constant, for the BHR implants, this varied with implant size [214]. Thus, implant type and head diameter recorded for each resurfaced hip were used to determine the offset for the centre of the femoral component, hence the HJC, which was also the origin of the acetabular coordinate system required for component orientation calculations.



$$d = \cos\left(\frac{\alpha}{2}\right) \times r_{FC} \qquad \text{(Equation 7-1)}$$

$$r_{AC} = \sin\left(\frac{\alpha}{2}\right) \times r_{FC} \qquad \text{(Equation 7-2)}$$

where:

HJC = Hip joint centre = Centre of femoral component

d = distance from cup face to the hip joint centre

r_{FC} = radius of femoral component

α = angle subtended by acetabular component: for Conserve Plus, α is constant at 170°; for BHR, α depends on the component size [214].

r_{AC} = internal radius of acetabular component

Figure 7-5: A schematic diagram illustrating the parameters used to calculate hip joint centre.

7.4.5 Validity of CT Cup Orientation Measurements

Validity is evidence or justification that an instrument measures what it is intended to measure. Criterion validity relates to how the instrument compares with the established 'gold standard' instrument [215]. Currently, there is no established gold standard method of measuring acetabular component orientation of MoMHRA. Thus, CT-based acetabular component orientation measurement could only be compared to another established method.

The Ein Bild Roentgen Analyse (EBRA) digital measurement system (University of Innsbruck, Austria) is a computerised method for measuring implant position from digitised plain radiographs. It is a method that has been validated and has been widely used in the literature [216-218]. Furthermore, EBRA has been reported to be a reliable and valid tool for predicting early failure of MoMHRA implants [93, 219]. The EBRA method has been reported to be accurate within ± 0.8° for acetabular cup inclination and ± 1.7° for anteversion in THA [218]. Therefore, the acetabular component inclination and anteversion measured using the CT images in the first 12 resurfaced hips were compared with measurements using the EBRA system (Figure 7-6). Radiographs used in this series were taken using a standard technique (Chapter 3).

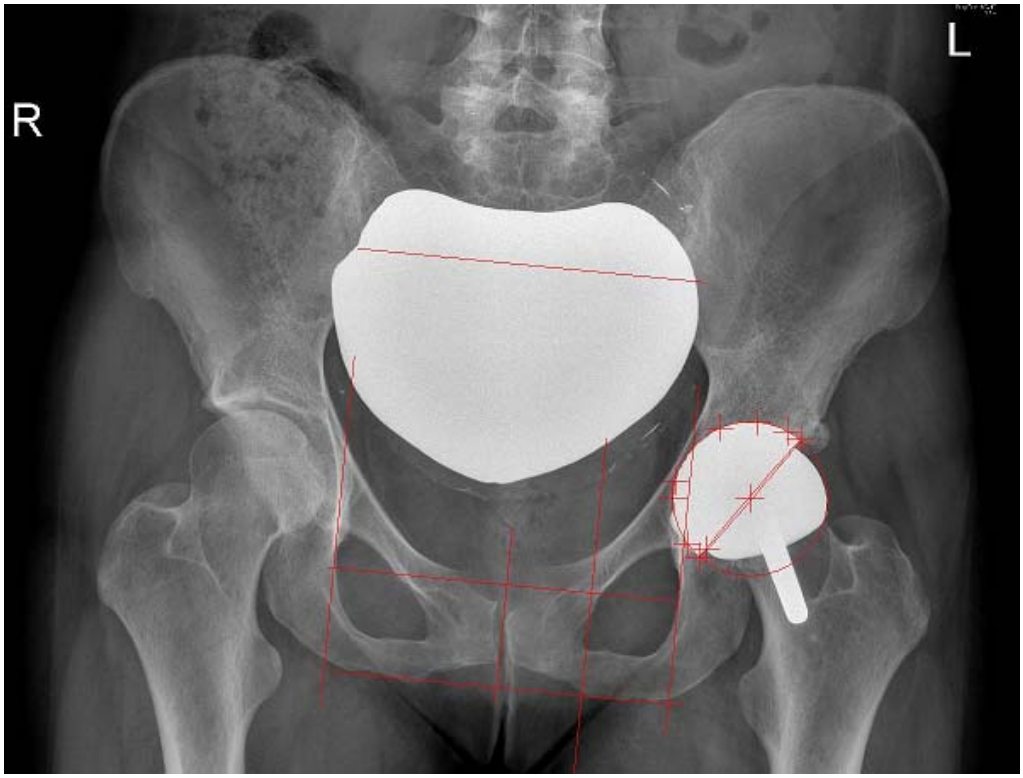


Figure 7-6: EBRA digital measurement system with the reference lines drawn in red.

The inclination and anteversion determined anatomically, radiographically, and by direct observation at the time of operation differ as they have different spatial arrangements [188]. The CT-based measurements define anatomical orientation, referred to as the true or three-dimensional orientation. This is different from radiographic orientation determined using the EBRA. The relationship between these different ways of expressing the acetabular orientation is non-linear, thus EBRA (radiological) angles were mathematically converted to anatomical angles using the method described by Murray [188] (Appendix 6). There was a high degree of linear relationship between anatomical angles of CT-based measurements and mathematically converted EBRA angles: Pearson's correlation coefficient (r): r = 0.90 for inclination and r = 0.86 for anteversion.

A high degree of linear correlation does not imply accuracy of either method. However, it was concluded that the CT-based method could reliably be used to compare acetabular orientations between patient groups in this study.

7.5 Results

Of the 21 MoMHRA patients analysed, data from 2 patients in the non-pseudotumour group were excluded due to loss of the sacrum marker during motion analysis in one patient and movement artefact in CT images in another patient. Thus, complete data from 19 patients (30 hips) were available for analysis.

7.5.1 Edge-Loading

As stated previously, edge-loading was defined to occur when the force path was plotted within a distance equal to or less than 10% of the cup radius from the edge of the acetabular cup (zone 1). During walking, edge-loading was observed in 23% of patients (3/13: 1 male, 2 females) in the non-pseudotumour group compared to all patients (6/6) in the pseudotumour group.

During more strenuous activities of daily living such as rising from a chair and stair climbing, edge-loading was observed in all patients in both groups. In patients with bilateral implants (3 patients in the pseudotumour group and 8 patients in the non-pseudotumour group), the occurrence of edge-loading was seen in both hips in all patients.

7.5.2 Zone Duration of Force Paths

Although edge-loading occurred in both patient groups 1 and 2, the distribution of the time spent by the force path in each zone differed significantly. During stance phase of walking, the duration of force path in zone 1 (edge-loading zone) was greater in the pseudotumour group (39% of the stance phase) compared with the three patients in the non-pseudotumour group (15% of the stance phase) who were found to be edge-loading ($p = 0.05$). The force paths in the pseudotumour group were located in zone 1 for the longest duration of the total weight bearing phase, while the longest duration occurred in zone 2 for the non-pseudotumour group (Figure 7-7). In fact, in the pseudotumour group, the total duration of the force paths in zone 1 and 2 accounted for 75% of the total weight-bearing phase. This represented a two-fold increase compared to the time distribution in the corresponding zones observed in the non-pseudotumour group.

The differences in time distribution of the force path between the patient groups were activity-dependent (Figure 7-7). With stair climbing, the differences were accentuated. There was a four-fold significant increase in the zone 1 (edge-loading zone) duration in the pseudotumour group (51% of the stance phase) of the stance phase compared to the non-pseudotumour group (11% of the stance phase) ($p = 0.02$). This indicated that the edge-loading lasted for five times longer in the pseudotumour group than the control group for each stair climbing activity. In fact, the highest zone duration per cycle always occurred in zone 1 for the pseudotumour group, while it occurred in zone 3 for the non-pseudotumour group. In the pseudotumour group, force paths in zones 1 and 2 accounted for 79% of the total weight-bearing phase. This compared with 24% of the weight bearing

phase in the non-pseudotumour group. The overall trend in time distribution of hip force loci between stair ascent and descent was similar in both groups.

The differences between the two groups were less pronounced during rising from and sitting down to a chair (Figure 7-7). In fact, the highest zone duration occurred in zone 1 for both groups, suggesting that rising from and sitting down to a chair was the most provocative activity in the non-pseudotumour groups, in terms of edge-loading. A statistically non-significant increase in zone 1 duration was observed in the pseudotumour group compared to the non-pseudotumour group ($p = 0.15$).

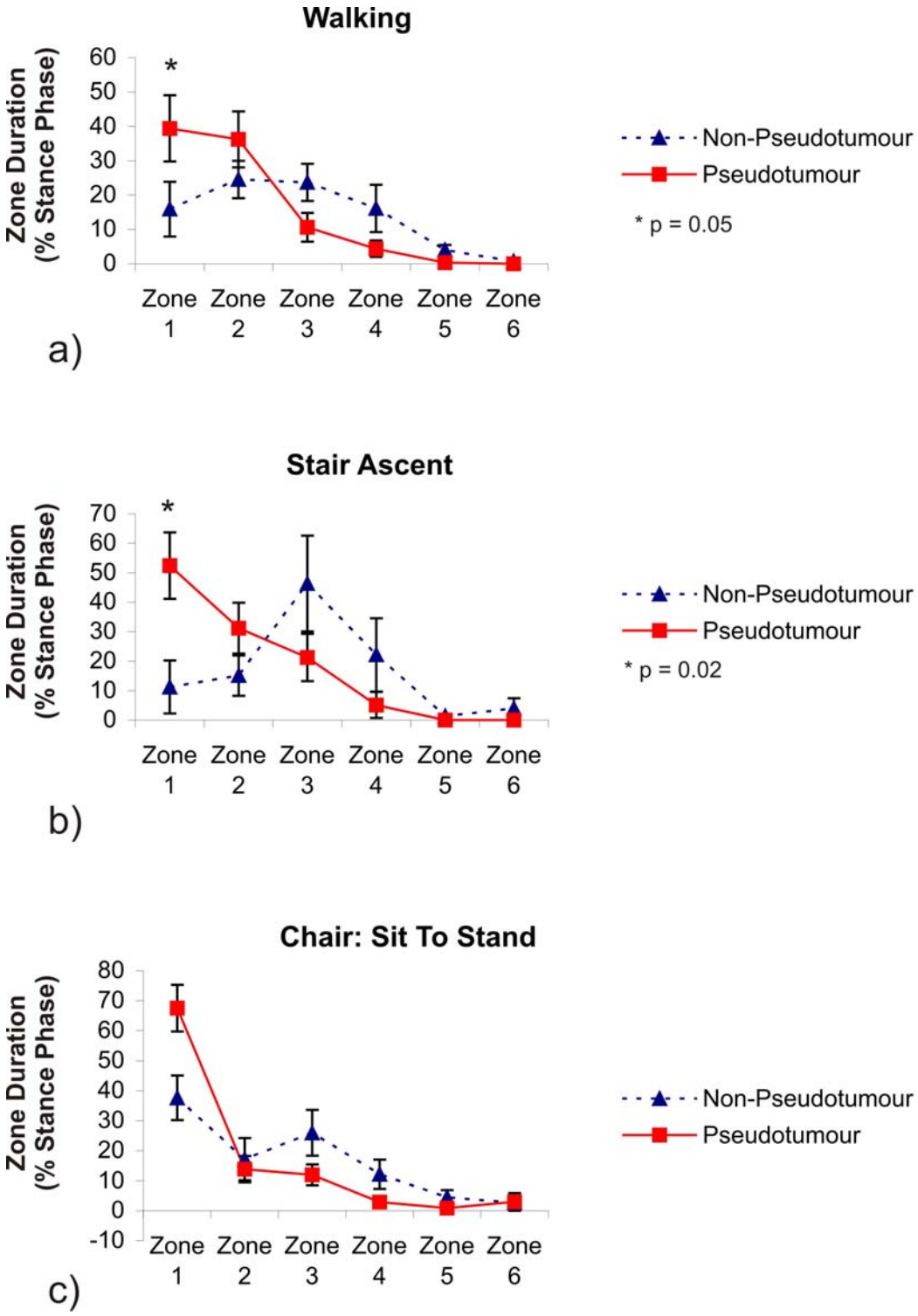


Figure 7-7: Distribution of zone duration during functional activities: walking (a), stair climbing (b), and rising from a chair (c). Zone 1 is defined as the edge-loading zone. The error bars represent standard errors of mean. Asterisk (*) indicates significant difference between the two MoMHRA patient groups.

7.5.3 Force Impulse Distribution of Force Paths

Overall, a similar trend was observed with normalised force impulse distribution of force paths as seen with zone duration (Figure 7-8). During walking, normalised force impulse in zone 1 (edge-loading) during the weight bearing phase was significantly greater in the pseudotumour group compared with the three patients in the non-pseudotumour group who were found to be edge-loading ($p = 0.04$). The comparative differences in force distribution of the force path between the two patient groups were also activity-dependent.

With stair climbing, the relative differences were accentuated. There was a significant four-fold increase in the value of normalised force impulse located in zone 1 (edge-loading) in the pseudotumour group compared with the non-pseudotumour group ($p =0.04$). This indicated that edge-loading occurred with four times greater force impulse in the pseudotumour group than the non-pseudotumour group for each stair climbing cycle. In fact, the highest normalised force impulse occurred in zone 1 (edge-loading) for the pseudotumour group, compared to zone 3 for the non-pseudotumour group. The overall trend in force impulse between stair ascent and descent was similar for both groups. However, the relative differences were less during rising from and sitting down to a chair. There was a non-significant increase in normalised force impulse in zone 1 (edge-loading) during the weight bearing cycle in the pseudotumour group compared with the non-pseudotumour group ($p = 0.20$). The highest normalised force impulse occurred in zone 1 for both groups, suggesting that rising from and sitting down to a chair was the most provocative activity for the non-pseudotumour group, in terms of edge-loading normalised force impulse distribution.

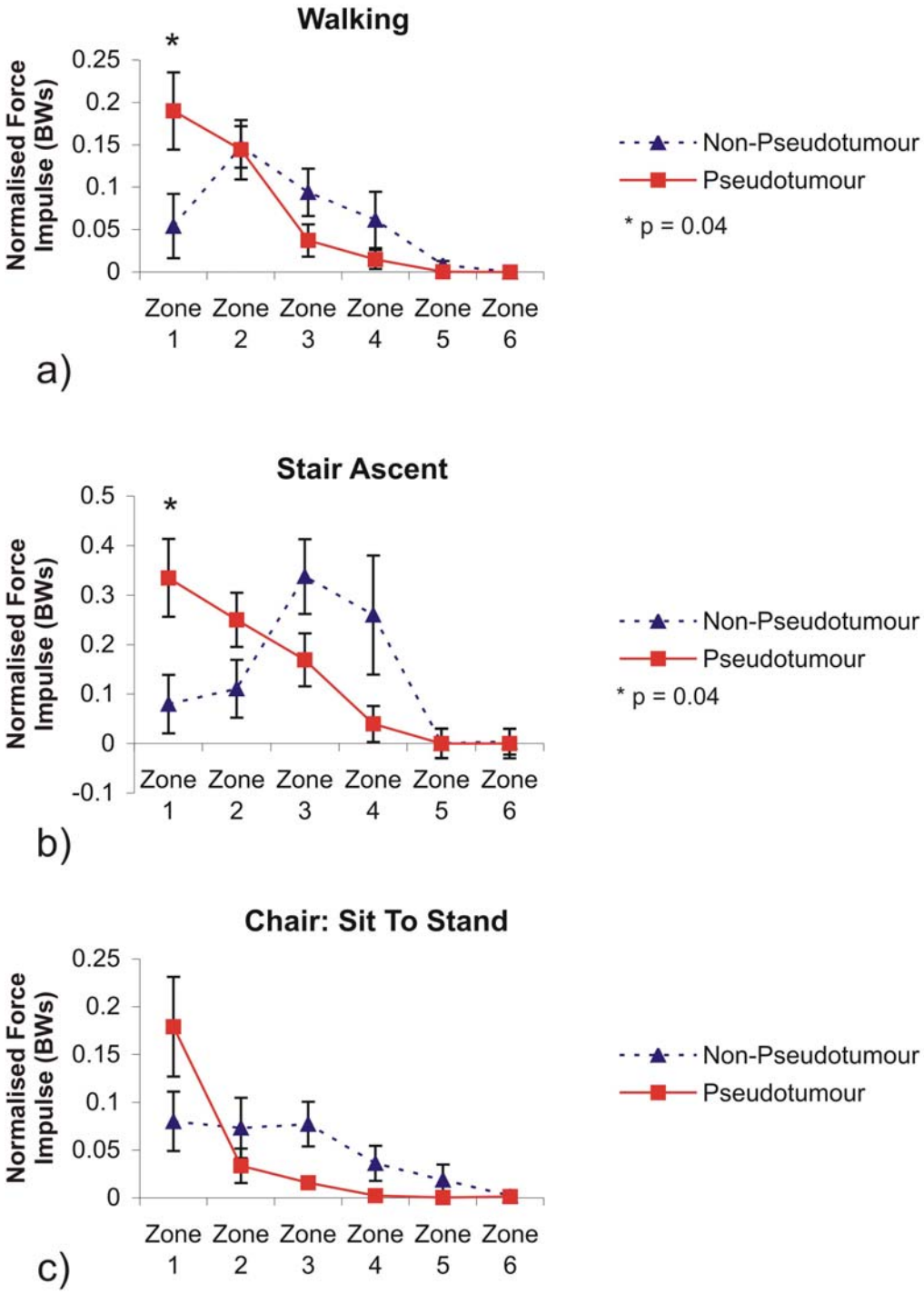


Figure 7-8: Distribution of normalised hip joint force impulse (calculated from the area under force vs. time curve) in each zone during functional activities: walking (a), stair climbing (b), and rising from a chair (c). Zone 1 is defined as the edge-loading zone. The error bars represent standard errors of mean. Asterisk (*) indicates significant difference between the two MoMHRA patient groups.

7.5.4 Acetabular Cup Orientation

In comparison with the non-pseudotumour group, the pseudotumour group was associated with: (1) higher median acetabular cup inclination: 52.0° (range 35.5°- 60.7°) vs. 45.1° (range 27.5°- 62.0°), p=0.10; (2) higher median acetabular anteversion: 21.2° (range 8.8°- 47.0°) vs. 16.0° (range 3.4°- 35.0°, p=0.18); and (3) significantly higher combined inclination and anteversion angle: 75.6° (range 58.4°-100.0°) vs. 58.75° (range 30.1°-90.0°), p=0.04. Although a variation in acetabular inclination and anteversion was observed between the right and the left resurfaced hips in all patients with bilateral MoMHRA in the study, there was no statistically significant difference between the right and left hips (paired t-test, p=0.51 for inclination and p=0.35 for anteversion).

The majority (16/21) of the acetabular cup inclination and anteversion values of the hips in the non-pseudotumour group was found within the safe zone of Lewinnek [202] (Figure 7-9). On the contrary, the cup orientation values in the pseudotumour group were found within the safe zone in one third (3/9) of the hips with the remaining two thirds (6/9) outside the safe zone.

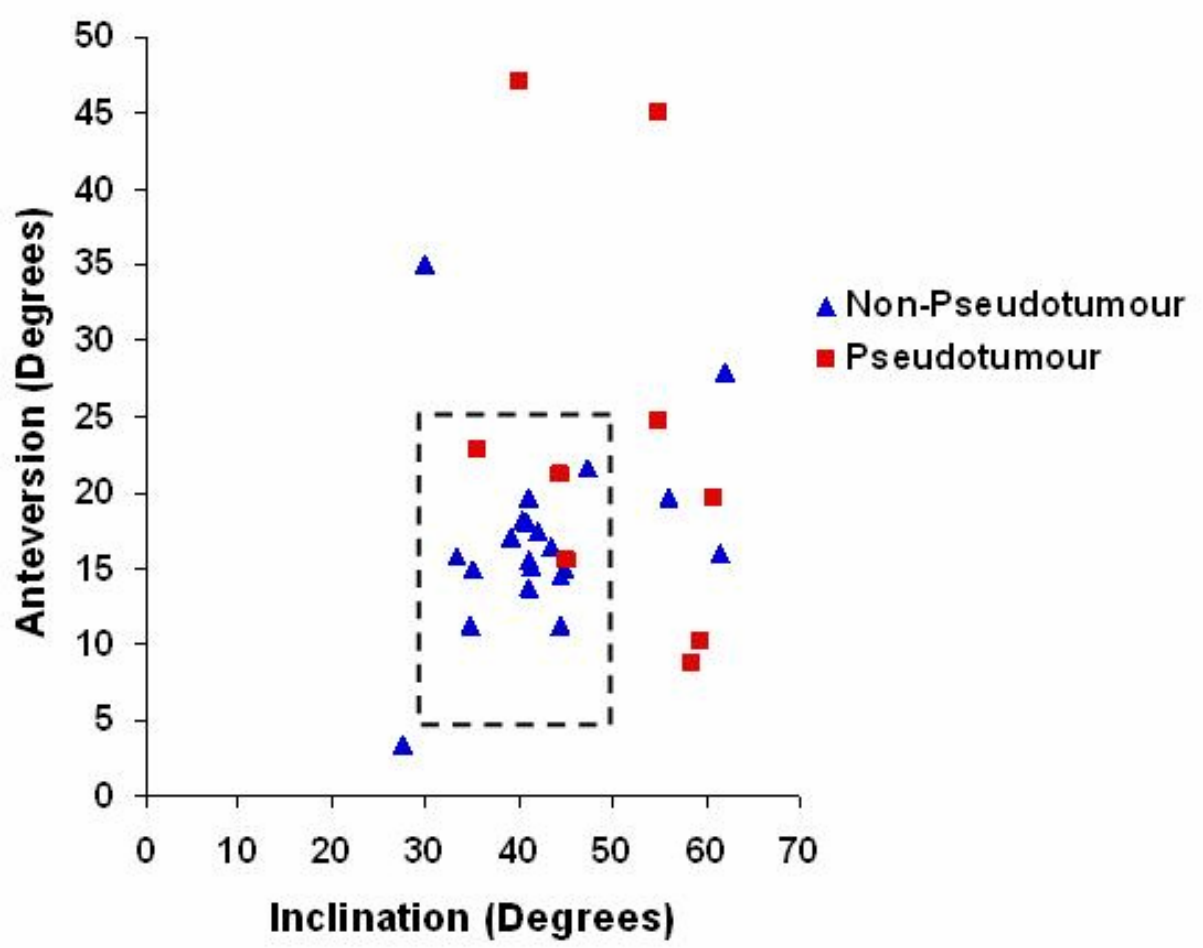


Figure 7-9: Values for the acetabular cup inclination and anteversion of the hips with pseudotumours (n = 9) and the hips without pseudotumours (n = 21). The safe zone, as defined by Lewinnek *et al* [202], is outlined by the dotted rectangle.

7.5.5 Serum Metal Ion Levels

In comparison with the non-pseudotumour group, the pseudotumour group had (Figure 7-10): (1) significantly higher median serum cobalt levels: 14.3 μg/l (range 10.6-64.1 μg/l) vs. 1.9 μg/l (range 1.2-5.0 μg/l), $p<0.001$; and (2) significantly higher median serum chromium levels: 21.2 μg/l (range 13.8-45.2) vs. 1.8 μg/l (range 0.7-7.6 μg/l), $p< 0.001$.

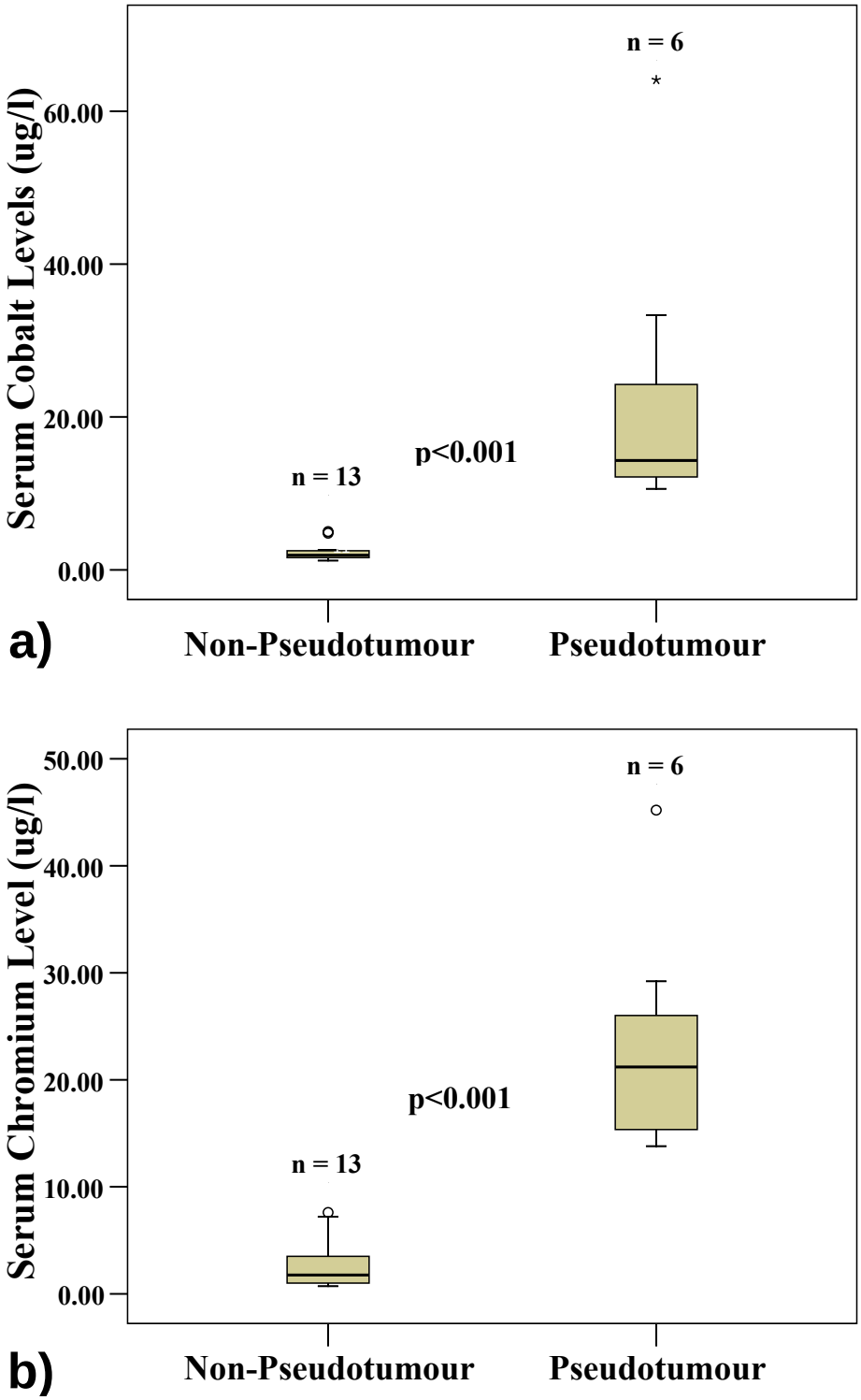


Figure 7-10: Boxplots showing differences in median serum cobalt (a) and serum chromium (b) level measurements between the patient groups. The number of patient per group is denoted by *n*.

7.6 Discussion

Edge-loading has been suggested as a possible mechanism that leads to increased wear in MoMHRA implants [92, 124, 154, 155]. However, edge-loading *in vivo* has not been previously investigated in MoMHRA patients. This study focused on determining whether edge-loading occurs *in vivo* by calculating the dynamic loci of hip joint segment force (force paths) experienced by MoMHRA patients during functional activities, using integrated data from three-dimensional motion analysis and CT scanning.

The results of this study demonstrated that edge-loading, which was defined as the force path occurring at a distance less than 10% of the cup face radius from the acetabular component edge, occurred in MoMHRA patients both with and without pseudotumours. Edge-loading was observed during normal activities of daily living, such as walking, stair climbing and rising from a chair. The observation of edge-loading in patients with well functioning MoMHRAs is consistent with the multi-directional *in vivo* wear paths measured in patients with well functioning THA [183]. The three-dimensional loci of points on the acetabulum over which the femoral component moves demonstrated the wear path extended to the edge of acetabular cups during level-ground walking. Furthermore, *in vivo* studies using video fluoroscopy with three-dimensional fitting have demonstrated that edge-loading with heelstrike can occur during normal walking due to microseparation (pistoning) of hip bearings [174, 175]. Moreover, edge-loading has been suggested to occur during stair climbing and rising from a chair in ceramic-on-ceramic

bearings based on a retrieval study of bearing couples from non-mechanical failures [158].

Although edge-loading occurred in MoMHRA patients both with and without pseudotumours during functional activities, zone duration and force impulse distribution differed significantly. Across the group general trends emerged. Edge-loading in the pseudotumour group was characterised by significantly longer (up to four-fold increase or 70% of weight bearing cycle) time distribution as well as greater amount (up to seven-fold increase) of normalised force impulse distribution in the edge-loading zone 1, compared to the non-pseudotumour group. Therefore, edge-loading in patients with pseudotumours occurred when significantly greater magnitudes of force impulse were experienced near the edge of the acetabular component for a significantly longer period of time. The significant differences in time and force impulse distribution of force paths in the edge-loading zone were activity-dependent, with proportionally greater difference observed during stair climbing. During a 12-hour period, it has been reported that patients with total hip arthroplasty (THA) stair climb 42 cycles, with estimates of 15,000 cycles per year [220, 221]. These significant increases in time and force impulse distribution of force paths in the edge-loading zone during more strenuous activities of daily living may be important factors responsible for increased wear in MoMHRA patients with pseudotumours.

With repeated episodes of loading in the same location, the MoM surfaces may be expected to conform geometrically (self-polish), thereby increasing the contact area and

reducing the contact stress. This self-limiting phenomenon may be offset *in vivo* by an activity-dependent multi-directional dynamic edge-loading process, which has the potential to disrupt favourable fluid-film lubrication modes [162]. Potential factors that would determine whether edge-loading leads to a self-limited phenomenon in contrast to so-called runaway wear may include the frequency, time duration and magnitude with which contact force occurs between the femoral head component and acetabular cup edge.

It may be hypothesised that there is a cumulative threshold of contact stress that must be exceeded by repeated episodes of edge-loading before resulting in significant wear. Therefore, edge-loading can be a 'benign' process that occurs during activities of daily living in patients with well functioning MoMHRA. However, once the contact stress generated by edge-loading exceeds the tolerance of the MoM bearing due to increase in frequency, duration and/or magnitude of contact force, a vicious cycle of wear may ensue. This is consistent with the observation that the edge-loading with significantly increased duration and magnitude of force impulse was measured during functional activities in MoMHRA patients with pseudotumours. It is thus feasible that prolonged edge-loading *in vivo* observed in these patients with pseudotumours in this study may lead to the *in vitro* edge-loading wear pattern seen in the retrieval study (Chapter 6). Furthermore, the *in vivo* observation of edge-loading with significantly increased duration and magnitude of force impulse would, in part, explain significantly elevated serum metal levels in the pseudotumour patient group. The pseudotumour group patients in the current study had more than a seven-fold elevation of median serum cobalt (14.3 μg/l vs. 1.9

μg/l) and a twelve-fold elevation of chromium ion levels (21.2 μg/l vs. 1.8 μg/l) compared to the non-pseudotumour group. In fact, no patient in the pseudotumour group had 'normal' median serum and aspirate levels of cobalt and chromium ions reported in well functioning MoMHRA [17, 79, 82, 125].

Edge-loading modelled in this study is dependent on both the direction of the resultant hip joint segment force vector as well as the orientation of the acetabular component. With metal-on-metal articulation, steep cup inclination can cause edge-loading of the femoral head on the acetabular cup. A rigid cup rim articulating on a rigid femoral head create will create high stress concentrations that may lead to runaway wear. Retrieval studies of metal-on-metal prostheses have confirmed that acetabular components with high inclination angle demonstrate increased wear secondary to edge loading [154, 222]. In addition, elevated serum and joint fluid levels of chromium and cobalt ions have been measured with steep acetabular component positioning in MoMHRA patients [92]. In the current study, there was a trend towards patients in the pseudotumour group having a steeper acetabular component, although the difference was not statistically significant ($p=0.10$). However, the current result is consistent with the clinical study (Chapter 3), in which no significant difference in radiographic inclination angle was found between the patient groups in a much larger cohort of 201 MoMHRA implanted hips. In addition, the median inclination angle of acetabular component in the pseudotumour group 52.0° (range 35.5°- 60.7°) in the current study was within 7° of the reported 'optimal' inclination angle [92, 201]. Therefore, a relatively small increase of inclination angle

measured in the pseudotumour group, on its own, was unlikely to be a dominant risk factor in edge-loading.

Recently, increased anteversion combined with increased inclination has been reported to be associated with elevated concentration of metal ions in whole blood [93]. Increases in anteversion and inclination have been suggested to decrease cover of the femoral component by the acetabular cup, thus decreasing the area for generation of fluid-film lubrication. This is consistent with the current study finding that the pseudotumour group patients, with significantly elevated metal ion levels compared with the non-pseudotumour group, were found to have a significantly greater median combined inclination and anteversion angle values (75.6°, range 58.4°-100.0°, vs. 58.75°, range 30.1°-90.0°, p=0.04). Although the significance of absolute values of combined acetabular orientation angles in the coronal and sagittal plane are not known, the concept of combined angles can be used within the framework of the current *in vivo* study model to illustrate the relationship between the acetabular orientation and edge-loading. For a given dynamic loci of hip joint segment force, an increase in either inclination or anteversion of the acetabular component would move the force path (intersection between the hip force vector and the cup) towards the edge of component. Thus, the shift in loci towards the edge of the cup may result from changes in cup orientation in one or two planes: increase in inclination or version independently, or increase in both inclination and version simultaneously. Therefore, a change of acetabular component orientation in two planes, such as increase in both inclination and anteversion angles, would increase the risk of edge-loading.

Edge-loading calculated in this *in vivo* study also depends on the direction of resultant hip joint segment force vector generated for a given orientation of the acetabular component. Thus, edge-loading may occur if the direction of the hip joint force vector is changed towards the rim of a well positioned acetabular component. This may also occur due to impingement. Impingement is a dynamic process of mechanical abutment conflict [223]. Femoral neck-to-acetabular component impingement may lead to subluxation of hip bearings. As a result, edge-loading may ensue at the opposite side of the impingement site as the hip joint force vector directs non-concentric loading of the femoral component against the acetabular cup edge. As hip resurfacing surgery retains the native proximal femoral geometry, the ratio of width of the head to the neck is much smaller than in conventional hip replacement [224]. Hip impingement may therefore occur more often in resurfaced hips when compared to conventional THR. However, acetabular cup orientation also influences the likelihood of femoral neck-to-acetabular component impingement [223]. Edge-loading in the patients with pseudotumours in this study may, in part, be attributed to the malposition of the acetabular component as the cup orientation in the majority of the pseudotumour hips was found to be outside the safe zone of Lewinnek [202]. This would increase the risk of the impingement-subluxation phenomenon, and hence edge-loading, especially during more strenuous functional activities. Edge-loading, in turn, would lead to violation of fluid-film lubrication with subsequent increase in MoM wear. For this reason, acetabular cup orientation has been suggested to be more critical with MoMHRA than conventional THA as the wear associated with edge-loading can cause disruption of fluid-film lubrication [92]

To summarise, the malposition of the acetabular cup (i.e. significant increase of combined inclination and anteversion angle) in the pseudotumour group may contribute to edge-loading in a number of ways. Firstly, it may decrease cover of the femoral component by the acetabular cup, thus decreasing the area for generation of fluid-film [92]. Secondly, it may also contribute to edge-loading by increasing the risk of impingement-subluxation phenomenon. Thus, the elevated concentration of metal ion levels in the pseudotumour group can be explained, in part, by an increase in the combined inclination and anteversion angle which favours the edge-loading process.

Although explained in part by acetabular cup malposition, the aetiology of edge-loading is likely to be multi-factorial. Edge-loading was observed in both the control group and the pseudotumour group of MoMHRA patients with well positioned acetabular components (i.e. within the safe zone). This indicates that other important dynamic factors may also be at play. These probably include implant, patient and surgical factors. Different implant designs may influence safe cup inclination and anteversion angles. Based on the current *in vivo* study model, implants with a greater angle subtended by the acetabular component (included angle) would shift the loci of hip joint force vector away from the cup edge for any given orientation by providing more cover. Although the implants in the pseudotumour group were predominantly BHR's (8/10) which have a lower included angle, the number of implants in this study was too small to detect any difference. The patient selection was matched in order to minimise confounding factors such as gender, age, femoral component size, as well as time since index surgery.

However, there may be additional factors that were not considered in this study. Even in ideally reconstructed hips, patients who are particularly flexible have a risk of osseous impingement at the extremes of motion. Women may be more likely to develop hip impingement as they have more risk factors. These risk factors include: smaller sized implant, a greater range of movement; and more joint laxity than men [225]. This may, in part, explain significantly higher prevalence of pseudotumours in female patients. In patients with joint laxity, edge-loading at heelstrike may also increase due to microseparation of the head from a well positioned cup.

Furthermore, the variables causing impingement may be additive. Bone impingement, soft tissue mass impingement, or a reduction in the muscle forces that normally hold the hip reduced may all cause subluxation of hip bearings. The exact point at which impingement occurs will depend on the bone anatomy of each individual patient. The presence of anterior femoral neck osteophytes not resected at the time of index operation would also increase the risk of anterior impingement postoperatively. Patients with the underlying pathological deformity such as femoro-acetabular impingement, characterised by the lack of femoral head-neck offset, may lead to impingement. As the femoral-head neck junction is preserved in hip resurfacing, either the malpositioninig of components or inadequate correction of deformity would increase the post-operative risk of impingement. Therefore, in patients with underlying pathological deformities, it may be more critical to improve the head-neck sagittal offset intra-operatively by judicious removal of anterior neck osteophytes or anterior translation of the femoral component. Lastly, the presence of a soft tissue pseudotumour mass about the hip joint may also

contribute to the risk of the impingement-subluxation phenomenon with subsequent increased edge-loading in MoMHRA patients.

The results of this study need to be considered in light of the potential limitations. Inaccurate placements of markers leads to inaccurate kinematic and kinetic results. Low inter-rater reliability in landmark palpation has been reported [226]. For this reason, the marker placement was carried out by the investigator for all study patients. Accuracy could have been further reduced during motion analysis by movement artefacts created by the relative motion of skin markers with respect to the underlying bones [177]. However, the error assessment has demonstrated that that potential source of errors such as variation in walking cadence, and velocity in each patient were repeatable and systematic.

The mathematical models that were used in the data processing computer software to estimate the hip joint force vector relied on a number of assumptions. Body segments were assumed to be rigid bodies, which do not change in shape or size. The rigid body assumption is required to establish a frame of reference within each body segment. In reality, these conditions do not exist. However, deformation occurring within any one segment can be considered to be negligible in comparison to the overall limb movements. Furthermore, resultant hip joint segment force measured in this study is a computational quantity derived from combined measurement of body position and simultaneous measurement of ground reaction force using an inverse dynamics technique, which in turn relies on rigid body assumption. The resultant hip joint segment force therefore

represents the sum of hip joint reaction forces and muscle forces. As such, hip joint segment force does not provide any specific information in terms of muscle activation or the stress on the MoMHRA implants involved in the articulation. However, the focus of the study was on the comparative values between the two groups, which would have been similarly affected by these model assumptions.

Three-dimensional orientation of the femoral components was not measured in this study. This was because there was poor repeatability of CT coordinate measurement of femoral component, which would have led to unacceptable error. However, contrary to THA, anteversion of the femoral component in MoMHRA has been reported to have a minimal effect on impingement [227]. Two-dimensional surface projection of three-dimensional spherical data may have led to slight distortion of the image at the edge of the sphere. However, this distortion was minimised by normalising the acetabular cup internal radius to the external femoral head component radius.

The power of the study may be low due to small sample sizes. The sample size of the pseudotumour group was limited clinically by the number of patients with radiologically confirmed diagnosis from the earlier clinical study. However, the selection of the control group was carefully matched (with a ratio of 2:1) for gender, age, femoral component size, as well as time since index surgery in order to minimise confounding factors. Despite the small number of patients, the trends observed were consistent and significant differences were found. The results of this study highlight trends that may be confirmed with greater sample size.

In conclusion, edge-loading in MoMHRA patients with pseudotumours occurred *in vivo* with significantly longer duration and greater magnitude of force impulse compared to the patients with well functioning MoMHRA during activities of daily living. Although the acetabular component malposition, such as increase in both inclination and anteversion angles, appears to be an important factor in edge-loading, the aetiology of edge-loading is likely to be multi-factorial. Further research is required to elucidate the relative importance of implant, patient, and surgical factors that lead to edge-loading. The results of the current *in vivo* study support the observation of edge-loading wear in the *in vitro* retrieval study. Therefore, this suggests that edge-loading is an important mechanism that leads to localised high wear, with subsequent elevation of metal ion levels in MoMHRA patients with pseudotumours.

7.7 Summary

- The results of the current *in vivo* study demonstrated that edge-loading in patients with pseudotumours occurred with a significantly greater magnitude of hip joint force impulse occurring close to the edge of the acetabular components for a significantly longer period of time, compared to the patients without pseudotumours. Therefore, the null hypothesis, which has stated that there is no difference in edge-loading (as measured by force path) between MoMHRA patients with pseudotumours and MoMHRA patients without pseudotumours during functional activities of daily living, was rejected.
- This *in vivo* finding supports the *in vitro* retrieval study (Chapter 6) findings of edge-loading of acetabular cup components in the pseudotumour group.
- Although malposition of acetabular component orientation, such as increases in both inclination and anteversion angles, appears to be an important factor in edge-loading, the aetiology of edge-loading is likely to be multi-factorial.
- The significant increase in time and force impulse distribution of force paths in the edge-loading zone were activity-dependent, with proportionally greater difference observed during more strenuous activities such as stair climbing.
- Therefore, it is concluded that edge-loading is an important *in vivo* mechanism responsible for localised high wear and subsequent elevation of metal ion levels in MoMHRA patients with pseudotumours during functional activities.

CHAPTER 8 CONCLUSIONS, CLINICAL RELEVANCE AND FUTURE WORK

8.1 Review of Research Objectives

Metal-on-metal hip resurfacing arthroplasty is increasingly being used as an alternative treatment option for young and active patients with significant hip osteoarthritis due to the limitations of conventional total hip arthroplasty. According to the 2008 National Joint Registry England and Wales Annual Report [2], the total number of hip resurfacing procedures accounted for 46% (1585 of 3471) of all primary hip arthroplasty procedures performed in the patient group younger than 55 years of age**.** Despite the satisfactory short-term implant survivorship, abnormal periprosthetic soft-tissue pseudotumour masses relating to the hip joint are being increasingly reported. These were found be locally destructive, requiring revision surgery in a high proportion (75%) of patients. Furthermore, the outcome of revision surgery for pseudotumour is inferior to the outcome of other MoMHRA revisions as well as the outcome of primary THA matched cases [43]. In addition, the reports of these soft-tissue masses are emerging from a number of orthopaedic centres across the United Kingdom [39-41]. However, there is currently no definitive evidence of potential mechanisms involved in the pathogenesis of such destructive soft tissue masses. It was therefore necessary to investigate this clinically important complication in order to provide evidence-based recommendations to minimise such an adverse clinical outcome in the future.

The scope of this thesis was therefore to determine whether an emerging clinical complication (pseudotumour) with a high revision burden results from a local biological reaction to increased wear particle burden, generated by excessive MoMHRA implant wear. This thesis set out to examine the research question in the following manner:

- Firstly, a clinical study was designed to establish the prevalence of, and the relationship between, serum levels of metal ions and presence of pseudotumours in patients with MoMHRA.
- Secondly, *in vitro* experiments were conducted to investigate the role of metal-induced hypersensitivity and cytotoxic effects of large amounts of metal nanoparticles and metal ions as potential biological reactions mediating the occurrence of pseudotumours in patients with MoMHRA.
- Thirdly, a retrieval study analysed the bearing surface wear of MoMHRA implants from patients with pseudotumours and compared these to retrievals for other revision indications.
- Lastly, an *in vivo* study was performed to investigate the role of edge-loading as a potential wear mechanism leading to elevated production of metal particles and metal ion levels in MoMHRA patients.

The main conclusions of these studies are discussed in the following section.

8.2 Conclusions

A review of the literature (Chapter 2) demonstrated that despite increasing cases of pseudotumours being reported, the current available information is limited to a small number of descriptive studies with anecdotal association of elevated metal ion levels in

patients with pseudotumour. This presented the case for further studies designed to explore potential mechanisms involved in pathogenesis of soft tissue pseudotumours.

A clinical study (Chapter 3) was necessary to confirm anecdotal findings and establish a framework for the remainder of the thesis. The clinical study investigated the prevalence of, and association between, pseudotumours and serum metal ion levels in patients with MoMHRA. The overall prevalence of pseudotumour was found to be 4%, with a very high prevalence of 30% in females with bilateral MoMHRA implants. The prevalence was considerably higher than previously estimated, thereby justifying the case for further studies designed to explore potential mechanisms involved in pathogenesis of this clinically important complication. The study also established that pseudotumour was associated with elevated metal ion levels. There was up to a six-fold elevation of serum and thirteen-fold elevation of hip aspirate levels of metal ion levels in patients with pseudotumours compared with patients without pseudotumours. In fact, pseudotumours were not detected in those patients who had normal levels of metal ions. This suggested that pseudotumours do not occur if the MoM articulations are well functioning.

It was postulated that pseudotumours are likely to be biological reactions to large amount of metal debris generated *in vivo* due to excessive wear. Two potential biological reactions mediating the occurrence of pseudotumours in patients with MoMHRA were then investigated. An *in vitro* clinical study (Chapter 4) was designed to assess systemic hypersensitivity responses to metal ions in patients with pseudotumour using the lymphocyte proliferation test. The study demonstrated that systemic exposure and

lymphocyte reactivity to cobalt and chromium, principal elements in the alloy used in the MoMHRA, and nickel, a common sensitiser, did not differ in patients with pseudotumour compared to those patients without pseudotumours. It is concluded that systemic hypersensitivity type IV reaction, mediated by lymphocyte reactivity to these metals, is not the dominant biological reaction mediating the occurrence of soft tissue pseudotumours.

A further *in vitro* experiment was conducted to determine whether a local cytotoxic effect of large amounts of metal wear debris may be the potential biological response. To achieve this, the effects of metal nanoparticles and metal ions on the viability of macrophages were separately investigated *in vitro* (Chapter 5). The results of this study demonstrated that cobalt nanoparticles and ions have dose-dependent effects on the viability of macrophages *in vitro*. It is concluded that the local cytotoxicity of high concentrations of cobalt nanoparticles phagocytosed by macrophages leading to necrosis may be an important biological reaction involved in the occurrence of soft tissue pseudotumours. It also suggested that lack of differences in hypersensitivity testing may be due to *in vivo* cytotoxic effects of increased metal ion levels on local lymphocytes.

Subsequent research focused firstly on assessing the magnitude of bearing surface wear that occurs in pseudotumour patients, and secondly on elucidating the potential wear mechanism responsible for the increased implant wear in these patients. In order to measure implant wear in patients with pseudotumours, an *in vitro* retrieval study was conducted (Chapter 6). The retrieval study demonstrated that MoMHRA implants revised

due to pseudotumour are associated with significantly greater linear wear rates of both the femoral head and the acetabular cup components. Implants in the pseudotumour group had up to a four-fold increase of median linear wear rate of the femoral component and greater than a five-fold increase of median linear rate of the acetabular component, in comparison with implants in the non-pseudotumour group. This *in vitro* finding supported the *in vivo* findings of elevated metal ion concentrations in the serum and the hip aspirates from patients with pseudotumours (Chapter 3). It is concluded that pseudotumour in contemporary MoMHRA implants is associated with increased wear at the MoM articulation. Wear on the acetabular cup component in the pseudotumour group always involved the edge, indicating edge-loading of the bearing. This highlighted that edge-loading with the loss of fluid film lubrication may be the dominant wear generating mechanism in MoMHRA patients with pseudotumour.

An *in vivo* motion analysis study was then developed (Chapter 7) to investigate edge-loading as a mechanism that can lead to the increased wear in patients with pseudotumours. The results of the *in vivo* study demonstrated that edge-loading in patients with pseudotumours occurred with significantly greater magnitude of hip joint force impulse near the edge of the acetabular component for a significantly longer period of time, compared to the patients without pseudotumours. Edge-loading in the pseudotumour group was characterised by up to four-fold increase or 70% of weight bearing phase time distribution and up to seven-fold increase of normalised force impulse distribution in the edge-loading zone. This *in vivo* finding supported the *in vitro* retrieval study (Chapter 6) finding of edge-loading in the pseudotumour group. Therefore, it is

concluded that edge-loading is an important *in vivo* mechanism responsible for localised high wear and subsequent elevation of metal ion levels in MoMHRA patients with pseudotumours during functional activities. Although the risk of edge-loading is influenced by acetabular component malposition, edge-loading is likely to be multi-factorial in its aetiology and further work is required to investigate the relative importance of implant, surgical and patient factors.

It is therefore concluded that the occurrence of soft tissue pseudotumour represents a local biological reaction to high metal debris load generated by excessive MoMHRA implant wear. Edge-loading is likely be an important factor contributing to increased wear of MoMHRA implants, leading to dose-dependent cytotoxicity and subsequent necrosis of periprosthetic soft tissues in susceptible patients.

8.3 Clinical Relevance

The current work presented in this thesis has contributed to the body of knowledge and understanding of pseudotumour, a clinically significant complication that occurs in patients following MoMHRA. For the clinicians and the surgeons involved in the care of MoMHRA patients, the findings of this thesis would be informative in a number of ways:

- Clinicians need to be aware of pseudotumours as a possible differential diagnosis during clinical evaluation of patients with unexplained symptoms following MoMHRA, even with normal appearance of plain radiographs. In these patients, further radiological investigation utilising soft-tissue imaging modalities such as ultrasound or MRI is recommended.

- Surgeons should undertake the MoMHRA procedures with great care, especially in females, in the knowledge that even with satisfactory acetabular component position, pseudotumours can occur.
- The *in vitro* study provided evidence that systemic hypersensitivity type IV reaction, mediated by lymphocyte reactivity to these metals, is not the dominant biological reaction in the occurrence of the soft tissue pseudotumours. Therefore, the study results do not support the routine use of lymphocyte transformation tests to screen patients pre-operatively.
- The study findings have implications for surgical technique. Although edge-loading was observed in MoMHRA patients with well positioned acetabular components, the majority of pseudotumour group patients were found to have malpositioned acetabular components on CT-based measurements. Therefore, this study highlighted the importance of accurate acetabular component implantation during MoMHRA. Improvement would, however, require a multifaceted approach that involves surgeon training as well as improvement in instruments. This is because acetabular anteversion is difficult to assess during surgery, especially with lateral patient positioning, as pelvic flexion on operating table is influenced by bracing method, the state of the other hip and the spine [228]. This variation of pelvic position on the operating table may not be evident to the surgeon. In addition, the use of MoMHRA acetabular component has reduced acetabular sector angles to less than 170° and requires nearly complete coverage of the cup by bone, which can promote implant inclination in excess of 50°. Technically, this

preparation is difficult because the acetabular preparation is done with reamers that have a 180° angle [223].

- Pseudotumours may develop several years following the surgery. This highlights the need for regular clinical outcome assessment of MoMHRA patients. This is of a particular importance in MoMHRA patients as MoMHRA is a relative new type of implant with short-term survivorship data.

In this thesis, an *in vivo* study was developed to investigate edge-loading in patients with pseudotumours. This involved the introduction of a novel methodology in assessing *in vivo* edge-loading utilising the combination of motion analysis and CT scans. The *in vivo* study was able to estimate the amount of edge-loading, and provided insight into the parameters that may be important. The *in vivo* edge-loading demonstrated in this study has implications for testing of MoMHRA implants *in vitro*. Studies that use standard hip simulators to reproduce the forces of normal walking may be unrealistic. Hip simulator studies must include edge-loading if they are to provide an indication of *in vivo* performance of new bearings. The data collected from such hip joint simulator studies would more accurately predict MoMHRA bearing wear *in vivo*. In addition, this study could be used to assess the effects of variables such as implant design on the locus of force relative to cup *in vivo* in patients with MoMHRA. Furthermore, in conjunction with finite element (FE) models of the resurfacing implants, the current study could be used to calculate MoMHRA implant contact stress during functional activities. Moreover, it may be feasible that the motion analysis and CT scans can be used during pre-operative

planning in order to determine the patient-specific safe zone of acetabular component orientation relative to the native acetabulum.

The results of the studies presented in this thesis provide evidence that support a relationship between the increased metal wear particle generation and the occurrence of an adverse local biological reaction with a high revision burden, pseudotumour. This justifies the heightened concerns in the literature over the unknown risks of long-term exposure to metal debris, especially as metal-on-metal hip resurfacing procedures are increasingly being used in younger active patients. Therefore, the evidence presented in this thesis reinforces the need for continuing clinical surveillance as well as the need for further studies to understand and reduce wear in patients with MoMHRA.

8.4 Recommendations for Future Studies

Although the current thesis provided evidence that pseudotumour is a dose-dependent wear-related biological reaction, there are important areas that need further investigation. Thus, it is hoped that further work raised by the current thesis will overcome important inherent limitations of the studies presented in this thesis, thereby providing additional insights into this clinically important complication.

The cross-sectional study (Chapter 3) was limited by its study design and a relatively small number of pseudotumour cases identified. Thus, interpretation of any trend present within this patient group should be done so with caution. It remains unknown as to why pseudotumour does not occur in all patients with elevated serum levels. A longitudinal

study is needed to provide important information as to whether these patients are at risk of developing pseudotumours later on. Moreover, such a study will also provide information as to whether the prevalence of pseudotumours in MoMHRA patients increases with longer follow-up, due to increased wear as a function of time and use.

The evidence provided in the study does not elucidate the reason for the high prevalence in females with bilateral implants. A large multi-centre prospective study would be able to control confounding factors in order to confirm this trend and identify potential risk factors. It is likely that the individual biologic response to the presence of wear debris may vary, reflecting a different toxic-effect threshold or immunological intolerance. Female prevalence may be attributed to cumulative effects of multiple gender differences such as local anatomy, smaller component size, range of motion, and the prevalence of localised periprosthetic metal-hypersensitivity reactions. Therefore, it is likely that pseudotumour occurs in the individual who has both idiosyncratic susceptibility as well as excess wear debris generation from the bearing surfaces. However, further studies are required to investigate these potential factors. Furthermore, in light of increasing awareness of pseudotumours, a clinical study would be required to assess whether earlier detection of pseudotumour and subsequent earlier revision surgery leads to improved clinical outcome.

Due to the limitations of skin patch testing, *in vitro* lymphocytic proliferation testing (Chapter 4) is considered to represent a more clinically appropriate method of assessing lymphocyte reactivity to metals. However, the local periprosthetic hypersensitivity cannot

be entirely excluded as the test utilised measures systemic hypersensitivity response. Thus, the next stage of investigation would involve measuring local lymphocyte reactivity in hip aspirates. This was not feasible in the current study as there was insufficient volume of hip aspirates available. Therefore, it would be beneficial for a future study to consider measuring lymphocyte reactivity in the local periprosthetic environment. Similarly, measurements of various cytokines in the hip aspirates would also provide additional information regarding the inhibition or activation of macrophages in the periprosthetic environment *in vivo* (Chapter 5). In addition, it remains unclear as to why the pseudotumours have only recently been reported in patients with contemporary MoMHRA, given that the MoM bearing has been in use during the past three decades. As the biological reaction to wear debris is influenced by size, shape and composition of the metal particles and ions, it is possible that the characteristics of wear debris generated from edge-loading of the contemporary MoMHRA implants may differ from the wear debris generated from earlier generations of MoMHRA implants and small diameter MoM bearings used in THA. However, further studies would be required to characterise wear debris generated from various implants with different designs and compare their biological responses.

Future research is required to develop reproducible techniques which will improve the reliability of correct alignment of the acetabular component during MoMHRA. This should include improved instrumentation, CT based pre-operative planning, navigation, and knowledge of the exact position of the hip and the components whilst the patient is on the operating table, which may allow a more accurate component size and position

tailored to each individual patient. A more accurate and reproducible component position may reduce the risk of edge-loading.

Another important line of future research highlighted by this thesis is the need for further *in vivo* investigation of edge-loading. The aetiology is likely to be multi-factorial and these may include implant, patient and surgical factors. *In vivo* studies of bony impingement and soft tissue mass impingement, which may all cause the impingement-subluxation phenomenon with subsequent edge-loading in MoMHRA patients, may help to identify these factors. This could be achieved by combining motion analysis with video fluoroscopy. This will also help to validate the *in vivo* study model (Chapter 7) used in this thesis. The ultimate objective of this and further work would be to identify the relative importance of these factors which lead to edge-loading in MoMHRA implants. Such evidence-based information will be pivotal for patient selection, surgical technique and design of future hip resurfacing implants in order to minimise the occurrence of such an adverse clinical outcome and ensure long-term implant survivorship in young and active patients.

APPENDIX 1: OXFORD HIP SCORE

1. During the past 4 weeks, how would you describe the pain you usually had from your hip?

None (1)	Very mild (2)	Mild (3)	Moderate (4)	Severe (5)

2. During the past 4 weeks, have you had any trouble with washing and drying yourself (all over) because of your hip?

No trouble at all (1)	Very little trouble (2)	Moderate trouble (3)	Extreme difficulty (4)	Impossible to do (5)

3. During the past 4 weeks, have you had any trouble getting in and out of a car or using public transport because of your hip?

No trouble at all (1)	Very little trouble (2)	Moderate trouble (3)	Extreme difficulty (4)	Impossible to do (5)

4. During the past 4 weeks, have you been able to put on a pair of socks, stocking or tights?

Yes, easily (1)	With little difficulty (2)	With moderate difficulty (3)	With extreme difficulty (4)	No, impossible (5)

5. During the past 4 weeks, could you do the household shopping on your own?

Yes, easily (1)	With little difficulty (2)	With moderate difficulty (3)	With extreme difficulty (4)	No, impossible (5)

6. During the past 4 weeks, for how long have you been able to walk before pain from your hip becomes severe (with or without a stick)?

No pain/more than 30 minutes (1)	16 – 30 minutes (2)	5 – 15 minutes (3)	Around the house only (4)	Not at all – pain severe on walking (5)

7. During the past 4 weeks, have you been able to climb a flight of stairs?

Yes, easily (1)	With little difficulty (2)	With moderate difficulty (3)	With extreme difficulty (4)	No, impossible (5)

8. During the past 4 weeks, after a meal (sat at a table), how painful has it been for you to stand up from a chair because of your hip?

Not at all painful (1)	Slightly painful (2)	Moderately painful (3)	Very painful (4)	Unbearable (5)

9. During the past 4 weeks, have you been limping when walking because of your hip?

Rarely/never (1)	Sometimes, or just at first (2)	Often, not just at first (3)	Most of the time (4)	All of the time (5)

10. During the past 4 weeks, have you had any sudden or severe pain – 'shooting', 'stabbing', or 'spasms' – from the affected hip?

No days (1)	Only 1 or 2 days (2)	Some days (3)	Most days (4)	Every day (5)

11. During the past 4 weeks, how much has pain from your hip interfered with your usual work (including housework)?

Not at all (1)	A little bit (2)	Moderately (3)	Greatly (4)	Totally (5)

12. During the past 4 weeks, have you been troubled by pain from your hip in bed at night?

No nights (1)	Only 1 or 2 nights (2)	Some nights (3)	Most nights (4)	Every night (5)

The Oxford Hip Score [123] was used with a 0 to 48 scale, with 48 being the best score, as recommended in the literature [116]. Thus, a total score recorded in the 12-60 scale (as above) was converted to a total score in the 0-48 scale by subtracting from 60:

Total Score (in 0-48 scale) = 60 – Total Score (in 12-60 scale).

APPENDIX 2: *IN VITRO* CYTOTOXICITY EXPERIMENTAL PROTOCOL

A. CELL CULTURE

I. Cell Preparation

Thawing of Cells

- Switch on the water bath set at 37°C
- Warm up tissue culture medium of 10% FBS (foetal bovine serum, M.B. Meldrum Ltd., UK) (50 ml) containing growth factors, αMEM (α Eagle minimum essential medium, Gibco BRL, Invitrogen Lt., Paisley, UK) (445ml) containing nutrients, and penicillin (100 U/ml)/streptomycin (100 µg/ml) (Gibco BRL, Invitrogen Ltd., Paisley, UK) (5 ml), by placing in the water bath for 30 minutes
- RAW 264.7 murine macrophage cell line (contained in the cryovials) is obtained from stock in liquid nitrogen
- Transport the cryovials back to the tissue culture laboratory and place them in the water bath
- Remove the cryovials from the water bath once thawed (5 minutes)

Re-Suspension of Cells:

- Add 2ml of fresh warm tissue culture medium to an universal tube
- Add thawed cells (1 ml)
- Add further 7 ml of fresh warm medium to make a 10ml solution
- Centrifuge at 1000 rpm for 5 minutes
- Re-suspend cells by adding 10 ml of fresh medium

Seeding of Cells

- Seed cells by placing 10ml solution containing re-suspended cells onto petridish (10 cm diameter)

Incubation

- Cells are cultured in 10% FBS containing penicillin/streptomycin and αMEM at 37°C CO_2 5%.

II. Preparation of Metal Ions/Particle Stock Solutions

1. Metal Ions

Prepare a 1000mM stock solution of metal ions:

a) Chromium (III) Chloride Hexahydrate

Molecular weight (MW) = 266.45

Thus, 1M = 266.24 g/L, and 1 mM = 266.24 mg/L = 0.26624 mg/mL

Hence, 1000 mM = 266.24 mg/mL = 2662.4 mg/10mL

b) Cobalt (II) Sulphate Heptahyrate

MW = 281.1

Hence, 1000 mM = 2811 mg/10mL

Perform serial dilutions of 1000 mM stock solution to prepare 1 μM, 10 μM and 100 μM of metal ion solutions

2. Metal Particles

Prepare a 1×10^{13} particles/mL stock concentration of metal nanoparticles:

a) Cobalt Nanoparticles

Density = 8900 kg/m^3 = mass in kg/volume in m^3

Thus, mass of 1 particle = density × volume of 1 particle

Assume a metal nanoparticle as a sphere:

Volume of 1 particle = $4/3\times\pi\times r^3$

Average particle diameter = 28 nm, radius (r) = 14 nm

Thus, volume of 1 particle (nm^3) = 11494.04 nm^3

Hence, mass of 1 particle (mg) = [8.90×10^9 mg / 1×10^{27} nm^3] × 11494.04 nm^3

$= 102296.96 \times 10^{-18} = 1.02 \times 10^{-13}$ mg

Therefore, mass of particle (mg)/mL = number of particle required/mL × 1.02×10^{-13} mg

Thus, 1×10^{13} particles/mL = 1.02×10^{0} mg/mL = 1.02 mg/mL

b) Chromium Nanoparticles

Density = 7140 kg/m^3

Average particle diameter = 30 nm, r = 15 nm

Volume of 1 particle (nm^3) = 14137.16nm^3

Hence, mass of 1 particle (mg) = 7.14×10^{9} mg / 1×10^{27} nm^3 × 14137.16 nm^3

= $100939.32 \times 10^{-18}$ = 1.01×10^{-13} mg

Thus, 1×10^{13} particles/mL = 1.01×10^{0} mg/mL = 1.1 mg/mL

c) Titanium Nanoparticles

Density = 4507 kg/m^3

Average particle diameter = 35 nm, r = 17.5 nm

Volume of 1 particle (nm^3) = 22449.30 nm^3

Hence, mass of 1 particle (mg) = 4.51×10^{9} mg / 1×10^{27} nm^3 × 2249.30 nm^3

= $101246.34 \times 10^{-18}$ = 1.01×10^{-13} mg

Thus, 1×10^{13} particles/mL = 1.01×10^{0} mg/mL = 1.01 mg/mL

Sterilise all nanoparticles by autoclaving

Sonicate all metal particle (Co, Cr, and Ti) stock concentrations for 10 minutes to re-suspend the particles using Tru-Sweep™ ultrasonic cleaner (Crest Ultraionic SDN, BHD, Malaysia)

Perform serial dilutions of 1×10^{13} particles/mL stock concentration to prepare 10^{7}, 10^{8}, 10^{9}, 10^{10}, 10^{11}, 10^{12}/ml concentrations of metal nanoparticles.

III. Co-Culture with Metal Ions/Particles

Cell Scraping:

- Take the petridish containing RAW 264.7 murine macrophage cell cultures from the incubator
- Use a disposable cell scraper to dislodge the adherent cells on the petridish

Cell Mixing

- Use a pipette with 10 mL tip
- Tilt the petridish containing RAW 264.7 murine macrophage cell cultures from the incubator
- Mix the total volume of cell cultures using pipette placed at the top part of the petridish, while avoiding excessive bubbles
- Repeat the cell mixing process three times

Cell Counting

- Pipette 20 µL from the petridish onto a cell-counter 4×4 grid glass-slip
- Count cells (on a 4×4 grid) using microscope and hand-held counter to determine the cell number per mL
- Calculate:
    - Total number of cells available = cell number per mL × total volume of culture medium
    - Cell number per well = volume per well (mL) × cell numbers/mL × number of wells

Sub-Culture of Cells into the Tissue Culture Plates

- 96-Wells (for Alamar Blue assay):
    - Open the lid of 96-wells and set the wells in a tilted position by placing it on the lid
    - Use the multi-release pipette (set the number of releases and the volume/release)
- 48-Wells (for Live/Dead Assay):
    - Place a coverslip into each well

  - Use the multi-release pipette (set the number of releases and the volume/release)
- Volume required per well is determined based on the total cell numbers available at a seeding density of 1×10^5 cells/cm^2

Incubate at 37°C CO_2 5% for 2-4 hours

Co-Culture with Metal Ions/Particles

- Use the multi-release pipette to add 200μL of various metal ion/particle concentration into each column of wells containing sub-cultured RAW 264.7 murine macrophage cells
- Nanoparticles:
  - Chromium nanoparticle concentrations at 10^7, 10^8, 10^9, 10^{10}, 10^{11}, 10^{12}, 10^{13} particles/ml
  - Cobalt nanoparticle concentrations at 10^7, 10^8, 10^9, 10^{10}, 10^{11}, 10^{12}, 10^{13} particles/ml
  - Titanium nanoparticle concentrations at 10^7, 10^8, 10^9, 10^{10}, 10^{11}, 10^{12}, 10^{13} particles/ml
- Metal ions:
  - Chromium (III) chloride hexahydrate concentrations at 1 μM, 10 μM, 100 μM, 1000 μM
  - Cobalt (II) sulphate heptahyrate concentrations at 1 μM, 10 μM, 100 μM, 1000 μM
- Medium alone: a negative control
- Use a new pipette tip for each group in order to avoid cross-contamination of different agents and concentrations

Feeding of Cells at Day 1 and Day 3:

- Remove the remaining medium from each well containing RAW 264.7 murine macrophage cell cultures using the vacuum suction unit

- In order to avoid drying out cells in the wells, repeat the process every two rows of wells
- Use a multi-release pipette to add fresh 200μL of tissue culture medium in to each well

B. VIABILITY ASSAYS

I. Alamar Blue (AB) Assay

Preparation of 5 % Alamar Blue (AB)

- Switch on the water bath
- Prepare a 5 % AB in 30 mL solution
    - Add 1.5 mL of AB Blue assay and 28.5 mL of αMEM into the centrifuge tube to make 1.5 mL AB dye in 30 mL solution (i.e. 5%)
- Place the tube containing the AB solution in the water bath

Addition of Alamar Blue

- Obtain the 96-wells containing RAW 264.7 murine macrophage cells co-cultured in the presence of various metal ions/nanoparticle concentrations from the incubator
- Remove the medium from each well using the vacuum suction unit
- Use a new tip for each agent to avoid contamination
- Begin from the lowest to the highest concentration to avoid contamination
- Add 100 μL of the 5% AB solution into each well
- In order to avoid drying out wells, repeat the process every two rows, using a new pipette tip each row

Incubate for 2 hours (record time)

Transfer of Supernatant into the 96-Well Microplate for Analysis

- Transfer 90 μL (leaving 10 μL behind to avoid cells in wells drying up) from each well into a new AB 96-well microplate for analysis
- Add 90 μL of AB solution alone to the 'background' column of microplate wells (thus, containing AB dye only to measure the background reading)
- Do not add AB into a column of microplate wells which contain sequentially diluted (1:2 ratio) concentrations of cells (required to calculate the conversion factor from RFU to cell number)

Alamar Blue Microplate Fluorometer

- The system incorporates an oxidation-reduction indicator, which is detected using a SpectraMAXGeminiXS microplate fluorometer at an excitation wavelength of 530 nm and an emission wavelength of 590 nm, with a cut-off at 570 nm.
- Insert the 96-wells microplate into the fluorometer cradle
- Open SoftMAX®PRO icon on the desk top
- Analyse using its attached software SoftMAX®PRO (Molecular Devices, Sunnyvale, CA) and reported as relative fluorescent units (RFU)
- Run the process three times for repeatability
- Save As – Export in .txt format

Repeat the entire process at day 4

II. Live/Dead Assay

Cell Washing with PBS solution

- Obtain 48-well from the incubator containing RAW 264.7 murine macrophage cells co-cultured in the presence of various metal ions/nanoparticle concentrations from the incubator
- Wash cells using the PBS solution
- Place in the incubator for 3-5 minutes

Prepare LD Assay Solution

- Turn off the fume cabinet light (LD assay is light-sensitive)
- Add 1.5 mL of PBS solution into a cryovial
- Obtain Calcein and EthD-1 (kept in the refrigerater drawer), wrapped in the foil
- Thaw Calcein and EthD-1
- Add 1.5 µL (1 in 1000 dilution with 3 mL PBS) of Calcein (for LIVE assay – stains living cell cytoplasm green) into the cryovial
- Add 1.5 µL (1 in 1000 dilution with 3 mL PBS) of EthD-1 (for DEAD assay – stains dead cell nucleus red) into the cryovial

Repeat Cell Washing with PBS

Addition of LD Assay

- Add 100 µL of LD assay into the two wells per group ONLY (as two wells assigned per group for each day 1 and day 4)
- Incubate for 15-30 minutes

Repeat Cell Washing with PBS Solution

Transfer Coverslips Containing Cells onto the Glass Slide for Cell Counting

- Use the hypodermic needle (green) and forceps to remove two day 1 coverslips per group onto the glass slip (use one coverslip per group)
- Place drops of PBS solution, using a disposable pipette, onto each coverslip, then cover with the rectangular glass coverslip

Live/Dead Assay Cell Counting

- Radiance 2000 Laser Confocal Scanning Microscope (Bio-Rad Microscience Ltd. Herts, UK) with LaserSharp 2000 software
- Open LaserSharp 2000 icon on the desktop
- Save three images per well

Repeat the entire process at day 4

APPENDIX 3: MOTION ANALYSIS PROTOCOL

Patient Preparation

Anthropometric data were collected for each patient; weight in kilograms, height, inter-ASIS distance, leg length measured from the ASIS to the medial malleolus, knee width measured between medial and lateral epicondyles, ankle width measured between medial and lateral malleoli). The length measurements were all made in metres and were required for the kinematic and kinetic analyses.

Patient Details

Name	
Date of Birth	
Patient Code	
Date of Test	

Anthropometric Data

Height (cm)	
Weight (kg)	
Inter ASIS Distance (cm)	

	Right	Left
Leg Length (cm)		
Knee Width (cm)		
Ankle Width (cm)		

Motion Analysis Marker Placement

Twenty-three 14 mm diameter retroreflective markers were attached using hypoallogenic double-sided tape to the lower limbs of each patient at anatomical landmarks to define seven lower limb segments (pelvis, and a right and left thigh, shank, and foot). Attachment of the markers on anatomical landmarks as performed in accordance with the protocol recommended previously by Davis *et al* [189].

Marker Set Description

Lower Limb Segment	Marker Label	Marker Placement
Pelvis	SACR	Placed mid-way between the posterior superior iliac spines
	LASIS	Placed directly over the left anterior superior iliac spine
	RASIS	Placed directly over the right anterior superior iliac spine
Thigh	THI (R and L)	Mid-thigh marker positioned over the lower lateral one-thirds of the way down the thigh, just below the swing of the hand (the height is not critical)
	THIA (R and L)	Anterior thigh at the same levels as THI marker
	THL (R and L)	Medial femoral epicondyle
	KNEE (R and L)	Lateral femoral epicondyle
Shank	TUB (R and L)	Tibial tuberosity
	TIB (R and L)	Mid-shank marker positioned approximately two-thirds of the way down the thigh from the KNEE marker, along the axis of the THI markers in the sagittal plane
Foot	ANK (R and L)	Lateral malleolus ankle
	MMA (R and L)	Medial malleolus ankle
	HEEL (R and L)	Placed on the calcaneous at the same height above the plantar surface of the foot as the toe marker
	TOE (R and L)	Placed over the second metatarsal head

Static Trial:

Patients stood in a natural standing position inside the capture volume on one of the force platforms. Data were captured for four seconds and then reconstructed to check that it was complete. The data collection was repeated in cases of any gaps or large body movements. This data was used to perform static calibration, in order to calculate the rotation offsets of the markers on the thigh and shank segments. A set of three static trials and the anthropometric data measured was used for calibration.

Vicon Nexus software was used to reconstruct data to ensure that all markers can be seen and the ground reaction force is normal prior to proceeding with the activities.

Walking:

Each patient walked at a normal cadence along a twelve-metre walkway incorporating two force platforms at the centre of capture volume. Patients were allowed to continue walking until the observed stride length and cadence did not appear to change. For kinetic data, the patients were required to strike force plates cleanly. It was important that this occurred without coaching in order to avoid interfering with the patient's natural gait. Thus, care was taken to ensure the patients did not target the force platform. This was achieved by instructing the patients to begin their walk at different starting points, thereby adjusting the position of the foot strike on the force platforms. Walking was repeated until three clean right and left foot strikes on either one of the two force platforms were achieved.

Rising from and Sitting onto a Chair:

Prior to data collection, the chair height was adjusted such that knees are flexed at 90° to accommodate the patient's varying body habitus and to ensure the patient's comfort while performing the activity. The chair was positioned next to the force platforms in the capture volume. Patients were instructed to sit upright on the chair with their arms crossed on their chest (to avoid arms obscuring the markers) and a foot on each force platform. Data was recorded from the time the patients rose to a standing position, and then sitting back down at a self-selected speed. The trial was repeated three times.

Stair Climbing:

A two-step staircase was positioned at the outside boundary of the two adjacent force platforms (A and B). Patients were instructed to stand with one foot (target foot) placed on force platform A while another foot (non-target foot) resting outside the force platform A, effectively making the force platform A the first step, and begin ascent using the non-target foot that was outside the platform A. Patients were instructed to turn around and commence descent using the non-target foot, completing the stair descent by landing the target-foot onto the second force platform B. Patients were then asked to repeat the process by alternating foot. Six trials were completed: three starting with the left foot as the target-foot, and three with the right foot as the target-foot. Data was captured for the

duration of the task. Patients performed stair climbing at their own pace. All patients were able to complete stair climbing easily and without pain.

Multi-Modality CT Marker Placement

In order to ensure that the same pelvic coordinate system could also be defined in CT scan images, the pelvic motion markers (R/L ASIS and SACR) were replaced at the identical anatomical locations with radio-opaque multi-modality markers (Multi-Modality MM3002 marker (Intermark Medical, Innovations LTD. in Bromley Kent, UK). This was carried out at the end of the motion analysis, prior to the patient leaving the motion analysis laboratory to the CT scanning suite. The presence of three multi-modality markers was checked in the CT scanning suite prior to the commencement of the scan.

APPENDIX 4: LOW DOSE HIP CT SCANNING PROTOCOL

Hip Protocol for CT scanner				64 slice
Area	kV	mA	Scan length (cm)	Collimation
ASIS	100	60	~2	32x1.2mm
Hips	100	100	~9	32x0.6mm
Distal Femur	100	60	5	32x1.2mm

All three scan regions have the same characteristics as follows.

1. The lateral and AP offsets of each slice have the same coordinate position (i.e. all slices must sit exactly above or below each other and not be shifted off to one side)
2. The scaling of each pixel in the different regions are the same.
3. The image size in pixels are the same in every region (i.e. all image slices should be, for example 512x512 pixels, there should NOT be one region, for example, of 512x512 and one of 256x256
4. There is no gantry tilt and no care dose (i.e. the kV and mAs is no greater than stated).

APPENDIX 5: RISK ASSESSEMENT FOR IONISING RADIATION

In order to ensure that the additional radiation exposure from low-dose hip CT scans to the study patients in Chapter 7 (who have already undertaken plain radiographs during their previous participation in the research study in Chapter 3), the expert risk assessment was sought. This was attained from Radiation Protection Advisers, Department of Medical Physics and Clinical Engineering, Churchill Hospital, Oxford, UK.

The total effective dose of 7 mSv was estimated to be extra to normal clinical practice. This dose has a life time fatal cancer induction risk of approximately 1 in 4000. It can also be described as the additional dose received by a person moving to an area having higher background radiation (e.g. Cornwall) for a period of about 2 years. Therefore, the total additional exposure to ionising radiation planned in this research study was considered by the clinical radiation experts as reasonable and that the risks to be acceptable.

APPENDIX 6: CT VS. EBRA ACETABULAR CUP ANGLES

The radiological angles measured by EBRA were mathematically converted to anatomical angles (CT-based measurements) using the method described by Murray [188]. Equations connecting radiographic (R), anatomical (A), inclination (*i*), and anteversion (*a*) were as follows:

$$\mathrm{Tan}(\mathrm{A}a) = \mathrm{Cos}(\mathrm{R}i) \times \mathrm{Cos}(\mathrm{R}a)$$
$$\mathrm{Sin}(\mathrm{R}a) = \mathrm{Tan}(\mathrm{A}i) \times \mathrm{Cos}(\mathrm{A}a)$$

APPENDIX 7: PUBLICATIONS AND CONFERENCE PROCEEDINGS

Publications in Peer Review Journals

1. Metal-on-metal hip resurfacing arthroplasty: a review of periprosthetic biological reactions.
G. Mabilleau*, Y.M. Kwon*, H. Pandit, D.W. Murray, A. Sabokbar.
Acta Orthop. 2008; 79(6): 734-47.
** both authors have made equal contributions to the paper*

2. Dose-dependent cytotoxicity of clinically relevant cobalt nanoparticles and ions on macrophages *in vitro*.
Y. M. Kwon, Z. Xia, S. Glyn-Jones, D.J. Beard, H. S. Gill, D. W. Murray
Biomedical Materials 2009; 4(2): 25018.

3. Asymptomatic pseudotumours following metal-on-metal hip resurfacing arthroplasty: prevalence and metal ion study.
Y.M. Kwon, S. Ostlere, P. McLardy-Smith, P. Monk, N. Athanasou, H. S. Gill, D.W. Murray
Journal of Bone and Joint Surgery [Am] 2009. In press

4. Lymphocyte proliferation responses in patients with pseudotumours following metal-on-metal hip resurfacing arthroplasty.
Y.M. Kwon, P. Thomas, B. Summer, H. Pandit, A. Taylor, D.J. Beard, D. W. Murray, H. S. Gill
Journal of Orthopaedic Research 2009. In press

5. Hip resurfacings revised for inflammatory pseudotumours have a poor outcome.
G. Grammatopoulos, H. Pandit, Y.M. Kwon, R. Gundle, P. McLardy-Smith, D.J. Beard, D.W. Murray, H.S. Gill
Journal of Bone and Joint Surgery [Br] 2009. In press

Conference Proceedings

1. Lymphocyte proliferation responses in patients with pseudotumours following metal-on-metal hip resurfacings
Y.M. Kwon, Ostlere, S, Thomas, P, Summer, B, McLardy-Smith, P, Taylor, A, Monk, A P; Gill, H S, Murray, D W
The 55th Orthopaedic Research Society Annual Meeting, Las Vegas, February, 2009
New Investigator Recognition Award (NIRA) for Best Paper Presentation
Award Sponsored by Association of American Bone and Joint Surgeons

2. Metal ion levels in pseudotumours associated with metal-on-metal hip resurfacings.
Y.M. Kwon, S. Ostlere, P. McLardy-Smith, R. Gundle, D. Whitwell, C.L.M. Gibbons, N.A. Athanasou, H.S. Gill, D.W. Murray
Podium presentation, The 55th Orthopaedic Research Society Annual Meeting, Las Vegas, February, 2009

3. Prevalence of asymptomatic pseudotumours in patients with metal-on-metal hip resurfacing.
Y.M. Kwon, P. McLardy-Smith, S. Ostlere, H. Pandit, A.P. Monk, R.A. Taylor, D. Beard, H.S. Gill, D.W.Murray
Podium presentation, The American Academy of Orthopaedic Surgeons Meeting, Las Vegas, February, 2009

4. *In vivo* modulation of osteoclast functions in patients with MoM hip resurfacing
G. Mabilleau, Y.M. Kwon, H.S. Gill, D.W. Murray, A. Sabokbar
Podium presentation, The American Academy of Orthopaedic Surgeons Meeting, Las Vegas, February, 2009

5. Outcome of failed hip resurfacing revised to THR depends on revision indication
H.S. Gill, G. Grammatopoulos, H. Pandit, Y.M. Kwon, P. McLardy-Smith, D.J. Beard, D.W. Murray
Podium presentation, The 55th Orthopaedic Research Society Annual Meeting, Las Vegas, February, 2009

6. Pseudotumours following metal-on-metal hip resurfacing arthroplasty: prevalence and metal ion study.
Y.M. Kwon, S. Ostlere, P. McLardy-Smith, R. Gundle, D. Whitwell, C.L.M. Gibbons, A. Taylor, H. Pandit, S. Glyn-Jones, N. Athanasou, D.J. Beard, H. S. Gill, D.W. Murray
Podium presentation, British Hip Society Annual Scientific Meeting, Manchester, March, 2009

7. Early to mid-term outcome of failed hip resurfacing revised to THR depends on revision indication.
G. Grammatopoulos, H. Pandit, Y.M. Kwon, P.J. Singh, R. Gundle, P. McLardy-Smith, D.J. Beard, D.W. Murray, H.S. Gill
Podium presentation, British Hip Society Annual Scientific Meeting, Manchester, March, 2009

8. *In vitro*.cytotoxicity of clinically relevant metal nanoparticles on macrophages.
Y.M. Kwon, Z. Xia, H.S. Gill, D.W. Murray
Podium presentation, the European Federation of National Associations of Orthopaedics and Traumatology (EFORT), Vienna, June, 2009

9. Measurements of metal ion levels in patients with soft tissue mass following metal-on-metal hip resurfacings.
Y.M. Kwon, Ostlere, S, McLardy-Smith, P, Gundle, R, Whitwell, D, Gibbons, CLM, Athanasou, NA, Gill, H S, Murray, D WPodium presentation, the European Federation of National Associations of Orthopaedics and Traumatology (EFORT), Vienna, June, 2009
Selected as a Finalist for the Best Free Paper

10. The use of lymphocyte transformation tests in patients with soft tissue mass following metal-on-metal hip resurfacings.
Y.M. Kwon, Ostlere, S, Thomas, P, Summer, B, McLardy-Smith, P, Taylor, A, Monk, A P; Gill, H S, Murray, D W
Podium presentation, European Federation of National Associations of Orthopaedics and Traumatology (EFORT), Vienna, June, 2009
Selected as a Finalist for the Best Free Paper

11. Pseudotumours following metal-on-metal hip resurfacing arthroplasty: metal ion and lymphocyte proliferation study.
Y.M. Kwon, P. Thomas, B. Summer, P. McLardy-Smith, S. Ostlere, R. Gundle, D. Whitwell, C.L.M. Gibbons, N. Athanasou, H.S. Gill, D.W. Murray
Podium presentation, British Orthopaedic Research, Newcastle, June, 2009
Awarded Best Paper Presentation

12. Cytotoxicity of clinically relevant cobalt nanoparticles and ions on macrophages *in vitro*.
Y.M. Kwon, Z. Xia, S. Glyn-Jones, D.J. Beard, H.S. Gill, D.W. Murray
Poster presentation, British Orthopaedic Research, Newcastle, June, 2009

REFERENCES

1. Shimmin, A., P.E. Beaule, and P. Campbell, *Metal-on-metal hip resurfacing arthroplasty.* J Bone Joint Surg Am, 2008. **90**(3): p. 637-54.
2. *National Joint Registry England and Wales Annual Report*. 2008.
3. Buergi, M.L. and W.L. Walter, *Hip resurfacing arthroplasty: the Australian experience.* J Arthroplasty, 2007. **22**(7 Suppl 3): p. 61-5.
4. *United States Food and Drug Administration. New device approval: Birmingham hip resurfacing*. May 2006 [cited; Available from: http://www.fda.gov/cdrh/mda/docs/p040033.html (date last accessed 12 December 2008).
5. Amstutz, H.C., et al., *Resurfacing THA for patients younger than 50 year: results of 2- to 9-year followup.* Clin Orthop Relat Res, 2007. **460**: p. 159-64.
6. Hing, C.B., et al., *The results of primary Birmingham hip resurfacings at a mean of five years: AN INDEPENDENT PROSPECTIVE REVIEW OF THE FIRST 230 HIPS.* J Bone Joint Surg Br, 2007. **89**(11): p. 1431-8.
7. Nishii, T., et al., *Five-year results of metal-on-metal resurfacing arthroplasty in Asian patients.* J Arthroplasty, 2007. **22**(2): p. 176-83.
8. Steffen, R.T., et al., *The five-year results of the Birmingham Hip Resurfacing arthroplasty: AN INDEPENDENT SERIES.* J Bone Joint Surg Br, 2008. **90**(4): p. 436-41.
9. Treacy, R.B., C.W. McBryde, and P.B. Pynsent, *Birmingham hip resurfacing arthroplasty. A minimum follow-up of five years.* J Bone Joint Surg Br, 2005. **87**(2): p. 167-70.
10. Daniel, J., P.B. Pynsent, and D.J. McMinn, *Metal-on-metal resurfacing of the hip in patients under the age of 55 years with osteoarthritis.* J Bone Joint Surg Br, 2004. **86**(2): p. 177-84.
11. Freeman, M.A. and G.W. Bradley, *ICLH surface replacement of the hip. An analysis of the first 10 years.* J Bone Joint Surg Br, 1983. **65**(4): p. 405-11.
12. Head, W.C., *Total articular resurfacing arthroplasty. Analysis of component failure in sixty-seven hips.* J Bone Joint Surg Am, 1984. **66**(1): p. 28-34.

13. Ritter, M.A., et al., *Failure mechanisms of total hip resurfacing: implications for the present.* Clin Orthop Relat Res, 2006. **453**: p. 110-4.
14. Sieber, H.P., C.B. Rieker, and P. Kottig, *Analysis of 118 second-generation metal-on-metal retrieved hip implants.* J Bone Joint Surg Br, 1999. **81**(1): p. 46-50.
15. Jacobs, J.J., J.L. Gilbert, and R.M. Urban, *Corrosion of metal orthopaedic implants.* J Bone Joint Surg Am, 1998. **80**(2): p. 268-82.
16. Germain, M.A., et al., *Comparison of the cytotoxicity of clinically relevant cobalt-chromium and alumina ceramic wear particles in vitro.* Biomaterials, 2003. **24**(3): p. 469-79.
17. Back, D.L., D.A. Young, and A.J. Shimmin, *How do serum cobalt and chromium levels change after metal-on-metal hip resurfacing?* Clin Orthop Relat Res, 2005. **438**: p. 177-81.
18. Brodner, W., et al., *Serum cobalt levels after metal-on-metal total hip arthroplasty.* J Bone Joint Surg Am, 2003. **85-A**(11): p. 2168-73.
19. Clarke, M.T., et al., *Levels of metal ions after small- and large-diameter metal-on-metal hip arthroplasty.* J Bone Joint Surg Br, 2003. **85**(6): p. 913-7.
20. MacDonald, S.J., et al., *Metal-on-metal versus polyethylene in hip arthroplasty: a randomized clinical trial.* Clin Orthop Relat Res, 2003(406): p. 282-96.
21. Savarino, L., et al., *Ion release in patients with metal-on-metal hip bearings in total joint replacement: a comparison with metal-on-polyethylene bearings.* J Biomed Mater Res, 2002. **63**(5): p. 467-74.
22. Gillespie, W.J., et al., *Development of hematopoietic cancers after implantation of total joint replacement.* Clin Orthop Relat Res, 1996(329 Suppl): p. S290-6.
23. Keegan, G.M., I.D. Learmonth, and C.P. Case, *Orthopaedic metals and their potential toxicity in the arthroplasty patient: A review of current knowledge and future strategies.* J Bone Joint Surg Br, 2007. **89**(5): p. 567-73.
24. Shimmin, A.J., J. Bare, and D.L. Back, *Complications associated with hip resurfacing arthroplasty.* Orthop Clin North Am, 2005. **36**(2): p. 187-93, ix.

25. Willert, H.G., et al., *Metal-on-metal bearings and hypersensitivity in patients with artificial hip joints. A clinical and histomorphological study.* J Bone Joint Surg Am, 2005. **87**(1): p. 28-36.
26. Brodner, W., et al., *Does the placenta inhibit the passage of chromium and cobalt after metal-on-metal total hip arthroplasty?* J Arthroplasty, 2004. **19**(8 Suppl 3): p. 102-6.
27. Ladon, D., et al., *Changes in metal levels and chromosome aberrations in the peripheral blood of patients after metal-on-metal hip arthroplasty.* J Arthroplasty, 2004. **19**(8 Suppl 3): p. 78-83.
28. Ziaee, H., et al., *Transplacental transfer of cobalt and chromium in patients with metal-on-metal hip arthroplasty: a controlled study.* J Bone Joint Surg Br, 2007. **89**(3): p. 301-5.
29. Silva, M., C. Heisel, and T.P. Schmalzried, *Metal-on-metal total hip replacement.* Clin Orthop Relat Res, 2005(430): p. 53-61.
30. Tharani, R., F.J. Dorey, and T.P. Schmalzried, *The risk of cancer following total hip or knee arthroplasty.* J Bone Joint Surg Am, 2001. **83-A**(5): p. 774-80.
31. Boardman, D.R., F.R. Middleton, and T.G. Kavanagh, *A benign psoas mass following metal-on-metal resurfacing of the hip.* J Bone Joint Surg Br, 2006. **88**(3): p. 402-4.
32. Campbell, P., et al., *Metal sensitivity as a cause of groin pain in metal-on-metal hip resurfacing.* J Arthroplasty, 2008. **23**(7): p. 1080-5.
33. Fang, C.S., et al., *The imaging spectrum of peri-articular inflammatory masses following metal-on-metal hip resurfacing.* Skeletal Radiol, 2008. **37**(8): p. 715-22.
34. Gruber, F.W., et al., *Cystic lesion of the groin due to metallosis: a rare long-term complication of metal-on-metal total hip arthroplasty.* J Arthroplasty, 2007. **22**(6): p. 923-7.
35. Hart, A., Sabah, S., Henkel, J., Lewis, A., Cobb, J., Sampson, B., Mitchell, A., Skinner, J.A., *The painful metal-on-metal hip resurfacing.* Journal of Bone & Joint Surgery - British Volume, 2009. **91**(6): p. 738-44.

36. Madan, S., R.L. Jowett, and M.I. Goodwin, *Recurrent intrapelvic cyst complicating metal-on-metal cemented total hip arthroplasty.* Arch Orthop Trauma Surg, 2000. **120**(9): p. 508-10.
37. Pandit, H., et al., *Pseudotumours associated with metal-on-metal hip resurfacings.* J Bone Joint Surg Br, 2008. **90**(7): p. 847-51.
38. Toms, A.P., et al., *MRI of early symptomatic metal-on-metal total hip arthroplasty: a retrospective review of radiological findings in 20 hips.* Clin Radiol, 2008. **63**(1): p. 49-58.
39. Ollivere, B.J., Durrah, C., Barker, T., Nolan, J., Porteous, M. *Early clinical failure of the Birmingham metal-on-metal hip resurfacing is associated with metalosis and soft tissue necrosis*. in *British Hip Society Annual Scientific Meeting*. 2009. Manchester, United Kingdom.
40. Langton, D.J., Jameson, S.S., Joyce, T.J., Natu, S., Logishetty, R., Tullocj, C., Nargol, A.N. *Adverse reactions to metal debris following large bearing metal on metal arthroplasty*. in *British Hip Society Annual Scientific Meeting*. 2009. Manchester, United Kingdom.
41. Board, T., Mohan, S., Gambhir, A., Porter, M. *Clinical experience of revision of resurfacing hip arthroplasty for ALVAL*. in *American Academy of Orthopaedic Surgeons Annual Meeting*. 2009. Las Vegas, USA.
42. Pandit, H., et al., *Necrotic granulomatous pseudotumours in bilateral resurfacing hip arthoplasties: evidence for a type IV immune response.* Virchows Archiv, 2008. **453**(5): p. 529-34.
43. Grammatopoulos, G., Pandit, H., Kwon, Y.,M., Gundle, R., McLardy-Smith, P., Beard, D.J., Murray, D.W., Gill, H.S., *Hip resurfacings revised for inflammatory pseudotumours have a poor outcome.* Journal of Bone & Joint Surgery - British Volume, 2009. **In Press**.
44. Grigoris, P., et al., *The evolution of hip resurfacing arthroplasty.* Orthop Clin North Am, 2005. **36**(2): p. 125-34, vii.
45. Head, W.C., *Wagner surface replacement arthroplasty of the hip. Analysis of fourteen failures in forty-one hips.* J Bone Joint Surg Am, 1981. **63**(3): p. 420-7.

46. Clarke, I.C., et al., *Current concepts of metal-on-metal hip resurfacing.* Orthop Clin North Am, 2005. **36**(2): p. 143-62, viii.
47. Murray, D., *Survival analysis*, in *Assessment Methodology in Orthopaedics*, P.B. Pynsent, Fairbank, J, Carr A, Editor. 1997, Butterworth-Heinemann: Oxford. p. 19-28.
48. Murray, D.W., A.J. Carr, and C. Bulstrode, *Survival analysis of joint replacements.* J Bone Joint Surg Br, 1993. **75**(5): p. 697-704.
49. Revell, M.P., et al., *Metal-on-metal hip resurfacing in osteonecrosis of the femoral head.* J Bone Joint Surg Am, 2006. **88 Suppl 3**: p. 98-103.
50. Mont, M.A., et al., *Use of metal-on-metal total hip resurfacing for the treatment of osteonecrosis of the femoral head.* J Bone Joint Surg Am, 2006. **88 Suppl 3**: p. 90-7.
51. Shimmin, A.J. and D. Back, *Femoral neck fractures following Birmingham hip resurfacing: a national review of 50 cases.* J Bone Joint Surg Br, 2005. **87**(4): p. 463-4.
52. Lilikakis, A.K., S.L. Vowler, and R.N. Villar, *Hydroxyapatite-coated femoral implant in metal-on-metal resurfacing hip arthroplasty: minimum of two years follow-up.* Orthop Clin North Am, 2005. **36**(2): p. 215-22, ix.
53. De Smet, K.A., *Belgium experience with metal-on-metal surface arthroplasty.* Orthop Clin North Am, 2005. **36**(2): p. 203-13, ix.
54. Mont, M.A., P.S. Ragland, and D. Marker, *Resurfacing hip arthroplasty: comparison of a minimally invasive versus standard approach.* Clin Orthop Relat Res, 2005. **441**: p. 125-31.
55. Beaule, P.E., et al., *Risk factors affecting outcome of metal-on-metal surface arthroplasty of the hip.* Clin Orthop Relat Res, 2004(418): p. 87-93.
56. Beaule, P.E., et al., *Metal-on-metal surface arthroplasty with a cemented femoral component: a 7-10 year follow-up study.* J Arthroplasty, 2004. **19**(8 Suppl 3): p. 17-22.
57. in *Orthopaedic Basic Science*, S. Simon, Editor. 1994, American Academy of Orthopaedic Surgeons. p. 439.

58. Anissian, H.L., et al., *The wear pattern in metal-on-metal hip prostheses.* J Biomed Mater Res, 2001. **58**(6): p. 673-8.

59. Dowson, D., et al., *A hip joint simulator study of the performance of metal-on-metal joints: Part II: design.* J Arthroplasty, 2004. **19**(8 Suppl 3): p. 124-30.

60. Dowson, D., et al., *A hip joint simulator study of the performance of metal-on-metal joints: Part I: the role of materials.* J Arthroplasty, 2004. **19**(8 Suppl 3): p. 118-23.

61. Howie, D.W., et al., *The long-term wear of retrieved McKee-Farrar metal-on-metal total hip prostheses.* J Arthroplasty, 2005. **20**(3): p. 350-7.

62. McKellop, H., et al., *In vivo wear of three types of metal on metal hip prostheses during two decades of use.* Clin Orthop Relat Res, 1996(329 Suppl): p. S128-40.

63. Amstutz, H.C., et al., *Mechanism and clinical significance of wear debris-induced osteolysis.* Clin Orthop Relat Res, 1992(276): p. 7-18.

64. Jacobs, J.J., et al., *Metal release in patients who have had a primary total hip arthroplasty. A prospective, controlled, longitudinal study.* J Bone Joint Surg Am, 1998. **80**(10): p. 1447-58.

65. Doorn, P.F., et al., *Metal wear particle characterization from metal on metal total hip replacements: transmission electron microscopy study of periprosthetic tissues and isolated particles.* J Biomed Mater Res, 1998. **42**(1): p. 103-11.

66. Mabilleau, G., et al., *Influence of fluoride, hydrogen peroxide and lactic acid on the corrosion resistance of commercially pure titanium.* Acta Biomater, 2006. **2**(1): p. 121-9.

67. Wang, J.Y., et al., *Prosthetic metals impair murine immune response and cytokine release in vivo and in vitro.* J Orthop Res, 1997. **15**(5): p. 688-99.

68. Catelas, I., et al., *Comparison of in vitro with in vivo characteristics of wear particles from metal-metal hip implants.* J Biomed Mater Res B Appl Biomater, 2004. **70**(2): p. 167-78.

69. Cobb, A.G. and T.P. Schmalzreid, *The clinical significance of metal ion release from cobalt-chromium metal-on-metal hip joint arthroplasty.* Proc Inst Mech Eng [H], 2006. **220**(2): p. 385-98.

70. Brodner, W., et al., *[Serum cobalt and serum chromium level in 2 patients with chronic renal failure after total hip prosthesis implantation with metal-metal gliding contact]*. Z Orthop Ihre Grenzgeb, 2000. **138**(5): p. 425-9.

71. Daniel, J., Ziaee, H, Pradhan, C, McMinn, D, *Renal clearance of metal ions: Is the renal threshold being breached at higher metal levels?*, in *54th Annual Meeting of the Orthoipaedic Research Society*. 2008: San Francisco. p. Paper No. 57.

72. Marker, M., et al., *Metal-on-metal hip implants: do they impair renal function in the long-term? A 10-year follow-up study.* Arch Orthop Trauma Surg, 2007.

73. Daniel, J., Ziaee, H., Alinovi, R., McMinn. D. in *54th Annual Meeting of the Orthopaedic Research Society*. 2008. San Francisco, USA.

74. Daniel, J., Ziaee, H, Alinovi, R, McMinn, D, *Early markers of nephrotoxicity in patients with metal on metal bearings for over ten years*, in *54th Annual Meeting of the Orthopaedic Research Society*. 2008: San Francisco. p. Poster No. 1803.

75. MacDonald, S.J., W. Brodner, and J.J. Jacobs, *A consensus paper on metal ions in metal-on-metal hip arthroplasties.* J Arthroplasty, 2004. **19**(8 Suppl 3): p. 12-6.

76. Merritt, K., T.D. Crowe, and S.A. Brown, *Elimination of nickel, cobalt, and chromium following repeated injections of high dose metal salts.* J Biomed Mater Res, 1989. **23**(8): p. 845-62.

77. Case, C.P., et al., *Development of a routine method for the determination of trace metals in whole blood by magnetic sector inductively coupled plasma mass spectrometry with particular relevance to patients with total hip and knee arthroplasty.* Clin Chem, 2001. **47**(2): p. 275-80.

78. Muniz, C.S., et al., *Reference values for trace and ultratrace elements in human serum determined by double-focusing ICP-MS.* Biol Trace Elem Res, 2001. **82**(1-3): p. 259-72.

79. Daniel, J., et al., *Blood and urine metal ion levels in young and active patients after Birmingham hip resurfacing arthroplasty: four-year results of a prospective longitudinal study.* J Bone Joint Surg Br, 2007. **89**(2): p. 169-73.

80. Vendittoli, P.A., et al., *Chromium and cobalt ion release following the Durom high carbon content, forged metal-on-metal surface replacement of the hip.* J Bone Joint Surg Br, 2007. **89**(4): p. 441-8.

81. Rasquinha, V.J., et al., *Serum metal levels and bearing surfaces in total hip arthroplasty.* J Arthroplasty, 2006. **21**(6 Suppl 2): p. 47-52.

82. Hart, A.J., et al., *The association between metal ions from hip resurfacing and reduced T-cell counts.* J Bone Joint Surg Br, 2006. **88**(4): p. 449-54.

83. Back, D.L., et al., *Early results of primary Birmingham hip resurfacings. An independent prospective study of the first 230 hips.* J Bone Joint Surg Br, 2005. **87**(3): p. 324-9.

84. Heisel, C., et al., *The relationship between activity and ions in patients with metal-on-metal bearing hip prostheses.* J Bone Joint Surg Am, 2005. **87**(4): p. 781-7.

85. Brodner, W., et al., *Cup inclination and serum concentration of cobalt and chromium after metal-on-metal total hip arthroplasty.* J Arthroplasty, 2004. **19**(8 Suppl 3): p. 66-70.

86. Brodner, W., et al., *Does the placenta inhibit the passage of chromium and cobalt after metal-on-metal total hip arthroplasty?* J Arthroplasty, 2004a. **19**(8 Suppl 3): p. 102-6.

87. Lhotka, C., et al., *Four-year study of cobalt and chromium blood levels in patients managed with two different metal-on-metal total hip replacements.* J Orthop Res, 2003. **21**(2): p. 189-95.

88. Jacobs, J.J., et al., *Cobalt and chromium concentrations in patients with metal on metal total hip replacements.* Clin Orthop Relat Res, 1996(329 Suppl): p. S256-63.

89. Coleman, R.F., J. Herrington, and J.T. Scales, *Concentration of wear products in hair, blood, and urine after total hip replacement.* Br Med J, 1973. **1**(5852): p. 527-9.

90. Daniel, J., et al., *The validity of serum levels as a surrogate measure of systemic exposure to metal ions in hip replacement.* J Bone Joint Surg Br, 2007. **89**(6): p. 736-41.

91. Daniel, J., et al., *The effect of the diameter of metal-on-metal bearings on systemic exposure to cobalt and chromium.* J Bone Joint Surg Br, 2006. **88**(4): p. 443-8.
92. De Haan, R., et al., *Correlation between inclination of the acetabular component and metal ion levels in metal-on-metal hip resurfacing replacement.* J Bone Joint Surg Br, 2008. **90**(10): p. 1291-7.
93. Langton, D.J., et al., *The effect of component size and orientation on the concentrations of metal ions after resurfacing arthroplasty of the hip.* Journal of Bone & Joint Surgery - British Volume, 2008. **90**(9): p. 1143-51.
94. Jacobs, J.J., et al., *Can metal levels be used to monitor metal-on-metal hip arthroplasties?* J Arthroplasty, 2004. **19**(8 Suppl 3): p. 59-65.
95. De Haan, R., et al., *Correlation between inclination of the acetabular component and metal ion levels in metal-on-metal hip resurfacing replacement.* Journal of Bone & Joint Surgery - British Volume, 2008. **90**(10): p. 1291-7.
96. Dizdaroglu, M., et al., *Free radical-induced damage to DNA: mechanisms and measurement.* Free Radic Biol Med, 2002. **32**(11): p. 1102-15.
97. Bacon, B.R., et al., *Hepatic lipid peroxidation in vivo in rats with chronic iron overload.* J Clin Invest, 1983. **71**(3): p. 429-39.
98. Marnett, L.J., *Lipid peroxidation-DNA damage by malondialdehyde.* Mutat Res, 1999. **424**(1-2): p. 83-95.
99. Heath, J.C., M.A. Freeman, and S.A. Swanson, *Carcinogenic properties of wear particles from prostheses made in cobalt-chromium alloy.* Lancet, 1971. **1**(7699): p. 564-6.
100. Visuri, T., et al., *Cancer risk after metal on metal and polyethylene on metal total hip arthroplasty.* Clin Orthop Relat Res, 1996(329 Suppl): p. S280-9.
101. Hallab, N., K. Merritt, and J.J. Jacobs, *Metal sensitivity in patients with orthopaedic implants.* J Bone Joint Surg Am, 2001. **83-A**(3): p. 428-36.
102. Benson, M.K., P.G. Goodwin, and J. Brostoff, *Metal sensitivity in patients with joint replacement arthroplasties.* Br Med J, 1975. **4**(5993): p. 374-5.
103. Evans, E.M., et al., *Metal sensitivity as a cause of bone necrosis and loosening of the prosthesis in total joint replacement.* J Bone Joint Surg Br, 1974. **56-B**(4): p. 626-42.

104. Witzleb, W.C., et al., *Neo-capsule tissue reactions in metal-on-metal hip arthroplasty.* Acta Orthop, 2007. **78**(2): p. 211-20.

105. Hallab, N.J., K. Mikecz, and J.J. Jacobs, *A triple assay technique for the evaluation of metal-induced, delayed-type hypersensitivity responses in patients with or receiving total joint arthroplasty.* J Biomed Mater Res, 2000. **53**(5): p. 480-9.

106. Davies, A.P., et al., *An unusual lymphocytic perivascular infiltration in tissues around contemporary metal-on-metal joint replacements.* J Bone Joint Surg Am, 2005. **87**(1): p. 18-27.

107. Doorn, P.F., et al., *Tissue reaction to metal on metal total hip prostheses.* Clin Orthop Relat Res, 1996(329 Suppl): p. S187-205.

108. Hallab, N.J., et al., *Lymphocyte responses in patients with total hip arthroplasty.* J Orthop Res, 2005. **23**(2): p. 384-91.

109. Park, Y.S., et al., *Early osteolysis following second-generation metal-on-metal hip replacement.* J Bone Joint Surg Am, 2005. **87**(7): p. 1515-21.

110. Korovessis, P., et al., *Metallosis after contemporary metal-on-metal total hip arthroplasty. Five to nine-year follow-up.* J Bone Joint Surg Am, 2006. **88**(6): p. 1183-91.

111. Milosev, I., et al., *Survivorship and retrieval analysis of Sikomet metal-on-metal total hip replacements at a mean of seven years.* J Bone Joint Surg Am, 2006. **88**(6): p. 1173-82.

112. Shahrdar, C., et al., *Painful metal-on-metal total hip arthroplasty.* J Arthroplasty, 2006. **21**(2): p. 289-93.

113. Campbell, P., et al., *Metal Sensitivity as a Cause of Groin Pain in Metal-on-Metal Hip Resurfacing.* J Arthroplasty, 2008.

114. Hartz, A. and J.L. Marsh, *Methodologic issues in observational studies.* Clin Orthop Relat Res, 2003(413): p. 33-42.

115. Chan, F.W., et al., *The Otto Aufranc Award. Wear and lubrication of metal-on-metal hip implants.* Clin Orthop Relat Res, 1999(369): p. 10-24.

116. Murray, D.W., et al., *The use of the Oxford hip and knee scores.* J Bone Joint Surg Br, 2007. **89**(8): p. 1010-4.

117. Breidahl, W.H., et al., *Power Doppler sonography in the assessment of musculoskeletal fluid collections.* AJR Am J Roentgenol, 1996. **166**(6): p. 1443-6.
118. Cardinal, E., et al., *Role of ultrasound in musculoskeletal infections.* Radiol Clin North Am, 2001. **39**(2): p. 191-201.
119. Chau, C.L. and J.F. Griffith, *Musculoskeletal infections: ultrasound appearances.* Clin Radiol, 2005. **60**(2): p. 149-59.
120. Pelsser, V., et al., *Extraarticular snapping hip: sonographic findings.* AJR Am J Roentgenol, 2001. **176**(1): p. 67-73.
121. Laskin, A. and J.P. Cowin, *Automated single-particle SEM/EDX analysis of submicrometer particles down to 0.1 microm.* Anal Chem, 2001. **73**(5): p. 1023-9.
122. Dawson, J., et al., *Comparison of measures to assess outcomes in total hip replacement surgery.* Qual Health Care, 1996. **5**(2): p. 81-8.
123. Dawson, J., et al., *Questionnaire on the perceptions of patients about total hip replacement.* J Bone Joint Surg Br, 1996. **78**(2): p. 185-90.
124. De Smet, K., et al., *Metal ion measurement as a diagnostic tool to identify problems with metal-on-metal hip resurfacing.* Journal of Bone & Joint Surgery - American Volume, 2008. **90 Suppl 4**: p. 202-8.
125. Vendittoli, P.A., M. Ganapathi, and M. Lavigne, *Blood and urine metal ion levels in young and active patients after Birmingham hip resurfacing arthroplasty.[comment].* Journal of Bone & Joint Surgery - British Volume, 2007. **89**(7): p. 989; author reply 989-90.
126. Walter, L.R., et al., *Distribution of chromium and cobalt ions in various blood fractions after resurfacing hip arthroplasty.* J Arthroplasty, 2008. **23**(6): p. 814-21.
127. Rooker, G.D. and J.D. Wilkinson, *Metal sensitivity in patients undergoing hip replacement. A prospective study.* J Bone Joint Surg Br, 1980. **62-B**(4): p. 502-5.
128. Jacobs, J.J., et al., *Wear particles.* J Bone Joint Surg Am, 2006. **88 Suppl 2**: p. 99-102.
129. Nyfeler, B. and W.J. Pichler, *The lymphocyte transformation test for the diagnosis of drug allergy: sensitivity and specificity.* Clin Exp Allergy, 1997. **27**(2): p. 175-81.

130. Thomas, P., et al., *Hypersensitivity to titanium osteosynthesis with impaired fracture healing, eczema, and T-cell hyperresponsiveness in vitro: case report and review of the literature.* Contact Dermatitis, 2006. **55**(4): p. 199-202.

131. Thomas, P., et al., *Intolerance of osteosynthesis material: evidence of dichromate contact allergy with concomitant oligoclonal T-cell infiltrate and TH1-type cytokine expression in the peri-implantar tissue.* Allergy, 2000. **55**(10): p. 969-72.

132. Basketter, D.A., et al., *Nickel, cobalt and chromium in consumer products: a role in allergic contact dermatitis?* Contact Dermatitis, 1993. **28**(1): p. 15-25.

133. Hallab, N.J., et al., *Immune responses correlate with serum-metal in metal-on-metal hip arthroplasty.* J Arthroplasty, 2004. **19**(8 Suppl 3): p. 88-93.

134. Jacobs, J.J. and N.J. Hallab, *Loosening and osteolysis associated with metal-on-metal bearings: A local effect of metal hypersensitivity?* J Bone Joint Surg Am, 2006. **88**(6): p. 1171-2.

135. Granchi, D., et al., *Expression of the CD69 activation antigen on lymphocytes of patients with hip prosthesis.* Biomaterials, 2000. **21**(20): p. 2059-65.

136. Lee, S.H., et al., *Human monocyte/macrophage response to cobalt-chromium corrosion products and titanium particles in patients with total joint replacements.* J Orthop Res, 1997. **15**(1): p. 40-9.

137. Xia, Z. and J.T. Triffitt, *A review on macrophage responses to biomaterials.* Biomed Mater, 2006. **1**(1): p. R1-9.

138. Matthews, J.B., et al., *Evaluation of the response of primary human peripheral blood mononuclear phagocytes to challenge with in vitro generated clinically relevant UHMWPE particles of known size and dose.* J Biomed Mater Res, 2000. **52**(2): p. 296-307.

139. Matthews, J.B., et al., *Comparison of the response of primary human peripheral blood mononuclear phagocytes from different donors to challenge with model polyethylene particles of known size and dose.* Biomaterials, 2000. **21**(20): p. 2033-44.

140. Yagil-Kelmer, E., et al., *Comparison of the response of primary human blood monocytes and the U937 human monocytic cell line to two different sizes of alumina ceramic particles.* J Orthop Res, 2004. **22**(4): p. 832-8.

141. Brockhaus, F. and B. Brune, *Overexpression of CuZn superoxide dismutase protects RAW 264.7 macrophages against nitric oxide cytotoxicity.* Biochem J, 1999. **338 (Pt 2)**: p. 295-303.

142. Drapier, J.C. and J.B. Hibbs, Jr., *Differentiation of murine macrophages to express nonspecific cytotoxicity for tumor cells results in L-arginine-dependent inhibition of mitochondrial iron-sulfur enzymes in the macrophage effector cells.* J Immunol, 1988. **140**(8): p. 2829-38.

143. *Orthopaedic Basic Science*, ed. S.R. Simon. 1994, Chicago, USA: American Academy of Orthopaedic Surgeons. 470.

144. Catelas, I., et al., *Effects of digestion protocols on the isolation and characterization of metal-metal wear particles. I. Analysis of particle size and shape.* Journal of Biomedical Materials Research, 2001. **55**(3): p. 320-9.

145. Nakayama, G.R., et al., *Assessment of the Alamar Blue assay for cellular growth and viability in vitro.* J Immunol Methods, 1997. **204**(2): p. 205-8.

146. O'Brien, J., et al., *Investigation of the Alamar Blue (resazurin) fluorescent dye for the assessment of mammalian cell cytotoxicity.* Eur J Biochem, 2000. **267**(17): p. 5421-6.

147. Roden, M.M., et al., *A novel cytolysis assay using fluorescent labeling and quantitative fluorescent scanning technology.* J Immunol Methods, 1999. **226**(1-2): p. 29-41.

148. Bland, J.M. and D.G. Altman, *Statistical methods for assessing agreement between two methods of clinical measurement.* Lancet, 1986. **1**(8476): p. 307-10.

149. Papageorgiou, I., et al., *The effect of nano- and micron-sized particles of cobalt-chromium alloy on human fibroblasts in vitro.* Biomaterials, 2007. **28**(19): p. 2946-58.

150. Allen, M.J., et al., *The effects of particulate cobalt, chromium and cobalt-chromium alloy on human osteoblast-like cells in vitro.* J Bone Joint Surg Br, 1997. **79**(3): p. 475-82.

151. Catelas, I., Petit, A., Zukor, D.J., Huk, O.L., *Cytotoxic and apoptotic effects of cobalt and chromium ions on J774 macrophages - Implication of caspase-3 in the apoptotic pathway.* J Mater Sci Mater Med, 2001. **12** (10): p. 949-53.

152. Case, C.P., et al., *Widespread dissemination of metal debris from implants.* J Bone Joint Surg Br, 1994. **76**(5): p. 701-12.

153. Merritt, K. and S.A. Brown, *Release of hexavalent chromium from corrosion of stainless steel and cobalt-chromium alloys.* Journal of Biomedical Materials Research, 1995. **29**(5): p. 627-33.

154. Campbell, P., et al., *The John Charnley Award: a study of implant failure in metal-on-metal surface arthroplasties.* Clin Orthop Relat Res, 2006. **453**: p. 35-46.

155. Hussain, A., Counsell, L., Kamali, A. . *Clinical effects of edge loading on metal-on-metal hip resurfacings*. in *British Hip Society*. 2009. Manchester, United Kingdom.

156. Altman, D.G., *Statistics in Practice*. How large a sample? , ed. S.M. Gore, Altman, D.G. 1982, London: British Medical Association.

157. Lusty, P.J., et al., *Wear and acetabular component orientation in third generation alumina-on-alumina ceramic bearings: an analysis of 33 retrievals [corrected][erratum appears in J Bone Joint Surg Br. 2008 Apr;90(4):543]*. Journal of Bone & Joint Surgery - British Volume, 2007. **89**(9): p. 1158-64.

158. Walter, W.L., et al., *Edge loading in third generation alumina ceramic-on-ceramic bearings: stripe wear.* Journal of Arthroplasty, 2004. **19**(4): p. 402-13.

159. Shon, W.Y., et al., *Impingement in total hip arthroplasty a study of retrieved acetabular components.* Journal of Arthroplasty, 2005. **20**(4): p. 427-35.

160. Taylor, S., M.T. Manley, and K. Sutton, *The role of stripe wear in causing acoustic emissions from alumina ceramic-on-ceramic bearings.* Journal of Arthroplasty, 2007. **22**(7 Suppl 3): p. 47-51.

161. Witzleb, W.-C., Guenther, K., Hanisch, U., Ziegler, J., Guenther, K-P., *In vivo wear rate of the Birmingham Hip Resurfacing Arthroplasty.* Journal of Arthroplasty, 2008. **Epub ahead of print**.

162. Udofia, I.J. and Z.M. Jin, *Elastohydrodynamic lubrication analysis of metal-on-metal hip-resurfacing prostheses.* Journal of Biomechanics, 2003. **36**(4): p. 537-44.

163. Liu, F., et al., *Importance of head diameter, clearance, and cup wall thickness in elastohydrodynamic lubrication analysis of metal-on-metal hip resurfacing prostheses.* Proceedings of the Institution of Mechanical Engineers. Part H - Journal of Engineering in Medicine, 2006. **220**(6): p. 695-704.

164. Liu, F., et al., *Development of computational wear simulation of metal-on-metal hip resurfacing replacements.* Journal of Biomechanics, 2008. **41**(3): p. 686-94.

165. Taylor, S.J., et al., *Telemetry of forces from proximal femoral replacements and relevance to fixation.* Journal of Biomechanics, 1997. **30**(3): p. 225-34.

166. Bergmann, G., et al., *Hip joint forces during load carrying.* Clinical Orthopaedics & Related Research, 1997(335): p. 190-201.

167. Bergmann, G., F. Graichen, and A. Rohlmann, *Hip joint loading during walking and running, measured in two patients.* Journal of Biomechanics, 1993. **26**(8): p. 969-90.

168. Davy, D.T., et al., *Telemetric force measurements across the hip after total arthroplasty.* Journal of Bone & Joint Surgery - American Volume, 1988. **70**(1): p. 45-50.

169. Watanabe, Y., et al., *Biomechanical study of the resurfacing hip arthroplasty: finite element analysis of the femoral component.* J Arthroplasty, 2000. **15**(4): p. 505-11.

170. Brand, R.A., et al., *A model of lower extremity muscular anatomy.* Journal of Biomechanical Engineering, 1982. **104**(4): p. 304-10.

171. Komistek, R.D., et al., *Mathematical model of the lower extremity joint reaction forces using Kane's method of dynamics.* Journal of Biomechanics, 1998. **31**(2): p. 185-9.

172. Bergmann, G., F. Graichen, and A. Rohlmann, *Is staircase walking a risk for the fixation of hip implants?* Journal of Biomechanics, 1995. **28**(5): p. 535-53.

173. Lu, T.W., et al., *Validation of a lower limb model with in vivo femoral forces telemetered from two subjects.* Journal of Biomechanics, 1998. **31**(1): p. 63-9.

174. Dennis, D.A., et al., *"In vivo" determination of hip joint separation and the forces generated due to impact loading conditions.* Journal of Biomechanics, 2001. **34**(5): p. 623-9.

175. Komistek, R.D., et al., *In vivo comparison of hip separation after metal-on-metal or metal-on-polyethylene total hip arthroplasty.* Journal of Bone & Joint Surgery - American Volume, 2002. **84-A**(10): p. 1836-41.

176. Chiari, L., et al., *Human movement analysis using stereophotogrammetry. Part 2: instrumental errors.* Gait & Posture, 2005. **21**(2): p. 197-211.

177. Leardini, A., et al., *Human movement analysis using stereophotogrammetry. Part 3. Soft tissue artifact assessment and compensation.* Gait & Posture, 2005. **21**(2): p. 212-25.

178. Leardini, A., et al., *A new software tool for 3D motion analyses of the musculo-skeletal system.* Clinical Biomechanics, 2006. **21**(8): p. 870-9.

179. Mont, M.A., et al., *Gait analysis of patients with resurfacing hip arthroplasty compared with hip osteoarthritis and standard total hip arthroplasty.* J Arthroplasty, 2007. **22**(1): p. 100-8.

180. Shrader, M.W., Bhowmik-Stoker, M., Jacofsky, M.C., Jacofsky, D.J., *Gait and stair function in total and resurfacing hip arthroplasty.* Clin Orthop Relat Res, 2009. **467**(6): p. 1476-1484.

181. Bennett, D., et al., *The influence of wear paths produced by hip replacement patients during normal walking on wear rates.* Journal of Orthopaedic Research, 2008. **26**(9): p. 1210-7.

182. Bennett, D., et al., *Gait kinematics of age-stratified hip replacement patients--a large scale, long-term follow-up study.* Gait & Posture, 2008. **28**(2): p. 194-200.

183. Bennett, D., et al., *Wear paths produced by individual hip-replacement patients--a large-scale, long-term follow-up study.* Journal of Biomechanics, 2008. **41**(11): p. 2474-82.

184. Ackland, M.K., W.B. Bourne, and H.K. Uhthoff, *Anteversion of the acetabular cup. Measurement of angle after total hip replacement.* Journal of Bone & Joint Surgery - British Volume, 1986. **68**(3): p. 409-13.

185. Hassan, D.M., et al., *Radiographic calculation of anteversion in acetabular prostheses.* Journal of Arthroplasty, 1995. **10**(3): p. 369-72.

186. Cobb, J.P., *Computer navigation versus conventional total knee replacement.[comment].* Journal of Bone & Joint Surgery - British Volume, 2007. **89**(8): p. 1130; author reply 1130-1.

187. Olivecrona, H., et al., *A new CT method for measuring cup orientation after total hip arthroplasty: a study of 10 patients.* Acta Orthop Scand, 2004. **75**(3): p. 252-60.

188. Murray, D.W., *The definition and measurement of acetabular orientation.* J Bone Joint Surg Br, 1993. **75**(2): p. 228-32.

189. Davis, R.B., Ounpuu, S., Tyburski, D., Gage, J.R., *A gait analysis data collection and reduction technique.* Human Movement Science, 1991. **10**: p. 575-587.

190. Cowley, M.S., Armstrong, P.F., *A multi-segment kinematic and kinetic foot model.* Gait & Posture, 2001. **13**: p. 297.

191. Bell, A.L., D.R. Pedersen, and R.A. Brand, *A comparison of the accuracy of several hip center location prediction methods.* Journal of Biomechanics, 1990. **23**(6): p. 617-21.

192. Kadaba, M.P., H.K. Ramakrishnan, and M.E. Wootten, *Measurement of lower extremity kinematics during level walking.* Journal of Orthopaedic Research, 1990. **8**(3): p. 383-92.

193. Kadaba, M.P., et al., *Repeatability of kinematic, kinetic, and electromyographic data in normal adult gait.* Journal of Orthopaedic Research, 1989. **7**(6): p. 849-60.

194. Ramakrishnan, H.K. and M.P. Kadaba, *On the estimation of joint kinematics during gait.* Journal of Biomechanics, 1991. **24**(10): p. 969-77.

195. Rodosky, M.W., T.P. Andriacchi, and G.B. Andersson, *The influence of chair height on lower limb mechanics during rising.* Journal of Orthopaedic Research, 1989. **7**(2): p. 266-71.

196. McFadyen, B.J. and D.A. Winter, *An integrated biomechanical analysis of normal stair ascent and descent.* Journal of Biomechanics, 1988. **21**(9): p. 733-44.

197. Roys, M.S., *Serious stair injuries can be prevented by improved stair design.* Applied Ergonomics, 2001. **32**(2): p. 135-9.

198. Riener, R., M. Rabuffetti, and C. Frigo, *Stair ascent and descent at different inclinations.* Gait & Posture, 2002. **15**(1): p. 32-44.

199. Hart, A., Sabah, S., Mitchell, A., Sampson, B., Henkel, J., Adam, J., Skinner, J. *New technology to investigate the unexplained painful metal-on-metal hip resurfacing*. in *American Academy of Orthopaedic Surgeons Annual Meeting*. 2009. Las Vegas.

200. Biedermann, R., et al., *Reducing the risk of dislocation after total hip arthroplasty: the effect of orientation of the acetabular component.* Journal of Bone & Joint Surgery - British Volume, 2005. **87**(6): p. 762-9.

201. Williams, D., M. Royle, and M. Norton, *Metal-on-metal hip resurfacing: the effect of cup position and component size on range of motion to impingement.* Journal of Arthroplasty, 2009. **24**(1): p. 144-51.

202. Lewinnek, G.E., et al., *Dislocations after total hip-replacement arthroplasties.* Journal of Bone & Joint Surgery - American Volume, 1978. **60**(2): p. 217-20.

203. Wu, G., et al., *ISB recommendation on definitions of joint coordinate system of various joints for the reporting of human joint motion--part I: ankle, hip, and spine. International Society of Biomechanics.[see comment]*. Journal of Biomechanics, 2002. **35**(4): p. 543-8.

204. Meriam, J.L., Kraige, L.,G., *Engineering mechanics: Dynamics*. Third ed. 1993, New York: John Wiley & Sons, Inc.

205. Bobbert, M.F. and H.C. Schamhardt, *Accuracy of determining the point of force application with piezoelectric force plates.* Journal of Biomechanics, 1990. **23**(7): p. 705-10.

206. Mita, K., et al., *An investigation of the accuracy in measuring the body center of pressure in a standing posture with a force plate.* Frontiers of Medical & Biological Engineering, 1993. **5**(3): p. 201-13.

207. Gill, H.S., O'Connor, J.,J., *A new testing rig for force platform calibration and accuracy tests.* Gait & Posture, 1997. **5**: p. 228-32.

208. Fleiss, J.L. and P.E. Shrout, *The effects of measurement errors on some multivariate procedures.* American Journal of Public Health, 1977. **67**(12): p. 1188-91.

209. Amstutz, H.C., et al., *Metal-on-metal hybrid surface arthroplasty. Surgical Technique.* J Bone Joint Surg Am, 2006. **88 Suppl 1 Pt 2**: p. 234-49.

210. Harrington, M.E., et al., *Prediction of the hip joint centre in adults, children, and patients with cerebral palsy based on magnetic resonance imaging.* Journal of Biomechanics, 2007. **40**(3): p. 595-602.
211. Kirkwood, R.N., E.G. Culham, and P. Costigan, *Radiographic and non-invasive determination of the hip joint center location: effect on hip joint moments.* Clinical Biomechanics, 1999. **14**(4): p. 227-35.
212. Leardini, A., et al., *Validation of a functional method for the estimation of hip joint centre location.* Journal of Biomechanics, 1999. **32**(1): p. 99-103.
213. Stagni, R., et al., *Effects of hip joint centre mislocation on gait analysis results.* Journal of Biomechanics, 2000. **33**(11): p. 1479-87.
214. Boardman, T., Walter, W.L. *When is 45 degrees not 45 degrees: Analysis of the true inclination angle of resurfacing sockets*. in *British Hip Society*. 2009. Manchester, United Kingdom.
215. Morris, T.W., *Assessment Methodology in Orthopaedics*, ed. P.B. Pynsent, Fairbank, J.C.T., Carr, A.J. 1997, Oxford: Butterworth-Heinemann.
216. Ilchmann, T., U. Kesteris, and H. Wingstrand, *EBRA improves the accuracy of radiographic analysis of acetabular cup migration.* Acta Orthopaedica Scandinavica, 1998. **69**(2): p. 119-24.
217. Phillips, N.J., I. Stockley, and J.M. Wilkinson, *Direct plain radiographic methods versus EBRA-Digital for measuring implant migration after total hip arthroplasty.* Journal of Arthroplasty, 2002. **17**(7): p. 917-25.
218. Wilkinson, J.M., et al., *Precision of EBRA-Digital software for monitoring implant migration after total hip arthroplasty.* Journal of Arthroplasty, 2002. **17**(7): p. 910-6.
219. Beaule, P.E., et al., *EBRA-FCA for measurement of migration of the femoral component in surface arthroplasty of the hip.* Journal of Bone & Joint Surgery - British Volume, 2005. **87**(5): p. 741-4.
220. Morlock, M., et al., *Duration and frequency of every day activities in total hip patients.* Journal of Biomechanics, 2001. **34**(7): p. 873-81.
221. Bergmann, G., et al., *Hip contact forces and gait patterns from routine activities.[see comment]*. Journal of Biomechanics, 2001. **34**(7): p. 859-71.

222. Bowsher, J.G., et al., *Surface damage after multiple dislocations of a 38-mm-diameter, metal-on-metal hip prosthesis.* Journal of Arthroplasty, 2008. **23**(7): p. 1090-6.

223. Malik, A., A. Maheshwari, and L.D. Dorr, *Impingement with total hip replacement.* Journal of Bone & Joint Surgery - American Volume, 2007. **89**(8): p. 1832-42.

224. Beaule, P.E., et al., *The femoral head/neck offset and hip resurfacing.* J Bone Joint Surg Br, 2007. **89**(1): p. 9-15.

225. Sharma, L., *Local factors in osteoarthritis.* Current Opinion in Rheumatology, 2001. **13**(5): p. 441-6.

226. della Croce, U., A. Cappozzo, and D.C. Kerrigan, *Pelvis and lower limb anatomical landmark calibration precision and its propagation to bone geometry and joint angles.* Medical & Biological Engineering & Computing, 1999. **37**(2): p. 155-61.

227. Vendittoli, P.A., et al., *Factors affecting hip range of motion in surface replacement arthroplasty.* Clinical Biomechanics, 2007. **22**(9): p. 1004-12.

228. Wines, A.P. and D. McNicol, *Computed tomography measurement of the accuracy of component version in total hip arthroplasty.* Journal of Arthroplasty, 2006. **21**(5): p. 696-701.